MOLECULAR CHARACTERIZATION OF MARINE BACTERIA AND THEIR ENZYMES FOR TEXTILE AZO DYE DECOLORIZATION

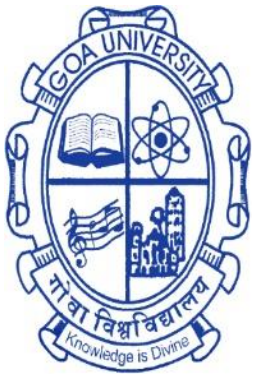
A Thesis submitted in partial fulfilment for the Degree of

DOCTOR OF PHILOSOPHY

in the

School of Biological Sciences and Biotechnology

Goa University



By

NADINE ANA DE SOUZA

CSIR- National Institute of Oceanography

Dona Paula, Goa

JULY 2024

DECLARATION

I, **Nadine Ana de Souza**, hereby declare that this thesis represents work which has been carried out by me and that it has not been submitted, either in part or full, to any other University or Institution for the award of any research degree.

Place: Taleigao Plateau **Nadine Ana de Souza**

Date:

CERTIFICATE

I hereby certify that the work was carried out under my supervision and may be placed for evaluation.

Dr. C. Mohandass

Research Guide
Chief Scientist & Scientist-in-Charge (Retd.)
CSIR- National Institute of Oceanography, Regional Centre
Mumbai – 400 053

ACKNOWLEDGEMENT

At the culmination of this thesis, I would like express my gratitude to all the individuals who have been instrumental in helping me achieve this milestone.

To begin with, I thank Almighty God, for all the opportunities and blessings he has bestowed upon my family and me.

My Research Guide, Dr. C. Mohandass, Chief Scientist (Retd.), for his unwavering and unconditional support. His expertise, understanding, patience, and encouragement was instrumental in the success of my research work and writing of this thesis.

I am indebted to Dr. N. Ramaiah, former Chief Scientist and former Head of Biological Oceanography Division, NIO, Goa, who introduced me to the world of academic research. He inculcated in me scientific temper and ethics and helped me realize the power of critical reasoning.

I thank Dr. S. K. Singh, Director, and Dr. S.W.A. Naqvi, former Director, at CSIR-National Institute of Oceanography, for all the facilities and allowing me to be a part of this esteemed institute.

My sincere thanks to the members of my DRC committee, Prof. Sandeep Garg and Prof. Sarita Nazareth, former Heads, Department of Microbiology, Goa University. Their invaluable feedback and constructive criticism have tremendously shaped this work and widened my research perspectives. I am truly grateful to them for their time and for all the support extended.

I gratefully acknowledge the funding received from the Council for Scientific and Industrial Research, New Delhi through the Project PSC0206 without which this research would not have been possible.

A special thank you to Dr. Samir Damare, Principal Scientist, CSIR-NIO for his guidance and helpful insights. His expertise and technical knowledge immensely contributed to the proteomic analysis in this study.

I extend my sincere gratitude to Dr. Rakhee Khandeparkar, Principal Scientist, CSIR-NIO for her constant support and generosity. I am also thankful to Mr. Ram Murti Meena, for helping with the sequencing of samples throughout my research.

I appreciate my colleagues and friends for their scientific contributions and all their help especially Dr. Elroy, Dr. Mandar, Dr. Pankaj, Dr. Ujwala, Dr. Jasmine, Dr. Akhila, Shruti, Naseera, Dr. Larissa, Dr. Bliss, Dr. Cindrella, Dr. Devika, Dr. Geeta and Dr. Sagar. Thank you to Marsha and Amruta who started the bioremediation journey with me. Many others have contributed to my successful completion whose names I could not include here for want of space. I thank them all.

My most profound gratitude to my mother and my sisters. You have been my biggest support and your unfailing love, concern and faith has seen me through it all. Thank you for being my constant source of strength and anchor throughout this journey. Thank you, Aaron, Ava and Judah, for cheering me on.

Finally, I thank with all my love, Joel and Dylan for their patience and encouragement and for being a precious part of me.

Nadine Ana de Souza

Contents

1 Introduction and Review of Literature 1

1.1 Introduction 1

1.2 The dyeing industry 2

1.3 The chemistry of dyes 3

1.4 Toxicity of textile dyes. 7

1.4.1 Impact of textile effluent on environment 7

1.4.2 Impact of textile effluent on human health 11

1.5 Treatment of textile dye containing wastewater 12

1.5.1 Physico-chemical methods 12

1.5.2 Biological methods 14

1.6 Factors affecting bacterial dye decolorization 20

1.7 Biochemical Mechanisms of bacterial dye decolorization 21

1.8 Molecular basis of dye decolorization 27

1.9 Significance of this study 28

2 Screening, Isolation and Identification of Dye Decolorizing Bacteria 31

2.1 Introduction 31

2.2 Materials and Methods 32

2.2.1 Sampling 32

2.2.2 Measurement of physico-chemical parameters 35

2.2.3 Microbiological analysis 35

2.2.4 Screening and isolation of dye decolorizing bacterial strains 36

2.2.5 Identification of dye decolorizing bacterial strains 37

2.2.6 Phylogenetic analysis 40

2.2.6 Primary dye decolorization assays 40

2.3 Results 41

2.3.1 Measurement of physico-chemical parameters 41

2.3.2 Microbiological analysis 41

2.3.3 Identification of dye decolorizing bacterial strains 43

2.3.4 Primary decolorization assay 44

2.4 Discussion 57

3 Optimization of Azo Dye Removal by Dye Decolorizing Bacteria 61

3.1 Introduction 61

3.2 Materials and Methods 62

3.2.1 Growth and decolorization assay of the dye decolorizing bacterial isolate 62

3.2.2 Optimization of various growth conditions for maximum dye decolorization 62

3.2.3 Decolorization of reactive azo dyes in presence of heavy metals. 66

3.3 Results 66

3.3.1 Growth and decolorization assay of the dye decolorizing bacterial isolate 66

3.3.2 Optimization of various growth conditions for maximum dye decolorization 68

3.3.3 Decolorization of reactive azo dyes in presence of heavy metals. 74

3.4 Discussion 80

4 Bioremediation and Detoxification of Reactive Azo Dyes 85

4.1 Introduction 85

4.2 Materials and Methods 86
4.2.1 Decolorization of different dye classes 86
4.2.2 Enzyme assays for analysis of dye decolorizing activity 88
4.2.3 Biodegradation analysis 90
4.2.4 Toxicity analysis 90
4.2.5 Decolorization of textile effluent 91
4.2.6 Statistical analysis 92
4.3 Results 93
4.3.1 Decolorization of different dye classes 93
4.3.2 Enzyme assays for analysis of dye decolorizing activity 93
4.3.3 Biodegradation analysis 93
4.3.4 Toxicity analysis 103
4.3.5 Decolorization of textile effluent 105
4.4 Discussion 112

5 Proteomic Characterization of Dye Decolorizing Bacteria 117

5.1 Introduction 117
5.2 Materials and Methods 119
5.2.1 Microorganisms and growth conditions 119
5.2.2 Cellular protein extraction 119
5.2.3 Protein estimation and methanol precipitation 120
5.2.4 Gel electrophoresis 120
5.2.5 In-solution digestion 121
5.2.6 Mass Spectrometry and Protein Identification 121
5.3 Results 123
5.3.1 Gel electrophoresis 123
5.3.2 Protein identification 123

5.3.3 Functional characterization of expressed proteins 124

5.3.4 Comparison of differentially expressed proteins 124

5.3.5 Dye decolorization induced changes in abundance of expressed proteins 125

5.4 Discussion 135

6 Molecular Characterization of Genes involved in Dye Decolorization 139

6.1 Introduction 139

6.2 Materials and Methods 140

6.2.1 Bacterial strain and culture conditions 140

6.2.2 PCR amplification and sequencing of azoreductase gene 140

6.2.3 Quantitative analyses of the azoreductase gene expression using Real Time-quantitative PCR (RT-qPCR) 141

6.3 Results 143

6.3.1 PCR amplification and sequencing of azoreductase gene 143

6.3.2 Quantitative analyses of the azoreductase gene expression 143

6.4 Discussion 159

7 Summary and Conclusions 163

Appendix 169

References 173

Publications and Conferences

List of Tables

1.1 Major synthetic dye classes used in the textile industry and the mode of their application to specific fiber types 5

1.2 Bacterial strains decolorizing various azo dyes 16

2.1 Physico-chemical characteristics of water samples 42

2.2 Physico-chemical characteristics of sediment samples 43

2.3 Morphological and physiological characteristics of dye decolorizing bacterial isolates 47

2.4 Biochemical tests and production of physiological enzymes by dye decolorizing bacterial isolates 49

2.5 16S rDNA sequence-based identification and NCBI GenBank accession numbers of dye decolorizing bacteria 50

2.6 Decolorization assay of reactive azo dyes at 100 mgL^{-1} 52

2.7 Decolorization assay of reactive azo dyes at 250 mgL^{-1} 53

2.8 Decolorization assay of reactive azo dyes at 500 mgL^{-1} 54

3.1 Optimum parameters for maximum decolorization of reactive azo dyes, individually and in combination 79

4.1 Details of different classes of dyes used to check decolorization 87

4.2 Activity of various enzymes during dye decolorization 94

4.3 Effect of reactive dyes and dye degraded metabolites on the hatching (%) of *Artemia salina* (brine shrimp) cysts 103

4.4 Effect of reactive dyes and dye degraded metabolites on the survival of *Artemia salina* (brine shrimp) nauplii (%) 104

4.5 Phytotoxicity studies of reactive dyes and dye degraded metabolites using *Vigna radiata* 105

4.6 Physico-chemical characteristics of raw textile effluent from Kanpur 111

5.1 Proteins up-regulated during decolorization of Reactive Black 5 azo dye . 132

5.2 Proteins up-regulated during decolorization of Reactive Green 19 azo dye 133

5.3 Proteins up-regulated during decolorization of Reactive Red120 azo dye . 134

6.1 List of primer sets used for PCR amplification of azoreductase gene 149

List of Figures

1.1 The diverse chemical structures of some synthetic dyes 4

1.2 Schematic diagram of water consumed and wastewater composition of wet process for cotton textile industry 9

1.3 Methods for treatment and removal of dyes from textile wastewater 13

1.4 Schematic representation of different mechanisms of azo dye reduction 22

1.5 Proposed mechanisms for the reduction of azo dyes by whole bacterial cell 26

2.1 Sampling locations located in (CM) Choraõ Mangroves, (DM) Divar Mangrove site, (RS) Ribandar saltpans. 33

2.2 Dye decolorizing bacteria (DDB) belonging to different representative bacterial genera isolated from mangrove and saltpan, water and sediment samples 45

2.3 Phylogenetic tree showing relationship between dye decolorizing bacteria 51

2.4 Primary decolorization assay of (A) RB5 (B) Reactive Green 19 (C) Reactive Red 120 (D) Reactive Blue 163 using *Shewanella seohaensis* NIO_14d 55

3.1 Growth curve and decolorization percent of *Shewanella seohaensis* NIO_14d . . . 67

3.2 Effect of aeration on the extent of decolorization by *Shewanella seohaensis* NIO_14d 69

3.3 Effect of pH on the extent of decolorization by *Shewanella seohaensis* NIO_14d 69

3.4 Effect of temperature on the extent of decolorization by *Shewanella seohaensis* NIO_14d 71

3.5 Effect of dye concentration on the extent of decolorization by *Shewanella seohaensis* NIO_14d 71

3.6 Effect of different medium strengths, carbon sources and nitrogen sources on the extent of decolorization by *Shewanella seohaensis* NIO_14d 75

3.7 Effect of different electron donors, NaCl concentrations and heavy metals on the extent of decolorization by *Shewanella seohaensis* NIO_14d 77

4.1 Decolorization of various azo, triarylmethane and anthraquinone dyes by *Shewanella seohaensis* NIO_14d 95

4.2 FTIR analysis of RB5, RG19 and RR120 decolorized dye samples versus untreated reactive azo dye controls 97

4.3 Spectroscopic analysis **(**UV-Visible spectrum) of treated and untreated samples of simulated textile dye wastewater and Textile effluent from Kanpur, India . . . 107

4.4 Collection of effluent samples from outside a textile mill in Kanpur, India 109

4.5 Decolorization of Effluent samples by *Shewanella seohaensis* NIO_14d 109

5.1 SDS-PAGE protein profiles for *Shewanella seohaensis* NIO_14d grown in the presence and absence of reactive azo dyes 127

5.2 Functional classification of identified proteins 129

5.3 Venn diagrams comparing up-regulated proteins entities in dye challenged *Shewanella seohaensis* NIO_14d versus control 131

6.1 Agarose gel electrophoresis (1%) of PCR products of total genomic DNA from *Shewanella seohaensis* NIO_14d with primer for gene *so3585* 145

6.2 Phylogenetic relationship of NAD(P)H dependent oxidoreductase from *Shewanella seohaensis* NIO_14d 147

6.3 Dye decolorization (%) and azoreductase activity of *Shewanella seohaensis* NIO_14d during decolorization of RB5 150

6.4 Dye decolorization (%) and azoreductase activity of *Shewanella seohaensis* NIO_14d during decolorization of RG19 151

6.5 Dye decolorization (%) and azoreductase activity of *Shewanella seohaensis* NIO_14d during decolorization of RR120 152

6.6 Relative expression (RQ) of the azoreductase gene (*SO3585*) gene of *Shewanella seohaensis* NIO_14d in the presence of Reactive Black 5 153

6.7 Relative expression (RQ) of the azoreductase gene (*SO3585*) gene of *Shewanella seohaensis* NIO_14d in the presence of Reactive Green 19 155

6.8 Relative expression (RQ) of the azoreductase gene (*SO3585*) gene of *Shewanella seohaensis* NIO_14d in the presence of Reactive Red 120 157

List of Abbreviations

°C	Degree Celsius
µL	Microliter
µM	Micromolar
CFU	Colony forming unit
BIS	Bureau of Indian Standards
BOD	Biochemical oxygen demand
bp	Basepair
BSA	Bovine Serum Albumin
CM	Chorao mangrove
COD	Chemical oxygen demand
COG	Clusters of Orthologous groups
DM	Divar mangrove
DNA	Deoxyribonucleic acid
DO	Dissolved oxygen
kDa	Kilodalton
KEGG	Kyoto Encyclopedia of Genes and Genomes
LC-MS-QToF	Liquid chromatography mass spectrometry quadropole
Mg / Kg	Milligram / Kilogram
Mg L^{-1}	Milligram / Litre
ml	Milliliter
mM	Millimolar
MPP	Mass Profiler Professional
MS	Mass Spectrometry
MSM	Mineral Salt Medium
NA	Nutrient agar
NADH	Nicotinamide adenine dinucleotide
NB	Nutrient broth
nm	Nanometer
OD	Optical density
PBS	Phosphate buffered baline
PCR	Polymerase chain reaction
pH	power of Hydrogen
PSU	Practical Salinity Scale
RB5	Reactive Black 5
RBL163	Reactive Blue 163

RG19	Reactive Green 19
ROS	Reactive oxygen species
rpm	Rounds per minute
rRNA	Ribosomal ribonucleic acid
RR120	Reactive Red 120
RS	Ribandar saltpan
RT	Room temperature
RT-qPCR	Real Time - quantitative Polymerase chain reaction
SDS-PAGE	Sodium dodecyl sulfate - Polyacrylamide gel electrophoresis
SWNA	Seawater nutrient agar
TDS	Total dissolved solids
TE	Tris-EDTA
TN	Total nitrogen
TS/TSS	Total solids/Total suspended solids
TVC	Total viable bacterial counts
UV	Ultraviolet

Chapter 1

Introduction and Review of Literature

Chapter 1

Introduction and Review of Literature

1.1 Introduction

"The Earth is what we all have in common" – **Wendell Berry**

From the mightiest beings to the invisible microbes, the Earth holds them all. Through the ages, Life has evolved, grown, and sustained on this planet. The habitats on Earth span a myriad landscapes, right from the depths of the ocean to the highest peaks, each providing a niche to its own unique life forms.

Microorganisms, Earth's tiniest creatures, are invisible yet impactful and are closely intertwined with the functioning of this planet. Their diverse populations, both known and unknown, encompass bacteria, fungi, protozoa, viruses and other micro fauna. These ubiquitous life forms have conquered every imaginable space terrestrial, aquatic and atmospheric. Their remarkable abilities of decomposition, biotransformation, energy generation and nutrient assimilation support their growth and survival in diverse ecological niches. They play a significant role in maintaining the homeostasis of various ecosystems. They contribute beneficial functions in ecological recycling owing to their capability to transform complex molecules into simpler ones. Through their growth, reproduction and respiration they balance and maintain a healthy ecological functioning. Global biogeochemical cycling of elements is inherently managed by microbial activity. Any intrusion of these pathways and cycles by either natural or anthropogenic causes can significantly affect the ecosphere and its fine balance.

Growth and development of civilization has been exponential in the last two centuries. Rapidly increasing populations and indiscriminate industrialization have subjected the Earth's resources to varied stresses. The terrestrial, atmospheric and aquatic ecosystem has been at the receiving end of unregulated anthropogenic activities. Industries consume copious amounts of water and generate hazardous and toxic-laden effluents. In spite of prescribed regulations for the treatment and release of this wastewater, it is seen that contaminants find their way into surface and ground water bodies and hamper life processes by affecting the native organisms, vegetation, animals and humans.

Global economic growth and development has accompanied rampant industrialization. This has led to an incredible increase in the levels of pollution. Sensitive habitats are rapidly declining as a consequence of exposure to pollutants in excess of what they are equipped to handle. Over a period of time, this exposure results in several long as well as short term consequences including negative health effects and diseases, loss in biodiversity and economic losses.

1.2 The dyeing industry

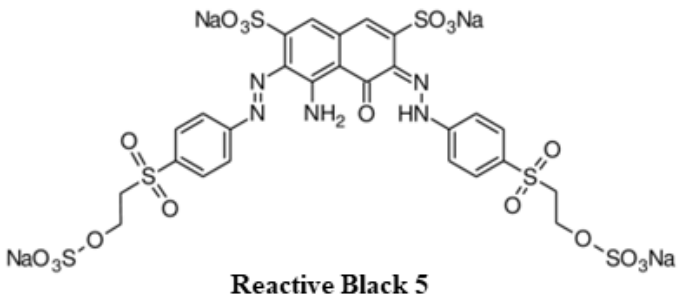
Dyes have a colorful past. The use of dyes began thousands of years ago. Mankind has been attempting to add color to the world around him since primitive times. The art of using color has been around since the Neolithic era. Archaeologists have uncovered evidence of Ancient Egyptians and European cave paintings with indications of the use of black, white, reddish and yellow pigments made from ochre (Brunello, 1973). The earliest existing written records of applying dyestuff to fabrics date back to 2600 BC (Křížová, 2015). Through the ages, dyes have undergone an evolution to develop into the vibrant colors we see today. The early years of dyeing fabrics were characterized by a rather limited range of colors. As civilizations advanced, they developed and improved upon the sources of dyes and pigments and the scope of their applications. Studies on the earliest-surviving colored fabrics and ancient manuscripts indicate the use of three sources of natural dyes: vegetable or plant, mineral and insect or animal dyes (Brunello, 1973). The 1850s heralded significant changes in the dyeing industry. In 1856, William Henry Perkin, an English chemist, while attempting to synthesize quinine, serendipitously created a purple-colored compound called mauveine. This marked the discovery of the first synthetic dye and creation of a new generation of dyes (Holme, 2006). The Industrial revolution led to a boom in the textile industry which then prompted the increasing demand for newer and more easily utilizable textile dyes. This brought to light the limitations of natural dyes and pigments which were in use thus far. Synthetic dyes were found to be largely advantageous in that they were easy to apply, readily available and economically cost effective. From then on, synthetic dyes were prevalent across a wide variety of industries including textile, pharmaceutical, leather, paper, cosmetic and food industries. This made the synthetic dye industry gigantic with more than 7×10^5 metric tons of global production of synthetic dyes per year (McMullan

et al., 2001). Of this, textile industries are reported to use a major quantity with consumption of over 10,000 tons of such dyes (Chandanshive *et al*., 2020

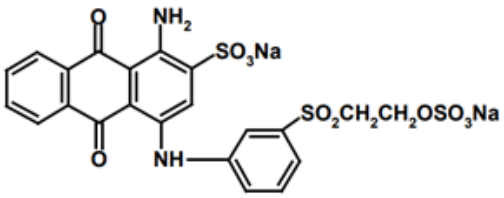
1.3 The chemistry of dyes

Synthetic dyes are organic molecules which possess color and specific structural characteristics which dictate their behavior (Millbern *et al*., 2022). The chemical structure of dye molecules is made up of a chromophore which is an aromatic group that absorbs light in the visible spectrum (400 – 700 nm) and which functions in fixing the dye within or into the fibers. It bears a conjugated system which is a structure with alternating double and single bonds (Ali, 2010). Additionally, synthetic dyes exhibit electron resonance which acts as a stabilizing influence (Abrahart, 1977). Most dyes also include an electron withdrawing or donating component known as auxochrome which may include carboxylic acid, sulfonic acid, amino, and hydroxyl groups. Although these groups do not directly contribute to the color, they can modify or intensify the hue of the dye and are commonly utilized to enhance dye solubility. There exists considerable structural diversity amongst different classes of synthetic dyes (**Figure 1.1**).

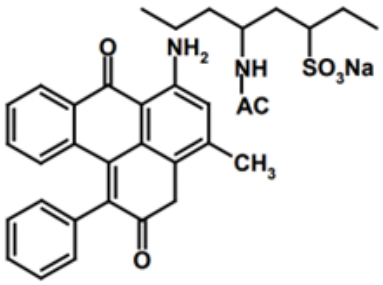
Dyes are classified based on their chemical composition, by the method of their application or by the types of fibers to which they can be applied (Kirk-Othmer, 1993). For instance, there are specific dyes for materials like nylon, cotton, or polyester, each offering unique coloration properties. Alternatively, dyes can be classified based on their mode of application which includes categories like direct dyes, reactive dyes, acid dyes, vat dyes, metal-complex dyes, disperse dyes, and azoic dyes, among others (Vandevivere *et al*., 1998). **Table 1.1** illustrates the major classes of synthetic dyes used in the textile industry and their application to specific fiber types. However, it is important to note that these classification systems are more relevant in the context of practical dye application technology, rather than in discussions primarily focused on the process of dye synthesis and the underlying chemistry involved. According to a chemical classification system, synthetic dyes are grouped based on the nature of their chromophores. As such, the various classes of industrially significant dyes include azo, anthraquinone, diazonium, sulfur, indigoid, triphenylmethyl (trityl), triarylmethane, nitro and phthalocyanine derivatives (Forgacs *et al*., 2004).



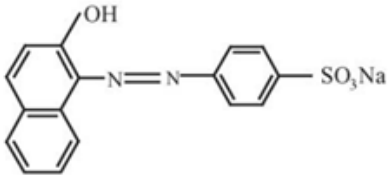
Reactive Black 5



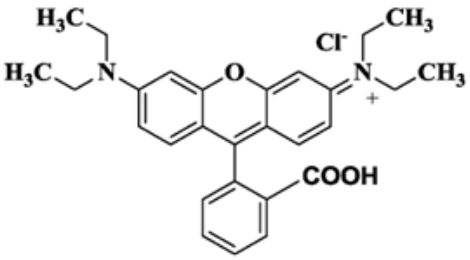
Remazol Brilliant Blue R



Poly R 478



Acid Orange 7



Rhodamine B

Figure 1.1: The diverse chemical structures of some synthetic dyes

Table 1.1: Major synthetic dye classes used in the textile industry and the mode of their application to specific fiber types (Modified from Souza *et al*., 2022)

Classes	Fiber type	Method of application
Acid dye	nylon, wool, silk	Neutral to acid dye baths
Basic dye	Modified nylon, polyester	Acid dye baths
Direct dye	cotton, rayon, leather, nylon	Neutral or slightly alkaline baths containing additional electrolytes
Dispersed dye	polyester, polyamide, acetate, plastic, acrylic	High or low-temperature pressure transport methods.
Reactive dye	cotton, nylon, silk, wool	Under the influence of heat and pH of the alkaline medium, dye reacts with the fiber functional group, and covalently bonds.
Sulfur dye	cotton, rayon	Aromatic substrate covered with sodium sulfide and reoxidized to sulfur-containing products, insoluble in fiber.
Vat dye	cotton, rayon	Water-insoluble dyes are solubilized by reduction with sodium hydrosulfite and exhausted into the fiber and reoxidized

Azo dyes constitute one of the largest classes of synthetic dyes and as described by Shah, (2014) account for more than 60% of the dyes produced annually. They currently dominate the dye chemistry industry, both in terms of production volume and usage. These dyes have far reaching applications and are frequently used across numerous sectors, including food, pharmaceuticals, paper manufacturing, cosmetics, textiles, and leather industries (Chang *et al*., 2001). Azo dyes are aromatic hydrocarbons and are known to be derivatives of benzene, toluene, naphthalene, phenol and aniline (Puvaneswari *et al*., 2006). These compounds bear the functional group R-N=N-R', in which R and R' can be either aryl or alkyl and are grouped as mono-, di-, tri- or poly- azo based on the number of (-N=N-) bonds present. Azo dyes display high stability and resistance to microbial attack. A complex chemical structure and electron withdrawing capacity makes these dyes xenobiotic and recalcitrant to biodegradation (Dave *et al*., 2015).

The characteristic structural features of a typical reactive azo dye molecule are:

1. the reactive system, which enables formation of covalent bonds between the dye and substrate,
2. the chromophoric group, contributing to the color
3. a bridging group that links the reactive system to the chromophore, and
4. solubilizing groups

The synthesis of azo compounds is anthropogenic and is performed in a simple two-step reaction process. The first step involves the diazotization of a primary aromatic amine. This is followed by a coupling reaction with electron rich nucleophilic groups such as amino and hydroxy (Benkhaya *et al*., 2020). The diazotization reaction is typically carried out in the presence of *in situ* generated nitrous acid (HNO_2). This nitrous acid is normally produced with hydrochloric acid and sodium nitrite. A primary aromatic amine, referred to as the "diazo component," is critical in the formation of color in azo dyes, as it offers a conjugated electron system next to the azo bond. This primary aromatic amine can be categorized into the following types: 1) aniline and its derivatives, 2) naphthylamines and naphthylaminesulfonic acids, and 3) diamines (Hunger, 2003). The end product of step one is a diazonium salt which is subject to a further reaction with “coupling components” resulting in a chemically stable azo dye.

1.4 Toxicity of textile dyes

Of the many applications, dyes find primary importance in textile manufacturing. China is amongst the leading global exporters of textiles followed by the European Union, India and USA (Ghaly *et al*., 2014). Consequently, these countries are also the major consumers of synthetic dyes and dyestuff. These synthetic dyes are largely preferred as they are cheaper to produce, brighter and possess high color fastness. As their production and use became more widespread, it brought with it an increased release of wastewater containing a toxic mixture of dyes and harmful chemicals. It has been estimated that every year in the textile industry, up to 200,000 tons of these dyes are lost to effluents during the dyeing and finishing operations. Besides the wastewater generated during the dyeing process, this has also been attributed to the inefficiency of the dyeing process (Ogugbue and Sawidis, 2011). In existing dyeing processes, the precise amount of unbound dyes ending up in wastewater, is unclear. However, it is roughly estimated that annually, over 15% or 280 kilotons of the total dye is lost worldwide (Kalyani *et al*., 2009; Prasad and Aikat, 2014). This loss could be attributed to the presence of unreactive, hydrolyzed dyes in the dye bath. Hydrolysis of a dye happens when the dye interacts with water molecules instead of bonding with the hydroxyl group of the fibers (Patil *et al*., 2010). The amount of dye lost in industrial applications depends on the type of dye used and varies from 2% loss for basic dyes to about 50% loss for certain reactive sulfonated dyes (McMullan *et al*., 2001). The direct discharge of wastewater containing such unfixed dyes into the environment presents considerable pollution and significant

1.4.1 Impact of textile effluent on environment

The textile industry poses a significant environmental concern both due to the volumes of water required for processing as well as the hazardous composition of the wastewater released (**Figure 1.2**). The most important constituent of textile wastewater is the presence of color due to dyes. Besides the inherent color, dye wastewater also exhibits characteristics of high alkalinity, excess biological oxidation demand, chemical oxidation demand and total dissolved solids (Kaushik and Malik 2009). The improper disposal of textile dye effluent, especially those containing azo dyes and their by-products, into aquatic ecosystems presents multiple environmental challenges. Besides being aesthetically unpleasant, such discharges significantly disturb aquatic ecosystems.

Pollution of water bodies is caused by intensely colored wastewater released from textile industries. The dark color impedes the penetration of sunlight thus reducing photosynthetic activity (Mohan *et al*., 2017). This results in diminished concentrations of dissolved oxygen, ultimately leading to a deterioration in overall water quality. Such alterations in the aquatic environment have been found to have acute toxic effects on both aquatic plants and animals, posing substantial threats to global biodiversity (Vandevivere *et al*., 1998). The presence of azo dyes has adverse effects on the total organic carbon (TOC), biological oxygen demand (BOD), and chemical oxygen demand (COD), all of which are crucial indicators of water health and cleanliness (Saratale *et al*., 2009c).

However, beyond color, the presence of these dyes in aqueous ecosystems presents serious environmental and health concerns as the dyes themselves as well as their transformation products are toxic, mutagenic and carcinogenic (Gürses *et al*., 2016). Liquid effluent from the textile manufacturing process contains high levels of toxic heavy metal residues like cadmium, copper, chromium and nickel. Textile effluents are also known to contain large amounts of salts and display high levels of dissolved and suspended solids along with high biological and chemical oxygen demand (Imtiazuddin *et al*., 2012). Wastewater released from textile dyeing and finishing industries contains a minimum of 72 toxic chemical of which at least 30 of these chemicals resist removal by conventional wastewater treatment procedures (Chen and Burns, 2006). The indiscriminate discharge of this untreated toxic soup inevitably leads to the destruction of natural habitats and compromises the quality and safety of aquatic and human life.

Besides the direct impact on aquatic ecosystems, there are numerous reports suggesting that textile dyes and their effluents can detrimentally affect plant life. These substances can hinder the germination rates and biomass growth of various plant species, disrupting crucial ecological functions. For instance, these plants often provide essential habitats for wildlife, protect soil from erosion, and contribute to soil fertility by supplying organic matter (Kapustka and Reporter, 1993; Ghodake *et al*., 2009).

The discoloration of water as a result of dye effluent can have significant negative impacts on fish in aquatic bodies. It can lead to neurological damage, metabolic stress, and even result in the death of fish. Fish are known to be highly sensitive to alterations in their aquatic environment, and any adverse changes can impact their biochemical, physiological, and histological parameters. A study by Kaur *et al*., (2013) documented

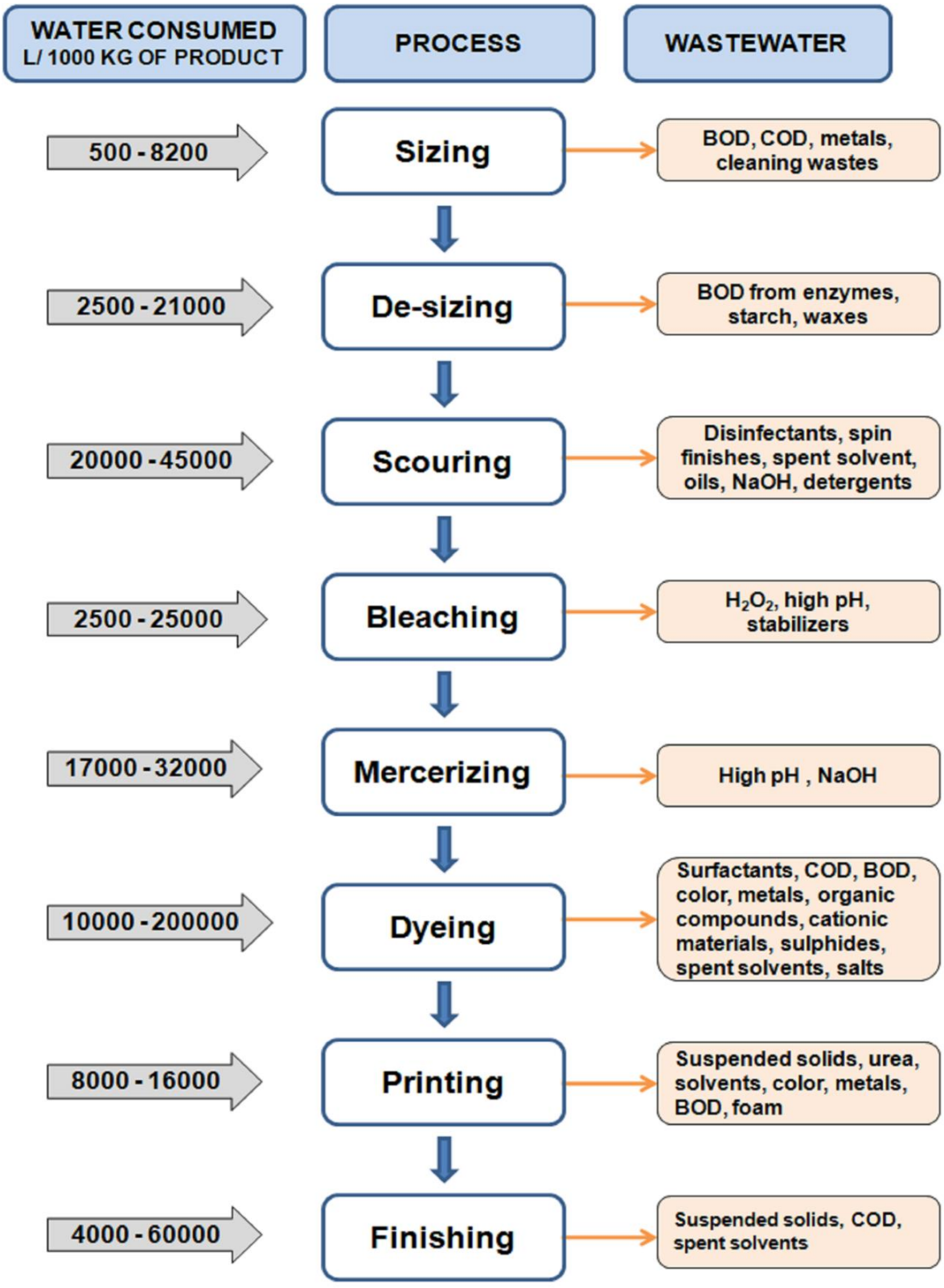


Figure 1.2: Schematic diagram of water consumed and wastewater composition of wet process for cotton textile industry (Ghaly *et al*., 2014; Yaseen and Scholz, 2019)

behavioral changes in the species *Cirrhinus mrigala* when exposed to sublethal concentrations of dyeing industry wastewater. Observed alterations included abnormal behaviors such as gulping air at the water's surface, erratic swimming, and increased gill movement. Similarly, Amwele *et al*., (2015) reported changes in behavior in the fish species *Oreochromis niloticus* after exposure to a specific type of metal complex dark green azo acid dye. Moreover, a study comparing the toxicity of treated and untreated textile industrial wastewater on the freshwater fish *Gambusia affinis* found that exposure to untreated water led to significantly higher mortality rates and showed cytotoxic effects on the fish's blood cells compared to those exposed to treated water (Soni *et al*., 2006). It is therefore clear that the widespread use and disposal of synthetic dyes in general and azo dyes in particular have broad and profound implications for environmental health and sustainability.

1.4.2 Impact of textile effluent on human health

The textile industry, while instrumental in the global economy, has a bearing on human health owing to the discharge of untreated effluents. Humans may be exposed to toxic dyes either directly through drinking water systems or indirectly through contaminated soil. Developing countries commonly use dye containing wastewater for agricultural soil irrigation (Garg and Kaushik, 2008; Imran *et al*., 2015). The recalcitrance and structural properties of dyes results in the accumulation and persistence of these chemicals in soils. Zhou, (2001) reported up to 456.2 mg of dye per kg of surface soil in the vicinity of textile processing units. The polluting nature of azo dyes as a result of the toxicity of the free dyes themselves and their transformation into toxic, mutagenic and carcinogenic amines, primarily as a result of anaerobic microbial reductive cleavage of the azo bond is well studied (Chung and Cerniglia, 1992; Asad *et al*., 2007). Exposure to azo dyes found in industrial effluents can occur in humans and other mammals either through ingestion or direct contact with the skin (Manickam and Vijay, 2021). Once ingested, the azo dyes are transformed into harmful amines by the intestinal microflora present in the human gut which can then adversely affect numerous tissues within the human body (Feng *et al*., 2012).

The acute exposure to azo dyes leads to irritation of eyes and skin, dermatitis and other allergic reactions (Mehra *et al*., 2021). A number of studies have reported the genotoxic

effects of azo dyes and heavy metals present in textile effluent (Sweeney *et al*., 1994; Mansour *et al*., 2007; Balakrishnan *et al*., 2016). Serra *et al*., (2008) implicated textile dyes in the occurrence of bladder cancer among textile workers. It is therefore imperative to tackle the problem of textile dye pollution and develop increasingly sustainable dyes and methods in the industry. The health of communities, and indeed the global population, is inextricably linked to the health of the environment, and we must take steps towards safeguarding both.

1.5 Treatment of textile dye containing wastewater

1.5.1 Physico-chemical methods

The removal of toxic dyes and chemicals from textile wastewater is critical before discharging it into the environment. Gahr *et al*., (1994) has described a typical dye house effluent to contain 0.6 – 0.8 g L^{-1} of dye. There exist numerous strategies for the treatment of dye containing wastewater (**Figure 1.3**). These include several conventional physical and chemical methods such as flocculation, coagulation/adsorption, membrane filtration, ozonation, irradiation and chemical degradation (Golab *et al*., 2005; Lopez-Grimau and Gutierrez, 2006; Eskandari *et al*., 2019). Commonly utilized techniques for treating wastewater, such as coagulation and flocculation, generate significant amounts of sludge, which necessitates safe disposal. Similarly, adsorption and membrane filtration methods can result in secondary waste streams that require additional treatment. While activated carbon (AC) stands as a highly effective adsorbent for various dye types, its high cost often discourages its use (Robinson *et al*., 2001). To make the process more economically viable, researchers have turned to cost-effective adsorbent materials such as peat, bentonite clay, fly ash, polymeric resins, ion exchangers, and numerous biological materials including corn cobs, maize stalks, and wheat straw for eliminating color from dye wastewater (Ramakrishna and Viraraghavan, 1997). However, the practical application of these adsorbents faces challenges due to issues with their regeneration or disposal, considerable sludge production, limited efficacy across a broad range of dyes, and still significant costs (Karcher *et al*., 2001; Anjaneyulu *et al*., 2005).

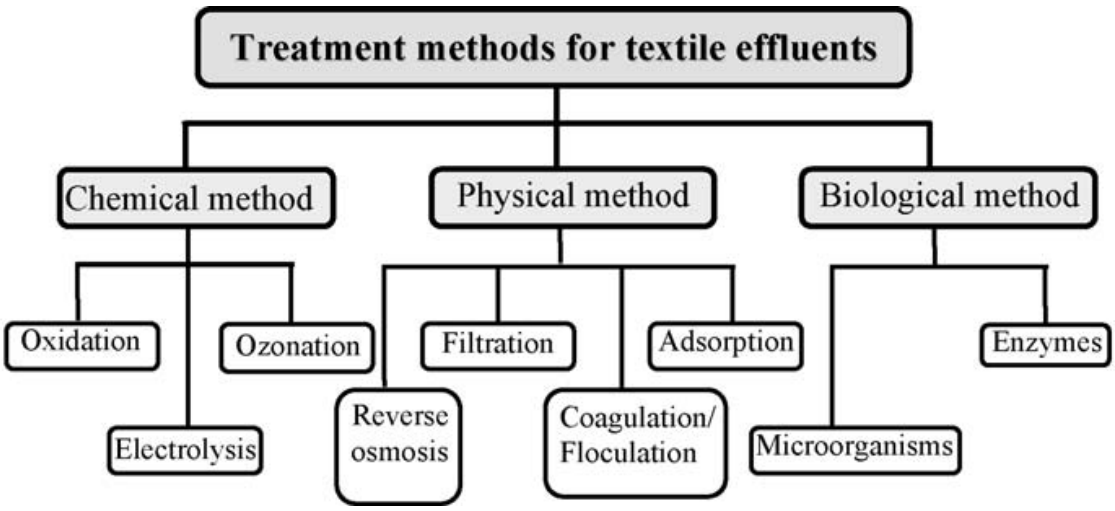


Figure 1.3: Methods for treatment and removal of dyes from textile wastewater (Adapted from Saratale *et al*., 2011)

Filtration techniques like ultrafiltration, nanofiltration, and reverse osmosis have been employed for water reuse and chemical recovery. In the textile sector, membrane usage offers promising opportunities for separating hydrolyzed dyestuffs and dyeing auxiliaries. This not only reduces the color, Biological Oxygen Demand (BOD), and Chemical Oxygen Demand (COD) of wastewater but is also beneficial for mercerizing and bleaching processes. However, the choice of filter type and porosity depends on the chemical composition of the wastewater and the specific temperature requirements of the process (dos Santos *et al*., 2007). Despite their utility, membranes come with significant disadvantages including high initial costs, the potential for membrane fouling, and the creation of secondary waste streams requiring further treatment (Robinson *et al*., 2001; dos Santos *et al*., 2007). These challenges have steered attention towards Advanced Oxidation Processes (AOP) and biological methods as viable alternatives for treating wastewater that contains dyes. AOP are processes that leverage powerful oxidizing agents (like hydrogen peroxide or Fenton's reagent) or heterogeneous photocatalysts such as titanium dioxide, zinc peroxide, manganese, and iron. These can be used with or without an irradiation source. AOP primarily function by generating hydroxyl radicals

that break down stubborn and harmful pollutants (Vandevivere *et al*., 1998; Alaton *et al*., 2002; Al-Kdasi *et al*., 2004). However, these methods are cost and energy intensive, are unable to completely remove azo dyes and their metabolites and present inherent difficulties of low operational efficiency. The disadvantages and limited applications of physical and chemical methods for the treatment of dye containing textile effluents makes bioremediation an attractive, environmentally friendly and economically viable solution.

1.5.2 Biological methods

A primary focus area in environmental science research harnesses microbial techniques for pollution management. Bioremediation capitalizes on the ability of microbes to adapt to toxic wastes, subsequently leading to the emergence of resistant strains that convert harmful chemicals into less toxic forms. Various biotechnological strategies, often employing microorganisms and occasionally combined with physicochemical processes, have drawn attention for their potential in effectively addressing pollution caused by azo dyes. Azo dyes are xenobiotic and resistant to natural biodegradation. Therefore, the employment of microbial or enzymatic methods for the thorough decolorization and degradation of such dyes from textile effluents holds several benefits. The substantial advantages of biological methods compared to physicochemical methods include their environmental-friendliness, cost-effectiveness, lower sludge production, the generation of non-toxic end products or their complete mineralization, and reduced water consumption (Banat *et al*., 1996; Rai *et al*., 2005). The success of microbial decolorization largely relies on the adaptability and activity of the chosen microorganisms. The identification and subsequent degradation by potent species offer promising perspectives in effluent treatment (Chen *et al*., 2008).

Several bacteria, fungi and algae have been reported to be capable of decolorizing and even mineralizing textile dyes (Pandey *et al*., 2007; Ali, 2010; Khan *et al*., 2013). Microorganism generally employ various biotransformation enzyme systems when exposed to recalcitrant compounds in their environment (Saratale *et al*., 2007).

Decolorization of azo dyes by bacteria

One of the earliest attempts to isolate bacteria for the degradation of azo dyes was carried out by Wuhrmann *et al*., (1980), wherein they identified *Bacillus cereus* capable of azo dye decolorization. Bacteria are extremely versatile in their abilities to bioremediate a number of environmental pollutants and toxic chemicals. Extensive research has been carried out to study diverse bacterial species and their ability to decolorize azo dyes under anaerobic, facultative anaerobic and aerobic conditions (Pandey *et al*., 2007; Saratale *et al*., 2011). The key step in bacterial degradation of azo dyes involves an enzymatic reduction of the azo bond leading to the formation of toxic aromatic amines under anaerobic conditions. These intermediates are further mineralized aerobically or anaerobically (Pandey *et al*., 2007). Bacterial bioremediation can be mediated by both pure cultures as well as microbial consortiums (Dave *et al*., 2015). The efficacy of the process depends on the type of azo dye and the operational conditions such as pH, temperature, dye concentration and presence of electron donors (Pearce *et al*., 2003). The synergistic action of mixed bacterial consortia may provide an improved system to tackle azo dye contaminated effluents (Saratale *et al*., 2011). Individual strains of the consortium may degrade different intermediates in the decolorization pathway leading to complete mineralization of azo dyes and a reduced probability of the occurrence of toxic amines (Forgacs *et al*., 2004). Despite these promising findings, some challenges remain. For instance, some dye degradation products can be toxic and may require further treatment. Additionally, not all azo dyes are susceptible to bacterial degradation, indicating the need for continued exploration of bacterial strains and their metabolic capabilities (Kudlich et al., 1997). **Table 1.2** summarizes some findings of various researchers investigating bacterial strains in isolation or consortium for the decolorization of azo dyes.

Table 1.2: Bacterial strains decolorizing various azo dyes (Modified from Khalid *et al*., 2010; Saratale *et al*., 2011; Dave *et al*., 2015)

Bacterial strain	Dye (Concentration)	% decolorization	Reference
Aeromonas hydrophila	Reactive Red 198,	60.2	Hsueh *et al*., (2009)
	Reactive Black 5,	80.9	
	Reactive Red 141,	66.5	
	Reactive Blue 171,	36.0	
	Reactive Yellow 84 (300 mg L^{-1})	33.7	
Acinetobacter calcoaceticus NCIM 2890	Direct brown MR (50 mg L^{-1})	91.3	Ghodake *et al*., (2009a)
Alcaligenes sp. AA09	Reactive Red BL 24 (50 - 200 mg L^{-1})	>90	Pandey and Dubey (2012)
Alishewanella sp. CBL-2	Sumifex Tourqi blue	83	Ajaz *et al*., (2018)
Bacillus sp. VUS	Navy Blue 2GL (50 mg L^{-1})	94	Dawkar *et al*., (2008)
Bacillus cereus ROC	Reactive Orange 16 Reactive Black 5 (250 mg L^{-1})	~80	Fareed *et al*., (2022)
Comamonas sp. UVS	Direct Red 5B (1.1 g L^{-1})	100	Jadhav *et al*., (2008a)
Citrobacter sp. CK3	Reactive red-180 (100 mg L^{-1})	95	Wang *et al*., (2009)
Enterobacter aerogenes ES014	Congo red (100 mg L^{-1})	81.5	Al-Ansari et al., (2022)
Geobacillus stearothermophilus (UCP 986)	Orange II (0.050 mM)	96-98	Evangelista-Barreto *et al.*, (2009)
Klebsiella pneumoniae R5-13	Methy1 Red (100 mg L^{-1})	98	Wong and Yuen (1996)

Table 1.2: Bacterial strains decolorizing various azo dyes **(continued)**

Bacterial strain	Dye (Concentration)	% decolorization	Reference
Proteus mirabilis	Red RBN (1 g L^{-1})	95	Chen *et al*., (1999)
Pseudomonas spp.	Reactive Blue 13 (200 mg L^{-1})	83.2	Lin et al., (2010)
Pseudomonas aeruginosa	Remazol Orange (200 mg L^{-1})	94	Sarayu and Sandhya, (2010)
Rhizobium radiobacter MTCC 8161	Reactive Red 141 (50 mg L^{-1})	90	Telke *et al*., (2008)
Shewanella decolorationis S12	Acid Red GR (150 mM)	100	Xu *et al*., (2007)
Shewanella sp.	Reactive Black 5 (250 mg L^{-1})	90	Imran *et al*., (2014)
Consortium TJ-1 *Aeromonas caviae, Proteus mirabilis* and *Rhodococcus globerulus*	Acid Orange 7 (200 mg L^{-1})	90	Joshi *et al*., (2008)
Consortium JW-2 *Paenibacillus polymyxa, Micrococcus luteus* and *Micrococcus* sp.	Reactive Violet 5R (100 mg L^{-1})	93	Moosvi *et al*., (2007)
Pseudomonas aeruginosa and *Bacillus circulans,* and (NAD1 & NAD6) isolates	Reactive Black 5 (100 mg L^{-1})	70-90	Dafale *et al*., (2008)

Decolorization of azo dyes by fungi

Fungi are a tenacious group of microorganisms with the ability to acclimatize to various environmental stresses. They are ubiquitous in nature and inhabit a variety of ecological niches including soil, detritus and living organisms. Their survival in adverse conditions is determined by their ability to rapidly adapt their metabolism to the available nutrients. They possess a unique enzyme system that can non-specifically oxidize a diverse set of recalcitrant aromatic compounds, including azo dyes (McMullan *et al*., 2001; Champagne & Ramsay, 2005). Their ability to breakdown and assimilate complex organic molecules makes them noteworthy for bioremediation of various environmental pollutants. One of the most studied fungal species in this regard is the white-rot fungus *Phanerochaete chrysosporium*, widely recognized for its ability to degrade azo dyes through lignin-degrading enzymes, mainly lignin peroxidase (LiP), manganese peroxidase (MnP), and laccase (Spadaro *et al*., 1992; Chagas and Durant, 2001; Enayatzamir *et al*., 2010). Furthermore, the fungus *Trametes versicolor* has also been reported for its capacity to degrade various azo dyes using laccase in combination with certain redox mediators (Selvam *et al*., 2012). Several other fungi have been studied for their azo dye decolorizing potential including *Pleurotus* (Hadibarata *et al*., 2013), *Penicillium* sp. (Gao *et al*., 2009), *Hypsizygus ulmarius* (Ravikumar *et al*., 2013) and Ganoderma sp. (Zhao et al., 2011) The extended growth phase and need for nutrient limiting conditions give fungi a disadvantage for use in removal od dyes from textile wastewater (Saratale *et al*., 2011). Moreover, as these white rot fungi are not indigenous to wastewater, their enzyme production levels are found to be inconsistent thereby reducing the efficiency of treating dye containing effluent (Robinson *et al*., 2001).

Decolorization of azo dyes by yeast

Yeasts are a largely unexplored microbial group in the process of azo dye decolorization. There are limited studies carried out on the ability of yeast to degrade various azo dyes. The use of yeast in bioremediation is advantageous owing to the shorter reaction time as compared to filamentous fungi which can be attributed to their faster growth rate (Dias *et al*., 2010). The biosorptive action of yeasts has been described as the likely non-enzymatic mechanism utilized for azo dye decolorization (Meehan *et al*., 2000; Dias *et al*., 2010). Šafaříková *et al*., (2005) evaluated the ability of Saccharomyces cerevisiae to

adsorb high concentrations of water-soluble dyes. Jadhav *et al*., (2008) reported the decolorization of triphenylmethane dyes by *Galactomyces geotrichum* MTCC 1360. The enzymatic degradation and decolorization of azo dyes have been studied in several yeast species. *Candida zeylanoides, Debaryomyces polymorphus* (Martins *et al.*, 1999; Yang *et al.*, 2003), *Issatchenkia occidentalis* (Ramalho *et al*., 2004), *Candida oleophila* (Lucas *et al*., 2006), and *Candida albicans* (Vitor and Corso, 2008) have been characterized in the decolorization of various azo dyes. A more recent study revealed that a salt tolerant yeast, *Cyberlindnera samutprakarnensis* could decolorize and degrade Acid Red B (ARB) with an efficiency of 97% under optimal conditions (Song *et al*., 2018).

Decolorization of azo dyes by algae

Although bacteria and fungi are the more preferred microbes for applications in bioremediation, photosynthetic algae and cyanobacteria have been identified as promising bioremediating agents in the treatment of dye containing wastewater. Vijayaraghavan and Yun, (2008) reported the role of an induced form of azoreductase in algal azo dye decolorization. The intrinsic ability of the algal biomass to adsorb chromophores and generate biomass through chromophore assimilation contributes to their ability to convert colored molecules to non colored ones (Saratale *et al*., 2011). Acuner and Dilek, (2004) showed the ability of several species of *Chlorella* and *Oscillatoria* are capable of completely metabolizing degrading azo dyes to simpler organic compounds or CO_2 with the formation of intermediate aromatic amines. Yan and Pan, (2004) reported the bioconversion and degradation of more than 30 azo compounds by *Chlorella pyrenoidosa*, *Chlorella vulgaris* and *Oscillateria tenuis*. The results from these investigations highlight the important role of algae in the removal of azo dyes and their degradative amines. Further, biosorption as a technology for the treatment of dye containing wastewater could be a viable alternative to the more costly methods in practice.

Decolorization of azo dyes by plants

Phytoremediation as a method for dye decolorization has gained attention in recent times. There exist many studies on the application of plants in the treatment of dye

wastewater. Patil *et al*., (2009) reported the use of plants in bioremediation as a cost effective and efficient technology for the removal of heavy metals and organic pollutants from contaminated soils and groundwater. Nilratnisakorn *et al*., (2007) studied the potential of narrow leaved cattails to remediate caustic reactive dye effluent. Plant roots in the rhizosphere show the ability to absorb dyes from the surrounding wastewater (Zhou and Xiang, 2013). Jayapal *et al*., 2018 successfully evaluated an integrated plant-microbe system operated in a sequential anaerobic-aerobic mode for the degradation of azo dyes and their metabolites. Plants are autotrophic and afford a large biomass requiring minimal nutrients making them an advantageous system for bioremediation. The treatment of contaminated wetlands by growing coco yam plants yielded a 72-77% decrease in color (Mbuligwe, 2005). Despite the obvious advantages, there exist certain challenges to the adoption of large-scale application of plants to treat effluents including tolerance levels towards various pollutants, the bioavailable fraction of the contaminants and the requirement of vast areas to efficaciously carry out remediation (Ghodake *et al*., 2009a).

1.6 Factors affecting bacterial dye decolorization

The efficiency of biological treatment methods for dye containing wasterwater is influenced by several physical and chemical parameters such as agitation level, temperature, oxygen, pH, dye concentration and structure, as well as the presence of electron donors and redox mediators, and various carbon and nitrogen sources (Krishnan *et al*., 2017). Therefore, a thorough understanding of these individual operational parameters is crucial to optimize the bacterial decolorization of azo dyes. Bacterial dye degradation is typically most efficient under anaerobic conditions, where oxygen levels in the reaction medium are kept low (Bouraie and Din, 2016). Optimal pH values for effective decolorization range from 6.0 to 10.0, and the most conducive temperature range for bacterial cell growth in the decolorization medium is 25-35°C (Pearce *et al*., 2003). The availability of a suitable electron donor is also vital for the biotreatment of dye-contaminated wastewater (Al-Amrani *et al*., 2014). Furthermore, the ease of decolorization is influenced by the specific molecular weight and structure of the azo dyes. Specifically, dyes with low molecular weight and simple structures show a higher rate of color removal. However, the rate of decolorization is impeded for dyes with

electron-withdrawing substitution groups including sulfonated azo dyes (Pandey *et al*., 2007). Kalyani et al., (2008) observed an inverse relationship between the rate of azo dye decolorization and the dye concentration. This could likely be due the toxicity of increased dye concentrations, inadequate bacterial biomass or blockage of enzymatic active sites by structurally diverse dyes and chemical substitution groups (Jadhav *et al*., 2008; Saratale *et al*., 2009b).

1.7 Biochemical Mechanisms of bacterial dye decolorization

Bacterial decolorization and degradation of azo dyes may be aerobic, anaerobic or a combination of the two and is initiated with the reductive cleavage of the azo bond (-N=N-). Enzymes, low molecular weight redox mediators, chemical reduction by biogenic reductants like sulfide, or a combination thereof may be involved in the mechanism of this reduction reaction (**Figure 1.4**). Additionally, the location of the reactions can be either intracellular or extracellular. Pearce *et al.*, (2003) described the unspecific nature of anaerobic bacterial reduction of azo dyes as compared to the aerobic process. The specific adaptation required by aerobic bacteria to decolorize azo dyes makes them less preferential for wastewater treatment in isolation.

Most azo dyes have substituted sulfonated groups and high molecular weight hindering their entry into the bacterial cell. As a result, degradation of sulfonated azo dyes is expected to be a largely extracellular process with the involvement of electron transport moieties for the transfer of reducing equivalents (Russ *et al*., 2000). Various bacterial oxidoreductive enzymes such as lignin peroxidase, laccases, tyrosinase, azoreductase, riboflavin reductase, NADH-DCIP reductase, polyphenol oxidase and aminopyrine N-demethylase have been primarily implicated in the decolorization/ degradation of azo dyes (Suzuki et al., 2001; Saratale *et al*., 2011; Dave *et al*., 2015).

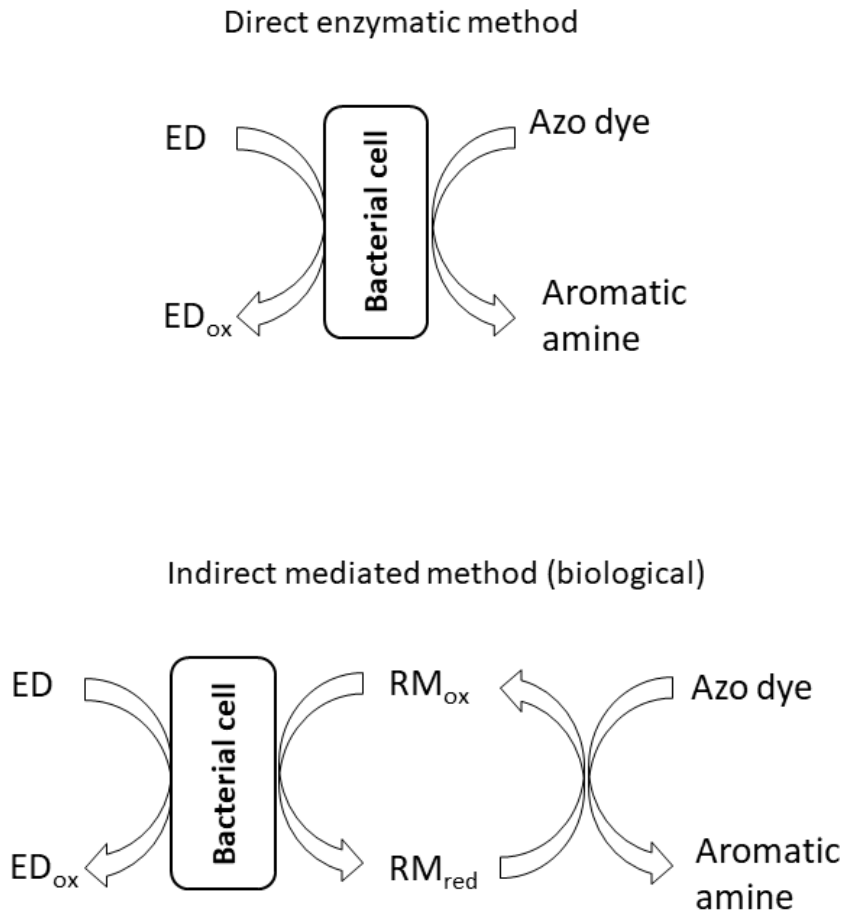


Figure 1.4: Schematic representation of different mechanisms of azo dye reduction, RM = Redox mediator; ED = electron donor (Modified from Pandey *et al*., 2007)

Tyrosinase

Tyrosinase (EC.1.14.18.1), is a monophenol monooxygenase, known to catalyze the oxidation of phenol using molecular oxygen as an oxidant. It has been used to remove phenol from contaminated sites and water (Wu *et al.*, 2001; El-Shora and Metwally, 2008). Tyrosinases catalyze a two-step enzymatic reaction: first the formation of *o*-diphenols by hydroxylation of monophenols followed by oxidation of *o*-diphenols to *o*-quinones (Duran and Esposito, 2000). The *o*-quinone formed may have an inhibitory effect on tyrosinase activity and hence these enzymes possess both cresolase and cathecolase activity (Kalme *et al*., 2009). During azo dye decolorization, this phenoloxidase acts as an oxidative enzyme marker. Studies have revealed the role of tyrosinase from *Comamonas* sp. UVS during decolorization of Red HE7B and Direct Blue GL (Jadhav *et al*., 2008) and from *Alcaligenes faecalis* PMS-1 in the decolorization of select azo dyes (Shah *et al*., 2012)

Laccase

Laccases (E.C.1.10.3.2), also known as phenol oxidases, are copper containing oxidoreductive enzymes. They display broad substrate specificity and catalyze the oxidation of inorganic as well as aromatic compounds with the reduction of oxygen to water (Majcherczyk *et al*., 1998). Laccases have been majorly studied in white rot fungi and some plants with few reports from bacteria (Gianfreda *et al*., 1999). Abadulla *et al*., (2000) studied the role of laccases from lignolytic fungi in decolorizing various synthetic dyes. Telke *et al*., (2009) reported a novel laccase-like phenol oxidase from *Bacillus* sp. ADR, involved in the degradation of C.I. Reactive Orange 16. A laccase enzyme from *Pseudomonas desmolyticum* NCIM 2112 was characterized for decolorization of various azo dyes (Kalme *et al*., (2009). Laccases mediate the direct cleavage of the azo group through a non-specific mechanism resulting in the lack of formation of aromatic amines (Dave *et al*., 2015). The results from these studies suggests the oxidative role played by these enzymes for complete mineralization of the dye molecules.

Lignin peroxidase

Lignin peroxidase (EC 1.11.1.14) is oxidoreductive enzyme and was first described in *Phanerochaete chrysosporium* by Tien and Kirk, (1984). These enzymes act on lignin as a substrate and can be classified under the broader category of ligninases. Their mode of action involves the use of peroxide as an acceptor. The enzyme has been employed to break down a wide array of persistent aromatic compounds, including three and four-ring polyaromatic hydrocarbons (PAHs), polychlorinated biphenyls, and synthetic dyes (Duran and Esposito, 2000; Dawkar *et al*., 2008). Sulfonated azo dye degradation by lignin peroxidases involves the oxidation of a phenolic group resulting in a radical formation at the azo bond bearing carbon atom. The phenolic carbon is hydrolytically cleaved to produce phenyldiazene, which can then be oxidized by a one-electron reaction generating N_2 with the concomitant loss of the azo linkage (Chivukula and Renganathan, 1995). While lignin peroxidase activity for azo dye decolorization is well documented in white rot fungi such as *Thelephora* sp. and *Phanerochaete chrysosporium* (Selvam *et al*., 2003; Verma and Madamwar, 2003), reports of this enzyme from bacteria are scarce. Dhanve *et al*., 2008 studied the asymmetric cleavage of azo dyes by lignin peroxidase activity in *Exiguobacterium* sp. RD3. In addition, investigators showed an increased azo dye degrading activity in purified forms of the enzyme obtained from *Bacillus* sp. strain VUS and from *Acinetobacter calcoaceticus* NCIM 2890 (Dawkar *et al*., 2008; Ghodake *et al*., 2009).

Azoreductase

Azoreductases (EC 1.7.1.6) are major group of enzymes with reducing activity and expressed in bacteria and fungi capable of decolorizing/degrading azo dyes. This enzyme is involved in the catalytic reductive cleavage of the azo (-N=N-) bond with the formation of resultant aromatic amines (Pandey *et al*., 2007). The mechanism of reduction is by the transfer of electrons through soluble flavins. Kehra *et al.,* 2005 explained the susceptibility of azo containing compounds to anaerobic as well as aerobic degradation. The presence of bacterial azoreductases decolorizing sulfonated azo dyes was first reported by Rafii *et al*., (1990) in bacterial strains belonging to *Clostridium* and *Eubacterium.* Extracellular azoreductases from these strains were constitutively produced and found to be oxygen sensitive. Many such unspecific cytoplasmic enzymes

with the ability to reduce azo bonds are found in various bacterial strains (Dave *et al*., 2015). Ghosh *et al.*, (1992) isolated nonspecific enzymes catalyzing azo bond reduction from aerobically grown cultures of *Shigella dysenteriae*. Similar activity was demonstrated in *E. coli* (Nakanishi *et al*., 2001), *Staphylococcus aureus* (Chen *et al*., 2005) and *Pseudomonas aeruginosa* (Nachiyar and Rajkumar, 2005). Further characterization of these enzymes indicated them to be flavoproteins (Pandey *et al*., 2007).

Azo dyes are broadly classified based on their structure, function and/or oxygen requirement. Abraham (2007) proposed a classification based on analysis of the secondary and tertiary amino acid structure owing to inherent inconsistencies in the primary sequence. Bacterial azoreductases represent novel families of enzymes with little similarity to other reductases (Saratale *et al*., 2011). Structurally azoreductases are mostly monomeric, although dimeric or tetrameric forms have been reported (Bafana and Chakrabarti 2008). On the basis of function, azoreductases may be classified as flavin dependent or flavin independent (Blümel and Stolz, 2003; Chen *et al*., 2005). The flavin dependent class of azoreductase are further categorized based on their cofactor requirement of NADH, NADPH or both (Singh *et al*., 2015).

Extensive research has been carried out on the purification and characterization of azoreductase enzymes from many bacteria, such as *Xenophilus azovorans* KF46F, *Pigmentiphaga kullae* K24, *Enterococcus faecalis*, and *Rhodobacter sphaeroides* have been extensively studied (Suzuki *et al*., 2001; Blümel and Stolz, 2003). Besides bacteria, this enzyme has also been found in rat and rabbit liver, intestinal microbiota (Chengalroyen and Dabbs, 2013) and environmental fungi (Chen, 2006) as well as halophilic organisms (Asad *et al*., 2007).

The complex structure and high molecular weight of sulfonated azo dyes impedes their uptake across the bacterial cell membrane. This casts doubts on the intracellular involvement of azoreductases. According to Russ *et al*., (2000), NADH, NADPH or FADH act as electron donors during the reduction of azo dyes. Since these cofactors are cytoplasmic, the reaction requires membrane transport systems to shuttle electrons to the membrane bound azoreductase in intact cells (Dave *et al*., 2015). Kudlich *et al*., (1997) endorsed the idea that the membrane-associated azo reductase activity, facilitated by redox compounds, is distinct from the soluble cytoplasmic nonspecific azo reductase.

The latter is accountable for reducing non-sulphonated dyes that permeate through the cell membrane. **Figure 1.5** shows the mechanism for azoreductase activity during decolorization of azo dyes in intact bacterial cells using redox mediators.

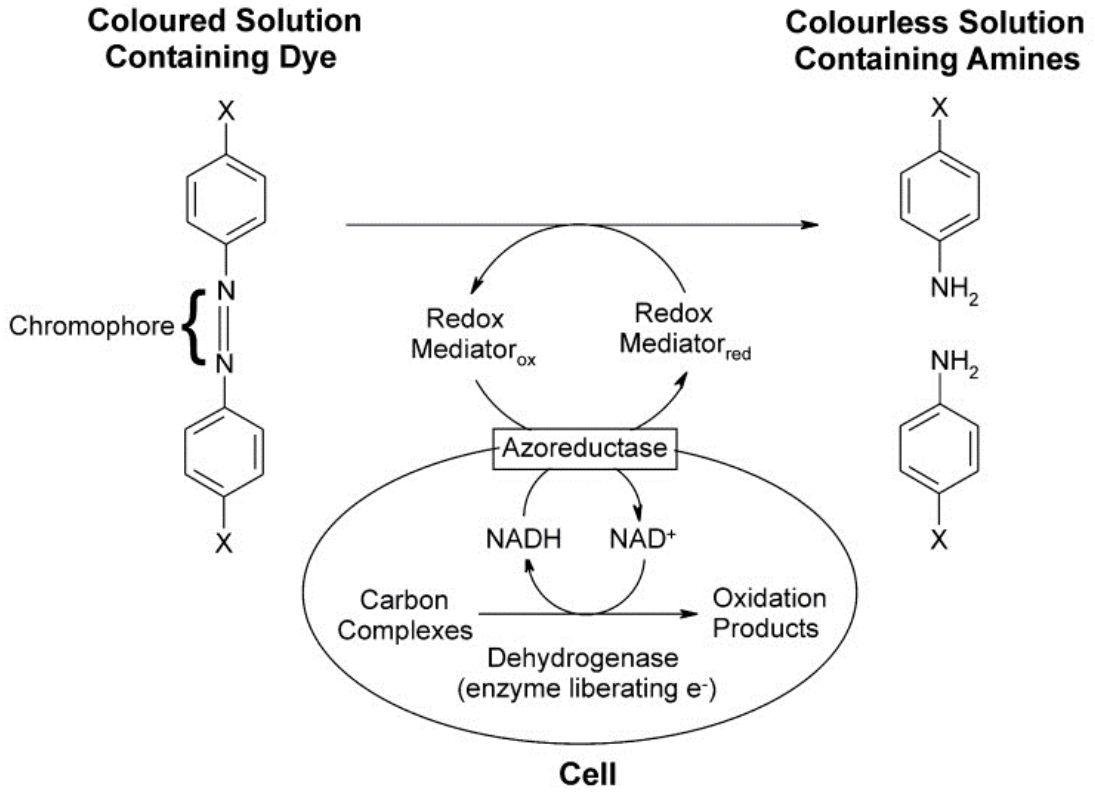


Figure 1.5: Proposed mechanisms for the reduction of azo dyes by whole bacterial cells (Adapted from Pearce *et al*., 2003)

1.8 Molecular basis of dye decolorization

Azo dyes, a predominant class of synthetic dyes utilized in industries, present a significant environmental concern due to their potential toxicity and recalcitrance. Research has increasingly pivoted towards understanding the genomic and proteomic basis of azo dye decolorization, providing novel insights into the molecular mechanisms underlying this process. Therefore, an in depth understanding of the microbial enzymes involved in azo dye decolorization and an evaluation of the functional genes involved is crucial. In recent years, a large number of azo dye decolorizing and degrading bacteria have been isolated and screened from diverse environmental habitats including dye containing wastewater (Kumari *et al*., 2016; Tang *et al*., 2018; Eskandari *et al*., 2019; Eslami *et al*., 2019; Pushpa *et al*., 2019; Srinivasan *et al*., 2019; Khaled *et al*., 2022). The vast majority of existing research has prioritized identifying and characterizing microorganisms capable of degrading azo dyes, in addition to assessing their capabilities for dye degradation (Chen *et al*., 2018). This has considerably advanced our comprehension of the azo dye degradation process and, through the examination of degradation byproducts, has hypothesized microbial degradation pathways of azo dyes. However, the explicit functional genes and their associated mechanisms involved in the microbial breakdown of azo dyes are not as widely reported.

Microbial degradation of azo dyes involves enzymatic breakdown, primarily mediated by azoreductases and oxidoreductive enzymes (Dave *et al*., 2015; Singh *et al*., 2015). These enzymes cleave the azo bonds and transform the dyes into less complex and often less toxic molecules. The genes encoding, their expression, regulation and resulting metabolic pathways have been elucidated in several organisms including *Pseudomonas, Pigmentiphaga*, *Bacillus*, *Enterococcus,* and *Escherichia* (Leelakriangsak, 2013). Significant genes, such as *azoR* and *azoA,* encoding prtoeins involved in catalytic azo dye cleavage have been identified in several bacterial species (Chen *et al*., 2010). Certain bacteria like *Shewanella decolorationis* S12 and *Pseudomonas luteola* harbor plasmids with azo dye reduction genes, which may provide them with a selective advantage in dye-contaminated environments (Xu *et al*., 2007; Chen *et al*., 2010).

In addition to gene identification, genomic studies have revealed that azo dye decolorization is often a complex process involving various metabolic pathways. In a study on *Bacillus subtilis*, genes related to electron transfer chains and energy

metabolism were found to be significantly up-regulated during dye decolorization (Valenzuela-García *et al*., 2020). This suggested a potential interaction between dye degradation and bacterial energy metabolism. One notable bacterial strain well studied for its azo dye degradation potential is *Shewanella oneidensis*. Genomic analysis of this bacterium has revealed genes for azoreductases, laccases and cytochromes are involved in dye degradation (Mugerfeld *et al*., 2009). Similarly, a recent transcriptomic study on the thermophilic strain *Anoxybacillus* sp. used RNA-Seq and qRT-PCR technology to confirm the role of NAD(P)H-flavin reductase, 2Fe-2S ferredoxin and NAD(P)-dependent ethanol dehydrogenase genes in Direct black G decolorization (Chen *et al*., 2020).

Proteomic analysis has also been a valuable tool in elucidating the molecular mechanisms of dye decolorization. Using advanced techniques such as 2D electrophoresis and mass spectrometry, studies have identified a range of proteins involved in azo dye degradation, including azoreductases, flavin reductases, and NAD(P)H-dependent enzymes (Feng *et al*., 2012). A metaproteomic approach to understanding potential azo dye degrading mechanisms was reported by An *et al*., (2020). Comprehensive *in silico* studies such as molecular docking of bacterial enzymes involved in dye decolorization can provide new insights into understanding and exploring interactions at the molecular level. Moreover, integrating various omics tools to study microbial azo dye decolorization could be impactful in developing more efficient systems for the bioremediation of textile wastewater.

1.9 Significance of this study

The dyeing industry constantly strives to develop various new synthetic dyes and continuous efforts are being made towards further developing these dyes to make them more sustainable, increase the scope of their application and reduce their impact on the environment. Keeping in mind these challenges, this study focused on screening and identifying potential bacteria, from marine and estuarine sources, capable of decolorizing dyes and exploring the molecular mechanisms they adopt in facilitating the process of dye decolorization. As dye wastewater contains high concentrations of salt, these salt tolerant bacteria would possess innate abilities to carry out dye decolorization under saline conditions. Proteomic analyses will provide insights into the changes in the protein

profile during decolorization of synthetic dyes. This knowledge will contribute to our understanding of the mechanism of decolorization of textile dyes and will aid in developing robust and efficient bioremediation steps for treating textile industry effluents. Investigations into the molecular framework of bacteria involved in dye decolorization would provide an assessment of the functional gene expression during this process. The detection of genes involved in azo dye decolorization and analysis of mRNA as an indicator of gene expression could significantly augment the understanding of the role of these genes in the pathways of dye decolorization. The work carried out for this research was planned in order to address the following major objectives

- **To select marine bacteria capable of textile azo dye decolorization**

  The rationale for pursuing this objective was to isolate salt tolerant bacteria from marine and estuarine sources. These isolates would then be screened for their ability to decolorize and detoxify high concentrations of synthetic textile azo dyes to eventually obtain isolates with maximum potential for bioremediation of textile wastewater.

- **To elucidate the proteomic characteristics of a select set of bacteria efficient in dye decolorization**

  The process of dye decolorization is mediated through a series of enzymatic reactions. The purpose of this objective was to identify the changes in the level of expressed proteins during the decolorization of textile azo dyes. This may help in elucidating the possible mechanism of action during dye decolorization and provide lacking information regarding the bacterial proteomic profile accompanying azo dye decolorization.

- **To evaluate the expression and regulation of genes encoding azo dye decolorization enzymes**

  Native bacteria possess inherent mechanisms to deal with pollutants and chemicals in their environment. The expression of their genes is tailored to survive stresses in their environment. Identifying the genes that play a key role in decolorization of azo dyes is useful in developing targeted technologies for the bioremediation of textile wastewater.

Chapter 2

Screening, Isolation and Identification of Dye Decolorizing Bacteria

Chapter 2

Screening, Isolation and Identification of Dye Decolorizing Bacteria

2.1 Introduction

Environmental habitats are strongly influenced by the various physical, chemical and biological processes that constitute it (Pace, 1997). These parameters in a given habitat share a closely interspersed relationship with each other. Physical conditions of temperature, pH and salinity affect the dynamics of the associated biota. Microorganisms are widely distributed across habitats including extreme conditions of high salinity, high pressure and high acidity. The complexity of their metabolic activity allows them to function in such a wide range of environmental conditions. The diverse distribution of microorganisms in the environment makes them a desirable resource for bioprospecting as potential agents of many useful compounds (Tanner *et al.*, 2017). Bacteria and fungi are well studied decomposers in aquatic and terrestrial ecosystem because of their ability to transform substrates. Their pivotal role as agents of bioremediation can be attributed to their diverse enzymatic systems. This allows them to efficiently convert organic matter to inorganic molecules thereby contributing to nutrient cycling in the environment (Thatoi *et al.*, 2013).

The marine environment encompasses oceans, estuaries, mangroves, lagoons and salt marshes where the salinity is in the range of 5 to 35 psu (practical salinity units) and it is home to abundant bacteria and fungi besides other life forms. Mangroves are amongst the most productive natural ecosystems. They are prolific in various living organisms including a rich genetic diversity of microorganisms (Thatoi *et al.*, 2013). These microorganisms are equipped with adaptive mechanisms to efficiently recycle molecules in their habitat. In spite of this, only a minute fraction of these microorganisms has been explored for their ecological role or their potential applications. Hence such an ecosystem offers a promising stock of organisms with bioremediation potential.

The widespread use of synthetic dyes across a gamut of industries has resulted in indiscriminate release of these dyes into the environment (Abd El-Rahim *et al*., 2017). This causes deleterious effects on the environment as well as reduces the quality of water bodies (Sarnaik and Kanekar, 1999). Azo dyes are amongst the largest class of recalcitrant synthetic dyes in use (Singh *et al*., 2015). The release of these dyes in wastewaters has raised concerns about their toxic effects on humans as well as on other organisms. The large amount of unbound dye in these effluents not only imparts dark coloration to the water bodies but additionally the dyes as well as their breakdown products have been shown to be carcinogenic and/or mutagenic in nature (Weisburger, 2002). Bioremediation offers an attractive, environmentally friendly and economically viable solution for the treatment of dye containing wastewater. Extensive studies have been carried out to indicate the potential role of bacteria in decolorizing and detoxifying a wide range of structurally different synthetic dyes (Bras *et al*., 2001; Chen *et al*., 2003; Mahmood *et al*., 2016). As a result, the development of successful and robust microbial based bioremediation technologies requires a better understanding of the microbial abundance and response to the presence of synthetic dyes. The isolation and characterization of culturable dye decolorizing bacteria would help evaluate the remediating potential of indigenous bacterial populations and identify prospective strains with enhanced capabilities for wastewater treatment.

2.2 Materials and Methods

2.2.1 Sampling

Three estuarine sources located in Goa along the west coast of India were selected for isolating potential dye decolorizing bacteria as shown in **Figure 2.1**. These sites are in the mangroves located at Choraõ (**CM;** 15°30'44.1" N 73°52'07.8" E) and Divar (**DM;** 15°30'30.6" N, 73°54'41.7" E) and saltpans situated at Ribandar (**RS;** 15°29'56.0" N, 73°50'46.6" E). Water samples were collected just below the surface using sterile polypropylene tubes. Sediment samples were collected at low-tide in undisturbed areas with the help of a core (0 - 5cm) in an aseptic zip lock bag. All samples were held on ice until further analysis in the laboratory.

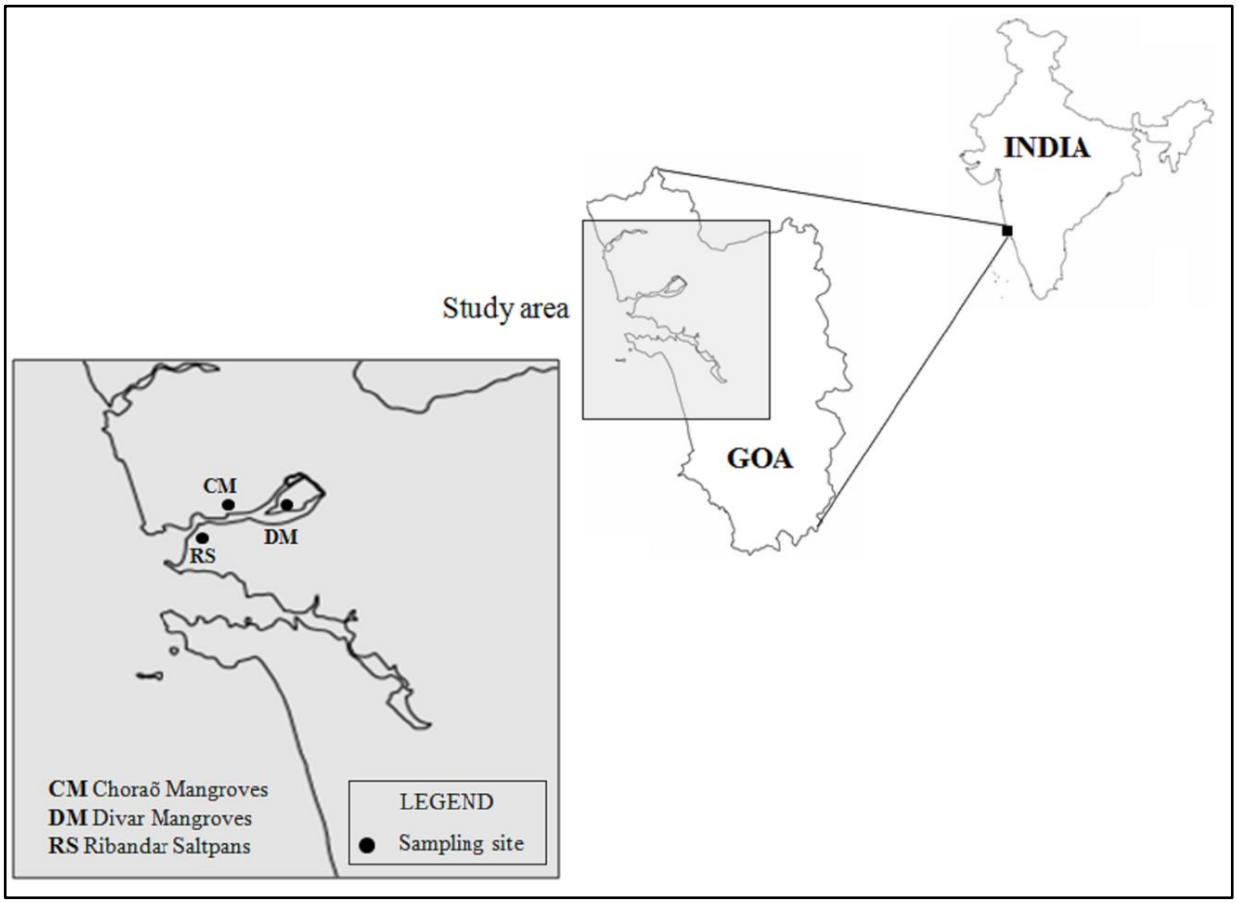


Figure 2.1: Sampling locations located in (**CM**) Choraõ Mangroves, (**DM**) Divar Mangrove site, (**RS**) Ribandar saltpans

2.2.2 Measurement of physico-chemical parameters

2.2.2.1 *Water samples*

The prevalent physico-chemical conditions at each sampling site were recorded. These included pH, temperature and salinity of the ambient sea water. Temperature at each location was measured on-site using a hand-held mercury thermometer. Salinity and pH of collected water samples was measured using a hand-held refractometer (ATAGO, ATC-S/Mill-E) and a bench top Accumet Basic AB15 – pH meter (Fisherbrand, USA) calibrated with standard buffers. Samples were also analyzed for dissolved oxygen (DO) level following Winkler's procedure (Parsons *et al*., 1984) (Appendix A). The levels of nutrients such as nitrate (NO_3-N) and nitrite (NO_2-N) were analyzed according to Parsons *et al*., (1984).

2.2.2.2 *Sediment samples*

The physical parameters such as temperature, pH and salinity of the overlying water were measured as described earlier. Basic descriptive statistics were applied on raw data sets with mean ± standard deviation of the water and sediment parameters determined separately for each sampling location.

2.2.3 Microbiological analysis

2.2.3.1 *Total viable counts*

Bacterial counts in the water and sediment samples were determined using standard dilution plate method. In order to enumerate the total viable bacterial counts (TVC**)**, water and sediment samples were processed accordingly, by serial dilution in sterile phosphate buffer (pH 7.2). Aliquots of 0.1 ml of sample dilution were spread in triplicate onto seawater nutrient agar (SWNA, with composition [L^{-1}]: peptic digest of animal tissue 5.0 g, sodium chloride 5.0 g, beef extract 1.5 g, yeast extract 1.5 g, agar 15 g, distilled water 1000 mL, pH 7.4 ± 0.2). Plates were incubated at 28°C for 24-48 h and bacterial counts were taken as colony forming units (CFU) mL^{-1}. Data was expressed as mean ± standard deviation (SD) of three replicate experiments.

2.2.3.2 *Sample Enrichment*

A selective enrichment culture technique using Mineral Salt Medium (MSM) amended with azo dye as the sole source of carbon and energy was used for enrichment of potential dye decolorizing bacterial strains from the collected samples (Sharma *et al*., 2004). Four reactive azo dyes (Sigma-Aldrich) i.e. Reactive Black 5 (**RB5**), Reactive Green 19 (**RG19**), Reactive Red 120 (**RR120**) and Reactive Blue 163 (**RBL163**) were used. 250 mL of sterile MSM (Appendix B) was prepared in 500 mL Erlenmeyer flasks with each of the azo dyes added to give a final concentration of 100 mg L^{-1}. Stock solutions of the dyes (10 g L^{-1}) were prepared and sterilized by membrane filtration using a 0.22-µm pore size membrane filter (Axiva, New Delhi). Each flask with the sterile medium was inoculated with 1 g of sediment sample or 10 mL of water sample. Flasks were incubated at 28°C for 7 days under agitated conditions (120 rpm). Repeated transfers of 2 % (v/v) inoculum were carried out in to fresh sterile MSM amended with increasing concentrations of reactive azo dyes (150 mg L^{-1} and 200 mg L^{-1}). Following incubation, the enriched cultures from the flasks were serially diluted and 100 µL aliquots were spread onto Mineral Salt agar plates amended with the four azo dyes. After 48 h incubation at 28 ± 2 °C, morphologically distinct bacterial colonies were picked up and streaked on sterile Nutrient agar (NA) plates.

2.2.3.3 *Purification and maintenance of bacterial cultures*

Distinct isolates obtained during initial isolation were purified separately by suspending in sterile saline and re-inoculating (by quadrant streak subculture) on Nutrient agar plates. Each pure isolate was grown in Nutrient broth (NB; HiMedia, Mumbai) (Appendix B) to a density of 1 OD at 600 nm (approx. 10^6 cells ml^{-1}). Liquid cultures (0.5 mL each) were transferred to sterile cryovials containing 0.5 mL 25% glycerol and stored at -80°C. The isolates were also maintained on sterile NA slants at 4°C for further analysis. 210 such pure isolates were obtained and were subject to further screening.

2.2.4 Screening and Isolation of Dye decolorizing bacterial strains

Preliminary studies to obtain bacteria with dye decolorizing potential were carried out using 50% Sea Water Nutrient agar (SWNA, with composition [L^{-1}]: peptic digest of animal tissue 5.0 g, sodium chloride 5.0 g, beef extract 1.5 g, yeast extract 1.5 g,

agar 15 g, distilled water 500 mL, sea water 500 mL, pH 7.4 ± 0.2) containing dye. All purified isolates were spot inoculated on dye-amended plates containing 200 mg L^{-1} of the reactive azo dyes. The plates were incubated at room temperature (RT) (28 ± 2 °C) for 24 – 48 h. The isolates showing zones of clearance were picked for further studies.

2.2.5 Identification of Dye decolorizing bacterial strains

2.2.5.1 *Morphological, physiological and biochemical characterization*

The morphological characteristics of the pure isolates of dye decolorizing bacteria were studied. Isolated colonies on nutrient agar were described with respect to their colony color and morphology. The Gram character for the selected isolates was determined by Gram staining (Gram, 1884). Motility of individual cells was determined by observing under light microscopy. Various biochemical tests were performed for the selected isolates using HiAssorted Biochemical test identification kit (HiMedia, India).

Further, all the pure isolates of bacteria were assessed for their abilities towards the production of physiological enzymes. These enzymes include oxidative (catalase and oxidase), reductive (nitrate and nitrite reductase), substrate specific hydrolytic enzymes (amylase, casease, lipase, ornithine decarboxylase and arginine dihydrolase). All biochemical activities were recorded qualitatively (+/-ve) as a part of taxonomic identification.

Catalase test: A well grown isolated colony of pure culture was picked up aseptically with a sterile loop and mixed with hydrogen peroxide solution (H_2O_2: 3% v/v) solution on a clean glass slide. Observation of bubble formation was considered as a positive test (Smibert and Krieg, 1994)

Cytochrome oxidase test: Oxidase test was performed using commercial tetramethyl-p-phenylenediamine dihydrochloride (TPPD: Himedia, DD018) discs. A smear of a loopful bacterial cell mass was spread on the disc. The development of dark purple colour within 10 to 15 seconds was considered as a positive test.

Nitrate reductase test: The isolates were inoculated in sterile nitrate broth and incubated at 28 ± 2 ºC for 24 h. Following incubation, development of a red color upon addition of sulphanilic acid and N, N-Dimethyl-α-naphthylamine indicated a nitrate reductase positive result.

Amylase test: Individual isolates were drop inoculated on nutrient agar plates containing 1 % starch and incubated at 28 ± 2 ºC for 24 h. Later, plates were flooded with Lugol's iodine solution (3% potassium iodide, 0.3% iodine). The presence of clear zone surrounding the colony was considered as a positive test for amylase production.

Casease test: Isolates were spot inoculated on Skim Milk agar plates (containing 2.8% skim milk powder) and incubated at 28 ± 2 ºC for 24 h. The presence of clear zone surrounding the colony was considered as a positive test for casease activity.

Lipase test: The production of lipase was determined using Nutrient agar amended with 1% Tween 80. Individual colonies were spot inoculated on the plates and incubated at 28 ± 2 ºC for 24 h. The formation of white precipitate around the colony was an indicator of lipase activity.

Ornithine decarboxylase test: Cultures were inoculated into nutrient broth containing 0.5% ornithine and incubated at 28 ± 2 ºC for 24 h. A violet color obtained following incubation indicates a positive result.

Arginine dihydrolase test: Cultures were inoculated into nutrient broth containing 0.5% arginine and incubated at 28 ± 2 ºC for 24 h. A purple color obtained following incubation indicates a positive result.

2.2.5.2 *Extraction of DNA*

For the extraction of DNA, the pure bacterial cultures were grown overnight in Luria Bertani broth (HiMedia, Mumbai) (Appendix B) and collected by centrifugation. Genomic DNA was extracted using the GenElute™ Bacterial Genomic DNA kit (Sigma-Aldrich, USA) following the manufacturer's instructions. Around 1.5 mL of overnight grown bacterial culture was centrifuged to obtain a cell pellet and the culture medium was discarded. Pellets were resuspended in 200 µL Lysozyme solution (~40mg/mL) and incubated at 37°C for 30 minutes. This was followed by addition of 20µL of RNase A solution. After incubation of this suspension for 2 minutes at room temperature, 20µL of Proteinase K solution and 200µL of Lysis Solution C were added, vortexed and incubated at 55°C for 10 minutes. 200µL of ethanol was then added to the lysate and homogenized. This entire solution was transferred to an activated Miniprep Binding Column assembled in a collection tube. The tube containing the column was centrifuged at 6500 x g for 1 minute following which the column was sequentially washed with the

two wash solutions provided and the collection tube changed at each step. The final elution was carried out in a fresh collection tube wherein the bound DNA was eluted by addition of Elution Solution. The quality and integrity of the eluted DNA was tested using Nanodrop and agarose gel electrophoresis, respectively.

2.2.5.3 *PCR amplification and purification*

The extracted DNA was amplified to obtain near full length 16S rRNA genes by polymerase chain reaction (PCR). The universal forward and reverse primers selected for amplification were 27F (5'-AGAGTTTGATCACTGGCTCAG-3') (Weisberg *et al*., 1991) and 1492R (5'-CTACGGCTACCTTGTTACGA-3') (Reysenbach *et al*., 1992) (BioServe). The final reaction tube volume was 25µL and contained 2µL of template DNA (added at a concentration of 30-50µg DNA μl^{-1}), 1µL each of forward and reverse primer (10pmol), 12µL of PCR Master Mix (Thermo, USA) and 9µL of Nuclease-free water (Thermo, USA). The PCR was performed using the following conditions: initial denaturation at 94°C for 4 min, followed by 35 cycles at 94°C for 1 min (denaturation), 55°C for 1 min (annealing), and 72°C for 1 min (extension). Final elongation was at 72°C for 20 min. The reaction was carried out in a Veriti 96 well Thermal Cycler (Applied Biosystems, USA). Amplification was confirmed by carrying out electrophoresis of the amplicons using a 0.8% agarose gel along with a 1kb molecular ladder. The amplified products were purified using a PCR purification kit GenElute™ PCR Clean-Up Kit according to the manufacturer's instructions. Products were stored at -20°C until further use.

2.2.5.4 *Sequencing*

Nucleotide sequences were determined by automated sequencing using the Applied Biosystems 3130*xl* Genetic Analyzer based on the principle of dideoxy chain termination. Sequencing was carried out using 1pmol each of the universal forward and reverse bacterial primers, 27F and 1492R. The 16S rRNA gene of each strain was assembled using DNA Baser Sequence Assembler and compared with the 16S rRNA gene database at the National Center for Biotechnology Information (NCBI; https:// www.blast.ncbi.nlm.nih.gov/Blast.cgi) using the BLAST search tool. Sequence identity was determined based on the closest reference match. Short sequences of less than 500bp, sequences with low similarity of lower than 90% and chimeric sequences were

removed. The identified sequences were submitted to NCBI GenBank database and accession numbers for these sequences were obtained.

2.2.6 Phylogenetic Analysis

The sequences obtained for each strain were used to construct phylogenetic trees by comparing to sequences of most closely related type/reference strains. The reference strains were selected based on the closest match with 16S rRNA sequences of the isolates under study and retrieved from GenBank database **(**https://www.ncbi.nlm.nih.gov/genbank/**)** (Wheeler *et al*., 2007). All sequences were converted to FASTA format and aligned using MEGA7 software (Kumar *et al*., 2016). After alignment, the phylogenetic tree was constructed using neighbor joining (NJ) algorithm (Tamura *et al*., 2004), and bootstrap analysis was performed to evaluate stability of relationships by performing 1000 replications of the dataset.

2.2.7 Primary dye decolorization assays

The dye decolorizing potential of the bacterial isolates obtained was determined by primary decolorization assays in nutrient broth (NB; HiMedia, Mumbai) (Appendix B) containing reactive azo dyes (Modi *et al*., 2010). The isolates were grown in NB to a density of 1 OD at 600 nm and used to inoculate into tubes containing the nutrient medium amended with the reactive azo dyes RB5, RG19, RR120 and RBL163 at concentrations of 100 mgL^{-1}, 250 $mgL^{-}1$ and 500 mgL^{-1}. The tubes were incubated at room temperature (RT) (28 ± 2 °C) for 24 h. Following incubation, the broth was centrifuged at 12,000 rpm for 10 min at 4°C and the absorbance of the cell-free supernatant was read spectrophotometrically at 597 nm for RB5, 630 nm for RG19, 522 nm for RR120 and 590 nm for RBL163. The uninoculated dye free culture medium was used as blank. The percentage of decolorization for different isolates was calculated using the following equation:

$$\text{Decolorization (\%)} = \frac{A_{\lambda,\text{initial}} - A_{\lambda,\text{final}}}{A_{\lambda,\text{initial}}} \times 100$$

where, $A_{\lambda,\text{ initial}}$ = initial absorbance and $A_{\lambda,\text{ final}}$ = absorbance after incubation

Data was expressed as mean ± standard deviation (SD) of three replicate experiments.

2.3 Results

2.3.1 Measurement of physico-chemical parameters

2.3.1.1 *Water samples*

The different physico-chemical parameters of water and sediment samples have been listed in **Table 2.1** and **Table 2.2**. Analysis of the water samples showed variations in temperatures ranging from 25˚C to 30.2˚C and pH range of 6.8 to 7.8. The salinity of the samples differed based on the sampling location with the samples from Ribandar saltpans recording the highest salinity. Variations in salinity in the mangrove locations were an outcome of frequent tidal changes experienced within this estuarine ecosystem. Dissolved oxygen levels showed a range of 3.42 to 5.14 mg L^{-1} while nitrate values ranged from 1.12 to 2.06 µmol L^{-1} and nitrite from 0.24 to 0.33 µmol L^{-1} respectively.

2.3.1.2 *Sediment samples*

The sediment parameters measured in the overlying water samples were found to be generally similar to the parameters of the water samples taken from that sampling location. However, the temperatures recorded of the sediment samples were slightly warmer in comparison to the water.

2.3.2 Microbiological analysis

2.3.2.1 *Abundance of bacterial populations*

Bacteria were found in all the samples obtained from Choraõ and Divar mangroves as well as Ribandar saltpans. It was observed that bacterial counts were higher in sediment samples as compared to water samples. The saltpans samples showed relatively lower counts in comparison to mangrove samples. The TVC of bacteria in mangrove water samples was much higher than in saltpan water sample as indicated in **Table 2.2**. Further, higher bacterial counts of 398.55 x 10^6 CFU mL^{-1} and 436.02 x 10^6 CFU mL^{-1} were recorded in mangrove sediment samples from Choraõ and Divar respectively. However, a lower TVC of 87.41 x 10^6 CFU mL^{-1} was measured in sediment collected from saltpans.

2.3.2.2 *Enrichment and Isolation of Dye decolorizing bacteria*

Selective enrichment using MSM was a useful technique to isolate potential dye decolorizing bacterial strains from the water and sediment samples. Following enrichment in the presence of four reactive azo dyes i.e. RB5, RG19, RR120 and RBL163, 210 morphologically distinct bacterial colonies were obtained. These were further purified and maintained on Nutrient agar slants and plates. Primary screening using dye amended plates yielded 81 bacterial isolates with the potential to decolorize 50 mg L^{-1} of the reactive azo dyes tested. A further screening carried out using 200 mg L^{-1} of the dyes yielded 15 bacterial strains showing the best decolorization ability. These isolates showed distinct clear zones around the bacterial colony on NA plates containing the dye.

Table 2.1: Physico-chemical characteristics of water samples

	Sampling Location		
	Choraõ Mangrove	**Divar Mangrove**	**Ribandar saltpans**
Temperature (˚C)	29.35 ± 0.05	28.39 ± 0.05	30.22 ± 0.05
pH	7.44 ± 0.03	7.83 ± 0.03	6.82 ± 0.04
Salinity (PSU)	27.24 ± 0.01	29.04 ± 0.04	32.24 ± 0.01
Dissolved Oxygen (mg L^{-1})	3.42 ± 0.06	5.14 ± 0.02	4.39 ± 0.02
Nitrite (µmol L^{-1})	0.31 ± 0.01	0.24 ± 0.03	0.33 ± 0.02
Nitrate (µmol L^{-1})	1.12 ± 0.02	1.24 ± 0.04	2.06 ± 0.01
CFU (no. x 10^3 mL^{-1})	407.61 ± 12.16	371.60 ± 8.20	34.21 ± 9.24

Table 2.2: Physico-chemical characteristics of sediment samples

	Sampling Location		
	Choraõ Mangrove	**Divar Mangrove**	**Ribandar saltpans**
Temperature (˚C)	31.35 ± 0.00	30.11 ± 0.01	31.05 ± 0.03
pH	7.14 ± 0.03	7.04 ± 0.02	8.11 ± 0.05
Salinity (PSU)	25.78 ± 0.00	27.34 ± 0.01	30.04 ± 0.06
CFU (no. x 10^6 mL^{-1})	398.55 ± 10.18	436.02 ± 15.20	87.41 ± 9.30

2.3.3 Identification of Dye decolorizing bacterial strains

2.3.3.1 *Morphological, Physiological and Biochemical Characteristics of Bacterial Isolates*

The 15 isolates were differentiated based on their morphological, cultural and biochemical characteristics. The various colony and cell morphologies as well as the temperature and pH for growth are shown in **Table 2.3**. The results of the biochemical tests and production of physiological enzymes were determined as shown in **Table 2.4**.

2.3.3.2 16*S rRNA based Identification and Phylogenetic Analysis*

The 15 dye decolorizing bacterial cultures obtained were identified on the basis of 16S rRNA gene sequencing. The purity of the extracted genomic DNA was confirmed based on A_{260nm}/A_{280nm} ratio and found to be within 1.7-2.0. Amplified product of ribosomal DNA in all the samples was approximately 1500 base pairs in size as confirmed in the 0.8% agarose gel. The sequences obtained for the dye decolorizing bacterial isolates represented >97% similarity to the matching phylotypes in the database. The sequence analysis showed the dye decolorizing bacterial isolates to belong to 4 genera as indicated in **Figure 2.2**. The results of identification of bacterial isolates by 16S rRNA gene

sequencing confirmed the results obtained in the biochemical tests. The GenBank accession numbers obtained for the isolates are listed in **Table 2.5**.

The phylogenetic tree created based on similarities in the 16S rDNA sequences for the different dye decolorizing bacterial isolates (**Figure 2.3**) shows high degree of similarity to related isolates and type strains. Based on the 16S rDNA sequences, the isolates are clustered into clades based on the degree of similarity or difference in rDNA sequence composition.

2.3.4 Primary decolorization assay

Initial decolorization studies showed the rapid and extensive decolorization of the four reactive dyes (RB5, RG19, RR120 and RBL163) at dye concentration of 100 mgL^{-1} by all the 15 isolates (**Table 2.6**). In comparative analysis of all the isolates tested, the bacterial isolate NIO_14d showed the maximum potential of azo dye decolorization and decolorized >98% of RB5, RG19 and RR120 and 88% of RBL163 within 24 hours of incubation. As shown in **Figure 2.4**, the isolates were further capable of efficient dye decolorization even at higher dye concentrations of 250 mgL^{-1} and 500 mgL^{-1} (**Table 2.7 and Table 2.8**). Of the four dyes tested, the extent of decolorization was found to be higher in RB5, RG19 and RR120 as compared to RBL163.

The primary decolorization studies provided a set of bacterial strains with considerable azo dye decolorization potential. Based on these results, the isolate NIO_14d which showed the best dye decolorization activity measured as percent decolorization was selected for further optimization and characterization studies. The isolate was identified as *Shewanella seohaensis* based on maximum similarity in NCBI database and was assigned with GenBank accession number KR922404.

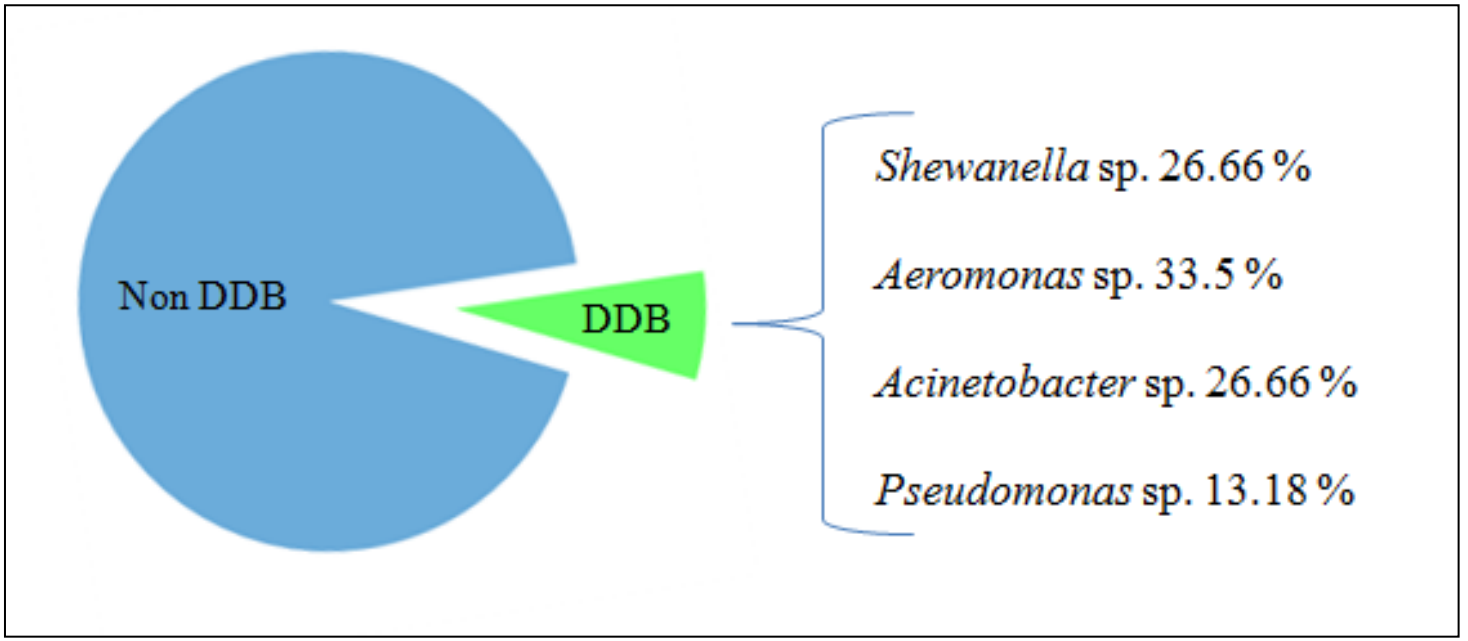


Figure 2.2: Dye decolorizing bacteria (DDB) belonging to different representative bacterial genera isolated from mangrove and saltpan, water and sediment samples

Table 2.3: Morphological and physiological characteristics of dye decolorizing bacterial isolates

Test	NIO_2c	NIO_3d	NIO_12c	NIO_13a	NIO_13b	NIO_14d	NIO_14l
Colony Morphology							
Shape	circular	circular	circular	circular	circular	circular	circular
Margin	entire	entire	entire	entire	entire	entire	entire
Elevation	raised	convex	convex	flat	convex	raised	convex
Surface texture	smooth	smooth	smooth	mucoid	smooth	smooth	smooth
Consistency	butyrous	butyrous	butyrous	butyrous	butyrous	butyrous	butyrous
Color	cream	cream	cream	greenish	off white	cream	cream
Opacity	opaque	opaque	opaque	translucent	translucent	opaque	translucent
Gram character	Gram negative rod	Gram negative rod	Gram negative rod	Gram negative rod	Gram negative rod	Gram negative rod	Gram negative rod
Motility	motile	motile	motile	motile	non motile	motile	motile
Growth conditions							
Temperature	25°C - 45°C	25°C - 40°C	25°C - 40°C	25°C - 40°C	25°C - 40°C	25°C - 35°C	25°C - 40°C
pH	6.0 – 8.0	6.0 – 8.0	6.0 – 8.0	7.0 – 9.0	6.0 – 8.0	6.0 – 8.0	6.0 – 8.0

Table 2.3 *(continued)*: Morphological and physiological characteristics of dye decolorizing bacterial isolates

Test	NIO_14s	NIO_14v	NIO_15c	NIO_15d	NIO_15e	NIO_15h	NIO_15m	NIO_15p
Colony Morphology								
Shape	circular	circular	circular	circular	circular	circular	circular	circular
Margin	entire	entire	entire	entire	entire	entire	entire	entire
Elevation	convex	convex	convex	convex	raised	convex	raised	convex
Surface texture	mucoid	mucoid	smooth	mucoid	smooth	smooth	smooth	smooth
Consistency	butyrous	butyrous	butyrous	butyrous	butyrous	butyrous	butyrous	butyrous
Color	white	off-white	cream	white	light pink	white	cream	white
Opacity	opaque	translucent	translucent	translucent	opaque	opaque	opaque	translucent
Gram character	Gram negative coccobacilli	Gram negative rod	Gram negative rod	Gram negative coccobacilli	Gram negative rod	Gram negative rod	Gram negative rod	Gram negative coccobacilli
Motility	non motile	non motile	motile	non motile	motile	non motile	motile	non motile
Growth conditions								
Temperature	25°C - 40°C	25°C - 40°C	25°C - 40°C	25°C - 40°C	25°C - 35°C	25°C - 40°C	25°C - 35°C	25°C - 35°C
pH	7.0 – 8.0	7.0 – 8.0	6.0 – 8.0	7.0 – 8.0	6.0 – 8.0	6.0 – 8.0	6.0 – 8.0	7.0 – 8.0

Table 2.4: Biochemical tests and production of physiological enzymes by dye decolorizing bacterial isolates

Isolate → / Test ↓	NIO_2c	NIO_3d	NIO_12c	NIO_13a	NIO_13b	NIO_14d	NIO_14l	NIO_14s	NIO_14v	NIO_15c	NIO_15d	NIO_15e	NIO_15h	NIO_15m	NIO_15p
Catalase	+	+	+	+	+	+	+	+	+	+	+	+	+	+	+
Oxidase	+	+	+	+	+	+	-	-	-	+	-	+	+	+	-
Nitrate reductase	+	+	+	-	+	+	-	-	-	+	+	+	+	+	+
Amylase	-	+	+	-	+	+	-	-	-	+	+	-	+	-	+
Casease	-	+	+	+	+	+	-	-	-	+	+	+	+	-	+
Lipase	-	+	+	-	+	+	-	+	+	+	+	+	+	-	+
Ornithine decarboxylase	-	-	-	-	-	-	-	-	-	-	-	-	-	-	-
Arginine dihydrolase	-	-	-	+	-	-	-	-	+	-	-	+	-	+	-
Citrate utilization	+	+	+	+	-	+	+	+	+	-	+	+	-	+	-
Lysine	-	-	-	-	-	-	-	+	+	-	+	-	-	-	+
Urease	-	-	-	+	-	-	+	-	-	-	-	-	-	-	-
Phenylalanine deaminase	+	-	+	-	-	-	-	+	+	-	+	+	-	-	+
H_2S production	-	+	-	-	-	-	-	-	-	-	-	-	-	-	-
Utilization of															
Glucose	+	+	+	+	+	+	+	+	+	+	+	+	+	+	+
Lactose	+	-	-	+	+	+	-	-	-	+	-	-	+	-	+
Arabinose	+	+	+	+	+	-	-	-	+	+	+	+	+	+	-
Sorbitol	-	-	-	-	-	-	-	-	-	-	-	-	-	-	-

Key: + : Positive reaction - : Negative reaction

Table 2.5: 16S rDNA sequence-based identification and NCBI GenBank accession numbers of dye decolorizing bacteria

Isolate	Source	NCBI GenBank Accession number	Nearest neighbor in NCBI database	Similarity (%)
NIO_2c	**RSW**	**MZ841641**	*Shewanella baltica*	99.79
NIO_3d	**DMW**	**KX062379**	*Aeromonas enteropelogenes* strain FDAARGOS_1509	99.85
NIO_12c	**CMW**	**KX062386**	*Aeromonas caviae* strain YPL5-62	99.86
NIO_13a	**DMW**	**OM736153**	*Pseudomonas putida*	100.00
NIO_13b	**DMsed**	**KX062380**	*Aeromonas dhakensis* strain P21	99.00
NIO_14d	**DMsed**	**KR922404**	*Shewanella seohaensis* strain S7-3	99.86
NIO_14l	**DMsed**	**KX062385**	*Pseudomonas oleovorans* strain ROA037	99.85
NIO_14s	**DMsed**	**KX062383**	*Acinetobacter tandoii* strain INA2	99.62
NIO_14v	**CMW**	**KX062384**	*Acinetobacter* sp. Z-1	99.73
NIO_15c	**CMsed**	**OM736155**	*Aeromonas hydrophila* strain GX5	99.29
NIO_15d	**CMsed**	**KX062381**	*Acinetobacter johnsonii* strain ATCC 17909	98.90
NIO_15e	**CMsed**	**OP903265**	*Shewanella putrefaciens* strain L6-5	99.71
NIO_15h	**CMsed**	**OP903270**	*Aeromonas* sp. ASNIH1	99.64
NIO_15m	**CMsed**	**OP903271**	*Shewanella sp. XF3-1*	99.72
NIO_15p	**RSW**	**KX062382**	*Acinetobacter sp.* strain PS-1	99.61

Key: **CMW** Choraõ Mangrove water, **CMsed** Choraõ Mangrove sediment, **DMW** Divar Mangrove water, **DMsed** Divar Mangrove sediment, **RSW** Ribandar saltpan water

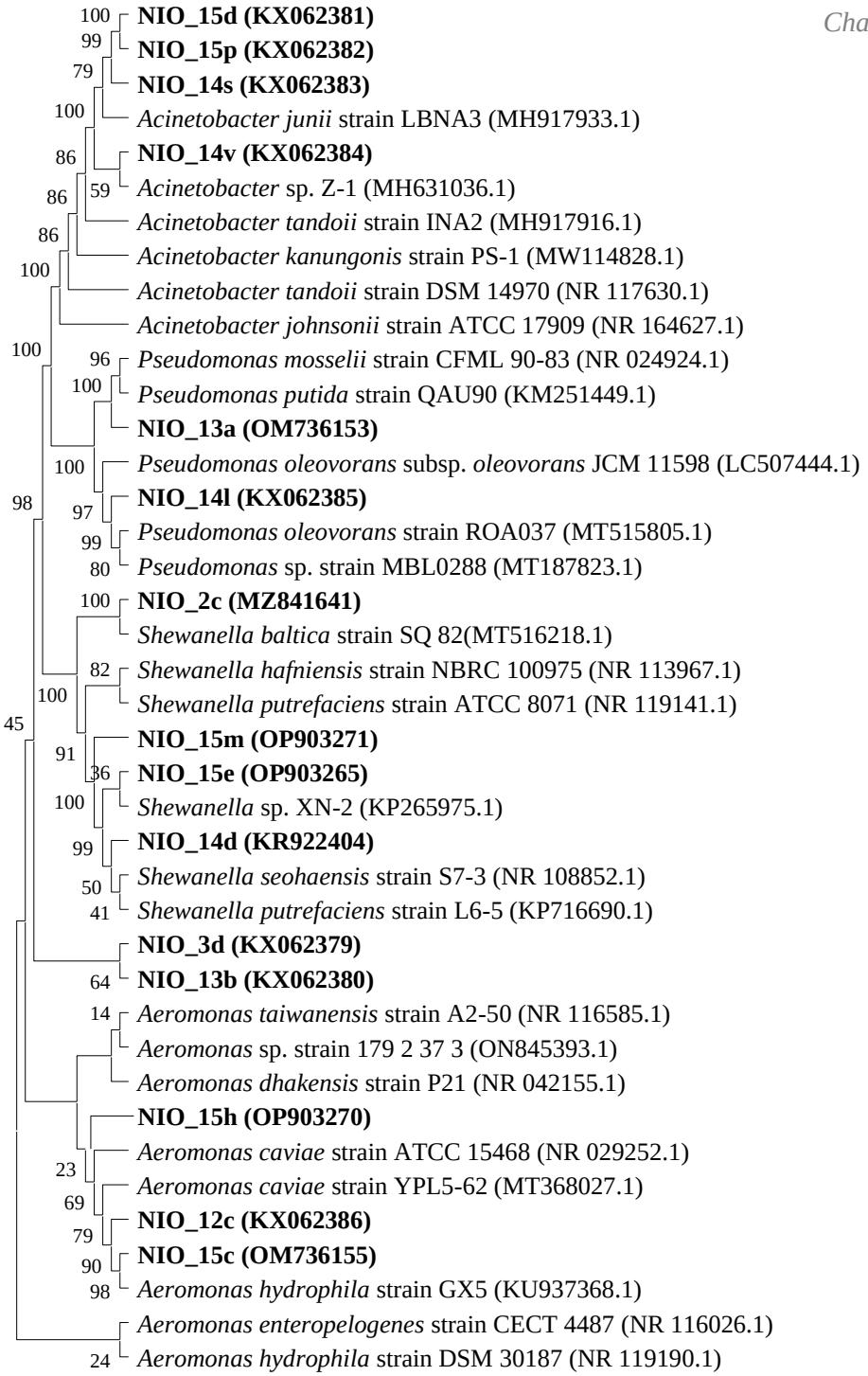


Figure 2.3: Phylogenetic tree showing relationship between dye decolorizing bacterial isolates obtained in this study. The tree was inferred from 16S rRNA sequence data obtained from GenBank database (accession number in parentheses) and constructed based on neighbour-joining (NJ) method. Bootstrap values were based on 1000 replicates and are shown as percentages at the branch nodes. Boldface type indicates isolate code of strains from this study, with the accession numbers given in brackets.

Table 2.6: Decolorization assay of reactive azo dyes at 100 mgL^{-1} (expressed as percent decolorization ± SD of three replicates)

Isolate	RB5	RG19	RR120	RBL163
NIO_2c	96.90 ± 0.26	88.63 ± 0.04	96.40 ± 0.01	86.80 ± 0.03
NIO_3d	94.71 ± 0.01	79.77 ± 0.14	84.76 ± 0.11	67.28 ± 0.13
NIO_12c	74.11 ± 0.13	71.00 ± 0.31	92.02 ± 0.13	63.80 ± 0.28
NIO_13a	82.00 ± 0.02	82.31 ± 0.22	97.00 ± 0.27	80.80 ± 0.15
NIO_13b	84.93 ± 0.01	84.53 ± 0.07	89.12 ± 0.09	75.37 ± 0.09
NIO_14d	**98.84 ± 0.04**	**99.47 ± 0.02**	**99.05 ± 0.11**	**88.85 ± 0.02**
NIO_14l	50.88 ± 0.04	81.05 ± 0.31	95.90 ± 0.21	66.00 ± 0.19
NIO_14s	58.70 ± 0.01	76.54 ± 0.25	85.84 ± 0.18	71.94 ± 0.11
NIO_14v	73.39 ± 0.11	71.32 ± 0.22	87.90 ± 0.20	72.11 ± 0.26
NIO_15c	85.40 ± 0.15	88.00 ± 0.19	90.24 ± 0.03	77.35 ± 0.23
NIO_15d	74.93 ± 0.01	89.17 ± 0.11	83.11 ± 0.12	80.04 ± 0.30
NIO_15e	95.14 ± 0.24	92.83 ± 0.24	95.84 ± 0.26	82.62 ± 0.17
NIO_15h	94.10 ± 0.17	94.05 ± 0.07	92.01 ± 0.09	61.00 ± 0.19
NIO_15m	86.22 ± 0.19	94.73 ± 0.03	96.34 ± 0.21	73.90 ± 0.25
NIO_15p	78.06 ± 0.28	89.83 ± 0.17	87.00 ± 0.30	60.04 ± 0.22

Table 2.7: Decolorization assay of reactive azo dyes at 250 mgL^{-1} (expressed as percent decolorization ± SD of three replicates)

Isolate	RB5	RG19	RR120	RBL163
NIO_2c	94.31 ± 0.05	81.11 ± 0.11	90.47 ± 0.20	69.00 ± 0.32
NIO_3d	92.00 ± 0.15	70.07 ± 0.09	76.32 ± 0.25	62.41 ± 0.08
NIO_12c	68.46 ± 0.17	69.13 ± 0.26	91.00 ± 0.02	48.03 ± 0.22
NIO_13a	77.04 ± 0.22	82.04 ± 0.01	94.32 ± 0.04	64.19 ± 0.15
NIO_13b	66.20 ± 0.36	76.28 ± 0.17	86.25 ± 0.19	66.16 ± 0.14
NIO_14d	**97.00 ± 0.06**	**96.39 ± 0.13**	**99.75 ± 0.03**	**71.05 ± 0.17**
NIO_14l	47.00 ± 0.03	72.14 ± 0.21	93.21 ± 0.30	42.76 ± 0.14
NIO_14s	45.24 ± 0.01	60.00 ± 0.03	77.30 ± 0.25	60.25 ± 0.19
NIO_14v	66.82 ± 0.18	60.01 ± 0.08	80.06 ± 0.06	61.30 ± 0.01
NIO_15c	82.72 ± 0.28	80.43 ± 0.25	88.03 ± 0.14	55.06 ± 0.02
NIO_15d	72.00 ± 0.15	82.33 ± 0.37	71.49 ± 0.18	68.41 ± 0.02
NIO_15e	93.10 ± 0.19	91.90 ± 0.15	92.81 ± 0.07	75.32 ± 0.26
NIO_15h	91.70 ± 0.21	92.79 ± 0.02	85.80 ± 0.13	47.15 ± 0.21
NIO_15m	83.02 ± 0.04	90.10 ± 0.06	90.12 ± 0.24	58.04 ± 0.03
NIO_15p	71.16 ± 0.23	85.13 ± 0.04	83.14 ± 0.05	55.00 ± 0.27

Table 2.8: Decolorization assay of reactive azo dyes at 500 mgL^{-1} (expressed as percent decolorization ± SD of three replicates)

Isolate	RB5	RG19	RR120	RBL163
NIO_2c	90.00 ± 0.15	75.45 ± 0.22	84.94 ± 0.06	63.24 ± 0.23
NIO_3d	90.67 ± 0.03	54.38 ± 0.26	62.01 ± 0.23	35.97 ± 0.17
NIO_12c	35.41 ± 0.04	66.80 ± 0.14	79.14 ± 0.21	33.04 ± 0.03
NIO_13a	40.00 ± 0.16	80.17 ± 0.02	63.19 ± 0.17	58.72 ± 0.05
NIO_13b	37.04 ± 0.37	72.00 ± 0.17	49.34 ± 0.01	40.05 ± 0.12
NIO_14d	**97.31 ± 0.01**	**95.30± 0.22**	**98.48 ± 0.16**	**66.19 ± 0.08**
NIO_14l	43.06 ± 0.19	48.36 ± 0.27	72.00 ± 0.21	31.97 ± 0.08
NIO_14s	37.24 ± 0.03	39.76 ± 0.23	54.03 ± 0.27	55.41 ± 0.08
NIO_14v	56.22 ± 0.07	58.11 ± 0.31	65.18 ± 0.22	52.74 ± 0.16
NIO_15c	80.34 ± 0.21	76.00 ± 0.15	60.01 ± 0.18	41.92 ± 0.09
NIO_15d	62.99 ± 0.23	71.19 ± 0.09	55.55 ± 0.03	64.00 ± 0.31
NIO_15e	87.10 ± 0.05	90.00 ± 0.03	62.97 ± 0.04	57.55 ± 0.22
NIO_15h	90.03 ± 0.12	85.40 ± 0.25	78.00 ± 0.11	41.03 ± 0.17
NIO_15m	73.02 ± 0.37	89.95 ± 0.24	87.62 ± 0.17	36.21 ± 0.12
NIO_15p	61.78 ± 0.04	67.08 ± 0.15	80.93 ± 0.03	46.20 ± 0.04

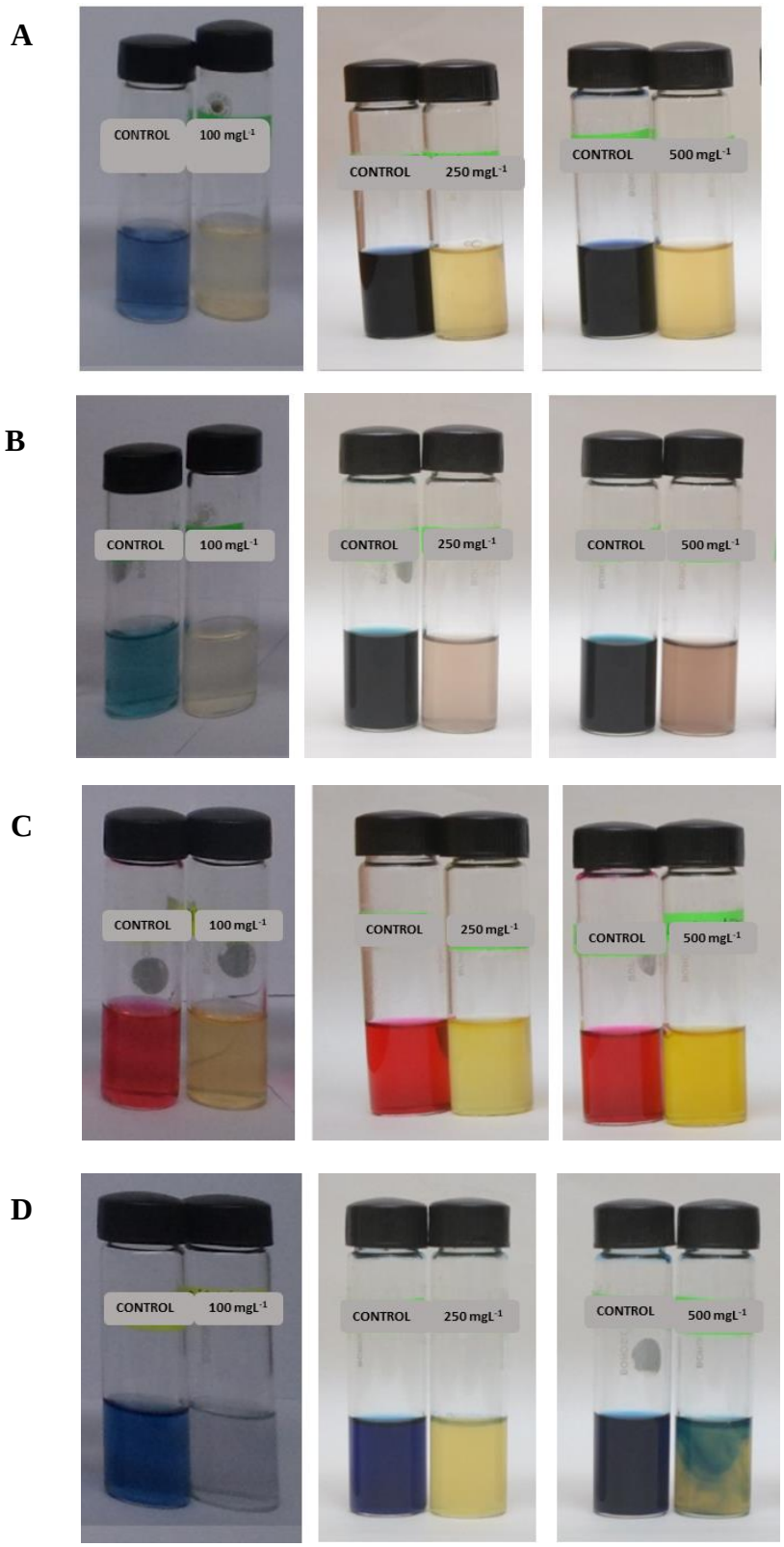


Figure 2.4: Primary decolorization assay of (A) RB5 (B) Reactive Green 19 (C) Reactive Red 120 (D) Reactive Blue 163 using *Shewanella seohaensis* NIO_14d

2.4 Discussion

Marine ecosystems are constantly under the influence of changing physical, chemical and biological parameters. Physical conditions such as temperature. pH, salinity and turbulence have a singificant effect on these environments (Lenihan, 1999; Varadharajan and Soundarapandian, 2014). The changes in physical processes can affect the water quality and this in turn can bring about changes in the spatio-temporal nutrient distribution as well as existing biological communities.

The complex and extremely productive mangrove ecosystems are subject to varying influences of biotic and abiotic environmental factors. These dynamic intertidal ecosystems are native to tropical and subtropical regions of the world. The rich, diverse microbial populations found in these habitats have significant impacts on the biogeochemical cycles occurring in these environments (Thorsten *et al*., 2001). Microbial species from these habitats are conferred with specialized physiological adapations because of the unique physico-chemical properties of the marine ecosystems where they occur (Raghukumar, 2008). Seasonal variations along with cyclic tides result in fluctuations in parameters especially salinity in the estuarine/mangrove environment. Similarly, hypersaline saltpans are frequently intermixed with tidal freshwater, brackish, and saltwater marshes (Linhoss and Underwood, 2016). These factors largely contribute to the biological diversity of these areas and presents a large collection of microorganisms with unknown and as yet unexplored techological potential (Thatoi *et al.*, 2013).

As a result of the use of a large amount of salt in dye industries, azo dye decolorization is often needed under hypersaline environments and low dissolved oxygen (Guo *et al*., 2020). Notwithstanding the deficiencies of bacterial enumeration using plate counts, culturable bacteria are useful to obtain insights on occurrence of certain bacteria as well as the isolation of potential bioremediators (Stanley and Konopka, 1985). An understanding of bacterial incidence is therefore important to understand the population dynamics in a given ecosystem. Measurment of the bacterial TVC in aquatic systems helps to evaluate the quality of the water and their relationship with relevant environmental factors. Ramaiah *et al*., (2007) have investigated the effects of raw sewage

disposal into the Mandovi estuary and published multiple reports (Ramaiah *et al*., 2001, 2002) of the presence of allochthonous microflora. The aspects of coastal pollution surveillance through bacterial incidence has been investigated in nearby tropical estuaries (Nagvenkar and Ramaiah, 2010). Further, D'Souza *et al*., (2006) and Verma *et al*., (2010) have isolated marine fungi from decaying wood obtained in Choraõ mangroves to treat textile wastewater. However, there are no reports outlining azo dye decolorizing bacteria in autochthonous populations from the sampling sites in this study. Keeping in mind that samples were collected during summer, the lower bacterial abundance in saltpans as compared to mangroves is possibly attributed to the adaptation of a limited number of bacteria to the extreme hypersaline environment.

The occurrence of dye decolorizing bacteria and fungi from various sources has been reported by several researchers (Stolz, 2001; Ali, 2010; Khan *et al.*, 2013; Bharathi *et al.*, 2022). Some of the bacterial and fungal strains characterized with dye decolorizing ability belong to genera such as *Bacillus* (Kumar *et al*. 2019), *Aeromonas* (Ji *et al.*, 2020; Du *et al.*, 2015), *Pseudomonas* (Mendes *et al.*, 2011; Bera and Tank, 2021), *Klebsiella* (Holkar *et al*., 2018), *Aspergillus* (Asses *et al.*, 2018), *Penicillium* (Gou *et al*., 2009), *Pleurotus* (Hadibarata *et al.*, 2013) and *Trametes* (Si *et al.*, 2013). Although most of these reports outline strains isolated from sites contaminated with dye effluents, there is a need for the biodiscovery of potential dye decolorizing bacteria from other environments. This provides opportunities to isolate and identify possible strains possessing new mechanisms and/or combinations of mechanisms of action as well as the unique properties marine environments confer on such bacteria. Saltpans are a largely under evaluated niche for the isolation of microorganisms with bioremediation potential. Pereira *et al*., (2013) isolated and characterized metal-tolerant bacterial strains from the Ribandar salt pans. Analysis of the mechanisms of metal removal indicated sulphate reduction pathways employed by these bacterial strains. Microorganisms use reductive mechanisms for bioremediation of various toxic and hazardous compounds including in detoxifying azo dye.

Of the 210 morphologically distinct bacterial colonies isolated from water and sediment of mangrove and saltpan samples, 15 isolates showed clear zones of decolorization on Mineral salt agar plates amended with 200 mgL^{-1} of reactive dyes. In an attempt to

explore bacterial isolates capable of decolorizing reactive azo dyes, bacteria belonging to four different genera, *Aeromonas, Acinetobacter, Pseudomonas and Shewanella*, were obtained in this study. The biochemical and morphological tests supported molecular identification and the bacterial strains showed major phenotypic characteristics of the related genera. All the isolates were positive for the production of catalase and were capable of utilizing glucose. Variations in responses were observed for the production of other physiological enzymes as well as utilization of lactose, arabinose and sorbitol. The isolates were mesophilic in nature which is typical of marine bacteria and their growth range was similar to the temperature and pH ranges of the collected samples.

Marine prokaryotes exhibit ecological resilience due to their constant exposure to fluctuating factors such as pH, salinity, sea surface temperature, water currents, precipitation and wind speed. While some of them undergo physical adaptations, many have the genetic capacity to perceive, process and integrate external stimuli, enabling them to rapidly adapt to changing environmental conditions (Lauro *et al*., 2009). As a result, they effectively regulate nutrient levels, including the influx and excretion of toxic chemicals. Numerous studies have documented the ability of marine bacteria to metabolize, break down or accumulate harmful substances (Dash et al., 2013). All the isolates evaluated rapidly decolorized 100 mgL^{-1} of the reactive azo dyes within 24 hours. This decolorization ability was retained in most of the isolates with an increase in the dye concentration to 500 mgL^{-1}. The strain NIO_14d showed the maximum dye decolorization and exhibited a decolorization percent of more than 95% even when exposed to higher dye concentrations. Although various bacterial species have been shown to decolorize and detoxify azo dyes (Ali, 2010), the structural complexity and high molecular weight of azo dyes results in a reduced efficiency of decolorization (Pearce *et al*., 2003). This study yielded a promising bacterial strain which is subjected to further molecular characterization experiments in order to understand the factors contributing to its ability to efficiently decolorize the reactive azo dyes tested.

To summarize, 15 bacterial isolates belonging to as many as 4 different readily cultivable genera were observed to have azo dye decolorizing potential. Although they cannot fully represent the functional and phylogenetic diversity that exists, these findings provide

insights into the dominant bacterial classes possessing inherent dye decolorizing capabilities. The primary advantage of cultivating these bacteria lies in the establishment of pure cultures, a prerequisite for marine biodiscovery, enabling their utilization in experimental investigations (Joint *et al.*, 2010). The results of this study suggest that the identification of dye decolorizing bacteria from mangrove and saltpan sources contributes to our understanding of the distribution of bacteria with dye decolorizing potential across diverse environmental settings. Moreover, these naturally occurring dye decolorizing bacterial isolates hold considerable promise as prospective candidates for the development of efficient bioremediation systems aimed at treating textile azo dye contaminated wastewater.

Chapter 3

Optimization of Azo Dye Removal by Dye Decolorizing Bacteria

Chapter 3

Optimization of Azo Dye Removal by Dye Decolorizing Bacteria

3.1 Introduction

Azo dyes are amongst the most prevalent class of synthetic dyes produced globally. They are predominantly used in textile, food, pharmaceutical, paper, leather and cosmetic industries (Chang and Lin, 2001). Azo dyes are aromatic compounds possessing one or more azo (-N=N-) groups and are a preferred class of synthetic dyes because of their chemical stability and ease of synthesis (Rafii *et al*., 1997). The presence of azo dyes in wastewater is concerning due to their recalcitrance, color and potential toxicity (Yoo *et al*., 2000). To date, many bacteria with dye decolorizing potential have been evaluated from different ecological niches (Pinheiro *et al*., 2022; Zafar *et al*., 2022; Pandey *et al*., 2007). Most have been isolated from dye containing wastewater and contaminated environments (Mahmood *et al*., 2011) but there also exist reports of dye decolorizing bacteria from uncontaminated environments (Khalid *et al*., 2012). Effective decolorization and degradation of azo dyes by microorganisms depends on several factors such as pH, temperature, aeration, dye concentration, chemical nature of dye, ionic strength of the system, nutrient components and type of microorganism used (Renganathan *et al*., 2006; Modi *et al*., 2010; Ambrósio *et al*., 2012; Singh *et al*., 2014). Kumar *et al.,* (2019) reported that the optimum values of various process parameters must be assessed in order to achieve successful decolorization and removal of azo dyes. Optimization of medium components by replacing constituents is a widely used method to determine the ideal sources of carbon and nitrogen for microbial bioremediation (Eskandari *et al*., 2019). This chapter focuses on the evaluation of various physico-chemical process parameters and medium components in order to obtain maximally efficient reactive azo dye decolorization by the isolate under study.

3.2 Materials and Methods

The optimization studies for maximum azo dye decolorization were carried out for the isolate *Shewanella seohaensis* NIO_14d which showed the highest decolorization potential as observed in the primary decolorization studies in Chapter 2.

3.2.1 Growth and decolorization assay of the dye decolorizing bacterial isolate

The growth profile and rate of decolorization by the dye decolorizing bacterial strain *Shewanella seohaensis* NIO_14d was measured spectrophotometrically. Erlenmeyer flasks (500 mL) containing 250 mL of sterile nutrient broth supplemented with reactive azo dyes RB5, RG19 and RR120 (Sigma-Aldrich) were inoculated with 1% (v/v) of pre-grown culture of *Shewanella seohaensis* NIO_14d. The dyes were added at a concentration of 100 mg L^{-1}. The flasks were incubated at 30°C under static conditions and samples were aliquoted every 3 hours. The samples were then centrifuged at 12,000 rpm for 10 minutes at 4°C and the cell-free supernatant color was read at the wavelength of maximum absorption of the dyes used, i.e. 597 nm for RB5, 630 nm for RG19 and 522 nm for RR120, using a Shimadzu UV-1800 spectrophotometer (Kyoto, Japan). Growth rate was measured by determining the absorbance of the culture sample at 600 nm (Dong *et al.*, 2003). Controls without dye and/or inoculum were maintained under identical conditions.

3.2.2 Optimization of various growth conditions for maximum dye decolorization

Various parameters such as the effect of medium components and physico-chemical parameters were analyzed in order to obtain maximum rate of azo dye removal. All optimization studies were carried out using three reactive azo dyes viz. RB5, RG19 and RR120 (Sigma-Aldrich), individually and a combination of the three dyes in a final concentration of 100 mg L^{-1} unless described otherwise. Aliquoted samples were centrifuged at 12,000 rpm for 10 minutes at 4°C and the cell-free supernatant was used to measure decolorization spectrophotometrically at the wavelength of maximum absorption of the dyes used, i.e. 597 nm for RB5, 630 nm for RG19, 522 nm for RR120 and 550 nm for dye combination.

The percentage of decolorization was calculated using the following equation:

$$\text{Decolorization (\%)} = \frac{A_{\lambda,\text{initial}} - A_{\lambda,\text{final}}}{A_{\lambda,\text{initial}}} \times 100$$

where, $A_{\lambda,\text{ initial}}$ = initial absorbance and $A_{\lambda,\text{ final}}$ = absorbance after incubation

3.2.2.1 *Effect of aeration*

Studies were carried out to determine the effect of oxygen on dye decolorization. Erlenmeyer flasks (250 mL) containing 100 mL of sterile nutrient broth supplemented with reactive azo dyes were inoculated with 1% (v/v) of pre-grown culture. The flasks were incubated at 30°C under static as well as shaker (150 rpm) conditions. Following 24 h incubation, decolorization was measured spectrophotometrically. Control was maintained for each condition without inoculating bacterial cells.

3.2.2.2 *Effect of pH*

The effect of varying pH on dye decolorization was tested in a pH range from 4 to 10. Here, 100 mL sterile nutrient broth of pH 4 - 10 was prepared and amended with 100 mg L^{-1} of the reactive dyes. The pH was adjusted with 1N HCl or 1N NaOH. The pH was maintained using specific buffer systems as mentioned: Citrate buffer (pH 4 and 5), phosphate buffer (pH 6, 7 and 8) and bicarbonate buffer (pH 9 and 10). Flasks were individually inoculated with 1% (v/v) of overnight grown culture and incubated at 30°C under static condition. The uninoculated dye free culture medium was used as a control under the same incubation conditions. After 24 hours incubation, aliquots of the culture were centrifuged at 12,000 rpm for 10 min at 4°C and the cell-free supernatant color was read at the maximum absorption wavelength for the respective dyes to calculate the percentage of decolorization.

3.2.2.3 *Effect of temperature*

Dye decolorization by the bacterial isolate was examined in the temperature range of 10°C - 50°C. Sterile nutrient broth (100 mL) with a final concentration of 100 mg L^{-1} of the reactive dye was inoculated with 1% (v/v) of pre-grown culture and incubated at 10, 20, 30, 40 and 50 °C under static conditions. After 24 hours of incubation, aliquots of the

culture were centrifuged at 12,000 rpm for 10 min at 4°C and the cell-free supernatant color was read at the maximum absorption wavelength for the respective dyes to calculate the percentage of decolorization. Uninoculated dye solutions were maintained as controls.

3.2.2.4 *Effect of dye concentration*

Studies were carried out to analyse the ability of the isolate to decolorize dyes of varying concentrations. The effect of dye concentration on the extent of decolorization was determined for the reactive dyes RB5, RG19, RR120 and for a combination of dyes. Flasks containing 100 mL sterile nutrient broth were prepared and the reactive dyes were individually added to give final concentrations of 50, 100, 250, 500, 750, 1000, 2000 and 5000 mg L^{-1}. The pre-grown bacterial culture (1% [v/v]) was added to the test flasks and incubated at 30°C under static condition. Uninoculated dye solutions were maintained as controls. Decolorization was monitored by measuring the absorbance of the decolorized broth after 24 hours and calculated as percentage of decolorization.

3.2.2.5 *Effect of medium strength*

In order to determine the optimum nutrient strength for dye decolorization, sterile nutrient broth (100 mL) was prepared in the following concentrations: 10%, 25%, 50%, 75% and 100% and amended with 100 mg L^{-1} of the reactive dyes. The pre-grown bacterial culture (1% [v/v]) was added to the test flasks and incubated at 30°C under static condition. Uninoculated dye solutions were maintained as controls. Decolorization was monitored by measuring the absorbance of the decolorized broth after 24 hours and calculated as percentage of decolorization.

3.2.2.6 *Effect of Carbon source*

To study the effect of various carbon sources on dye decolorization, a sterile mineral salt medium (100 mL) amended with 100 mg L^{-1} of the reactive dyes was prepared. The appropriate carbon sources (glucose, sucrose, lactose, xylose and starch) were added at a final concentration of 5 g L^{-1}. The pre-grown bacterial culture (1% [v/v]) was added to the test flasks and incubated at 30°C under static condition. Uninoculated dye solutions were maintained as controls. Decolorization was monitored by measuring the absorbance of the decolorized broth after 24 hours and calculated in terms of percentage.

3.2.2.7 *Effect of Nitrogen source*

The effect of different organic and inorganic nitrogen co-substrates on rate of dye decolorization was also analyzed. The nitrogen sources used were ammonium sulfate, urea, yeast extract, peptone, tryptone and casein at a concentration of 5 g L^{-1} and added to 100 mL of a sterile mineral salt medium amended with 100 mg L^{-1} of the reactive dyes. The pre-grown bacterial culture (1% [v/v]) was added to the test flasks and incubated at 30°C under static condition. Uninoculated dye solutions were maintained as controls. Decolorization was monitored by measuring the absorbance of the decolorized broth after 24 hours and calculated in terms of percentage.

3.2.2.8 *Effect of electron donors*

The ability of the isolate under study to decolorize reactive azo dyes in the presence of various electron donors was studied. The effect of five different electron donors (formate, lactate, acetate, pyruvate and succinate) on the rate of dye decolorization was determined. Sterile nutrient broth (100 mL) amended with 100 mg L^{-1} of the reactive dyes was prepared. Each of the electron donors were added in the form of their salts at a concentration of 20 mM. The pre-grown bacterial culture (1% [v/v]) was added to the test flasks and incubated at 30°C under static condition. Uninoculated dye solutions were maintained as controls. Decolorization was monitored by measuring the absorbance of the decolorized broth after 24 hours incubation and calculated in terms of percentage.

3.2.2.9 *Effect of NaCl concentration*

In an effort to determine the optimum NaCl concentration to facilitate maximum azo dye decolorization, a sterile mineral salt medium (100 mL) containing varying NaCl concentrations of 0-25% with an increment of 5% NaCl was prepared. The reactive dyes were added to give a final concentration of 100 mg L^{-1}. The pre-grown bacterial culture (1% [v/v]) was added to the test flasks and incubated at 30°C under static condition. Uninoculated dye solutions were maintained as controls. Decolorization was monitored by measuring the absorbance of the decolorized broth after 24 hours incubation and calculated in terms of percentage.

3.2.3 Decolorization of reactive azo dyes in presence of heavy metals

The ability of *Shewanella seohaensis* NIO_14d to decolorize azo dyes in the presence of various heavy metals was determined. The heavy metals studied were chromium, cadmium, lead, copper and nickel. Decolorization studies were carried out in sterile nutrient broth (100 mL) amended with the respective heavy metal salt at a final concentration of 100 µg mL^{-1}. The reactive dyes were added to give a final concentration of 100 mg L^{-1}. The pre-grown bacterial culture (1% [v/v]) was added to the test flasks and incubated at 30°C under static condition. Uninoculated dye solutions were maintained as controls. Decolorization was monitored by measuring the absorbance of the decolorized broth after 24 hours incubation and calculated in terms of percentage.

3.3 Results

The isolate NIO_14d used for optimization studies of maximum azo dye removal was identified as *Shewanella seohaensis* NIO_14d with GenBank accession number KR922404. The pure culture of the isolate was deposited at the Microbial Type Culture Collection (MTCC) of the CSIR-Institute of Microbial Technology, Chandigarh, India, under the accession number MTCC 25079.

3.3.1 Growth and decolorization assay of the dye decolorizing bacterial isolate

The growth profile of *Shewanella seohaensis* NIO_14d and extent of decolorization of the three reactive dyes in dye-amended nutrient broth suggest rapid decolorization (**Figure 3.1**). The culture achieved substantial decolorization of all three reactive dyes in the initial 3 hours of incubation with the dye itself.

In case of RB5, rapid decolorization (84.33%) was seen within the initial 3 hours and a maximum decolorization of 98.31% was achieved by 20 hours. Similarly, for RG19, decolorization of 78.5% was seen after 3 hours incubation of the culture with the dye whereas a maximum of 91.49% was achieved in 23 hours. Maximum decolorization of 97.07% of RR120 happened within 17 hours. It was observed that there was concomitant reduction in color of the reactive dyes along with active cell growth and considerable decolorization occurred in the early stages of growth.

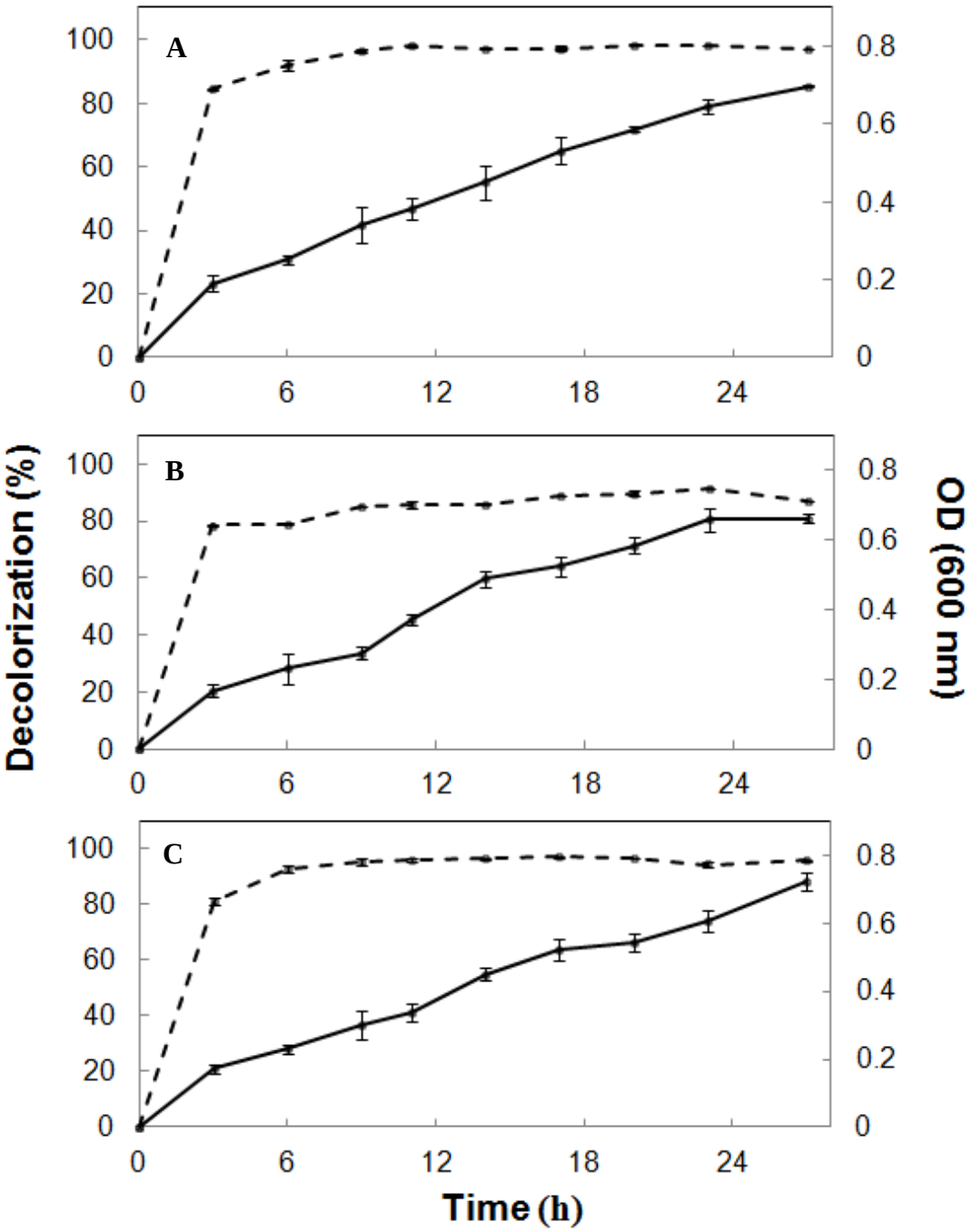


Figure 3.1: Growth curve (solid line) and decolorization percent (dashed line) of *Shewanella seohaensis* NIO_14d in nutrient broth amended with 100 mg L^{-1} of (**A**) Reactive Black 5 (**B**) Reactive Green 19 (**C**) Reactive Red 120. Data are expressed as mean ± standard deviation (SD) of three replicate experiments.

3.3.2 Optimization of various growth conditions for maximum dye decolorization

3.2.2.1 *Effect of aeration*

As seen in **Figure 3.2**, aeration has an effect on the extent of decolorization of reactive azo dyes. Although decolorization was achieved in both shaker as well as static conditions, a higher percent decolorization was observed under static conditions for the tested dyes individually and in combination. The isolate was able to decolorize more than 85% of the dyes individually and in combination.

3.2.2.2 *Effect of pH*

It was observed that dye decolorization was affected by the pH of the growth medium. A pH in the range of 6 to 9 was found to be optimum for maximum decolorization of the reactive azo dyes rather than extreme acidic or alkaline pH (**Figure 3.3**). The isolate was capable of decolorizing the individual and combination of test dyes at higher pH but not under acidic conditions of pH 5 and below.

3.2.2.3 *Effect of temperature*

This study indicated that dye decolorization occurs optimally in the mesophilic temperature range of 30°C to 40°C with more than 85% decolorization of dyes achieved within 24 hours (**Figure 3.4**).

3.2.2.4 *Effect of dye concentration*

The results (**Figure 3.5**) indicated the ability of the bacterial strain, *Shewanella seohaensis* NIO_14d to considerably decolorize varying concentrations of reactive dyes as well as a combination of dyes. At increased dye concentration of 2000 mg L^{-1}, decolorization of 90% (for RB5), 85% (for RG19), 92% (for RR120) and 79% (for a combination of dyes) was achieved. Interestingly, even at very high dye concentrations (5000 mg L^{-1}), the strain showed substantial decolorization of more than 70% of the reactive dyes (RB5, RG19, RR120 and a combination thereof) with 93.46% of RR120 being decolorized.

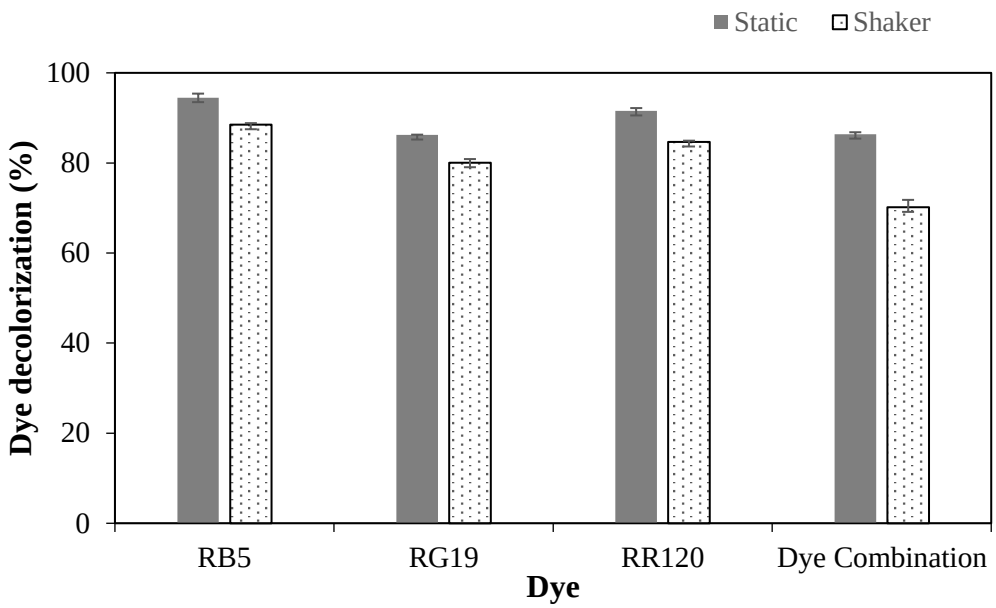


Figure 3.2: Effect of aeration on the extent of decolorization by *Shewanella seohaensis* NIO_14d in nutrient broth amended with reactive dye (100 mg L^{-1}). Data are expressed as mean ± standard deviation (SD) of three replicate experiments.

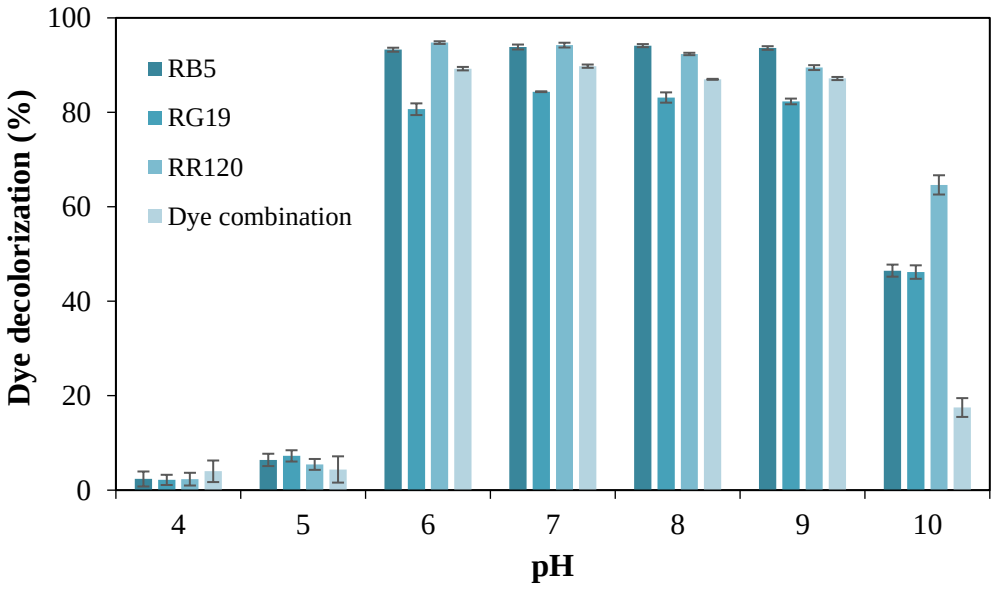


Figure 3.3: Effect of pH on the extent of decolorization by *Shewanella seohaensis* NIO_14d in nutrient broth amended with reactive dye (100 mg L^{-1}). Data are expressed as mean ± standard deviation (SD) of three replicate experiments.

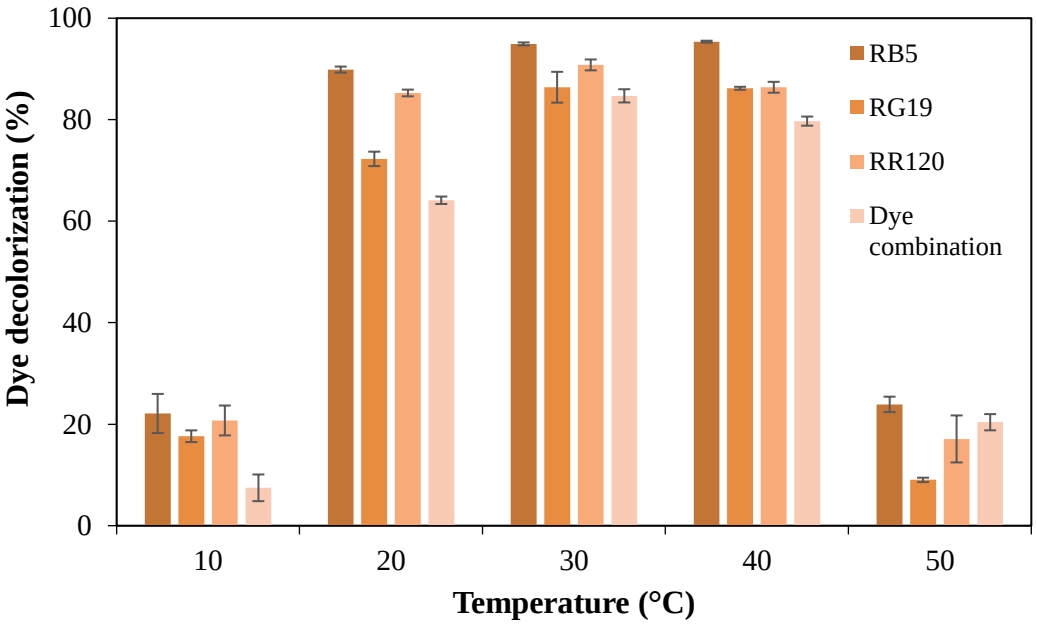


Figure 3.4: Effect of temperature on the extent of decolorization by *Shewanella seohaensis* NIO_14d in nutrient broth amended with reactive dye (100 mg L^{-1}). Data are expressed as mean ± standard deviation (SD) of three replicate experiments.

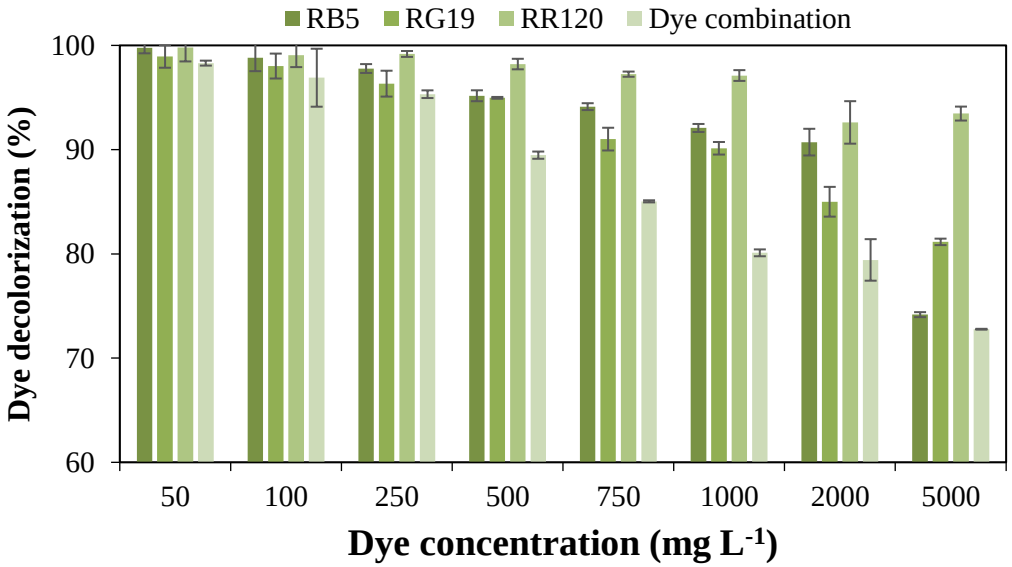


Figure 3.5: Effect of dye concentration on the extent of decolorization by *Shewanella seohaensis* NIO_14d in nutrient broth amended with reactive dye. Data are expressed as mean ± standard deviation (SD) of three replicate experiments.

3.2.2.5 *Effect of medium strength*

Shewanella. seohaensis NIO_14d was also capable of decolorizing reactive azo dyes in nutrient media of different strengths. Experimental results indicated that a 10% diluted nutrient medium was unfavorable for decolorization with the isolate capable of decolorizing only about 50% of the reactive dyes. Under low strength nutrient media, there were lower rates of decolorization and the extent of decolorization increased concomitantly with increasing medium strength (**Figure 3.6 (A)**).

3.2.2.6 *Effect of Carbon source*

The results as seen in **Figure 3.6 (B)** indicated the ability of the bacterial strain, *Shewanella seohaensis* NIO_14d to appreciably decolorize reactive dyes in the presence of various sugars. It was observed that of all the dyes tested, individually and in combination, the dye RR120 showed the highest decolorization (> 80%) irrespective of the sugar supplemented in the growth medium. Similarly, the sugar provided in the medium did not impact the decolorization of RG19 with more than 70% of the dye being decolorized. The isolate decolorized 72% of the mixture of dyes when grown in the presence of starch.

3.2.2.7 *Effect of Nitrogen source*

Different organic and inorganic nitrogen co-substrates present in the growth medium had a more significant effect on the dye decolorization. The presence of yeast extract, peptone or tryptone in the growth medium allowed the isolate to efficiently decolorize more than 80% of the reactive dyes within 24 hours (**Figure 3.6 (B)**). Only RB5 showed considerable decolorization when grown in media supplemented with inorganic nitrogen substrates such as urea and ammonium sulphate.

3.2.2.8 *Effect of electron donors*

The results represented in **Figure 3.7 (A)** show the ability of the bacterial strain, *Shewanella seohaensis* NIO_14d to considerably decolorize reactive dyes as well as a combination of dyes in the presence of various electron donors. Experimental results indicated that succinate and pyruvate enhanced the effects of dye decolorization as compared to the other electron donors. The strain showed decolorization of more than 87% of the reactive dyes (RB5, RG19 and RR120) when tested with succinate and pyruvate. Of the compounds studied, acetate was the least efficient at augmenting the

decolorization process with decolorization for a combination of dyes of as low as 51.92%.

3.2.2.9 *Effect of NaCl concentration*

As *Shewanella seohaensis* NIO_14d was a salt tolerant bacterial isolate from an estuarine source, we expected it to decolorize reactive dyes even in the presence of higher concentrations of NaCl. As recorded in **Figure 3.7 (B)**, in a medium lacking NaCl, the isolated achieved up to 99% decolorization of the individual dyes and dye combination. Further, in a medium containing 1% (w/v) NaCl, the isolate still decolorized more than 90% of the reactive dyes and dye combination. However, when the concentration of NaCl in the medium was increased to 10% (w/v) and further to 15% (w/v), the extent of dye decolorization significantly decreased. The isolate showed very limited growth at 20% (w/v) NaCl concentration and hence no dye decolorization was observed.

3.2.3 *Dye decolorization in the presence of heavy metals*

From **Figure 3.7 (C)**, it was seen that *Shewanella seohaensis* NIO_14d showed the ability to decolorize azo dyes in the presence of heavy metal salts. In general, the heavy metals did not adversely affect the decolorization activity of the isolate with more than 80% dye decolorization achieved. There was a slight reduction in decolorization activity in the presence of lead.

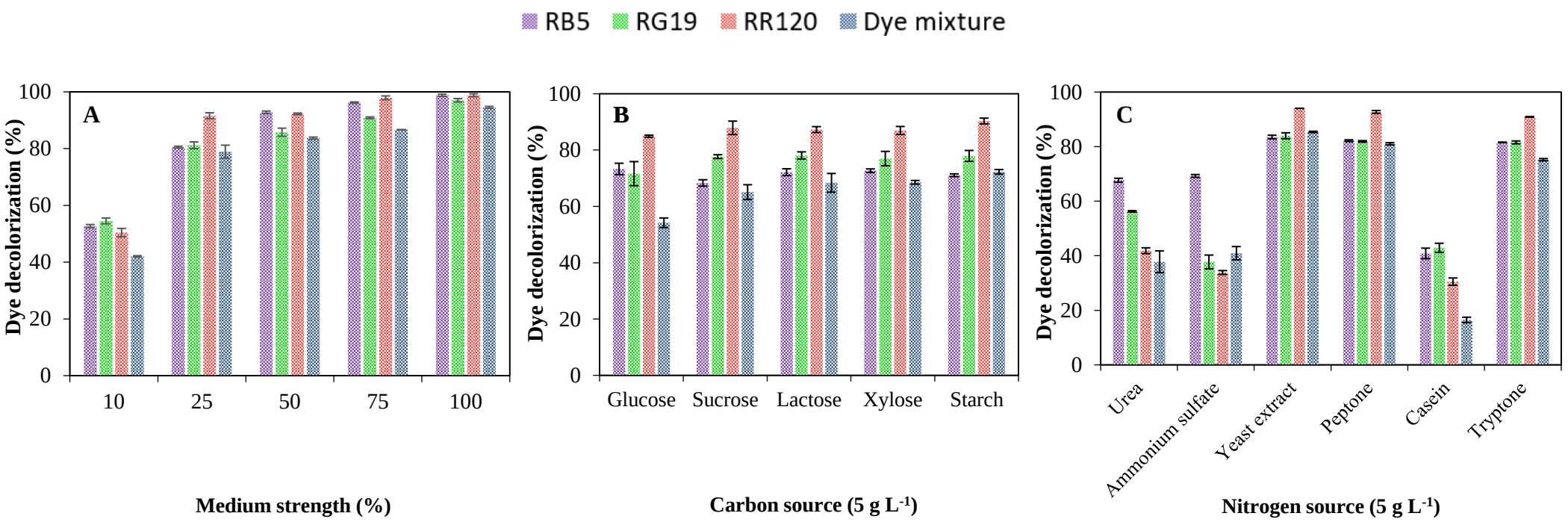


Figure 3.6: Effect of different (**A**) medium strengths (**B**) carbon sources and (**C**) nitrogen sources on the extent of decolorization by *Shewanella seohaensis* NIO_14d in nutrient broth amended with reactive dye (100 mg L^{-1}). Data are expressed as mean ± standard deviation (SD) of three replicate experiments.

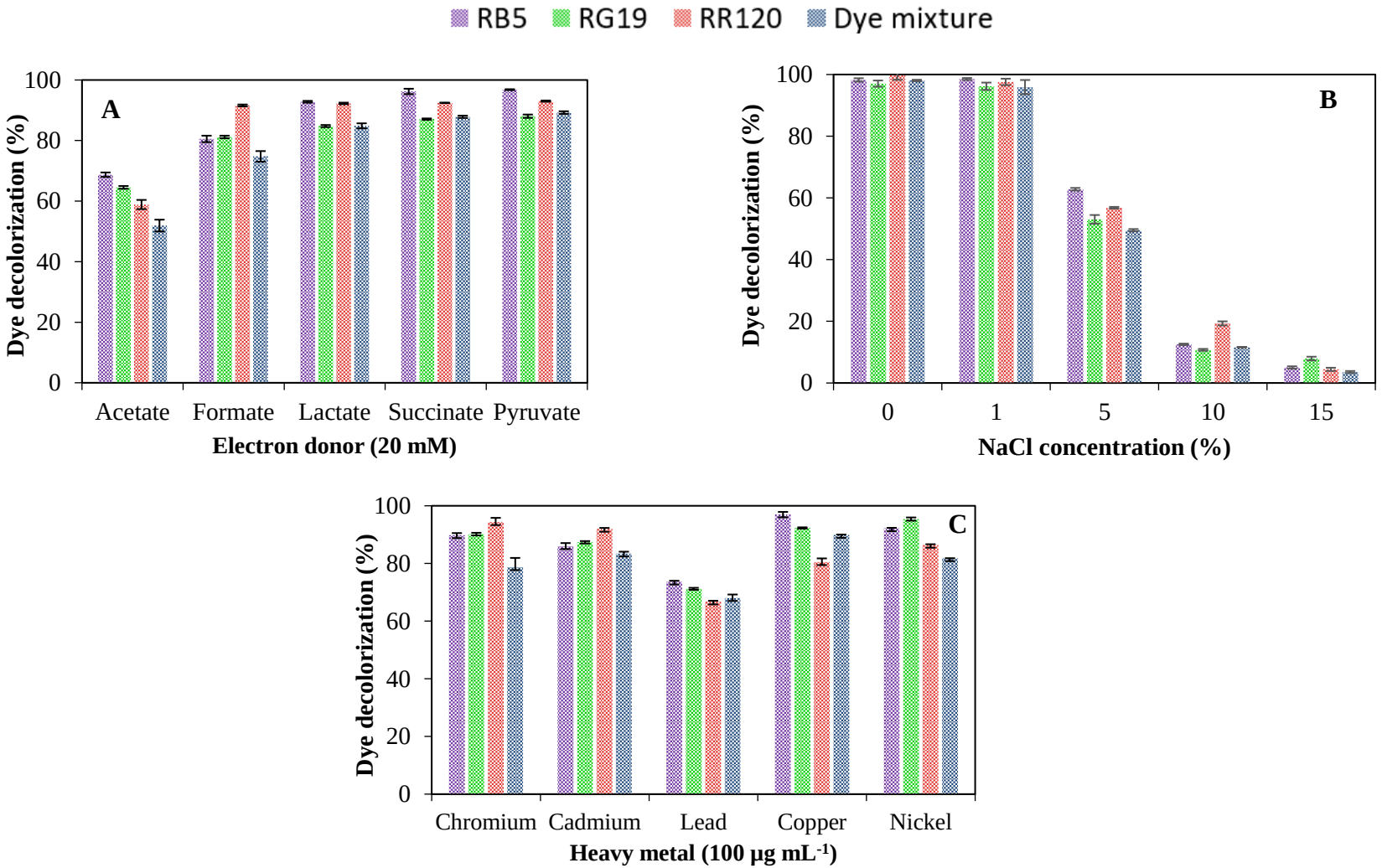


Figure 3.7: Effect of various (**A**) electron donors (**B**) NaCl concentrations and (**C**) heavy metals on the extent of decolorization by *Shewanella seohaensis* NIO_14d in nutrient broth amended with reactive dye (100 mg L^{-1}). Data are expressed as mean ± standard deviation (SD) of three replicate experiments.

Table 3.1: Optimum parameters for maximum decolorization of reactive azo dyes, individually and in combination

Parameter	RB5	RG19	RR120	Dye combination
Aeration	Static	Static	Static	Static
pH	8	7	6	7
Temperature (°C)	40	30	30	30
Dye concentration (mg L^{-1})	50	50	50	50
Medium strength (%)	100	100	100	100
Carbon source	Glucose	Lactose	Starch	Starch
Nitrogen source	Yeast extract	Yeast extract	Yeast extract	Yeast extract
Electron donor	Succinate/ Pyruvate	Pyruvate	Pyruvate	Pyruvate
NaCl concentration (%)	0 - 5	0	0	0

3.4 Discussion

Of the 15 isolates sourced from mangroves and saltpan environments, *Shewanella seohaensis* NIO_14d was the most promising isolate with the ability to rapidly decolorize more than 90% of all the reactive azo dyes tested. This bacterial isolate was selected to study the optimum operational parameters for maximum azo dye decolorization. Microorganisms have undergone processes such as isolation, selection, mutation and genetic engineering to enable efficient bioremediation. These techniques, as highlighted by Renner (1997) and Pieper and Reineke (2000), have resulted in microorganisms with the enhanced capability to degrade persistent pollutants and exhibit improved rates of degradation for specific target substances.

Time course of cell growth and color removal indicated that maximum decolorization by the isolate occurred in the first three hours of contact with the reactive dyes RB5, RG19 and RR120. In contrast to previous findings by Wu *et al*. (2009), the bacterial strain isolated in the present study demonstrated highly efficient decolorization capabilities. Within a short time of 23 hours, it successfully decolorized over 90% of RG19, while RR120 was decolorized by more than 90% in just 6 hours. In the aforementioned study, Wu *et al*. observed that *Shewanella oneidensis* WL-7 achieved only 36% decolorization rate of 100 µM of RB5 in approximately 12 hours. The level of decolorization of 100 mgL^{-1} reactive azo dye achieved by *Shewanella seohaensis* NIO_14d in this study is higher than that reported for other bacterial strains including *Bacillus cereus, Trichosporon beigelii* NCIM-3326, *Pseudomonas aeruginosa, Micrococcus glutamicus, Exiguobacterium sp. and Streptomyces krainskii* SUK-5 (Modi *et al*., 2010; Saratale *et al*., 2009a, b; Silveira *et al*., 2009; Dhanve *et al*., 2008). This indicates the potential of this isolate for use as an effective bioremediatory agent to treat azo dye containing wastewater.

The isolate showed a higher percent decolorization when incubated under static conditions as compared to shaker conditions. This finding aligns with previous research by Oturkar *et al*. (2011). Bor-Yann (2002) proposed that this disparity is likely attributed to the lower activity of azoreductase under aerobic conditions. In a recent review by Pinheiro *et al*. (2022), various treatment methods for azo dyes under anaerobic, aerobic, or anaerobic-aerobic sequential conditions were explored. Interestingly, this study indicated that considerable dye decolorization occurred even under aerobic conditions

implying that the isolate may require a certain amount of oxygen, as was also observed for *Pseudomonas luteola* by Bor-Yann (2002).

The pH value is a crucial factor in dye decolorization studies as it not only influences the decolorizing capacity but also affects color stability (Deng *et al*., 2008). The results from this study revealed that *Shewanella seohaensis* NIO_14d showed highest azo dye decolorizing activity within a pH range of 6 to 8. It was also observed that the isolate was capable of dye decolorization at pH 9. This observation highlights a desirable characteristic for microbial bioremediation systems especially considering that reactive azo dyes are bound to cotton fibers under alkaline dye bath conditions and high temperatures (Aksu, 2003). Additionally, as reported by Asad *et al*. (2007), it is pertinent to note that textile wastewaters are found to be typically alkaline in nature. Operational temperature in the mesophilic range (20 – 40 °C) did not impact the extent of dye decolorization. The combination of increased metabolic activity and improved growth at 30°C likely synergistically contribute to the observed optimum temperature for maximum decolorization.

The initial concentration of dye has a significant impact on the extent of dye decolorization by microbial isolates. In order to assess the decolorization ability of the isolate, it was subjected to reactive azo dyes in the concentrations ranging from 50 mgL^{-1} up to 5000 mgL^{-1}. At a dye concentration of 1000 mgL^{-1}, more than 90% of color removal was observed. Moreover, at a higher dye concentration of 2000 mgL^{-1}, the isolate could decolorize 90% of RB5 and RR120 and 85% of RG19. An exceptional strain, *Shewanella seohaensis* NIO_14d demonstrated remarkable tolerance to a dye concentration as high as 5000 mgL^{-1} while retaining its ability decolorize up to 93% of the reactive azo dyes individually within 24 hours. In contrast, a previous study by Kalyani *et al*. (2009) reported a longer duration of 114 hours required to remove 5000 mgL^{-1} of azo dye. Asad *et al*. (2007), studied the growth of bacterial strains in a medium containing 10,000 ppm of Remazol Black B. However, they did not evaluate the decolorization rate at this concentration and suggested that a reduction in cell growth could be attributed to the toxicity of dyes which may inhibit metabolic activities. The findings of the study were in agreement with results reported by Sponza and Isik (2004) where rate of decolorization was inversely proportional to initial dye concentration.

Dye decolorization is a physiological process accompanying active cell growth. A full strength nutrient medium supported optimum growth of the isolate and consequently allowed maximum dye decolorization. It is worth mentioning that when the nutrient strength reduced to 10%, the isolate could still decolorize more than 50% of the individual dyes and 42% of the dye combination. As reported by Senan and Abraham (2004), adaptability and survival of the microorganisms and activity of decolorizing enzymes influences the efficiency of decolorization. The resilience of the isolate in a low nutrient environment makes it suitable for use in treating nutrient-poor wastewater. The study evaluated the effect of various carbon and nitrogen sources on dye decolorization since azo dyes are chemically deficient as a nutrient source requiring supplementation of carbon and nitrogen in order to promote biodegradation (Nigam *et al*., 1995; Senan and Abraham, 2004). Carbon sources seemed to be less effective in promoting the decolorization process, even as the bacterial cells utilized the additional carbon sources instead of the dye compound as their primary carbon source (Saratale *et al.*, 2011). Experimental results showed that medium containing starch was optimum for the decolorization of RR120 and a mixture of dyes. Tony *et al*. (2009) showed enhanced decolorization of azo dyes with the use of 1.3 gL^{-1} starch in the medium. Reports indicate that the presence of glucose in the medium are inhibitory to azo dye decolorization (Chung *et al*., 1978; Khalid *et al*., 2008; Oturkar *et al*., 2011). In contrast, *Shewanella seohaensis* NIO_14d decolorized 73% of RB5 in the presence of glucose. This could be explained by glucose providing an increased source of reducing equivalents for azo bond cleavage, and enabling better decolorization (Carliell *et al*., 1996). The findings provide evidence that the inclusion of organic or inorganic nitrogen sources had a significant impact on the rate of decolorization. It was ascertained that media supplemented with organic nitrogen sources were more conducive to azo dye decolorization as compared to inorganic co-substrates. Specifically, when the medium was supplemented with yeast extract, it showed the highest level of decolorization compared to the when amended with inorganic compounds. This emphasizes the importance of organic co-substrates for the process of dye decolorization. In a study conducted by Chen *et al*. (2003), various nitrogen source supplements, including peptone, tryptone, monosodium glutamate, meat extract, beef extract, yeast extract and urea were examined to determine their effectiveness in enhancing the decolorization rate of 50 mgL^{-1} azo dye C.I. Reactive Red 198. The results revealed that yeast extract emerged as the most effective nitrogen source supplement. Further support for the impact of yeast extract on decolorization was

reported in various studies documented in the literature (Chang and Lin, 2000; Kodam *et al*., 2005; Moosvi *et al*., 2005).

It is crucial to investigate the impact of different electron donors and acceptors on bacterial azoreduction since these compounds are consistently found in the environment (Gerritse *et al*., 1999; He and Sanford, 2003]. Sodium acetate, sodium formate, sodium succinate, sodium citrate, and sodium pyruvate are examples of electron donors that have been found to accelerate the decolorization rate in previous studies (Hong *et al*., 2007; Telke *et al*., 2009). The findings of this study indicate 85% of color removal in the presence of succinate and pyruvate compared to decolorization levels as low as 51% with acetate as an electron donor. Based on these observations, it can be inferred that during the enzymatic decolorization process, which involves the transfer of electrons in a reduction reaction, certain compounds like succinate and pyruvate are more favorable as electron transfer agents. These compounds facilitate the decolorization process by contributing to the reduction of the azo dye.

The elevated levels of salt concentration arise as a result of batch processes utilized in both dye production and dye-consuming industries, reaching concentrations as high as 15-20% (Manu and Chaudhari, 2003). In general, when the sodium concentration exceeds 3 g L^{-1}, it can moderately impede various bacterial activities (De Baere *et al*., 1984). In the present study, the effect on NaCl on the decolorization of azo dyes, both individually and in combination, was examined. *Shewanella seohaensis* NIO_14d isolated in this study was salt tolerant and capable of decolorizing more than 90% of reactive azo dyes at 10 g L^{-1} NaCl concentration. More than 50% of dye decolorization was achieved at 50 g L^{-1} NaCl concentration with average rates of decolorization drastically declining as NaCl concentrations were raised above 10% (w/v). These results were in contrast to reported findings by Anjaneya *et al*., 2011 which indicated maximum decolorization in samples containing 10 g L^{-1} NaCl.

The isolate exhibited efficient azo dye decolorization of more than 80% in the presence of various heavy metals. This is in concurrence with previous reports of the ability of *Shewanella* species to reduce and detoxify heavy metals in its environment (Toes *et al*., 2008; Kang and So, 2016). Decolorization activity was observed to be lower in the presence of lead. This could be attributed to a possible inhibitory effect of lead on the growth of the bacterium and/or on the reducing activity of azoreductase. Textile dyeing

processes often involve the utilization of various heavy metals to stabilize the dye to the target surface, resulting in the presence of these toxic elements in textile wastewater (Rybicki *et al*., 2004; Murugesan *et al*., 2009). Consequently, it becomes crucial to have bioremediation agents that possess the ability to decolorize dyes even in the presence of these harmful heavy metals. This characteristic is imperative for effectively treating textile industry effluents and ensuring removal of both dyes and heavy metals from wastewater. A bacterial consortium capable of simultaneously bioaccumulating 80% of RB5 (59.3 mgL^{-1}) and 90% of Cr (VI) was characterized by Kilic *et al*., (2007). Cetin *et al*., 2008 reported the ability of sulfate reducing bacteria to decolorize 25–30% of 50 mg L^{-1} reactive dyes and removal of 95% of chromate after 72 hours of incubation. The high efficiency of decolorization in the presence of several heavy metals in this study, suggests a resilient microbial strain, although, the heavy metal reduction potential of the isolate will have to be further determined.

In summary, the findings derived from this study would help to provide a robust basis for further research on the development of a practical decolorization process using *Shewanella seohaensis* NIO_14d as a catalyst. These methods have been previously described by Chang and Lin (2000) for a fed-batch decolorization process and by Chang *et al*., 2001 for an immobilized cell system. Besides its durability and resilience, the isolate exhibits potential for further examination, suggesting the possibility of enhanced performance in industrial environments. However, a further evaluation is necessary to confirm this potential. The color removal rates observed in this study are notably high, on par with augmented strains or those obtained from contaminated environments. Consequently, the isolate holds significant value for bioremediation purposes, as it can be tailored to address specific contamination challenges.

Chapter 4

Bioremediation and Detoxification of Reactive Azo Dyes

Chapter 4

Bioremediation and Detoxification of Reactive Azo Dyes

4.1 Introduction

The textile and dyestuff manufacturing industries are the primary contributors to the release of dyes into the environment (Tony *et al*., 2009). As these industries use a wide range of synthetic dyes, the pollution caused by their effluents has reached concerning levels. Typically, colors become visible when the dye concentration exceeds 1 mg L^{-1}, and on average, effluents from textile manufacturing processes have been reported to contain concentrations of around 300 mg L^{-1} (O'Neill *et al*., 1999; Goncalves *et al*., 2000). Azo dyes dominate the textile industry as the most prevalent class of synthetic dyes, constituting approximately 80% of all dyestuff used, followed by the anthraquinone type (Tony *et al*., 2009). As described by Sarkar *et al*. (2017), the chromogenic nature of azo dyes is contributed by its azo group (-N=N-) in conjunction with sulphonic groups (SO^{3-}). Singh *et al*. (2014), proposed that azo dyes are electron-deficient xenobiotic compounds due to the presence of electron-withdrawing groups in their molecular structure. This leads to electron deficiency in the dyes, making them resistant to degradation. The anaerobic reduction of azo dyes leads to the formation of toxic aromatic amines. These dyes and their breakdown products have been reported to be carcinogenic and mutagenic and can persist in the environment, potentially bioaccumulate in organisms, and disrupt ecological balance (Myslak and Bolt, 1998; de Aragao Umbuzeiro *et al*., 2005). The release of aromatic amines from azo dyes, as well as their environmental impact, necessitates continuous research, regulation, and the adoption of safer alternatives. Amongst the various mechanisms for the removal of azo dyes by biological agents, the activity of reductive enzymes has been well studied (Pandey *et al*., 2007; Shah *et al*., 2013; Singh *et al*., 2015). In the context of enzymatic decolorization and degradation of azo dyes, azoreductases and laccases are two prominent enzyme families that have demonstrated significant promise (Stolz, 2001; Bafana *et al*., 2008; Saratale *et al*., 2011; Tian *et al*., 2019). Laccases, in particular, exhibit remarkable

potential in effectively decolorizing a wide array of well-known industrial dyes (Rodriguez *et al*., 1999; Reyes *et al*., 1999). Additionally, other enzymes such as manganese peroxidase (MnP), lignin peroxidase (LiP), and polyphenol oxidase (PPO) also hold considerable potential in the process of decolorization and degradation of azo dyes (Mielgo *et al*., 2003; Gomare *et al*., 2008; Kaushik and Malik, 2009; Guo *et al*., 2016).

Various analytical techniques are employed to investigate the potential process of dye decolorization and identify the resulting metabolites generated by bacterial treatment of azo dyes. UV–vis spectroscopy (UV–vis) serves as the principal method for assessing and quantifying dye decolorization. Moreover, various chromatographic methods and Fourier transform infrared spectroscopy (FTIR) spectroscopy and Nuclear Magnetic Resonance (NMR) serve as valuable analytical tools in dye degradation studies and enable researchers to understand the mechanisms involved in the process of dye decolorization. (Saratale *et al*., 2011). To assess the effectiveness of the microbial-mediated dye decolorization process, it is crucial to conduct diverse toxicity studies so as to monitor the characteristics of the decolorization and degradation byproducts. As detailed by Tan *et al*., (2005); Kalyani *et al*., (2008); Kalme *et al*., (2009) and Saratale *et al*., (2009c), the toxicity of the azo dye containing sample before and after treatment is assessed using various biological test organisms.

4.2 Materials and Methods

4.2.1 Decolorization of different dye classes

The bacterial isolate under study, *Shewanella seohaensis* NIO_14d, was tested for its ability to decolorize various other azo dyes as well as other chemical classes of dyes. Erlenmeyer flasks (250 mL) containing 100 mL of sterile nutrient broth were amended with 200 mg L^{-1} of each of the test dyes (Sigma-Aldrich). The dyes belonging to the following classes were tested: azo, anthraquinone and triarylmethane (**Table 4.1**). Pre-grown bacterial culture (1% [v/v]) was inoculated in the medium containing the respective dye and incubated at 28 ± 2 °C under static conditions. After 24 h, the samples were centrifuged at 12,000 rpm for 10 minutes at 4°C and the cell-free supernatant color was read spectrophotometrically (Shimadzu, Japan) at the wavelength of maximum

absorption of the dyes used. Decolorization was calculated in terms of % decolorization as follows:

$$\text{Decolorization (\%)} = \frac{A_{\lambda,\text{initial}} - A_{\lambda,\text{final}}}{A_{\lambda,\text{initial}}} \times 100$$

where, $A_{\lambda,\text{ initial}}$ = initial absorbance and $A_{\lambda,\text{ final}}$ = absorbance after incubation.

Table 4.1: Details of different classes of dyes used to check decolorization

Dye Class	Dye Name	Color Index Number	λ_{max} (nm)	Reference
Triarylmethane	Crystal Violet	42555	590	Güzel *et al*., 2014
	Victoria Blue	44045	599	Gomaa *et al*., 2008
Anthraquinone	Poly R 478	NA[#]	520	Enayatzamir *et al*., 2009
	Remazol Brilliant Blue R (RBBR)	61200	595	Enayatzamir *et al*., 2009
Azo	Direct yellow 27	13950	393	Adeel *et al*., 2015
	Direct blue 71	34140	587	Hafshejani *et al*., 2014
	Reactive orange 16	17757	494	Won *et al*., 2004
	Acid yellow 17	18965	400	Jaikumar *et al*., 2009
	Acid red 114	23635	514	Sanghi *et al*., 2006
	Methyl red	13020	520	Yang *et al*., 2013
	Congo red	22120	488	Si *et al*., 2015
	RB5	20505	597	Yu *et al*., 2010
	RG19	20575	630	Petrucci *et al*., 2015
	RR120	292775	522	Hafeez *et al*., 2018

[#]CI Number not reported

4.2.2 Enzyme assays for analysis of dye decolorizing activity

Assays were carried out to determine the presence and activity of three degradative enzymes known to be involved in dye decolorization viz. lignin peroxidase, laccase and azoreductase.

Preparation of Cell free extract

The pre-grown bacterial culture (1% v/v) was added to sterile nutrient broth medium containing the dyes RB5, RG19 and RR120 at a final concentration of 100 mg L^{-1} as well as to dye free nutrient medium. Cell free extracts were obtained by centrifugation at 7,000 rpm for 15 min at 4°C. The cells were then suspended in 50 mM potassium phosphate buffer (pH 7.4) (Appendix C) and sonicated (Ultrasonicator model no. SKL 250D) by keeping the sonicator at the output of 70 A. The conditions for sonication were maintained as 16 strokes each of 9 s, with 6 s interval for 4 min at 4°C. This homogenate was centrifuged, and supernatant was used as enzyme source (Kalme *et al*., 2007). Enzyme activity was then compared between the two samples (with and without dye).

(a) Lignin peroxidase

Assays were carried out in cuvettes (path length 1 cm) with a total volume of 1 ml. Lignin peroxidase activity was determined by monitoring the rate of oxidation of veratryl alcohol to veratraldehyde at 312 nm (Paszezynski *et al*.,1988). The reaction mixture was prepared with 2.5 mL of 40 mM veratryl alcohol, 20 mL of 150 mM d-tartaric acid buffer (pH 2.5) (Appendix C) and 2.5 mL of 8 mM H_2O_2. The final reaction mixture contained 500 µL of the above prepared reaction mixture to which was added 500 µL of cell free enzyme sample (Kalyani *et al*., 2008). The kinetic reaction was measured spectrophotometrically at 312 nm (ε312, 9300 M^{-1} cm^{-1}) for 1 min at 30 ± 2 °C. Reaction blanks were maintained containing all assay components except active enzyme. The enzyme assays were run in triplicate, and the average values were taken to calculate a unit of enzyme activity.

(b) Laccase

Laccase activity was determined by measuring the oxidation of the non-phenolic dye ABTS method (Naghdi *et al*., 2017). The ABTS is oxidized by laccase to a preferred state of the cation radical. The development of an intense blue-green color (λ_{max} at 420 nm) was considered as a measurement of the cation radical concentration which can be correlated to enzyme activity (Majcherczyk, *et al*., 1998). The reaction mixture (1 mL) containing 160 µL of ABTS (1.5 mM), 740 µL of 0.1 M sodium acetate buffer (pH 4.5) (Appendix C) and 100 µL of the cell free crude enzyme was incubated for 5 minutes. Oxidation of ABTS was monitored by estimating the increase in absorbance at 420 nm (ε420, 3.6×10^4 M^{-1} cm^{-1}) against a suitable blank. One unit of enzyme (U) was defined as the amount of laccase that oxidized 1 μmol of ABTS substrate per min.

(c) Azoreductase

Azoreductase enzyme activity were measured during dye decolorization of the reactive dyes RB5, RG19 and RR120 by *Shewanella seohaensis* NIO_14d using the method by Punj and John (2009). Assays were carried out in cuvettes (path length 1 cm) with a total volume of 1 ml. All substances were dissolved in 50 mM phosphate buffer (pH 7.2). The reaction mixture contained 250 µL of the respective dye (100 mg L^{-1}) prepared in phosphate buffer (Appendix B), resulting in a final concentration of 20 µM dye, 25 µL FMN (1mM) and 225 µL of cell free crude enzyme sample. The reaction was started by the addition of 0.5 mM NADH. The reduction in color absorbance was monitored photometrically in the first 5 minutes at λ_{max} for each dye. The molar extinction coefficients for the dyes were 35000 M^{-1} cm^{-1} for RB5 at 597 nm, 23300 M^{-1} cm^{-1} for RG19 at 630 nm and 32500 M^{-1} cm^{-1} for RR120 at 522 nm. One unit (U) of enzyme activity was defined as the amount of enzyme that catalyzes the degradation of 1 µmol of the reactive azo dye per min (Punj and John, 2009). All the enzymatic reactions were carried out at 30 ± 2 °C where reference blanks contained all components except the enzyme. All enzyme assays were run in triplicate, and the average values were taken to calculate enzyme activity.

4.2.3 Biodegradation analysis

4.2.3.1 *Metabolite Extraction*

In order to monitor the biodegradation of the reactive azo dyes, the metabolites produced after dye decolorization were extracted in an organic solvent. *Shewanella seohaensis* NIO_14d was grown in Nutrient broth containing 500 mg L^{-1} of the azo dyes RB5, RG19 and RR120. The biodegraded metabolites of reactive dyes after decolorization were extracted from the culture supernatant. After complete decolorization, the culture broth was centrifuged at 7000 rpm for 15 minutes at 4°C and an equal volume of ethyl acetate was used for extraction. The extract was dehydrated over anhydrous sodium sulphate (Na_2SO_4) and evaporated to dryness in a rotary vacuum evaporator (Equitron Roteva-8763). The crystals obtained were dissolved in a small amount of HPLC grade methanol (Babu *et al*., 2013).

4.2.3.2 *FTIR*

The biodegraded metabolites of reactive azo dyes (RB5, RG19 and RR120) were characterized by Fourier-transform infrared spectroscopy (FTIR) (Nicolet 5700, Thermo Fischer Corporation, USA) as per the procedure described by Babu *et al*., 2013. The extracted treated decolorized sample was mixed with potassium bromide (KBr) to prepare a pellet and scanned in the range of 4,000–400 cm^{-1}. The KBr pellet without sample was used as blank.

4.2.4 Toxicity analysis

4.2.4.1 *Using Artemia salina*

The toxicity of the dyes and their degradation products were analyzed by a standard bioassay procedure using the brine shrimp, *Artemia salina* (Prasad and Rao, 2013). In order to determine the toxicity of the free dyes as well as the degraded products, *Shewanella seohaensis* NIO_14d was grown in Nutrient broth containing 500 mg L^{-1} of the azo dyes RB5, RG19 and RR120. After decolorization, the samples were centrifuged at 12,000 rpm for 10 min at 4°C and the supernatant was filter sterilized using a 0.22 µm pore size filter. The cell-free supernatant (1 mL) was added to each well of a 24-well

plate (Costar, USA). The cysts of *Artemia salina* were hatched out in sterilized sea water (35 ppt) with aeration for 24 h to nauplii stage. Forty *Artemia salina* cysts or nauplii were added accordingly to the wells of the plate. The hatching of cysts and survival of nauplii was recorded after 24 hours of incubation at 30 °C. The bacteria-free dye samples were used as controls. Seawater was used as the positive control. Following incubation, the plates were checked to count the number of hatched cysts and surviving nauplii. Enumeration was carried out using a binocular microscope.

4.2.4.2 *Using Vigna radiata*

The phytotoxicity of the treated and untreated dye samples were measured using the seed germination assay as described by Singh *et al.*, (2015). In order to determine the toxicity of the free dyes as well as the degraded products, *Shewanella seohaensis* NIO_14d was grown in Nutrient broth containing 500 mg L^{-1} of the azo dyes RB5, RG19 and RR120. After decolorization, the samples were centrifuged at 12,000 rpm for 10 min at 4°C and cell free supernatant was filter sterilized using a 0.22 µm pore size filter. The filtrate was used to determine phytotoxicity.

Ten seeds of *Vigna radiata* were surface sterilized and placed in Petri plates on Whatman filter papers soaked in 5 mL of distilled water, untreated reactive dye and treated decolorized reactive dye respectively. The assay was carried out in triplicates and germination was monitored over 7 days. The phytotoxicity was assessed with respect to germination percentage, length of root and shoot after emergence. The following formula was used to calculate germination percentage:

$$\text{Germination (\%)} = \frac{\text{number of seeds germinated in treatment}}{\text{number of seeds germinated in control}} \times 100$$

4.2.5 Decolorization of Textile effluent

4.2.5.1 *Laboratory simulated textile dye wastewater*

Synthetic simulated textile dye wastewater was prepared in the laboratory by adding 250 mg L^{-1} of the individual dyes RB5, RG19 and RR120 to a solution of 10% NaCl solution. The pH of the solution was adjusted to 9 using 1N NaOH. The simulated dye wastewater was supplemented with 0.1% (w/v) yeast extract since previous studies indicated that an

organic nitrogen source boosts decolorization activity. *Shewanella seohaensis* NIO_14d was pre-grown in sterile nutrient broth and 1% of the inoculum was added to the simulated dye wastewater sample in Erlenmeyer flasks. The flasks were incubated at 30°C under static condition. Following decolorization of the solution (after 24 hours incubation), suitable aliquots were taken, centrifuged at 12,000 rpm for 10 minutes at 4°C and the resulting cell-free supernatant was used to determine the UV-visible absorption spectrum and measure the extent of decolorization. Uninoculated simulated textile dye wastewater was used as control.

4.2.5.2 *Raw Textile effluent obtained from Kanpur, India*

Effluent sample was collected from outside a textile mill located in Kanpur, India and transported in 10L cans. The physico-chemical parameters of the sample were characterized and the effluent sample was analyzed for decolorization by *Shewanella seohaensis* NIO_14d.

Flasks containing effluent amended with 0.1% (w/v) yeast extract since previous studies indicated that an organic nitrogen source boosts decolorization activity. The pre-grown culture was inoculated (1% [v/v]) and incubated at 30°C under static condition. After 24 hours incubation, suitable aliquots were taken, centrifuged at 12,000 rpm for 10 minutes at 4°C and the resulting cell-free supernatant was used to determine the UV-visible absorption spectrum and calculate the percentage of decolorization.

4.2.6 Statistical analysis

All experiments were carried out in triplicate. Basic descriptive statistics were applied to the raw data sets and the results were presented as mean ± standard deviation (SD). The data for enzyme assays was analyzed by one-way analysis of variance (ANOVA) with Tukey–Kramer multiple comparison test.

4.3 Results

4.3.1 Decolorization of different dye classes

Shewanella seohaensis NIO_14d was able to decolorize almost all the azo dyes tested except for Direct yellow 27 (**Figure 4.1**). The isolate also showed the ability to decolorize dyes belonging to other chemical classes. The color of the triarylmethane dye, Victoria blue, was reduced by 63.43% while, the anthraquinone dyes Poly R 478 and RBBR were decolorized 54% and 26.64% respectively.

4.3.2 Enzyme assays for analysis of dye decolorizing activity

The enzyme activity exhibited by *Shewanella seohaensis* NIO_14d varied for the three enzymes assayed as shown in **Table 4.2**. The isolate did not yield detectable levels of the enzyme laccase in response to exposure to reactive azo dyes. Very low levels of lignin peroxidase were measured in the medium after dye decolorization. However, a significant amount of the reductive enzyme azoreductase was produced by *Shewanella seohaensis* NIO_14d with a maximum of 0.48 ± 0.13 U min^{-1} ml^{-1} measured after decolorization of the dye RG19.

4.3.3 Biodegradation analysis

The FTIR spectrum, as observed in **Figures 4.2(A), 4.2(B) and 4.2(C)**, showed a comparison between the peaks obtained from untreated control reactive dyes RB5, RG19 and RR120 with the extracted metabolites after dye decolorization. The control showed specific peaks at 3448 cm^{-1} corresponding to the presence of medium N-H bond and peaks in the range of 1585 to 1604 cm^{-1} due to azo group (–N=N–) stretching. The asymmetric C–N stretching frequency appears in the range of 1289 to 1314 cm^{-1} due to the aromatic nature of the reactive dyes while symmetric stretching is seen at 2924 cm^{-1}. The FTIR spectrum of the samples obtained after the treatment of the dyes with *Shewanella seohaensis* NIO_14d showed differences in the peak positions when compared to the control. The spectrum did not show a peak at 3448 cm^{-1} corresponding to N–H. This is indicative of the absence of secondary and tertiary amines in the decolorized samples.

Table 4.2: Activity of various enzymes during dye decolorization

Sample	Lignin peroxidase[a]	Laccase[b]	Azoreductase[c]
Dye free Control	0.002 ± 0.06	0.008 ± 0.04	0.017 ± 0.04
RB5 after decolorization	0.038 ± 0.07*	BDL	0.381 ± 0.02*
RG19 after decolorization	0.002 ± 0.03*	BDL	0.48 ± 0.13*
RR120 after decolorization	0.01 ± 0.01	BDL	0.439 ± 0.22*

Mean ± standard deviation of triplicates

BDL: below detectable limit

*P<0.05; significant level based on one-way ANOVA with Tukey–Kramer test

[a] µmol of veratryl alcohol oxidized min^{-1} ml^{-1}

[b] μmol of ABTS oxidized min^{-1} ml^{-1}

[c] μmol of reactive dye reduced min^{-1} ml^{-1}

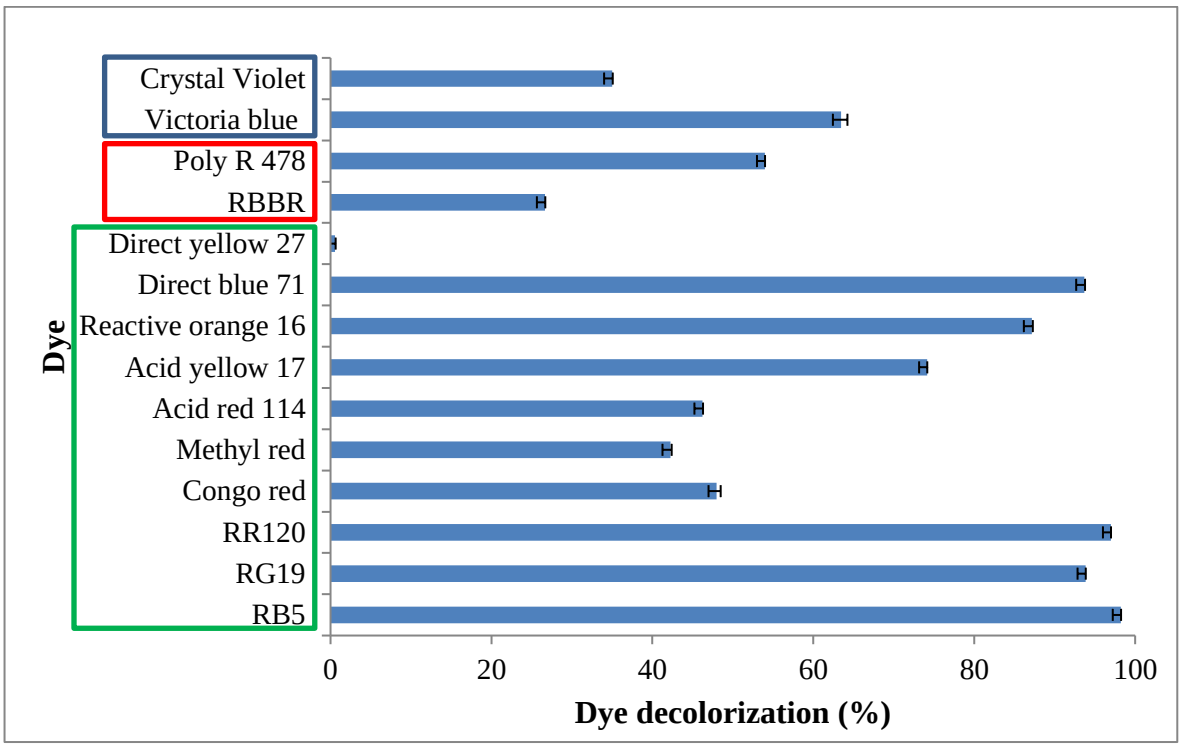


Figure 4.1: Decolorization of various azo ( ), triarylmethane ( ) and anthraquinone ( ) dyes by *Shewanella seohaensis* NIO_14d in nutrient broth amended with dye (100 mgL^{-1}). Data are expressed as mean ± standard deviation (SD) of three replicate experiments.

A

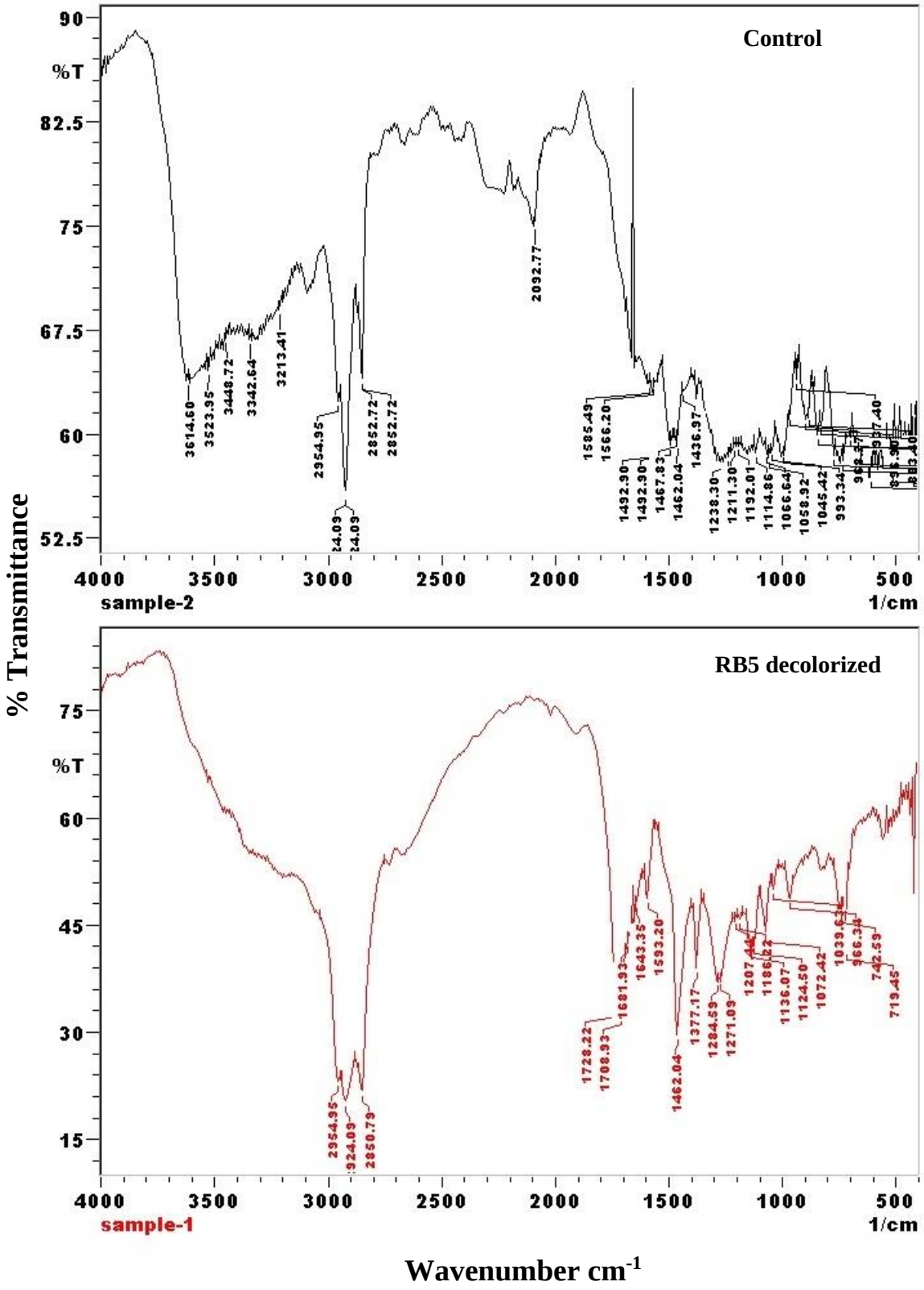


Figure 4.2 (A): FTIR analysis of RB5 decolorized dye samples versus untreated reactive azo dye controls (500 mg L^{-1}).

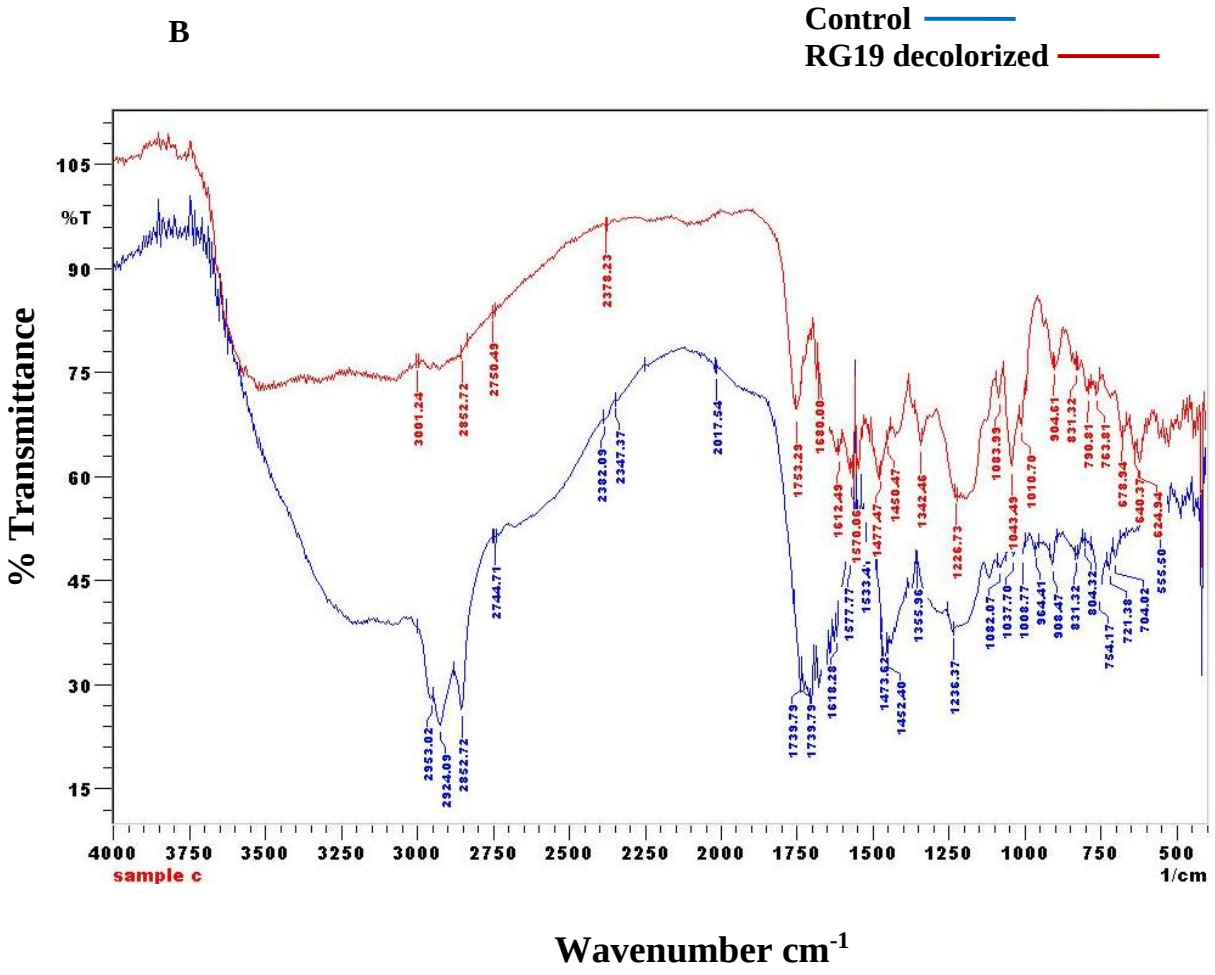


Figure 4.2 (B): FTIR analysis of RG19 decolorized dye samples versus untreated reactive azo dye controls (500 mg L^{-1}).

C

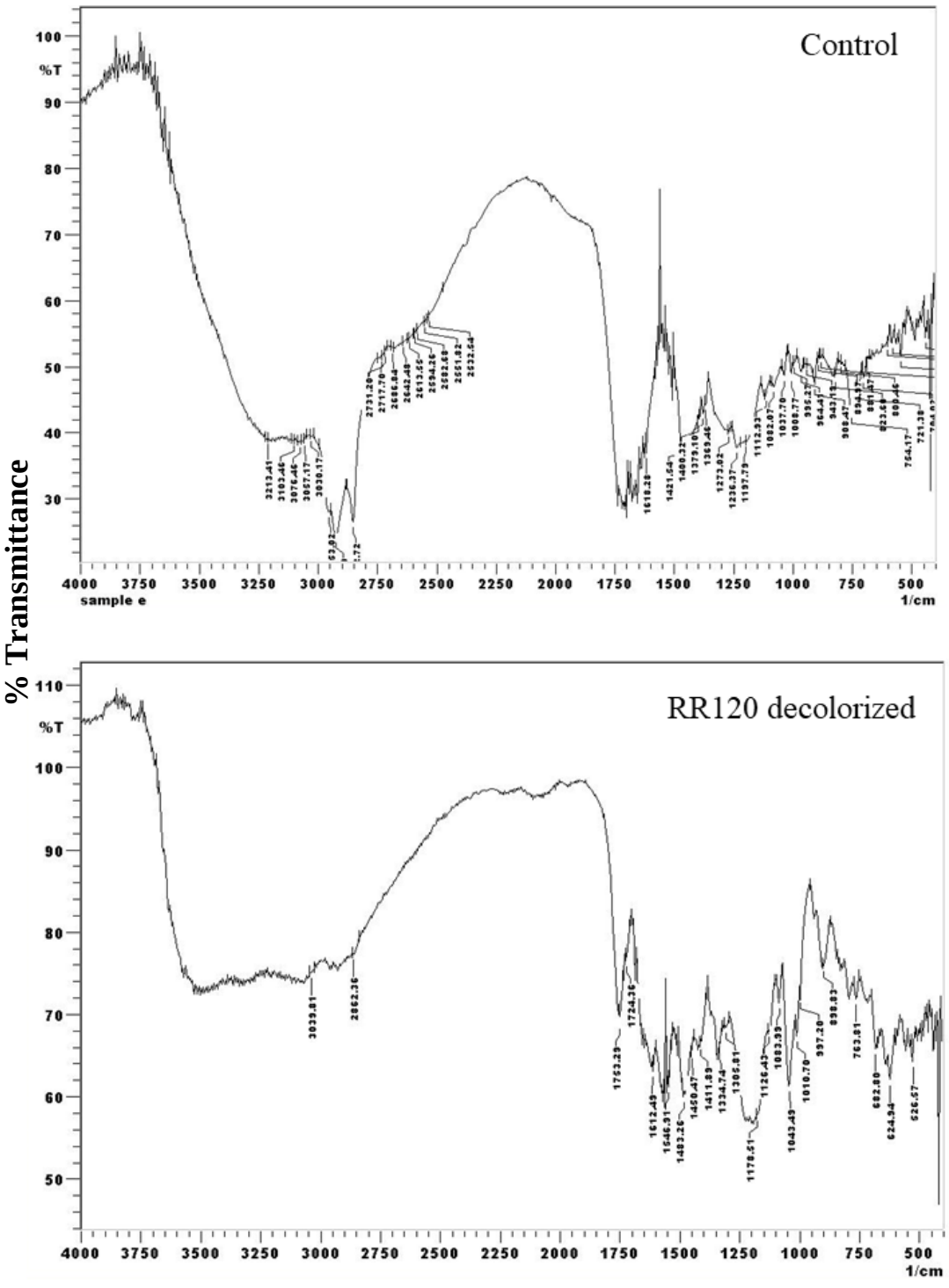


Figure 4.2 (C): FTIR analysis of RR120 decolorized dye samples versus untreated reactive azo dye controls (500 mg L^{-1}).

4.3.4 Toxicity analysis

4.3.4.1 *Using Artemia salina*

The reactive dyes and their decolorized metabolites were evaluated for their toxicity using the brine shrimp, *Artemia salina*. It was observed that the treated dye solution is less toxic to the hatching of *Artemia salina* cysts (**Table 4.3**). Amongst the dyes tested, the decolorized metabolites of RR120 did not affect hatching of the cysts with 100% hatching obtained. The decolorized metabolites of the other two dyes, RB5 and RG19, also did not impede cyst hatching with 84% and 77% hatching achieved in the presence of these dyes, respectively. In contrast, the untreated dye control was found to inhibit hatching indicating its toxic effects.

The survival of *Artemia salina* nauplii was much higher in treated decolorized dye solution as compared to the original dye as seen in **Table 4.4**. More than 85% of the brine shrimp nauplii were found to survive even after 24 hours of exposure to the decolorized dye metabolites as opposed to the untreated dye.

Table 4.3: Effect of reactive dyes and dye degraded metabolites on the hatching (%) of *Artemia salina* (brine shrimp) cysts after 24 hours

Treatment	**RB5**	**RG19**	**RR120**
Sea water control	100 ± 0.12	100 ± 0.04	100 ± 0.37
Untreated dye	6 ± 0.71	12 ± 0.42	4 ± 1.69
Decolorized dye metabolites	84 ± 0.82	77 ± 1.12	100 ± 0.12

Table 4.4: Effect of reactive dyes and dye degraded metabolites on the survival of *Artemia salina* (brine shrimp) nauplii (%) after 24 hours

Treatment	RB5	RG19	RR120
Sea water control	98 ± 0.74	99 ± 0.59	100 ± 1.52
Untreated dye	18 ± 1.46	10 ± 0.77	12 ± 1.52
Decolorized dye metabolites	88 ± 0.25	86 ± 0.03	90 ± 0.43

4.3.4.1 *Using Vigna radiata*

Phytotoxicity studies carried out using seeds of *Vigna radiata* (mung bean) showed higher toxicity of the untreated reactive dyes compared to the treated dye samples. The seeds exposed to the untreated dyes showed a poor germination rate of 14% for RB5, 6% for RG19 and 18% for RR120. The seeds exposed to the decolorized dye samples exhibited >85% germination after 7 days. Further, the average root and shoot length of the germinated seeds were comparable to that obtained with the distilled water control (**Table 4.5**). In sharp contrast, seeds exposed to the untreated dye samples RB5, RG19 and RR120 showed root lengths of 0.3 cm, 0.5 cm and 0.7 cm respectively. Likewise, the shoot length measured in cm was also much smaller in seeds which were in contact with the untreated dyes.

Table 4.5: Phytotoxicity studies of reactive dyes and dye degraded metabolites using *Vigna radiata*

Parameter	**Distilled water control**	**RB5 untreated**	**RB5 treated**	**RG19 untreated**	**RG19 treated**	**RR120 untreated**	**RR120 treated**
Germination (%)	100 ± 0.74	14 ± 1.68	85 ± 1.04	6 ± 0.83	89 ± 0.96	18 ± 1.08	86 ± 1.14
Root length (cm)	3.7 ± 0.74	0.3 ± 1.49	2.2 ± 0.39	0.5 ± 0.41	2.3 ± 0.97	0.7 ± 0.25	1.9 ± 1.84
Shoot length (cm)	2.9 ± 0.74	0.6 ± 0.94	1.8 ± 0.07	0.4 ± 1.16	1.9 ± 0.82	0.8 ± 1.53	2.1 ± 1.06

4.3.5 Decolorization of Textile effluent

4.3.5.1 *Laboratory simulated textile effluent*

UV-Visible spectroscopic analysis (200 – 800 nm) carried out for the simulated textile effluent prepared in the laboratory is shown in **Figure 4.3 (A)**. The peak observed in the spectrum at 600 nm was found to be drastically reduced after 24 hours of treatment following decolorization of the effluent sample by *Shewanella seohaensis* NIO_14d. Smaller peaks seen at 390 nm and 315 nm were also reduced after bacterial treatment.

Treatment of the laboratory simulated textile effluent with *Shewanella seohaensis* NIO_14d for 24 hours resulted in considerable decolorization of 89% (± 0.25 SD) of the sample as seen in **Figure 4.5 (A**).

4.3.5.2 *Textile effluent obtained from Kanpur, India*

The raw textile effluent collected from Kanpur, India (**Figure 4.4**) was treated with the bacterial isolate *Shewanella seohaensis* NIO_14d to determine its bioremediation potential. Interestingly, the isolate showed high potential in decolorizing the raw effluent to an appreciable extent of 73% (± 1.08 SD) as depicted in **Figure 4.5 (B).**

The physico-chemical parameters of the effluent tested according to APHA protocols have been listed in **Table 4.6**. The raw textile effluent had a dark green color and a string offensive odor. The pH of the effluent was found to be 10.17. The levels of total solids, total suspended and dissolved solids found in the effluent were extremely high (TS: 2833.33; TSS: 1340; TDS: 2750.48) and exceeded the permissible limits set by the Bureau of Indian Standards (BIS, 2009). BOD determined the amount of organic matter in the effluent and was much higher (420 mgL^{-1}) than the prescribed BIS limit of 30 mgL^{-1}. The COD measured to determine the level of pollution was also found to be almost 7 times higher than the allowed limits. The high amounts of COD, BOD, nitrates, nitrites, chlorides and total nitrogen observed were consistent with those in untreated effluents (Aslam *et al*., 2004).

The UV-Visible spectrum of the raw effluent showed a noteworthy reduction in the observed peaks at approximately 550 nm and 620 nm after 24 hours of treatment with the bacterial culture **Figure 4.3 (B)**. This was indicative of decolorization of the dark colored effluent to a lighter solution by the isolate.

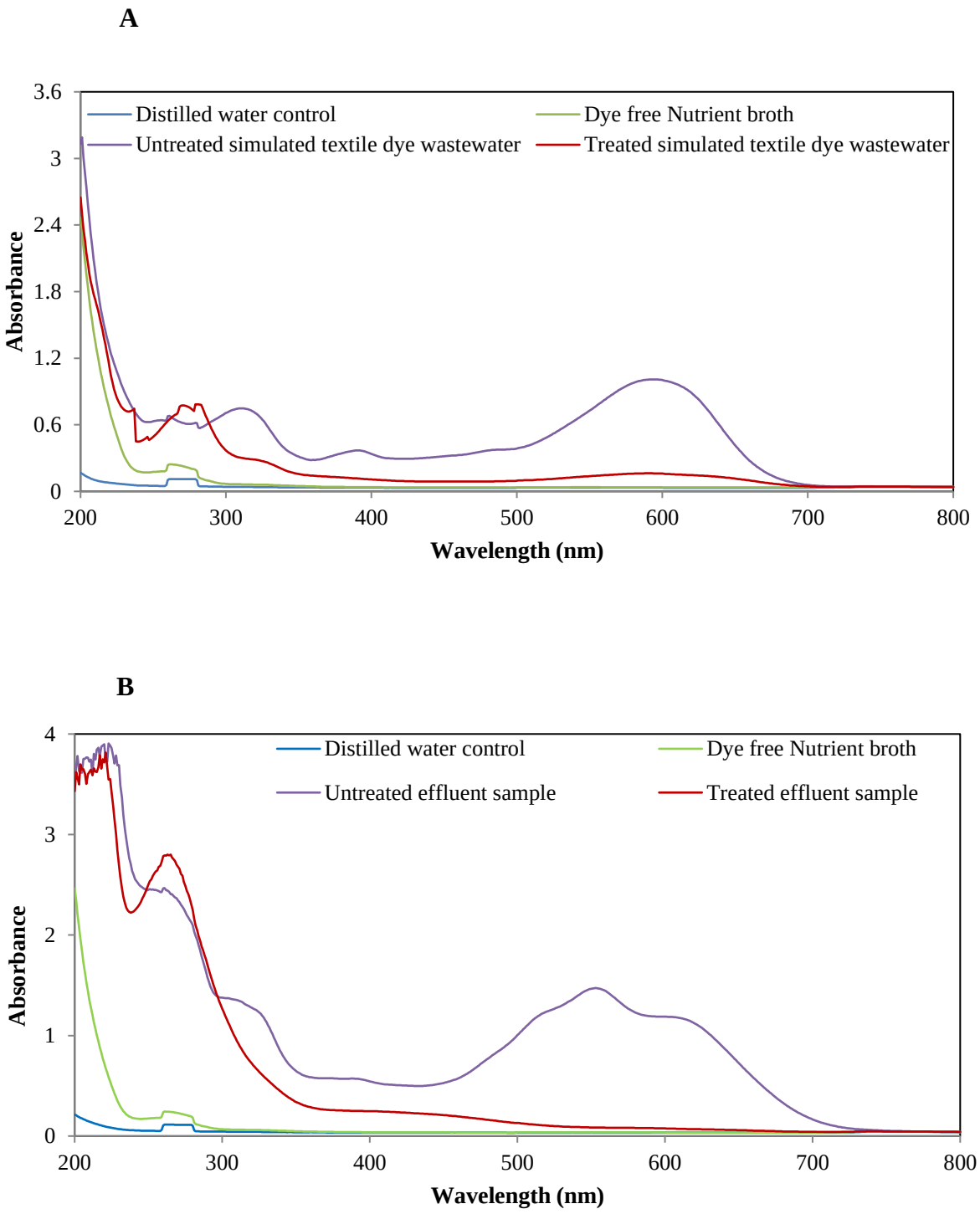


Figure 4.3: Spectroscopic analysis **(**UV-Visible spectrum) of treated and untreated samples of (**A**) simulated textile dye wastewater and (**B**) Textile effluent from Kanpur, India



Figure 4.4: Collection of effluent samples from outside a textile mill in Kanpur, India

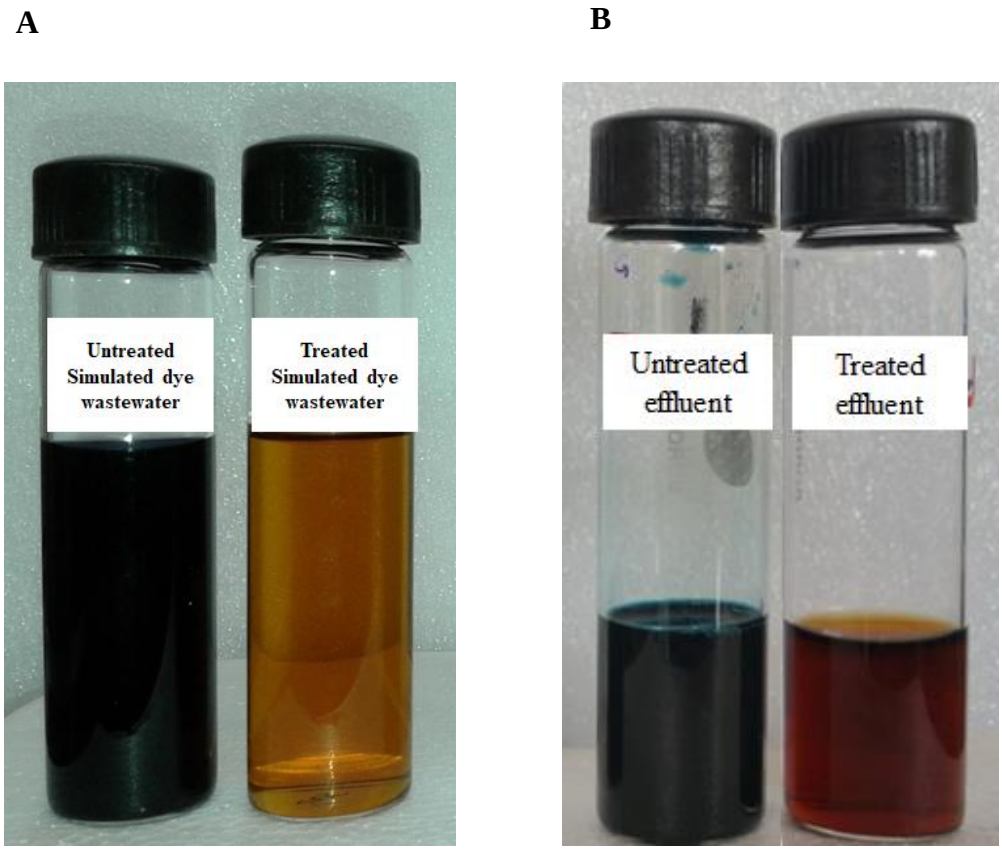


Figure 4.5: Decolorization of Effluent samples by *Shewanella seohaensis* NIO_14d. (**A**) simulated textile dye wastewater and (**B**) Textile effluent from Kanpur, India

Table 4.6: Physico-chemical characteristics of raw textile effluent from Kanpur, India

Parameter	**Raw Textile effluent**	**Permissible limits (BIS, 2009)**
pH	10.17 ± 0.00	5.5-9.0
Salinity (ppt)	15 ± 0.01	-
Total Solids (mgL^{-1})	2833.33 ± 24.03	2200
Total Suspended Solids (mgL^{-1})	1340 ± 24.03	100
Total Dissolved Solids (mgL^{-1})	2750.48 ± 29.19	2100
BOD (mgL^{-1})	420 ± 12.56	30
COD (mgL^{-1})	1700 ± 18.83	250
Nitrates (mgL^{-1})	164.5 ± 6.31	10
Nitrites (mgL^{-1})	1.73 ± 1.42	-
Total nitrogen (mgL^{-1})	636 ± 28.74	100
Chlorides (mgL^{-1})	1286.84 ± 18.17	200

Standard deviation, **n=3**

4.4 Discussion

The ability to decolorize, degrade and detoxify synthetic dyes is a key characteristic of microorganisms involved in the bioremediation of dye-containing wastewater. *Shewanella seohaensis* NIO_14d isolated in this study demonstrated the capability to decolorize a broad spectrum of synthetic dyes belonging to various chemical dye classes. Additionally, the isolate could detoxify the dye during the process of decolorization. Commercial textile dyeing processes utilize reactive dyes bearing chromophoric groups which are azo, anthraquinone and triphenylmethane in nature (Sudha *et al*., 2014). The large amount of unfixed dyes lost in the effluent have been reported to have an LD50 value of more than 200 mg/kg (Won *et al*., 2004). The complex aromatic structures of synthetic dyes render them xenobiotic and extremely recalcitrant to degradation. Mishra and Maiti (2018) reviewed the efficiency and various mechanisms of bacterial decolorization of three major classes *viz*. azo, anthraquinone and triphenylmethane dyes from wastewater. The findings of the study indicate that the isolate possesses the necessary mechanisms to efficiently decolorize not only azo dyes but also dyes belonging to the anthraquinone and triphenylmethane classes. The inability to decolorize the azo dye Direct yellow 27 is possibly due to the toxicity conferred by the dye which interferes with the metabolic functioning of the isolate and requires further investigation.

Oxido-reductive enzyme systems are the most common mechanism implicated in the bio-decolorization of textile dyes by microorganisms (Saratale *et al*., 2011). In an attempt to identify the enzymes associated with azo dye decolorization by *Shewanella seohaensis* NIO_14d, the enzyme activity of three known dye degrading enzymes was determined. An increased azoreductase activity of 0.38 – 0.48 μmol of reactive dye reduced min^{-1} ml^{-1} was found following dye decolorization by the isolate. There was no significant lignin peroxidase or laccase activity detected during the assay, possibly indicating that *Shewanella seohaensis* NIO_14d does not produce these enzymes to reduce and decolorize reactive azo dyes. Contrastingly, Telke *et al*., (2010) reported a laccase from *Pseudomonas* sp. SU-EBT responsible for Congo red decolorization. Lignin peroxidases for dye decolorization are best studied in white-rot basidiomycetes (Ollikka *et al*., 1993; Levin *et al*., 2004; Gomaa *et al*., 2008; Hadibarata *et al*., 2013; Rekik *et al*., 2019). However, there do exist few reports of bacterial lignin peroxidases capable of dye

decolorization (Gomare *et al*., 2008; Dawkar *et al.*, 2009; Ghodake *et al.*, 2009; Kalyani *et al.*, 2011).

The FTIR spectral analysis facilitates the recognition of interaction types and strengths present in azo dyes, which encompass diverse functional groups. By examining the FTIR spectra after bacterial biodegradation, researchers can obtain valuable insights into the alterations and interactions occurring within the dye molecules. This process offers valuable information about the degradation process itself and the disintegration of chemical bonds (Saratale *et al*., 2011). The changes in observed peaks in the FTIR spectra following azo dye decolorization are a suggestive of successful degradation of the reactive azo dyes by *Shewanella seohaensis* NIO_14d. The absence of a peak at 3448 cm−1 corresponding to N–H is indicative of the absence of secondary and tertiary amines in the decolorized samples. Further, absence of the peaks of azo bond (–N=N–) stretching at 1585 to 1604 cm^{-1} indicates the possible reductive cleavage of these bonds during the dye decolorization process.

It is crucial to assess the toxicity of the substances generated during the bacterial degradation of dyes in order to evaluate the quality of the treated wastewater and its potential impact on the environment. This evaluation is necessary before the effluent is ultimately released into the environment or water bodies. Since synthetic dyes have a profound impact on flora, fauna and human health, using various biotic organisms as indicators to determine the toxicity of the effluent is of significance. This study analyzed the toxicity of the dye samples before and after bacterial treatment using *Artemia salina* and *Vigna radiata*. The toxicity of the untreated reactive dyes compromised the hatching of *Artemia salina* (brine shrimp) cysts while post bacterial treatment, the metabolites of dye degradation allowed a high hatching percentage. In addition, when the *Artemia salina* nauplii were exposed to the decolorized metabolite, they exhibited a survival rate of over 85%. In contrast, the presence of the untreated dye resulted in a low survival rate ranging from 10% to 18%. These findings support the conclusion that the products of biodegradation of RB5, RG19 and RR120 are not toxic to *Artemia salina*. Similar conclusions on the toxicity of reactive dyes and their metabolites were drawn in studies carried out by Almeida and Corso (2016) and Sreedharan *et al*., (2021). The reduced toxicity of the secondary metabolites formed after decolorization of the reactive azo dyes, by the isolate, is evident from the results of the phytotoxicity studies. Low rates of

germination of *Vigna radiata* seeds could be attributed to the inhibitory effects of the toxic azo dyes as compared to 85% of germination seen in seeds exposed to treated dye samples. Similarly, the germinated seedlings showed enhanced root and shoot length following contact with treated dye metabolites in sharp contrast to the poor growth in presence of reactive dyes. It is evident that bacterial treatment effectively reduces the toxicity of the dyes and leads to the production of safer by-products. Kalyani *et al*., (2009) report comparable results on the non-toxic effects of the degradation products of azo dye reactive red 2 on seeds of *S. vulgare* and *P. mungo*.

UV-Visible (UV-Vis) spectroscopy (200-800 nm) is a powerful tool to analyze dye decolorization (Knapp and Newby, 1995). UV-Vis studies carried out on laboratory simulated textile effluent as well as raw effluent obtained from Kanpur showed a significant reduction in the sharp peak observed at λ_{max}. The decrease in the peak without a shift in λ_{max} indicates degradation of the dye molecules during decolorization and removal of the dark colored dye solution to a lighter solution with consequent decrease in color intensity. Similar results were observed by Babu *et al*. (2013) and Almeida and Corso (2016) when studying the microbial mediated decolorization of Victoria Blue B and Acid Blue 161 respectively. Additionally, as reported by Saratale *et al*., (2009a), an increase in absorbance towards the UV region is further evidence of the removal of the dye. The physico-chemical analysis of raw textile effluent obtained from Kanpur, India indicated a highly colored and alkaline wastewater likely due to the use of silica and sodium hydroxide in the textile dyeing process. The levels of various parameters including BOD, COD, nitrates, chlorides, TS, TSS and TDS in the effluent significantly exceeded permissible limits rendering the effluent unsafe for discharge into the environment. Although, the ability of *Shewanella seohaensis* NIO_14d to reduce these parameters was not analyzed in this study, the isolate was able to withstand the hostile nature of the raw textile effluent and achieve a measurable reduction in color intensity. In a previous study, Kurade *et al*., (2012) reported a bacterial-yeast consortium capable of reducing the BOD and COD of textile effluent samples. To enhance the bioremediating potential of the isolate in this study, further research is warranted to investigate its capabilities in reducing other polluting characteristics of the effluent.

The focus on artificial textile wastewater in research remains limited, despite the preparation and testing of various components to simulate actual wastewater from textile factories. Additionally, there is a lack of a comprehensive reference that summarizes and evaluates the reported wastewater constituents. Synthetic wastewater is essential for pilot-scale studies and when stable effluents from real sources are unavailable (Yaseen and Scholz, 2019). Notwithstanding these constraints, this study highlights the reactive azo dye decolorization and degradation potential of *Shewanella seohaensis* NIO_14d and its application in *in situ* bioremediation strategies. Thus, this study has added a marine bacterial isolate capable of efficiently decolorizing textile effluent and detoxifying reactive azo dyes. This can contribute to the efforts to mitigate pollutants using microbial bioremediative technologies.

Chapter 5

Proteomic Characterization of Dye Decolorizing Bacteria

Chapter 5

Proteomic Characterization of Dye Decolorizing Bacteria

5.1 Introduction

The understanding of synthetic dye decolorization, degradation, and detoxification by marine organisms has been rapidly expanding. However, there remains a significant gap in exploring the functional aspects of their abilities, particularly regarding species-specific deviations in well-established dye-microbe interactions and/or the resulting end products. Leveraging proteomics can offer valuable insights by elucidating the proteins and pathways involved in enzymatic degradation of synthetic azo dyes and facilitating biotransformation in specific species or strains. It remains pertinent to understand the mechanisms of aromatic dye decolorization to aid the development of effective bioremediation strategies. Proteins are both a structural and functional component of the cell and are fundamental to living systems, contributing to both molecular and metabolic intra-cellular events (Hassan *et al*., 2022). Bacterial proteome analysis is a widely recognized approach for obtaining a wealth of biological insights as cellular protein expression is linked to numerous unexplored biological processes. This makes it highly valuable for advancing functional proteomics in various biological systems (Patterson and Aebersold, 2003). Notably, proteomics has proven instrumental in identifying numerous natural gene products produced by microorganisms (Bumpus *et al*., 2009), as well as facilitating the development of novel halophilic enzymes (Choi *et al*., 2005).

Bacterial species employ numerous strategies to eliminate or discolor azo compounds from their surroundings including biosorption, bioaccumulation, reduction, oxidation, and sequential reduction-oxidation processes (Mahmood *et al*., 2016). Among various bacterial species, *Shewanella* stands out due to its diverse respiratory metabolic pathways, making it a promising candidate for bioremediation (Heidelberg *et al*., 2002). To gain valuable insights, it is crucial to comprehend and assess the changes in the organism's proteome during its growth. For instance, Zhao and Poh (2008) elucidate how different cellular

protein components of bacteria react differently to different environmental stimuli. Proteins may be either up- or down-regulated in response to exposure to various stresses in the environment (Gao *et al*., 2004). An *et al*., (2020) adopted an integrated metagenomic and metaproteomic analyses to investigate the functional genes and proteins involved in the decolorization of Direct Black G by thermophilic microflora. Proteomic analyses help to establish stress-response mechanisms in bacteria under dye exposure, critical for the evolution of more robust and effective decolorization strains. Proteomic data has further unveiled the interconnected pathways involved in dye decolorization, such as electron transport chain and secondary metabolite biosynthesis pathways, providing deeper insights into the bacterial metabolic machinery (Chen *et al*., 2020, Zhang *et al*., 2022). It is important to understand complex biological activities and interactions in order to reveal the molecular mechanisms involved in microbial remediation of environmental pollutants. This would aid in the development of increasingly promising bioremediation strategies.

This study used a gel-free proteomic approach to evaluate the changes in protein expression of *Shewanella seohaensis* NIO_14d during the decolorization of three reactive dyes, Reactive Black 5 (RB5), Reactive Green 19 (RG19) and Reactive Red 120 (RR120). A Liquid Chromatography Mass Spectrometry - Quadrupole Time of Flight (LCMS-QToF) system was employed to identify the differential expression of proteins and measure their abundance during dye decolorization.

5.2 Materials and Methods

5.2.1 Microorganism and growth conditions

The protein expression profile of the dye decolorizing bacterial isolate collected from an estuarine location in Goa, India was analyzed in this study. The strain NIO_14d was identified by 16S rDNA gene sequencing as *Shewanella seohaensis* (GenBank Acc. No.: KR922404) as discussed in **Section 3.2.5**. The culture was purified on seawater nutrient agar (SWNA containing [l^{-1}]: peptic digest of animal tissue 5.0 g, sodium chloride 5.0 g, beef extract 1.5 g, yeast extract 1.5 g, agar 15 g, distilled water 500 mL, sea water 500 mL, pH 7.4 ± 0.2) and a loopful of seed culture from an isolated colony was pre-cultured in 10 mL nutrient broth. For proteomic analysis, overnight grown culture was inoculated in sterile NB and grown until mid-exponential phase ($O.D_{600}$ ~ 0.4; time taken ca. 6h). This freshly prepared primary inoculum (1% (v/v)) was added to Erlenmeyer flasks (250 mL) containing 100 mL of sterile nutrient broth amended individually with 100 mg L^{-1} of the reactive dyes RB5, RG19 and RR120 (Sigma-Aldrich). Cells were harvested by centrifugation at 14,000 rpm at 4°C for 10 min. Cell pellets were washed twice with 1X Phosphate Buffer (PB containing [l^{-1}]: disodium hydrogen phosphate 1.42 g, potassium dihydrogen phosphate 0.24 g, distilled water 1000 mL, pH 7.4 ± 0.2) to ensure removal of media containing dyes. Inoculated dye-free NB was processed under the same conditions and used as control.

5.2.2 Cellular protein extraction

The cell pellets of *Shewanella seohaensis* NIO_14d, obtained at the time points 7 hours and 24 hours following dye decolorization, were washed twice with 1X PB and resuspended in 1 mL of protein extraction buffer along with zirconia beads and homogenized in a Fast-Prep®24 homogenizer (MP Biomedicals, USA) at 6.5 m/s for 40 seconds. The tubes were held on ice for rest duration (5min) between each homogenization step. Whole cell proteins were extracted using a urea-thiourea (UT) buffer containing [ml^{-1}]: urea 0.42 g, thiourea 0.15 g, CHAPS 0.4 g, IPG buffer (Immobilized pH gradient) 80 µL, Dithiothreitol (DTT) 0.03 g and 1M tris solution 200 µL. The bacterial cells and debris were then centrifuged at

14,000 rpm for 20 min at 4°C, and supernatant transferred to a fresh microcentrifuge tube. Residual proteins were further extracted by adding another 500 µL of urea-thiourea buffer to the cell debris in the zirconia bead bashing tube and re-homogenized. The supernatants were pooled and proteins in suspension were maintained in extraction buffer. Aliquots as required were used for proteomic analysis and the remaining protein samples were stored at -20°C for further use.

5.2.3 Protein estimation and methanol precipitation

A volume of 50 µL of the supernatant obtained from protein extraction was taken and 1:9 (v/v) 100% methanol (Fluka, MS grade) was added and incubated at 4°C for a minimum of 1h. Tubes were then centrifuged at 14,000 rpm for 20 min at 4°C and supernatant discarded followed by addition of 90% methanol (Friedman, 2007). After incubation and centrifugation, pellets were vacuum dried for 20 min at 30°C (care was taken not to over-dry). The vacuum dried samples were resuspended in 1 mL of TE buffer (pH 8.3) (**Appendix D**) containing 10 µL of 1X protease inhibitor (Serva, Germany).

Protein estimation was carried out following the standard procedure (Lowry *et al.*, 1951). To 1mL of sample, 5ml of Reagents A+B (**Appendix D**) were added and incubated at room temperature for 10 min. To this, 0.5mL of Folin and Ciocalteau's Phenol reagent was added and tubes were incubated in the dark for 30 min. Following dark incubation, absorbance was read at O.D660 with protein extraction buffer used as blank and Bovine serum albumin as standard for calibration. Absorbance readings were used to estimate protein content in each sample. Based on the calculations, suitable volumes were dispensed and used for methanol precipitation containing a fixed concentration of protein (for each sample). This was to ensure equal amount of protein was represented in each sample in subsequent tests

5.2.4 Gel electrophoresis

The bacterial proteins present in the extracts were resolved using Sodium dodecyl sulfate - Polyacrylamide gel electrophoresis (SDS-PAGE) in a Mini-Protean electrophoresis unit (Bio-Rad Laboratories), according to Laemmli (1970). Precipitated total protein samples

(100µg µL^{-1} each) resuspended in sample solubilizing buffer (15µL) (**Appendix D**) were heated in a dry bath at 95°C for 5min before being loaded on to a 6% stacking gel overlying a 12% resolving gel (**Appendix D**). A medium range protein molecular weight marker (97.4 - 14.3 kDa) (Perfect protein marker, GeNei) was prepared similarly. The tubes were subjected to a short spin to ensure the entire sample volume is loaded. Electrophoresis was carried out in 1X running buffer (**Appendix D**) at 90V for two hours. Gels were treated with fixative (**Appendix D**) for 1-2h, and stained using silver stain technique following the protocol described by Heukeshoven and Dernick, (1985). The stained gels were visualized (G-Box F3 Gel Documentation System, Syngene, UK) to check the quality of proteins before processing them further.

5.2.5 In-solution digestion

The quality of the protein samples was assessed based on visual appearance of protein bands obtained on SDS gels. In-solution digestion of the proteins was carried out using trypsin digestion following a method modified from Kinter and Sherman, (2000). Precipitated protein sample pellets were reconstituted using 6M urea as a chaotropic agent along with 200mM DTT and 200 mM iodoacetamide as reducing and alkylating agents, respectively. The mixture was incubated in dark conditions at room temperature. The urea concentration was diluted by adding 500µL of 50mM Tris-HCl. The extracted protein sample (100 µg) was digested with 1 mg mL^{-1} trypsin (20µg Proteomic grade Trypsin from porcine pancreas dissolved in 20µL of 1mM HCl, Sigma T6567, USA) at 37°C for 15 hours. After digestion, the samples were acidified to a pH of 2-3 using 100% formic acid (MS grade) before subjecting to mass spectrometry.

5.2.6 Mass Spectrometry and Protein Identification

5.2.6.1 *LC/MS-QToF analysis*

Aliquots (60 µL) of acidified tryptic digests were transferred to autosampler MS vials, sealed and analyzed using the in-house LCMS-QToF facility (6538 UHD Accurate Mass QTOF LC/MS, Agilent Technologies, USA). Eight µL sub-volumes of the digested

samples were injected into the auto-sampler in quadruplets on a Prot ID Chip 150 II 300A C18 150 mm column. The LC separations were carried out using deionized water (aqueous phase) and HPLC grade acetonitrile (ACN; organic phase) across a gradient elution with 0.1% Formic acid used as an adduct in both the aqueous and organic phases. The peptides were eluted using a standardized 71-minute protocol with a with a linear gradient of increasing acetonitrile concentration (2 to 90% for 50 min, 90% for 10 min and 90 to 2% for 3 min). The MS/MS spectra for the separated ions were acquired in the range of 50 to 2000 *m/z* in positive mode at 2 ppm accuracy. The spectral data was acquired using Mass Hunter Software ver. B.06.00 (Agilent Technologies, USA) (de Souza *et al*., 2019)

5.2.6.2 *Identification of Proteins*

The spectra obtained through Mass Hunter were used for protein identification and quantification using Spectrum Mill software ver. B.04.01.141 (Agilent Technologies, USA) by following the manufacturer's instructions. The MS/MS spectra acquired were searched against the genus-specific UniProtKB/Swiss-Prot database for *Shewanella*. The search was carried out at an accuracy of 50 ppm for MS and 100 ppm for MS/MS. In addition, a maximum of 2 missed cleavages was allowed. Auto-validation was carried out for the database matches using the default settings with a False Discovery Rate (FDR) of 1.2% to generate the protein and peptide summary files. Significant proteins had cut-off peptide scores in protein mode >1 with a scored peak intensity (SPI) of >10% for peptides.

5.2.6.3 *Statistical analyses*

Mass Profiler Professional (MPP) software ver. 14.5 (Agilent Technologies, USA) was used to analyze the protein hits generated in Spectrum Mill. The study was a high throughput discovery proteomics experiment and samples were run as four technical replicates. The proteins were identified in each of the replicates and grouped for each sample viz. dye-free control, RB5, RG19 and RR120. Each identified protein entity in the sample was filtered based on the frequency of occurrence in at least one condition. The differential significance was determined using a p-value cut-off of 0.2 and a fold- change

cut-off of 2.0 when comparing dye-free control samples versus dye-amended samples. The protein matches satisfying the cut-off criteria were cross-referenced with their UniProtK Accession numbers and classified based on their functions using the Kyoto Encyclopedia of Genes and Genomes, ver. 37 (KEGG) pathways database. Venn diagrams were created to identify proteins which were up-regulated during dye decolorization and categorize proteins found to be common to all the conditions.

5.3 Results

5.3.1 Gel electrophoresis

Proteins that were differentially regulated during azo dye decolorization by *Shewanella seohaensis* NIO_14d were analyzed in this study. The protein profile differed when the isolate was grown in the presence and absence of the azo dyes as seen from the intensity of the different bands in SDS-PAGE (**Figure 5.1**). The SDS-PAGE fragments for proteins suppressed or induced when the isolate was initially exposed to the azo dyes were found to be distinctly different from the proteins expressed by *Shewanella seohaensis* NIO_14d in decolorized dye samples after 24 hours. The protein profiles for the decolorized dye samples were found to be visually similar to the proteins produced by the isolate in dye-free NB with the exception of the possible induction of two protein fragments corresponding to 21 kDa and 17 kDa in size.

5.3.2 Protein identification

The proteomic profile of *Shewanella seohaensis* NIO_14d during azo dye decolorization was examined. The numbers of proteins expressed in medium with dyes was compared to that expressed in the dye-free control in order to determine the changes in the protein profile accompanying dye decolorization. The accession numbers of the identified proteins were referenced using the UniProtKB database (www.uniprot.org). Approximately, a total of 1182 functionally different protein hits were obtained from the data acquired using the MPP software ver. 14.5 (Agilent Technologies, USA). Of these, 507 entities were obtained

from the culture grown in the absence of the dyes (control), whereas, 423, 417 and 677 proteins were detected in *Shewanella seohaensis* NIO_14d grown in medium with RB5, RG19 and RR120, respectively. These proteins were inclusive of those detected at 7h as well as 24h during the process of dye decolorization.

5.3.3 Functional characterization of expressed proteins

The proteins identified from the UniProtKB database belonged to broad functional categories and were accordingly classified as shown in **Figure 5.2**. All the differentially expressed proteins were segregated into 15 broad categories based on their physiological functions assigned using the Kyoto Encyclopedia of Genes and Genomes, ver. 37 (KEGG) metabolic pathways (https://www.genome.jp/kegg/pathway.html) and Clusters of Orthologous Groups (COG) database. This allowed a comparative analysis of the proteins expressed between control and dye treatment. It was observed that the number of proteins differentially expressed during dye decolorization did not vary much compared to the dye free control. The maximum number of proteins identified were those involved in translation (84 for RR120, 62 for RG19, 71 for RB5 and 84 for dye-free NB) which made up ~15% of the total classified proteins. Following this, the largest group of proteins were those involved in energy metabolism (10.5%), amino acid metabolism (10.25%), cellular processes (9.4%) and membrane transport (9.3%).

The minimum numbers of identified proteins were those involved in the metabolism of other molecules including terpenoids, polyketides, flavonoids and secondary metabolite biosynthesis, accounting for only 0.6% of the total classified proteins. A fraction of the proteins did not have annotated matches in the UniProt database and were consequently grouped as proteins with “Miscellaneous & Unknown function”.

5.3.4 Comparison of differentially expressed proteins

Quantitative analysis of the protein profiles revealed significant differences in protein expression of *Shewanella seohaensis* NIO_14d exposed to reactive azo dyes. At 7 hours of

incubation of the isolate with the dyes, 176, 113 and 231 proteins were up-regulated during the decolorization of RB5, RG19 and RR120 respectively (**Figure 5.3A**). Further, at 24 hours following dye decolorization as many as 138, 219 and 520 proteins were up-regulated in *Shewanella seohaensis* NIO_14d grown in RB5, RG19 and RR120 respectively as compared that grown in the dye-free control (**Figure 5.3B**). As many as 29 (~5%) proteins were uniquely up-regulated for all the conditions compared in the early stages of dye decolorization (7 hours). As the dye decolorization progressed, 17 (~2%) commonly up-regulated proteins were identified at 24 hours. Each dye condition revealed a unique set of proteins with the most number of proteins observed when the isolate was grown in the presence of RR120 (**Figure 5.3**).

5.3.5 Dye decolorization induced changes in abundance of expressed proteins

Prominent proteins expressed by *Shewanella seohaensis* NIO_14d during the decolorization of RB5 are listed in **Table 5.1**. Similarly, up-regulated proteins identified during decolorization of Reactive Green 19 and Reactive Red 120 are summarized in **Tables 5.2** and **5.3** respectively. It was observed that during dye decolorization, many proteins predominantly up-regulated played a role in energy metabolism, especially the cellular oxidoreductases. Proteins commonly expressed in all three dye decolorizing conditions were an oxidoreductase FAD/NAD (P)-binding domain protein (SwissProt ID: A8GZW1) and an alkyl hydroperoxide reductase (SwissProt ID: A9KY42). At 24 hours of exposure, the alkyl hydroperoxide reductase was up-regulated by 1.54, 1.25 and 7.68 folds under RB5, RG19 and RR120 dye decolorizing conditions respectively. This oxidoreductase protein complex uses either NADH or NADPH as an electron donor for direct reduction of redox dyes or of alkyl hydroperoxides. It functions in cellular response to oxidative stress and was notably absent in the control sample without dye.

Additionally, multiple proteins with annotated roles in electron transport were found to be up-regulated during reactive azo dye decolorization. A fumarate reductase flavoprotein subunit (SwissProt ID: P83223) was up-regulated by 1.29, 16.00 and 1.66 in RB5, RG19 and RR120 decolorizing conditions respectively. Cytochrome c protein (SwissProt ID: A9L5Q8) which is also an electron transport protein, was identified in all three dye-

challenged samples as well as in dye-free control with a fold change of 1.18 (in RR120 decolorizing condition) and 16.00 (in RB5 and RG19 decolorizing conditions). Two NADH dependent oxidoreductases (SwissProt ID: B0TT30 and Q8EI38) were significantly up-regulated when compared to the isolate exposed to the dye-free control. An important observation revealed the detection of an FMN-dependent NADH-azoreductase obtained under RG19 decolorizing condition.

Shewanella seohaensis NIO_14d showed increased expression of two transport proteins during dye decolorization conditions. These were Na (+)-translocating NADH-quinone reductase subunit A detected during decolorization of RG19 (fold change of 16.00) and RR120 (fold change of 1.36) and TRAP dicarboxylate transporter (fold change of 16.00) detected during decolorization of RB5. A membrane protein with 3.59-fold increase, reported to be involved in aromatic hydrocarbon degradation was identified in RB5 decolorizing condition at 7 hours

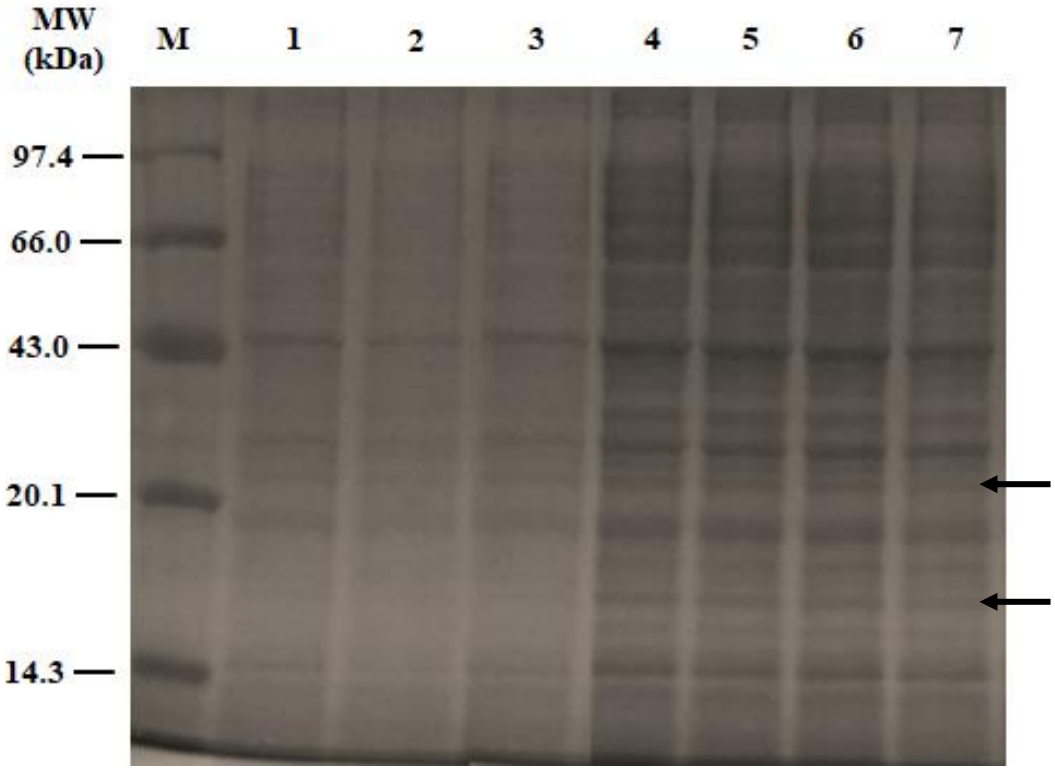


Figure 5.1: SDS-PAGE protein profiles for *Shewanella seohaensis* NIO_14d grown in the presence and absence of reactive azo dyes. *Lanes* **M,** Medium range protein molecular marker (14.3 - 97.4 kDa); **1**, isolate grown in RB5 at 0h; **2**, isolate grown in RG19 at 0h; **3**, isolate grown in RR120 at 0h; **4**, isolate from decolorized RB5 at 24h; **5**, isolate from decolorized RG19 at 24h; **6**, isolate from decolorized RR120 at 24h; **7**, isolate grown in dye-free NB. Arrows indicate major proteins expressed during dye decolorization. Molecular weight of protein standards in kDa are shown on the left side of gel.

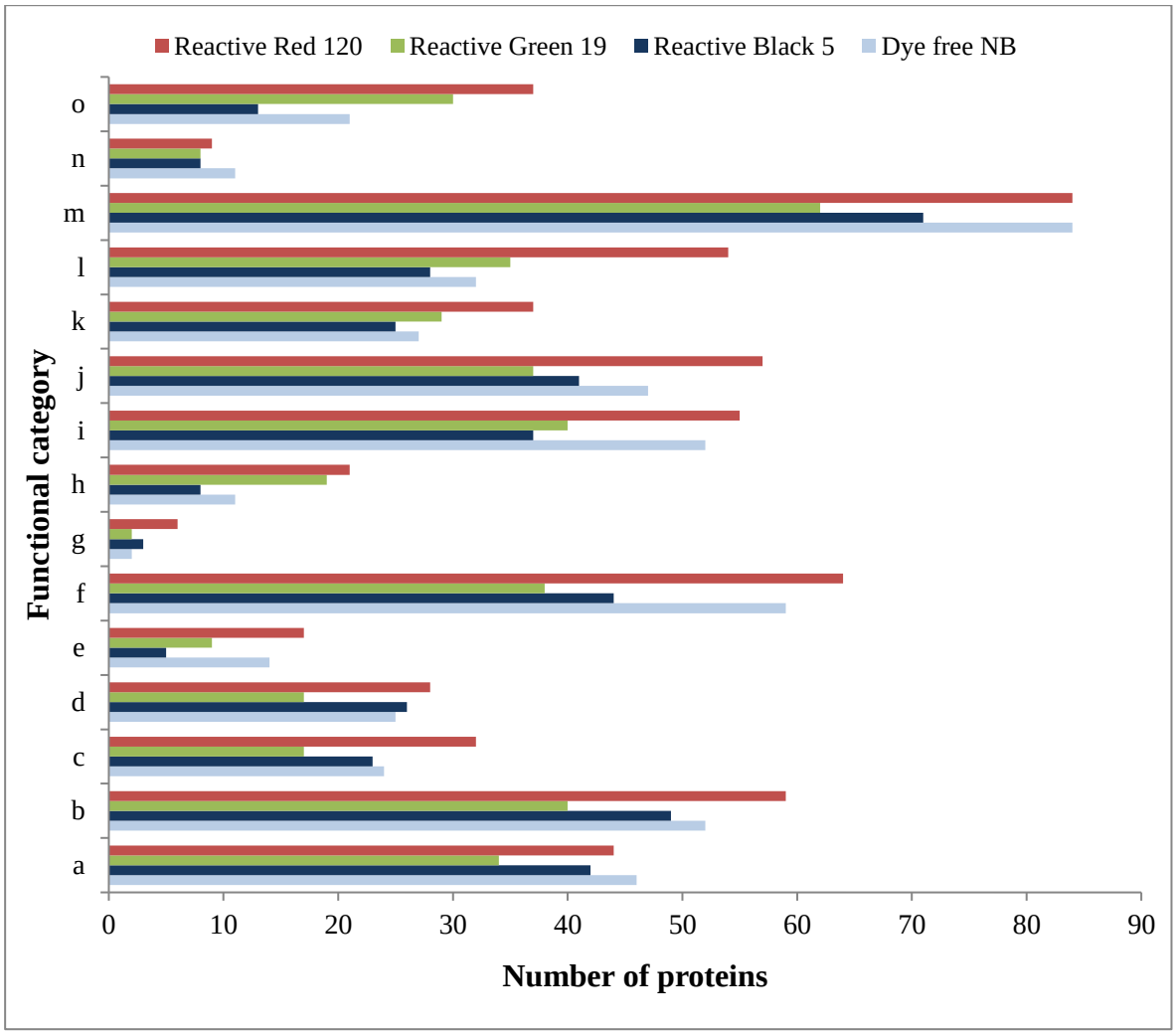


Figure 5.2: Functional classification of identified proteins expressed in dye-free nutrient broth compared to those expressed during decolorization of the reactive dyes: RR120, RG19 and RB5. Lowercase letters along the y-axis refer to the following categories of functional roles: (a) Carbohydrate metabolism; (b) Amino acid metabolism; (c) Lipid metabolism; (d) Nucleotide metabolism; (e) Cofactors and vitamins metabolism; (f) Energy metabolism; (g) Other metabolic processes; (h) Signal transduction; (i) Cellular process; (j) Transport; (k) Replication and repair; (l) Transcription; (m) Translation; (n) Protein folding, sorting and degradation; (o) Miscellaneous & Unknown function. (KEGG metabolic database, https://www.genome.jp/kegg/) (de Souza *et al*., 2019)

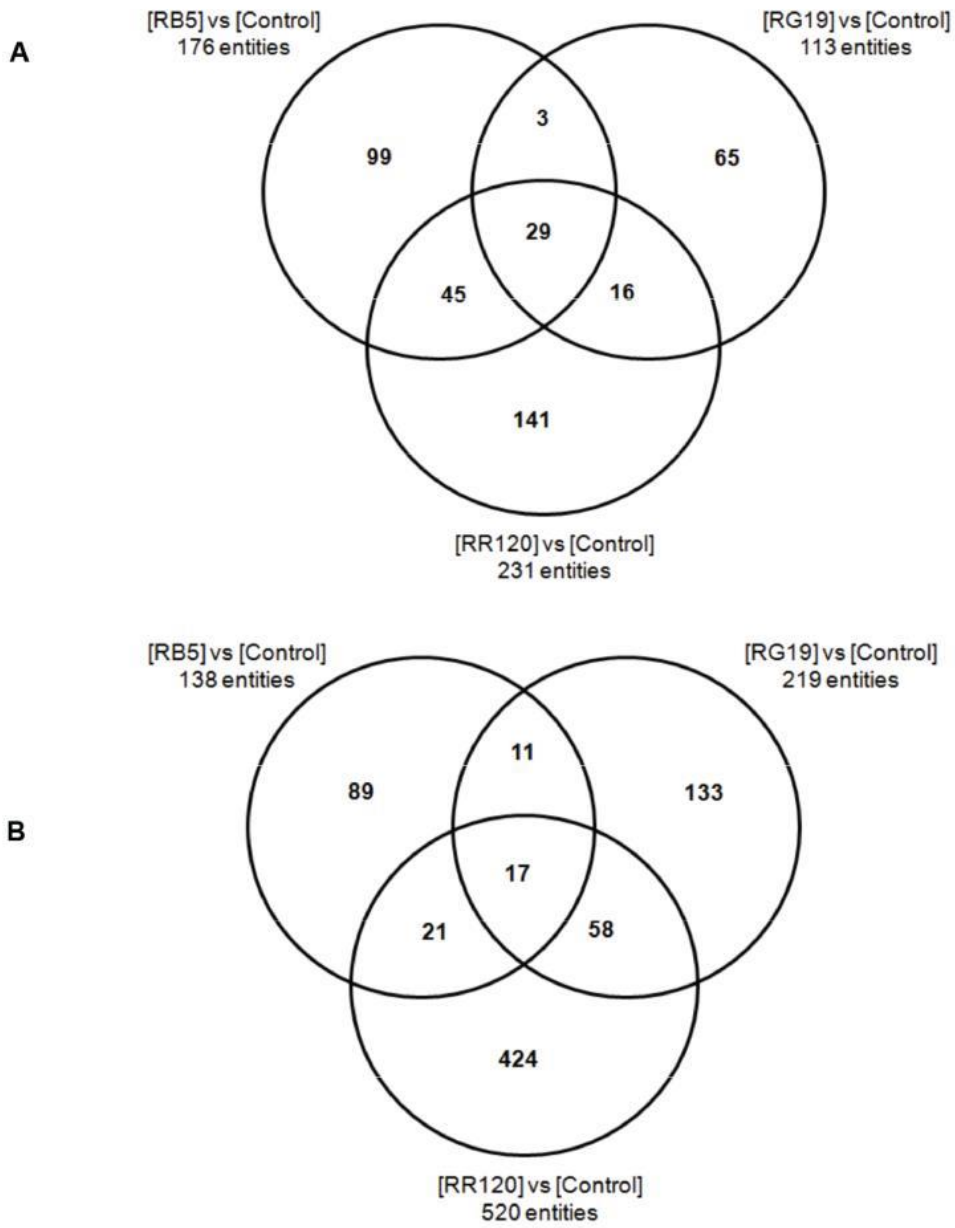


Figure 5.3: Venn diagrams comparing up-regulated proteins entities in dye challenged *Shewanella seohaensis* NIO_14d versus control (without dye). (**A**) Up-regulated entities at 7 hours; (**B**) Up-regulated entities at 24 hours of exposure to dyes (de Souza *et al*., 2019)

Table 5.1: Proteins up-regulated during decolorization of Reactive Black 5 azo dye (de Souza *et al*., 2019)

Swiss-Prot ID	Protein name	Gene based on protein ID	Protein Mass (Da)	Functional category[a]	MS/MS search score	Number of distinct peptides	% coverage[b]	Fold change[c]
A9L5Q8	Cytochrome c prime	*Sbal195_1300*	16506.6	energy metabolism	18.9	1	14.7	16.00
P83223	Fumarate reductase flavoprotein	*SO_0970*	62903.3	energy metabolism	129.43	8	24.6	1.29
A8GZW1	Oxidoreductase FAD/NAD(P)-binding domain protein	*Spea_0520*	26730	energy metabolism	6.84	1	2.9	1.08
Q8EI38	NADH-quinone oxidoreductase, subunit K	*nuoK*	11211.3	energy metabolism	3.61	1	12.7	16.00
A9KY42	Alkyl hydroperoxide reductase/ Thiol specific antioxidant	*Sbal195_1777*	22160.7	peroxiredoxin activity	49.09	4	24.8	1.54
A1S369	Alkyl hydroperoxide reductase	*Sama_0617*	20943.4	peroxiredoxin activity	56.8	4	29.1	16.00
Q8EI86	Alkyl hydroperoxide reductase peroxiredoxin component AhpC	*ahpC*	20971.4	peroxiredoxin activity	60.75	4	33.3	16.00
A4Y8D8	TRAP dicarboxylate transporter, DctP subunit	*Sputcn32_2500*	38006	membrane transport	5.6	1	7.6	16.00
A9KTX7	Membrane protein involved in aromatic hydrocarbon degradation	*Sbal195_2866*	46196.6	cellular process	35.54	2	8.7	3.59

[a] Functions are reported according to KEGG2 metabolic database (http://www.genome.jp/kegg/kegg2.html)

[b] Percent amino acid coverage

[c] Fold change compared to dye free control

Table 5.2: Proteins up-regulated during decolorization of Reactive Green 19 azo dye (de Souza *et al*., 2019)

Swiss-Prot ID	Protein name	Gene based on protein ID	Protein Mass (Da)	Functional category[a]	MS/MS search score	Number of distinct peptides	% coverage[b]	Fold change[c]
A9L5Q8	Cytochrome c prime	*Sbal195_1300*	16506.6	energy metabolism	12.92	1	14.7	16.00
A8GZW1	Oxidoreductase FAD/NAD(P)-binding domain protein	*Spea_0520*	26730	energy metabolism	6.49	1	2.9	2.94
A8FPZ7	FMN-dependent NADH-azoreductase	*azoR*	21205.9	energy metabolism	8.31	1	9.6	16.00
P83223	Fumarate reductase flavoprotein subunit	*SO_0970*	62903.3	energy metabolism	26.5	2	4.1	16.00
B0TT30	NADH:flavin oxidoreductase/NADH oxidase	*Shal_2030*	74360.4	energy metabolism	5.19	1	3.8	1.49
A9KY42	Alkyl hydroperoxide reductase/ Thiol specific antioxidant	*Sbal195_1777*	22160.7	peroxiredoxin activity	41.25	4	35.3	1.25
A8FYW2	Na (+)-translocating NADH-quinone reductase subunit A	*nqrA*	47902.9	membrane transport	38.55	3	9	16.00
B1KNE0	TRAP dicarboxylate transporter, DctP subunit	*Swoo_1732*	39527.3	membrane transport	4.79	1	7.5	16.00

[a] Functions are reported according to KEGG2 metabolic database (http://www.genome.jp/kegg/kegg2.html)

[b] Percent amino acid coverage

[c] Fold change compared to dye free control

Table 5.3: Proteins up-regulated during decolorization of Reactive Red 120 azo dye (de Souza *et al*., 2019)

Swiss-Prot ID	Protein name	Gene based on protein ID	Protein Mass (Da)	Functional category[a]	MS/MS search score	Number of distinct peptides	% coverage[b]	Fold change[c]
A9L5Q8	Cytochrome c prime	*Sbal195_1300*	16506.6	energy metabolism	12.96	1	14.7	1.18
A8GZW1	Oxidoreductase FAD/NAD(P)-binding domain protein	*Spea_0520*	26730	energy metabolism	6.61	1	2.9	3.32
P83223	Fumarate reductase flavoprotein subunit	*SO_0970*	62903.3	energy metabolism	65.37	4	12.4	1.66
BOTT30	NADH:flavin oxidoreductase/NADH oxidase	*Shal_2030*	74360.4	energy metabolism	4.85	1	3.8	16.00
A9KY42	Alkyl hydroperoxide reductase/ Thiol specific antioxidant	*Sbal195_1777*	22160.7	peroxiredoxin activity	58.04	4	35.3	7.68
Q8EI86	Alkyl hydroperoxide reductase peroxiredoxin component	*ahpC*	20971.4	peroxiredoxin activity	73.18	5	48.1	16.00
A4Y3Y6	Na (+)-translocating NADH-quinone reductase subunit A	*nqrA*	47856.1	membrane transport	77.97	6	23.1	1.36

a Functions are reported according to KEGG2 metabolic database (http://www.genome.jp/kegg/kegg2.html)

b Percent amino acid coverage

c Fold change compared to dye free control

5.4 Discussion

In this study, expressional proteomics was used to examine the protein expression during decolorization of reactive azo dyes. SDS-PAGE was carried out on whole cell protein extracts of *Shewanella seohaensis* NIO_14d grown in the presence and absence of three reactive dyes, RB5, RG19 and RR120. SDS-PAGE results revealed a differential protein profile before and after the decolorization of azo dyes. The gel electrophoresis observations indicate a preliminary induction of low molecular weight proteins. These up-regulated proteins are possibly representing a regulatory function in response to azo dye challenge in *Shewanella seohaensis* NIO_14d. There have been reports of oxidative and reductive bacterial enzymes being actively up-regulated (Liu *et al*., 2009b; Ryan *et al*., 2010; Zhang *et al*., 2013; Joshi *et al*., 2020), during the process of dye decolorization. These enzymes have been described to play a key role in the pathways of dye degradation and color removal.

In this study, SDS-PAGE allowed for visualization of protein profiles from whole-cell extracts during reactive azo dye decolorization. In solution LC-MS/MS analysis was used to further understand expressional proteomic differences in *Shewanella seohaensis* NIO_14d and investigate possible cellular metabolic components with pivotal roles in the decolorization pathway. The 1182 proteins identified were grouped into COG functional groups corresponding to 33% of the predicted 3545 protein coding ORF's within *Shewanella seohaensis* (Proteome ID: UP001062925). From the functional classification of identified proteins, it was observed that the presence of azo dyes did not significantly impact the number of detected proteins. Despite the dye challenge and decolorization process, essential cellular processes remained unaffected as evidenced by robust growth of the culture and expression of major metabolic proteins in all three dye challenged conditions. The presence of proteins without a predicted function highlights that there may still be uncharacterized proteins whose functions are yet to be annotated. Characterizing these proteins may offer suggestions to their potential role in metabolic and cellular pathways including dye degradation. This can be possible by adopting improved MS/MS search parameters or investing in improved metagenomic, metaproteomic and transcriptomic studies (An *et al*., 2020)

Shewanella strains have gained recognition as excellent candidates for bioremediation due to their ability to use a wide range of electron donors and acceptors, which helps mitigate the toxic effects of various contaminants (Hong and Gu, 2010). Their potential in bioremediation is attributed to specific cellular proteins, including cellular oxidoreductases, c-type cytochromes, and peroxiredoxins, which play crucial roles in the reductive metabolism of *Shewanella* species. Some of these proteins have also been implicated in the decolorization of azo dyes, as proposed by Chen *et al*., (2010). Numerous studies have focused on identifying and characterizing the molecular components involved in the dye decolorization process (Hong *et al*., 2007b; Brigé *et al*., 2008; Wu *et al*., 2009; Wang *et al*., 2010). Notably, the bacterial electron transport chain was first proposed to be involved in azo dye reduction by Kudlich *et al*., (1997). Peroxiredoxins, a class of enzymes with antioxidant protective functions, were also suggested to play a protective role in cells by Dubbs and Mongkolsuk (2007). The up-regulation of relevant oxidoreductases (oxidoreductase FAD/NAD(P)-binding domain protein) and peroxiredoxins (*ahpC* gene encoded alkyl hydroperoxide reductase) in dye-exposed *Shewanella seohaensis* NIO_14d indicates their potential involvement in the dye decolorization process. However, experimental validation of these proteins was not conducted in this discovery proteomic experiment.

Telke *et al*., (2009) and Thakur *et al*., (2014) have shown azo dye decolorization to proceed through a reductive enzymatic pathway. Moreover, Leelakriangsak, and Borisut (2012), and Mahmood *et al*., (2017), have well documented the activity of NADH-ubiquinone: oxidoreductase and FMN dependent NADH-azoreductase in the azo dye detoxification process. An increased expression of NADH:flavin oxidoreductase/NADH oxidase and 16 fold up-regulation of FMN-dependent NADH-azoreductase in *Shewanella seohaensis* NIO_14d was observed. Azoreductases have been described to utilize NADH and/or NADPH as an electron donor, and decolorize azo dyes into corresponding aromatic amines by reductive cleavage of azo bonds (Chen, 2006).

Quinones are widespread in nature, functioning as metabolites or byproducts of various organisms. They are capable of engaging in harmful redox cycling, resulting in an increased build-up of reactive oxygen species (ROS). The intracellular synthesis of these species, such as superoxide, hydrogen peroxide (H_2O_2), and hydroxyl radicals, can damage lipids, proteins,

and nucleotides (Deller *et al.*, 2008). Moreover, electrophilic quinones can react with cellular thiols via Michael addition, a reaction that forms S-adducts through covalent bonds. This reaction leads to the exhaustion of cellular thiols, subsequently triggering thiol-specific stress within cells (Rodriguez *et al.*, 2005). The use of quinone compounds to immobilize quinone-reducing microorganisms is considered a promising approach to enhance the anaerobic decolorization of xenobiotic azo dyes. Despite its potential, there is limited knowledge about how these microorganisms respond to immobilized quinones in the presence of azo dyes. Zhang *et al*., (2013) have investigated the response of quinone reducing *Escherichia coli* strain to immobilized anthraquinone-2-sulfonate reduction and acid red 18 dye decolorization. Contrastingly, Liu *et al*., (2009b) described an azoreductase which does not contribute to in vivo dye reduction but instead serves to protect against thiol-specific stress. Studies described by Ryan *et al*., (2010) proposed a novel mechanism of NADH quinone oxidoreductase to explain the contradiction of how the same enzyme can reduce both azo and quinone substrates. Two significantly up-regulated proteins Alkyl hydroperoxide reductase/ Thiol specific antioxidant and Na (+) translocating NADH-quinone reductase, observed in this study, could probably be attributed to exert such a dual role. In doing so, these proteins could have a likely role in color removal as well as a protective response to thiol specific stress. However, this warrants further investigation to establish a more objective relationship between the two processes.

Studies by Hong and Gu (2010), Hong *et al.*, (2007b), and Wang *et al*., (2010) have demonstrated that fumarate reductase enhances decolorization by transferring electrons during bacterial azo reduction. In line with these findings, the analysis of results from this study shows a significant up-regulation of the fumarate reductase flavoprotein subunit, suggesting its similar role in *Shewanella seohaensis* NIO_14d. This protein constitutes a part of the bacterial energy metabolism and is expressed during the decolorization of all three reactive azo dyes in this study. It is likely that energy metabolism and the shuttling of electrons concomitantly occur during dye decolorization and may play an active role in the process.

Transport proteins also play a vital role in the response of bacteria to environmental contaminants, including azo dyes and heavy metals. A transport protein, namely TRAP

dicarboxylate transporter, was found to be up-regulated in *Shewanella seohaensis* NIO_14d, indicating the probable involvement of this protein in transferring reducing electrons to the azo dye during the decolorization process, as previously described by Tang *et al*., (2007). Furthermore, cytochrome c proteins have been observed to be crucial components of the electron transport chain involved in reducing dye molecules and facilitating the decolorization process, as reported by Brigé *et al*., (2008). Consistent with these findings, multiple up-regulated cytochrome c proteins were identified in *Shewanella seohaensis* NIO_14d associated with the decolorization of the three reactive azo dyes. During decolorization of samples containing the azo dye RB5, a membrane protein involved in aromatic hydrocarbon degradation was identified. Gene Ontology (GO) annotation indicated that this 46.197 kDa polypeptide functions in membrane transport associated with the catabolism of aromatic hydrocarbons. The identification of this protein was based on the similarity hit to the polypeptide found in *Shewanella baltica* (strain OS195). Studies aimed at ex-situ expression of this and other up-regulated proteins would be highly valuable.

In summary, expressional proteomics enables a comprehensive investigation into alterations in protein makeup, along with the identification of proteins that are part of the reaction in a specific physiological condition (Vasseur *et al*., 1999). Utilizing this method provides a global perspective and a strategy to explore the molecular mechanisms underlying bioremediation, particularly the cellular responses to external stresses or stimuli. The protein profiles obtained from this study highlight the up-regulation of cellular oxidoreductases that likely function in electron transfer during azo dye decolorization. However, to fully comprehend the specific metabolic pathways in which these proteins operate, further investigations combining computational and other 'omics' techniques will be necessary. These integrated approaches will provide a deeper understanding of the molecular mechanisms underlying the efficient decolorization and detoxification processes performed by *Shewanella seohaensis* NIO_14d, making it a promising candidate for azo dye bioremediation.

Chapter 6

Molecular Characterization of Genes Involved in Dye Decolorization

Chapter 6

Molecular Characterization of Genes involved in Dye Decolorization

6.1 Introduction

Synthetic azo dyes constitute a significant heterogeneous environmental contaminant and present a serious threat to both, global environment and human health. The prevalence of these dyes in the environment has led to an increased interest in biological systems for the treatment of these pollutants. Many bacterial strains capable of facilitating the decolorization and complete mineralization of azo dyes under various conditions have been isolated and investigated (Sudha *et al*., 2018; Tang *et al*., 2018; Srinivasan *et al*., 2019; Chen *et al*., 2020; Neihsial *et al*., 2022). These studies have mainly focused on the characterization of dye degrading microorganisms and speculated on the pathways of dye degradation based on analysis of degradation products (Chen *et al*., 2020). Azo dye decolorization is largely driven by an enzymatic breakdown of the dye molecule. The various oxido-reductive enzymes with key functions in azo dye decolorization and degradation have been summarized by Singh *et al*., (2015) and Pinheiro *et al*., (2022). During the bioremediation process, the organisms undergo rapid genetic changes that enable them to acquire new metabolic pathways for the breakdown of xenobiotic substances (Igiri *et al*., 2018). It is thus important to identify the specific functional genes involved in microbial dye decolorization and understand their role in the degradation pathway. Consequently, conducting in-depth investigations into the crucial enzymes and functional genes involved in the degradation of azo dyes by bacteria can significantly enhance our comprehension of the gene regulation mechanisms employed by these bacteria during dye decolorization. This, in turn, could offer valuable theoretical insights to optimize the bioremediation of azo dyes effectively. Genomics tools have given new impetus to examine and identify key elements in microbial responses to azo dyes. Ooi *et al*., (2007), Mendes *et al*., (2011), Joshi et al., (2020) reported azo dye decolorization

related genes and how they contribute to color removal. The genes encoding azoreductases have been observed in multiple bacterial genera such as *Pseudomonas, Pigmentiphaga, Bacillus, Geobacillus, Enterococcus, Escherichia* and *Clostridium* (Leelakriangsak, 2013). The detection and molecular characterization of these genes is possible by specific primers designed to target and amplify the template. In recent years, there has been a widespread utilization of transcriptomics and quantitative real-time polymerase chain reaction (qRT-PCR) to investigate changes in gene expression in organisms when they are exposed to external stimuli (Sharma *et al*., 2022).

In this study, the azoreductase gene in *Shewanella seohaensis* NIO_14d was detected using gene specific primers and the gene expression was quantitatively analyzed by Real Time - quantitative PCR (RT-qPCR) during the decolorization of reactive azo dyes.

6.2 Materials and Methods

6.2.1 Bacterial strain and culture conditions

Shewanella seohaensis NIO_14d isolated and identified in Chapter 3 was selected for gene expression studies based on its high azo dye decolorizing potential and proteomic profile analysis in previous chapters.

6.2.2 PCR amplification and sequencing of azoreductase gene

The bacterial isolate was examined for the presence of genes involved in azo dye decolorization using specific PCR primers (**Table 6.1**). Genomic DNA was extracted (extraction procedure outlined in Section **3.2.5**) and used as template. The PCR reaction mixture (25 µl) contained 2 µl template DNA (30-50 µg DNA μl^{-1}), 1 µl each of forward and reverse primer (10 pmol) and 12 µl of PCR Master Mix (Thermo, USA). The volume was made up with nuclease-free water. Amplicons were obtained using the PCR program of initial denaturation at 94°C for 2 min, followed by 35 cycles at 94°C for 1 min (denaturation), 57°C for 30 sec (annealing), and 72°C for 2 min (extension). Final

elongation was at 72°C for 7 min. The reaction was carried out in a 96 well Thermal Cycler plate (Veriti 9902, Applied Biosystems, USA). The PCR product was detected on 1% agarose gel. The amplified product was cleaned up using GenElute™ PCR clean-up kit (Sigma-Aldrich, USA) as per the manufacturer's instructions. Gene sequencing was carried out using the Taq Dye Deoxy Terminator 32 cycle sequencing kit (Perkin-Elmer, USA) and analyzed in 373A automated DNA sequencer (3130x/Genetic analyzer, Thermo Fisher Scientific, USA). The sequence obtained was analyzed through the GenBank database.

6.2.3 Quantitative analyses of the azoreductase gene expression using Real Time - quantitative PCR (RT-qPCR)

6.2.3.1 *Culture conditions for gene expression studies*

Bacterial cells were grown in NB containing each of the reactive azo dyes RB5, RG19 and RR120 added at a concentration of 50 and 500 mgL^{-1}. Culture was sampled for analysis at the following time intervals during growth and decolorization: 0 h, 3 h, 6 h, 12 h and 24 h. Dye-free NB inoculated with *Shewanella seohaensis* NIO_14d was maintained as the control. Azoreductase activity and gene expression of *azoR* gene was studied at each sampling stage.

6.2.3.2 *Dye decolorization and Azoreductase assay*

The percentage of dye decolorization and the production of the azoreductase enzyme during decolorization was measured following the protocols as outlined in **Sections 4.2.1** and **5.2.2** respectively. Protein concentrations were quantified using the Bradford method with Bovine Serum Albumin (BSA) as the standard (Bradford, 1976).

6.2.3.3 *Total RNA extraction and cDNA synthesis*

The bacterial cells sampled at each time interval were pelleted by centrifugation at 7,000 rpm for 15 min at 4°C. Total RNA was extracted using Pure Link RNA Mini kit (Ambion, Life technologies). The cell pellet was resuspended in lysis buffer containing 1% of 2-mercaptoethanol and homogenized. The solution was centrifuged at 10,000 rpm for 5 min to obtain a clear supernatant. The homogenate was taken in fresh RNase-free

microcentrifuge tubes and 100% ethanol was added to form a visible precipitate. The sample was then loaded onto the binding columns provided in the RNA mini kit and further steps were followed as per the manufacturer's instructions. RNA was eluted out by addition of RNase-free water and stored at -20 °C. The extracted RNA was checked for purity and quantified using NanoDrop. The A_{260}/A_{280} ratio measured was approximately 2.0 indicating pure RNA. The RNA obtained was then converted to cDNA using the GenElute™ mRNA Miniprep Kit (Sigma-Aldrich). mRNA was converted to cDNA by using ReadyScript cDNA Synthesis Mix (Sigma-Aldrich). The final reaction mixture contained 4 µL ReadyScript cDNA Synthesis Mix, 1 µL of ~1µg RNA template, 15 µL of PCR grade water to give a total volume of 20 µL. The components were mixed gently and incubated in a thermal cycler with initial temperature of 25 °C for 5 min, followed by 42 °C for 30 min and finally at 85 °C for 5 min.

6.2.3.4 *Real Time-qPCR quantification of azoreductase gene expression*

Analysis of azoreductase gene expression was carried out using real time quantitative PCR (RT-qPCR). The *rpoB* gene encoding DNA-directed RNA polymerase, beta subunit was maintained as the internal control during the RT-qPCR run since there was hardly any change in the mean threshold cycle (Ct) values of *rpoB* gene expression over the growth period of the bacterial isolate from 0 h (Ct = 16.4) to 24 h (Ct = 16.3). The primers used in the study are listed out in **Table 6.1**. The efficiency of all the PCRs were determined and found to be between 97 and 100%. Amplification was carried out for three technical replicates in 96-well plates (total reaction volume of 20 µL) containing 1 µL cDNA, 200 nM of each gene specific primer pair and 5X qARTA Green qPCR mix (QARTA Bio) with the volume made up with nuclease-free water. PCR cycles were run using the cycling parameters of 95 °C for 15 min, followed by 40 cycles of 95 °C for 15 min and 60 °C for 1 min. The relative fold of induction was determined using the $2^{-\Delta\Delta}$Ct method (Livak and Schmittgen, 2001).

6.3 Results

6.3.1 PCR amplification and sequencing of azoreductase gene

The target azoreductase gene was successfully amplified by PCR from chromosomal DNA as the PCR template to yield a PCR product of ~500 bp in size (**Figure 6.1**). Using the primers for the gene *SO3585*, positive amplification was achieved for the gene in *Shewanella seohaensis* NIO_14d. This gene encodes an FMN dependent azoreductase in *Shewanella oneidensis* MR-1 (Mugerfeld *et. al*., 2009). The partial nucleotide sequence obtained was compared to the protein sequences in GenBank. The results indicated that the gene sequence from *Shewanella seohaensis* NIO_14d (GenBank Accession number OQ383380) showed 98.31% similarity to an NAD(P)H oxidoreductase from *Shewanella* sp. MR-4 (GenBank Accession number WP_011623745). As shown in **Figure 6.2**, the gene sequence obtained in this study showed a high similarity with NAD(P)H dependent oxidoreductases from *Shewanella* species as well as with NAD(P)H-FMN and ferric reductase (azoreductase) from *Bacillus subtilis*.

6.3.2 Quantitative analyses of the azoreductase gene expression

6.3.2.1 *Dye decolorization and Azoreductase assay*

Strain *Shewanella seohaensis* NIO_14d was challenged with concentrations of 50 and 500 mg L^{-1} of reactive azo dyes RB5, RG19 and RR120. At lower dye concentrations, the isolate rapidly achieved 98% of color removal for RB5 and RR120 and 92% for RG19 within the initial 3 hours of growth. This was accompanied by a concurrent peak in azoreductase activity (**Figures 6.3(a), 6.4(a) and 6.5(a)**). A gradual decline in the enzyme activity was seen once maximum decolorization was attained. Contrastingly, on exposure to a higher concentration of azo dye (500 mgL^{-1}), decolorization proceeded at a slower rate. Maximum decolorization was seen following 24 hours incubation with the dye. However, highest azoreductase activity was detected at 12 hours of growth of the isolate in dye containing medium (**Figures 6.3(b), 6.4(b) and 6.5(b))**. The azoreductase activity measured at 12 hours was 0.147, 0.173, and 0.403 U/mg protein during decolorization of

RB5, RG19 and RR120 respectively. Following this, a decrease in azoreductase activity was observed even as the isolate continued to decolorize the azo dye.

6.3.2.2 *Real Time-qPCR quantification of azoreductase gene expression*

The expression of the genes for azoreductase activity during the dye decolorization process was examined by measuring the levels of azoreductase specific gene expression in the cell culture as well as simultaneously determining the extent of dye decolorization and enzyme activity. The gene expression levels obtained by real time quantitative PCR (RT-qPCR) were normalized to that of the *rpoB* gene which encodes the beta subunit of DNA-directed RNA polymerase in the bacterial cell. The *rpoB* gene was selected as the internal control since its expression levels was found to be invariant during growth and decolorization of *Shewanella seohaensis* NIO_14d exposed to different dye concentrations. Quantitative values were obtained by using the comparative threshold cycle (ΔΔCT) method recommended by Applied Biosystems. The relative expression of the azoreductase gene (*so3585*) was determined three times in each of the experimental RNA samples and is expressed as the fold difference in the quantity of cDNA molecules present at different growth and decolorization stages. In samples containing 50 mg L^{-1} RB5 dye, azoreductase gene (*so3585*) expression drastically increased to show a 3.9-fold increase at 6 hours for a concentration of 50 mg L-1 of RB5 (**Figure 6.6**). As shown in **Figure 6.7**, at 6 hours after dye challenge, a 3.5-fold increase in gene expression was observed in *Shewanella seohaensis* NIO_14d exposed to RG19. A fold increase of 4.2 was seen in the gene expression during decolorization of 50 mgL^{-1} RR120 (**Figure 6.8**). In comparison, during decolorization of 500 mg L^{-1} of reactive azo dyes, the relative expression of the gene was up regulated at 12 hours corresponding to the peak in enzyme activity. The highest increase in fold change of 4.07 was seen in the decolorization of RR120. This time course study of gene expression shows that azoreductase gene (*so3585*) was differentially expressed in *Shewanella seohaensis* NIO_14d during different growth and decolorization stages and also at different dye concentrations.

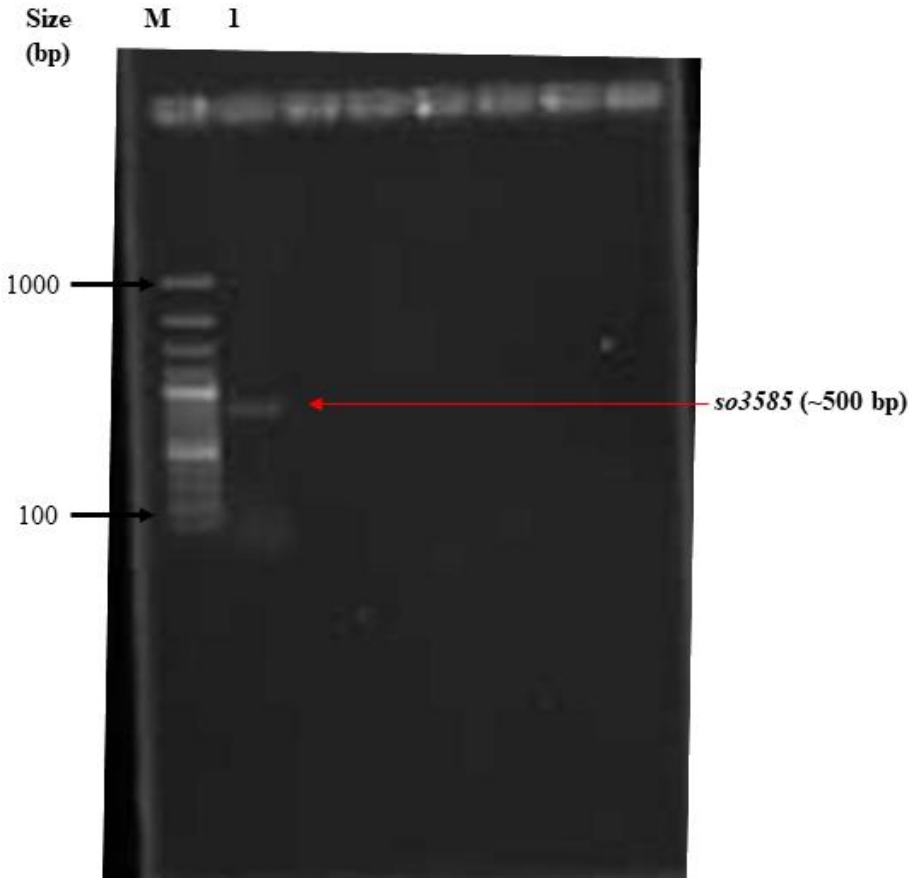


Figure 6.1: Agarose gel electrophoresis (1%) of PCR products of total genomic DNA from *Shewanella seohaensis* NIO_14d with primer for gene *so3585*. Lane **M**: 100 bp DNA ladder (Marker); Lane **1**: amplified PCR product of *Shewanella seohaensis* NIO_14d

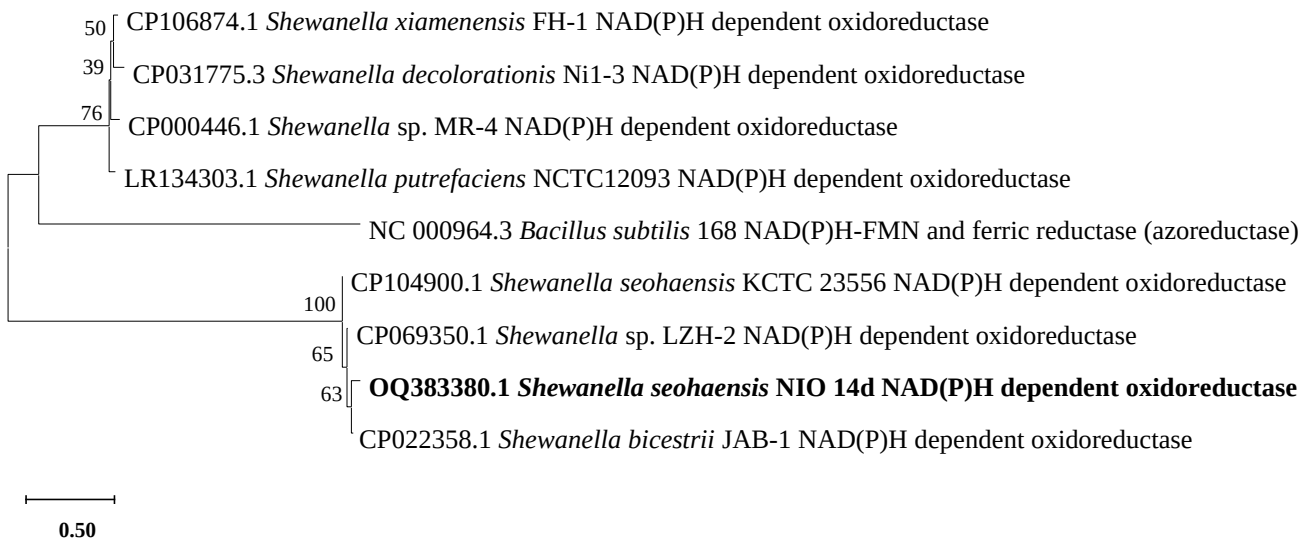


Figure 6.2: Phylogenetic relationship of NAD(P)H dependent oxidoreductase from *Shewanella seohaensis* NIO_14d obtained in this study with NAD(P)H dependent oxidoreductase from other bacterial species. The tree was constructed using neighbour-joining (NJ) method with bootstrap values (1000 replicates) as percentages at the branch nodes.

Table 6.1: List of primer sets used for PCR amplification of azoreductase gene

Target gene	**AS[#] (bp)**	**Organism**	**Primer sequence (5' - 3')** **F** Forward **R** Reverse orientation	**AT[*]** (°C)	**Reference**
SO3585	615	*Shewanella oneidensis* MR-1	**F** 5′-ATGAAGTTACTCATCGTCAGCA CC-3′ **R** 5′-TTACATACCGTAGCAGTATTCCTGC-3′	57	Mugerfeld *et al.*, 2009
For RT-qPCR					
SO3585	615	*Shewanella oneidensis* MR-1	**F** 5′-ATGAAGTTACTCATCGTCAGCA CC-3′ **R** 5′-TTACATACCGTAGCAGTATTCCTGC-3′	57	Mugerfeld *et al.*, 2009
rpoB	72	*Shewanella psychrophila* WP2	**F** 5′-CCGGTTCGCATGCTGAAG -3′ **R** 5′-TGCTGGTGTAGCAATCGGAAT-3′	60	Liu *et al.*, 2018

[#] Amplicon size in base pairs

[*] Annealing temperature

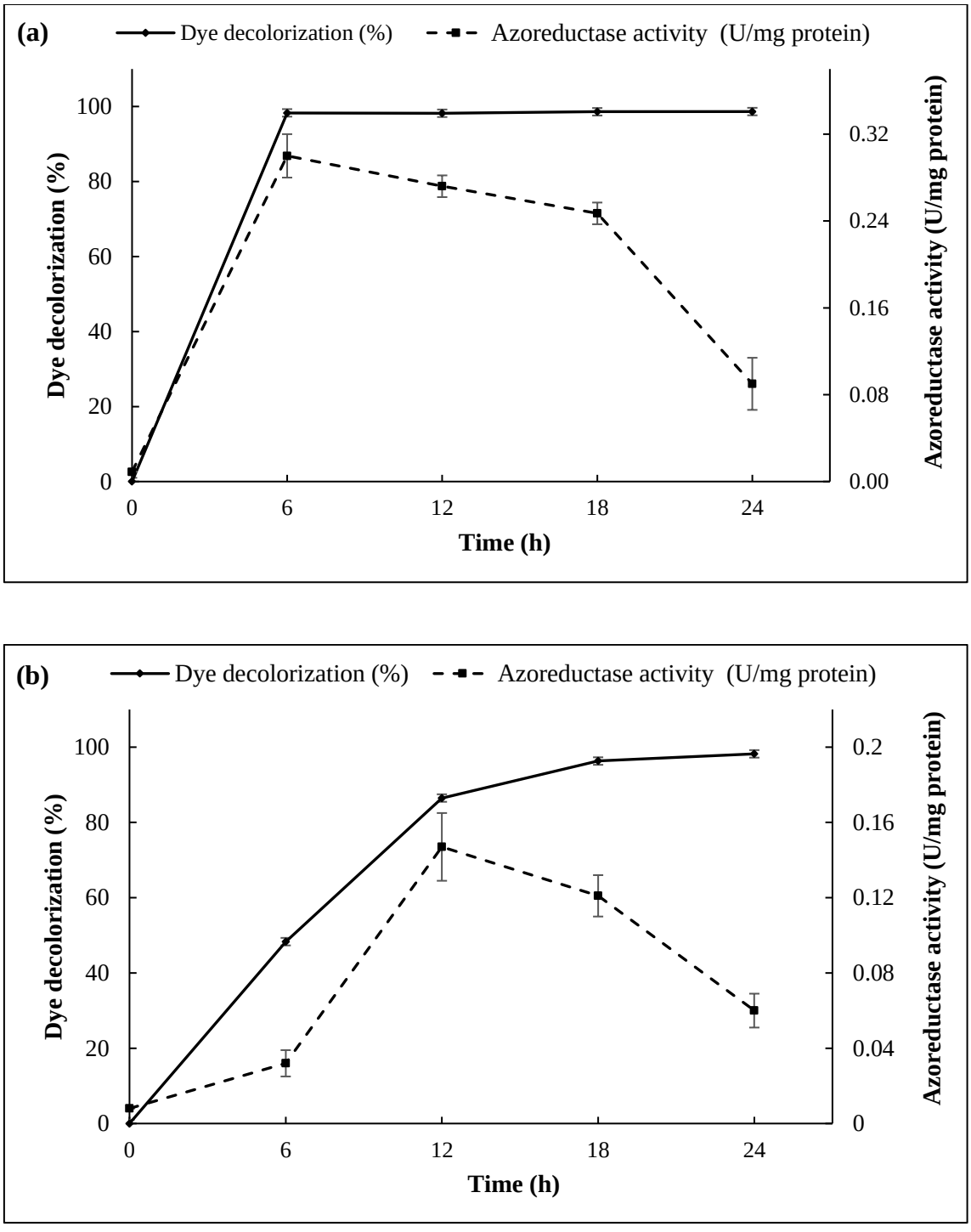


Figure 6.3: Dye decolorization (%) and azoreductase activity of *Shewanella seohaensis* NIO_14d during decolorization of RB5 at a concentration of (**a**) 50 mgL^{-1} and (**b**) 500 mgL^{-1}

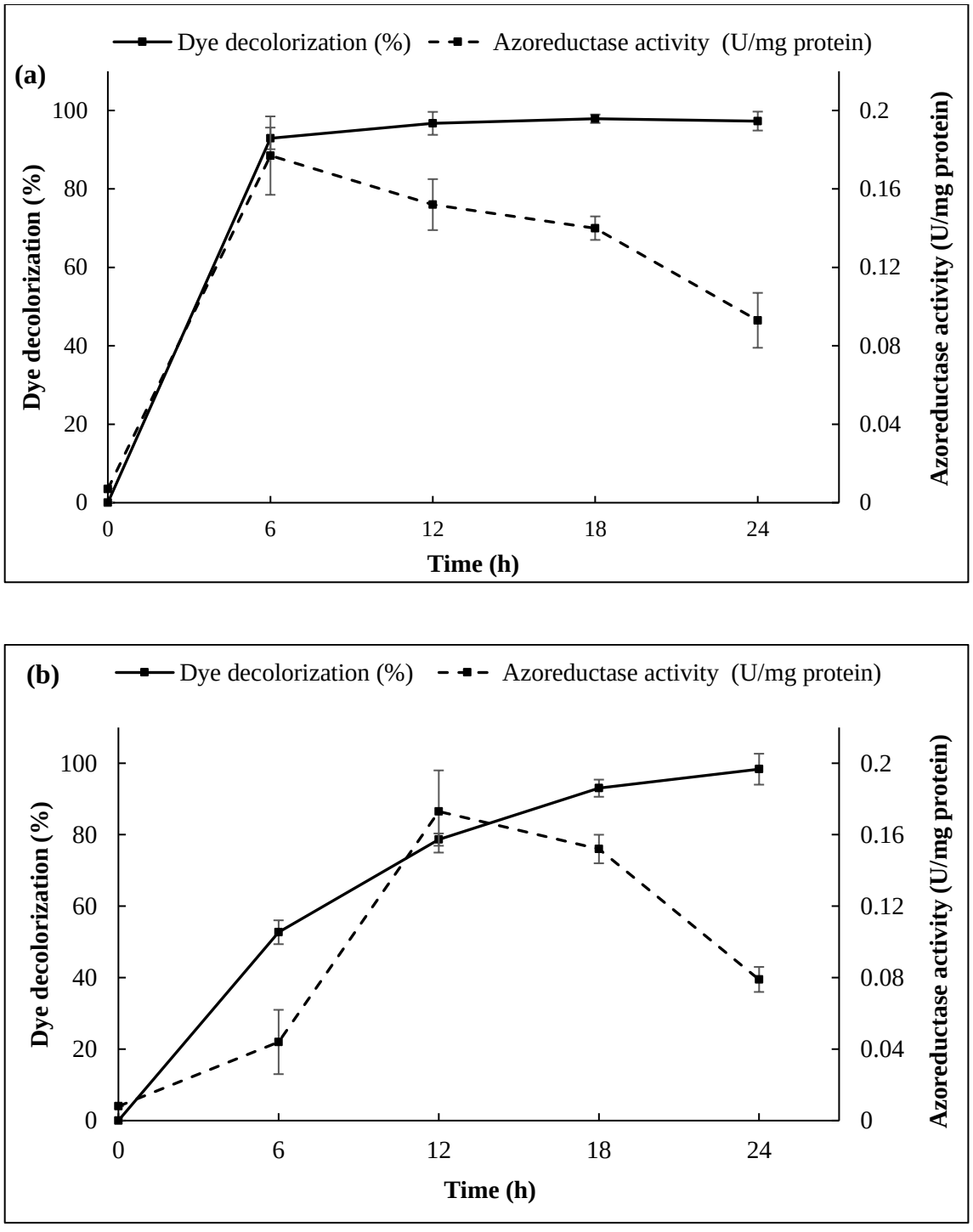


Figure 6.4: Dye decolorization (%) and azoreductase activity of *Shewanella seohaensis* NIO_14d during decolorization of RG19 at a concentration of (**a**) 50 mgL^{-1} and (**b**) 500 mgL^{-1}

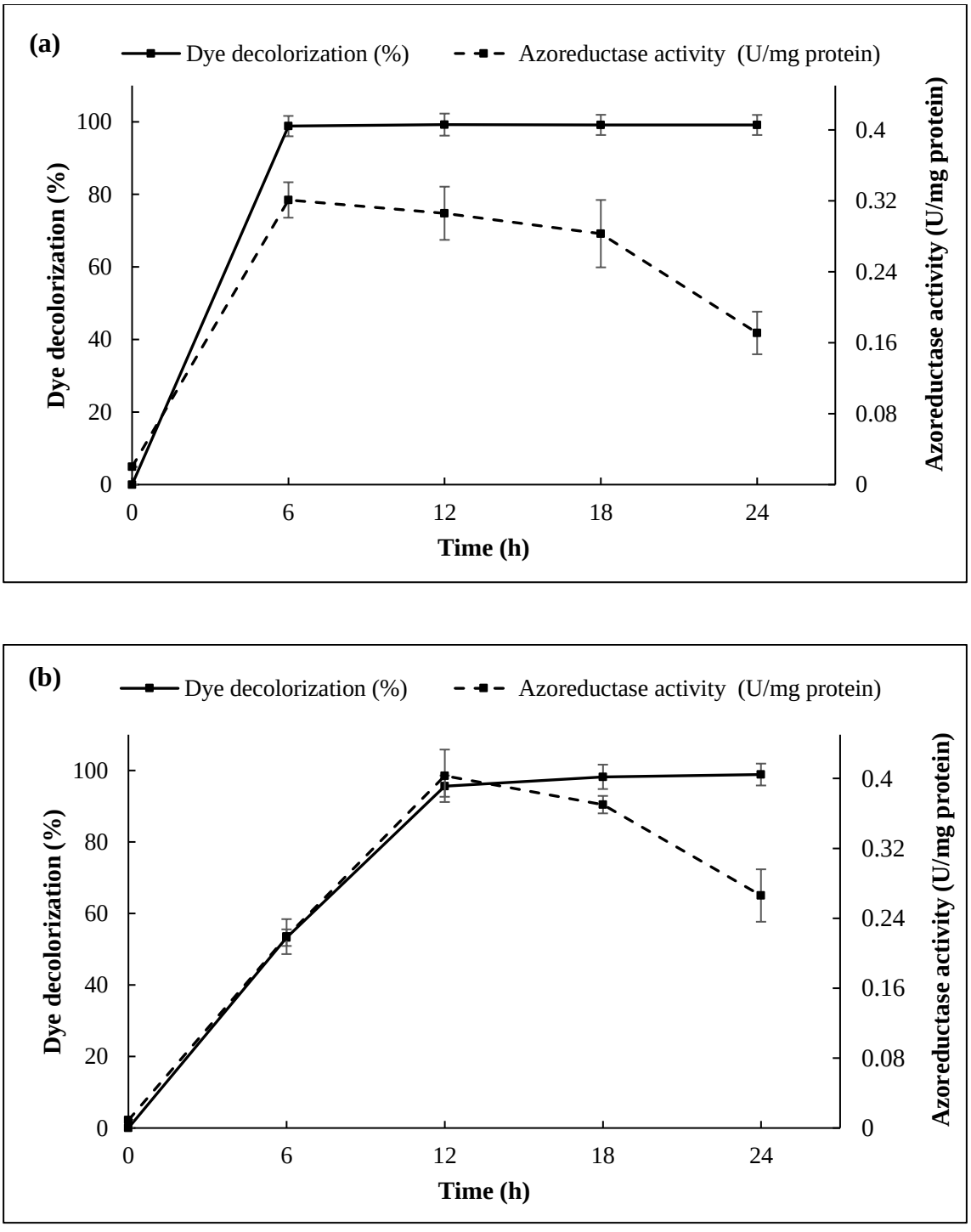


Figure 6.5: Dye decolorization (%) and azoreductase activity of *Shewanella seohaensis* NIO_14d during decolorization of RR120 at a concentration of (**a**) 50 mgL^{-1} and (**b**) 500 mgL^{-1}

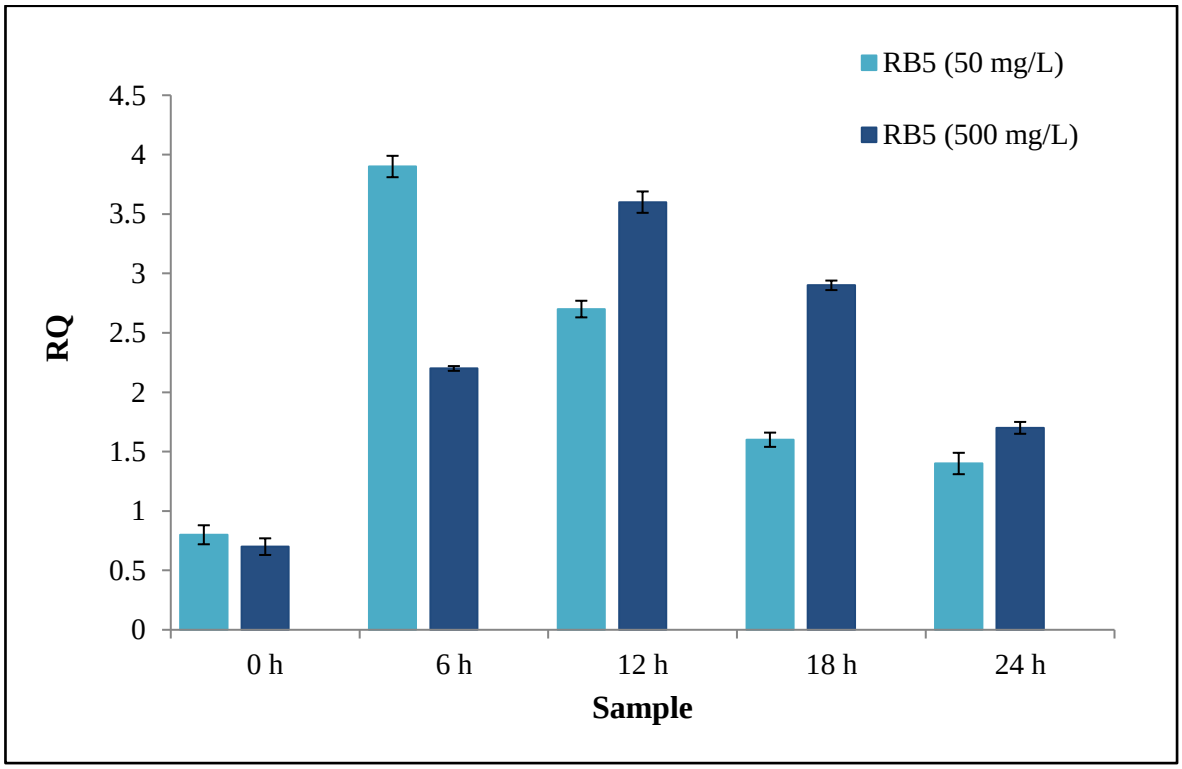


Figure 6.6: Relative expression (RQ) of the azoreductase gene (*SO3585*) gene of *Shewanella seohaensis* NIO_14d in the presence of Reactive Black 5 (RB5). Gene expressions in dye-challenged and dye-free control samples are normalized with respect to the internal control gene *rpoB*.

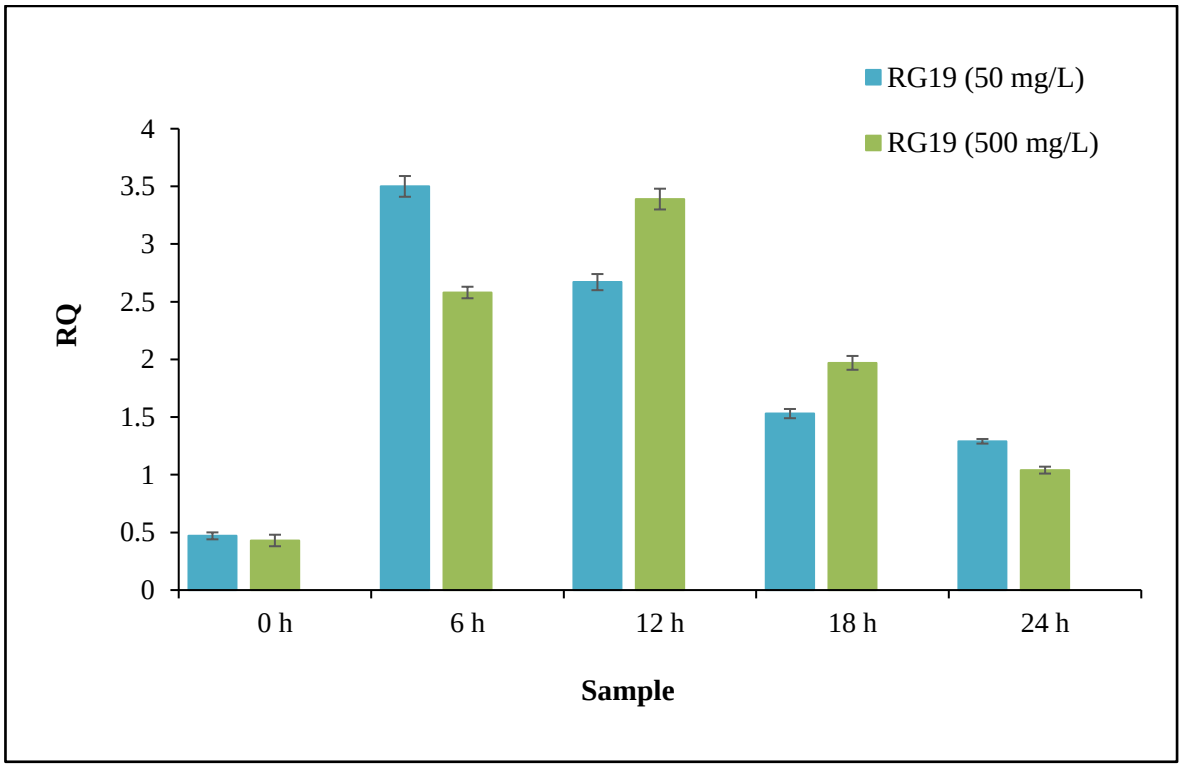


Figure 6.7: Relative expression (RQ) of the azoreductase gene (*SO3585*) gene of *Shewanella seohaensis* NIO_14d in the presence of Reactive Green 19 (RG19). Gene expressions in dye-challenged and dye-free control samples are normalized with respect to the internal control gene *rpoB*.

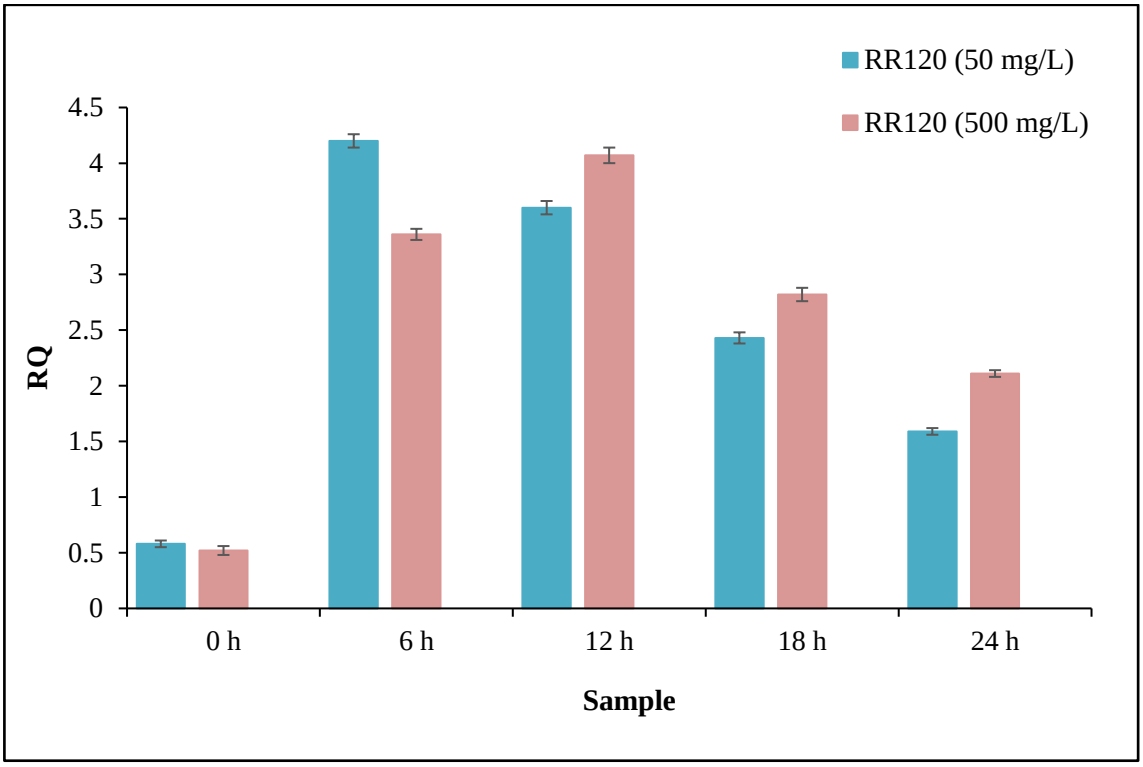


Figure 6.8: Relative expression (RQ) of the azoreductase gene (*SO3585*) gene of *Shewanella seohaensis* NIO_14d in the presence of Reactive Red 120 (RR120). Gene expressions in dye-challenged and dye-free control samples are normalized with respect to the internal control gene *rpoB*.

6.4 Discussion

Investigating azo dye decolorizing enzymes and understanding the expression of their functional genes is a crucial precursor to elucidate the molecular mechanisms involved. In this study, the differential expression levels of the gene encoding azoreductase enzyme putatively involved in the biodegradation of three reactive azo dyes was determined. Azo dye decolorization proceeds through enzymatically driven redox reactions by bacterial strains and suggests the role of genetic precursors in dye decolorizing bacteria (An *et al*., 2020). A previously reported gene, *SO3585*, with a putative azoreductase function was described (Mugerfeld *et al*., 2009). A positive amplification of this gene was detected in *Shewanella seohaensis* NIO_14d capable of decolorizing azo dyes RB5, RG19 and RR120. *SO3585* is a well-studied gene encoding a putative flavin mononucleotide dependent azoreductase and showing 28% sequence similarity to azoreductase from *Bacillus subtilis* as reported by Mugerfeld *et al*., (2009). Brown *et al*., (2006) demonstrated conserved regions in the derived amino acid sequence of *SO3585* from *Shewanella oneidensis* with characteristics of NADH_dh2 family of NAD(P)H oxidoreductases. Bafana and Chakrabarti (2008) reported the residues involved in NAD(P)H binding to be highly conserved across azoreductases in bacterial species. Various investigations have been carried out demonstrating the role of NAD(P)H dependent oxidoreductases in reductive transfer of electrons for dye decolorization (Chen *et al*., 2005; Punj and John, 2009; Mahmood *et al*., 2017; Abbas *et al*., 2020). In concurrence with these findings, the azoreductase gene amplified in this study showed high sequence similarity to NAD(P)H dependent oxidoreductase in *Shewanella* species as well as with NAD(P)H-FMN and ferric reductase (azoreductase) from *Bacillus subtilis* reported by Deller *et al*., (2006). This suggests the potential role of an NAD(P)H dependent oxidoreductase in *Shewanella seohaensis* NIO_14d in the azo dye decolorization pathway.

Azoreductase gene expression levels were quantitatively analyzed in the presence of varying concentrations of the test reactive azo dyes. It was observed that at lower dye concentrations, enzyme activity as well as dye decolorization was maximal at 3 hours of growth of the isolate followed by a gradual decline in activity. Interestingly, at a higher dye concentration, the enzyme activity peaked at 12 hours of growth despite maximum color removal being

achieved only after 18 hours. This possibly indicates the role of azoreductase in the initial stages of the multi-step azo dye degradation mechanism. This observation is in agreement with the known mechanisms of azoreduction as reviewed by Misal and Gawai (2018).

Bacteria undertake a range of strategies to carry out decolorization and degradation of various synthetic azo dyes. The process is determined by complex regulatory network, which further controls the expression of target genes. Thus, in order to understand this process, it is important to understand signaling and the response of the cells to xenobiotic molecules like azo dyes in their environment. Studying the azo dye decolorization process in *Shewanella* species using mRNA gene expression by RT-qPCR has not been extensively investigated. Töwe *et al*., (2007) reported the regulation of an azoreductase gene in *Bacillus subtilis* while Liu *et al*., (2009a) described the involvement of *AzoR* in resistance to thiol-specific stress caused by electrophilic quinones. Further, Ryan *et al*., (2010b) studied the expression of azoreductase genes during growth on different azo compounds using RT-PCR. More recently, a global transcription regulator cAMP receptor protein (*Crp*) (Gao *et al*., 2012), was found to be essential for the decolorization of azo dyes in *Shewanella putrefaciens* CN32 (Liu *et al*., 2020). The results from this study exhibited the up-regulation of azoreductase specific gene expression levels by real time quantitative PCR (RT-qPCR) when normalized to *rpoB* gene during azo dye decolorization. The functional gene was differentially expressed by *Shewanella seohaensis* NIO_14d over the time course of dye exposure. The increased fold change of azoreductase (*SO3585*) expression seen later, at 12 hours, when decolorizing higher dye concentrations was probably because of the adaptive influence exerted by increasing dye concentrations on bacterial growth and decolorizing ability.

The altered expression of genes and enzymatic activity involved in dye decolorization can be studied by identifying the contributing genetic determinants. The changes in gene mRNA levels directly reflect the dynamics of changing environment during the decolorization process. It would be appealing to extend this approach to identify and explore other genes playing roles in the pathway of dye decolorization and degradation to understand the complete process. Designing targeted primers to detect genes with implications in dye metabolism either in culture, in consortium or in environmental samples is a highly effective tool towards improving bioremediation strategies involving microorganisms.

The key strategy used in this work was to induce, measure, and track the expression of microbial dye decolorizing gene, while growing in culture conditions to eventually mimic the interactions in bioremediation environment. A synergistic approach of whole genome sequencing, transcriptome sequencing and qRT-PCR technology would provide critical contributions to identifying and understanding the cleanup of environmental contaminants. Although this method may be outside the scope of this study, it holds great promise in predicting metabolic processes of organisms in polluted environments and anticipating the microbial-facilitated reduction of contaminants, thereby expediting the bioremediation process.

Chapter 7

Summary and Conclusions

Chapter 7

Summary and Conclusions

Investigations on dye decolorizing microbial species are imperative for understanding and developing microbe mediated solutions to combat synthetic dye pollution. Preliminary studies on various bacterial species capable of decolorizing synthetic dyes reveal the detoxification abilities of numerous environmental isolates across different ecotypes. Indeed, microbial dye decolorization in general and azo dye degradation in particular is modulated through enzymatically driven reduction and oxidation mechanisms. As earlier reported, the environmental impact of pollution and synthetic dye-related waste disposal is extensive. Aquatic and coastal systems, in particular, are especially vulnerable to the presence of toxic substances. This study was carried out with the objective of isolating salt tolerant, azo dye decolorizing bacterial isolates and elucidating the proteomic and genomic characteristics accompanying dye decolorization. The hypotheses put forth were whether salt tolerant marine bacterial isolates could rapidly and effectively decolorize and detoxify high concentrations of reactive azo dyes in a measurable manner and whether any specific proteins and genes associated with dye decolorization were differentially regulated.

The following are some of the significant features from this work:

- Water and sediment samples obtained from Choraõ and Divar mangroves and Ribandar saltpans located in Goa yielded 81 bacterial isolates with the potential to decolorize 50 mg L^{-1} of reactive azo dyes. Further screening at a higher dye concentration gave 15 isolates exhibiting significant azo dye decolorization. These isolates were subjected to extensive biochemical characterization and belonged to the genera *Aeromonas*, *Acinetobacter*, *Pseudomonas* and *Shewanella* as identified from 16S rDNA gene sequencing and analysis.

- Of the isolates tested, *Shewanella seohaensis* NIO_14d, (GenBank Accession number KR922404), a gram-negative bacterium, obtained from Divar mangrove sediment

showed the highest dye decolorizing ability of >98% of three reactive azo dyes *viz*. Reactive Black 5, Reactive Green 19 and Reactive Red 120.

- This isolate was selected for further studies to optimize maximum dye decolorization. *Shewanella seohaensis* NIO_14d was capable of rapid and efficient decolorization of azo dyes as evidenced from more than 75% color removal occurring in the first three hours of contact with the reactive dyes RB5, RG19 and RR120.

- Optimization studies revealed that aeration had no negative effect on the ability of the isolate to decolorize reactive dyes. This is of significance as studies have shown that azo dye decolorization occurring under purely anaerobic conditions might lead to formation of toxic aromatic amines.

- The optimum operational temperature for decolorization was in the range 30 - 40 °C. Although the optimum pH for decolorization by the isolate was 7 – 8, the potential to decolorize the test dyes even up to pH 10 is a useful characteristic in the treatment of alkaline dye-containing wastewater.

- *S. seohaensis* NIO_14d is capable of decolorizing reactive azo dyes ranging in concentration from 5 mg L^{-1} to 5000 mg L^{-1}. Maximum decolorization was achieved in medium supplemented with yeast extract as a nitrogen source and starch as a carbon source. *S. seohaensis* NIO_14d efficiently decolorizes reactive dyes as well as a mixture of dye in the presence of electron donors such as succinate and pyruvate.

- The salt tolerant isolate obtained in this study, efficiently decolorized reactive dyes individually and in combination at NaCl concentrations of 0 to 5%. When NaCL concentration was further increased to 10%, decolorization drastically reduced.

- *S. seohaensis* NIO_14d displayed the ability to decolorize >80% reactive azo dyes in the presence of heavy metals like chromium, cadmium, lead, nickel and copper. This finding is of significance as textile effluents are known to contain intense amounts of heavy metals.

- When tested for its ability to decolorize alternative chemical classes of dyes and other azo dyes, *S. seohaensis* NIO_14d successfully decolorized a broad spectrum of dyes belonging to other chemical classes such as triarylmethane and anthraquinone dyes. The isolate also showed efficient color removal of various structurally different azo dyes.

- Enzyme assays indicated an increased production of azoreductase during dye decolorization by *S. seohaensis* NIO_14d as compared to enzyme in dye free nutrient broth. There was no significant lignin peroxidase or laccase activity detected although these enzymes have also been implicated in dye decolorization.

- Metabolite analysis showed the absence of secondary and tertiary amines post dye decolorization. *S. seohaensis* NIO_14d was able to decolorize the reactive azo dyes and mitigate their toxicity as corroborated by the hatching of *Artemia salina* cysts and survival of *Artemia salina* nauplii in the treated dye solution as compared to the original dye. Phytotoxicity studies showed a higher germination percent when seeds of *Vigna radiata* were exposed to the treated dye sample following decolorization by *S. seohaensis* NIO_14d as compared to untreated reactive azo dye.

- Both, laboratory simulated textile effluent as well as raw effluent obtained from Kanpur, India showed a sharp reduction in peak intensity at λ_{max} during UV-vis spectroscopic analysis. It can thus be concluded that the isolate shows potential to remove the color from the darkly colored wastewater.

- Expressional proteomic analysis revealed a set of up-regulated proteins (mainly cellular oxidoreductases) with potential roles in decolorization of azo dyes. Oxidoreductases, cytochrome c proteins and transport proteins identified in this study potentially help in transferring electrons during the reductive metabolism of azo dyes. Additionally, peroxiredoxins and quinone reductases detected in *S. seohaensis* NIO_14d could play a role in decolorization as well as function in response to cellular oxidative and thiol specific stress.

- Genomic analysis of *S. seohaensis* NIO_14d revealed an azoreductase gene (*so3585*) showing similarity to NAD(P)H oxidoreductase and having azoreductase activity. RT-qPCR analysis of the azoreductase gene expression levels during dye decolorization showed an increase in fold change at 6h during decolorization of 50 mgL^{-1} of dye and a fold increase at 12h in presence of 500 mgL^{-1} reactive dye. This increase in gene expression correlates to the time of maximum dye decolorization.

In conclusion, the findings of this study yielded a salt tolerant bacterial strain capable of efficiently decolorizing and detoxifying a very high concentrations of reactive textile azo dyes. The molecular characterization of the proteome and gene expression analysis carried out in this study has important implications in understanding the mechanism of azo dye decolorization by *Shewanella seohaensis* NIO_14d. This knowledge contributes to our understanding of the mechanism of decolorization of textile dyes and will aid in developing efficient bioremediation steps for treating textile industry effluents, designing strategies for understanding biodegradation and mineralization pathways and holistically improve the bioremediation process.

Future Prospects

While the utilization of marine microbes for remedial applications and biodiscovery is constrained by the challenge of accurately replicating natural conditions, marine bacteria still present several advantages. More detailed studies would give newer insights into the mechanisms adopted by microorganisms in degrading synthetic dyes in textile wastewaters. Studies aimed at ex-situ expression of proteins up-regulated during dye decolorization would be highly valuable. Delving deeper into understanding the regulation of azoreductase gene expression will lead to the use of strategies for targeted gene manipulation such as site directed mutagenesis to generate bacterial strains with higher biotransformation potential. Notwithstanding the limitations of this study, cloning and overexpressing the azoreductase gene could further promote the development of more robust microbial strains to tackle environmental pollutants. The advances in high-throughput ‘omics’ technologies have

significantly enhanced our ability to determine the efficacy of microbial bioremediation strategies and gain insights into the concomitant changes in microbial physiology and metabolism. A more detailed study of proteins coupled with metabolomics would act as a powerful tool to further determine the dye degradation mechanisms adopted by such dye decolorizing bacterial strains and provide insights into the interactions of regulatory factors participating in the decolorizing process. This would be helpful in evolving more efficient bioremediation efforts.

Appendix

A. Chemical estimation

Winkler's Titration (Parsons et al. 1984)
Sodium thiosulphate solution (0.0025M)
Sulphuric acid *conc.*
Winkler solution 1 (manganous sulfate)
Winkler solution 2 (alkaline-iodide)

Winkler solution 1 and 2 were added to samples collected in bottles to sequester dissolved oxygen in the sample. The precipitate formed on inverting the stoppered bottle is dissolved with sulphuric acid and titrated against Sodium thiosulphate solution using starch solution as an indicator.

Biochemical oxygen demand (BOD)
Phosphate buffer: 8.5 g KH_2P0_4, 21.75 g K_2HP0_4, 33.4 g $Na_2HP0_4 \bullet 7H_20$, and 1.7 g NH_4Cl was dissolved in 1L distilled water
Magnesium sulfate: 22.5 g $MgSO_4 \bullet 7H_20$ was dissolved in 1 L reagent water.
Calcium chloride: 27.5 g $CaCl_2$ was dissolved in 1 L distilled water
Ferric Chloride: 0.25 g $FeCl_3 \bullet 6H_20$ dissolved in reagent water. Dilute to 1 L.

B. Media Composition

Mineral Salt Medium

NaCl	1.0 g
$CaCl_2 \bullet 2H_2O$	0.1 g
$MgSO_4 \bullet 7H_2O$	0.5 g
KH_2PO_4	1.0 g
Na_2HPO_4	1.0 g

Dissolved in 1000 mL double distilled water (d/w)
pH adjusted to 7.2 with 1N NaOH

Nutrient broth		Luria Bertani broth	
Peptone	10.0 g	Tryptone	10.0 g
Beef extract	3.0 g	Yeast extract	5.0 g
NaCl	5.0 g	NaCl	10.0 g

Dissolved in 1000 mL double distilled water (d/w)
pH adjusted to 7.0 with 1N NaOH

C. Stains and Buffers

C.1 Stains

Gram stain reagents

Crystal violet

Solution A- 2g of crystal violet in 20mL ethanol
Solution B- 0.8g ammonium oxalate dissolved in 80mL d/w

Gram's Iodine

Dissolve 1g iodine and 2g Potassium iodide in 300mL d/w, filter through Whatman filter paper No. 1

Safranine

2.5g Safranine was dissolved in 10mL ethanol, and volume made up to 100mL with d/w and filtered through Whatman filter paper No. 1

C.2 Buffers

0.1M Sodium acetate buffer (pH 4.5)

Solution A (0.1M Sodium acetate trihydrate): 1.361 g $CH_3COONa \bullet 3H_2O$ 27.22 in 100 mL d/w
Solution B (0.1M acetic acid): 0.572 mL glacial acetic acid make the volume to 100 mL with d/w
For pH 4.5
Solution A (37mL) + solution B (63mL) =100mL 0.1M sodium acetate buffer

Phosphate buffer (pH 7.4)

Solution A (0.2M monobasic di-hydrogen phosphate): 2.76g NaH_2PO_4 in 100mL d/w

Solution B (0.2M dibasic hydrogen phosphate): 2.84g Na_2HPO_4 in 100mL d/w

For pH 7.4

Solution A (19mL) + solution B (81mL) =100mL 0.2M phosphate buffer

Tartaric acid buffer (pH 2.5)

Tartaric acid	1.13 g
Sodium tartrate dihydrate	0.58 g

Add distilled water to make up to 1 L.

TE buffer

10mL 0.11M Tris-HCl (pH 8.0) was diluted with 90mL d/w. To this 0.0372g EDTA was added. pH was adjusted to 8.

D. Reagents for molecular techniques

Protein extraction: Urea-Thiourea extraction buffer (5mL)

7M Urea	2.102g
2M Thiourea	0.761g
4% CHAPS	0.2g
0.8% IPG buffer	40 µL
20mM DTT	0.01542g
1M Tris HCl (pH 8.0)	100µL

CHAPS-Cholamidopropyl dimethylammonio-1-propanesulfonate

DTT – Dithiothreitol

IPG – ampholyte containing buffer

Cell cultures were pelleted and the growth medium was discarded. To the pellet, 500µL of extraction buffer was added, homogenized and centrifuged. The supernatant was transferred to a fresh microfuge tube and held at 4°C.

Folin lowry's method for Proteins estimation (Lowry *et al*., 1951)

Reagents	*Preparation*
Reagent A	2% Na_2CO_3 in 0.1N NaOH
Reagent B	0.5% $CuSO_4$ in 1% potassium sodium tartarate
Reagent C	Mixture of Reagent A + Reagent B (50 + 1mL), made prior use
Reagent D	Folin and Ciocalteau's phenol reagent (1:2, with d/w)
Standard bovine serum albumin solution	0.1mg BSA in 1mL d/w

To 100µL of protein sample, 900µL d/w + 5mL of Reagent C was added and incubated at room temperature for 10min. To this mixture, 0.5mL of Reagent D was added and the tubes were incubated for 30min in dark. Optical densities were measured at 660nm with protein extraction buffer used as blank. Concentrations were determined from standard graph using Bovine serum albumin as the standard.

SDS-PAGE

Stock solutions

Reagents	*Preparation*
Acrylamide/Bis acrylamide solution	29.2% acrylamide and 1.2% (w/v) was dissolved in d/w. pH was adjusted to 7.0 and stored at 4°C
Resolving gel buffer (1.5M TrisHCl, pH 8.8)	18.615g Tris base was dissolved in 100mL d/w. pH was adjusted to 8.8 with 6N HCl
Stacking gel buffer (0.5M TrisHCl, pH 6.8)	12.11g Tris base was dissolved in 100mL d/w. pH was adjusted to 6.8 with 6N HCl
Ammonium persulfate (10%)	0.1g APS was dissolved in 1mL d/w (fresh)

Electrophoresis buffer (1X)

Tris base	3.0 g
Glycine	14.4 g
SDS (10%)	10 mL
d/w	1L
pH	8.3

Sample buffer

0.5M Tris-HCl (1M, pH 6.8)	1.25 mL
Glycerol	2.5 mL
10% SDS	2 mL
0.5% (w/v) bromophenol blue	0.2mL
d/w	3.55 mL

Gel running buffer (10X)

Tris base	30.3 g/L
Glycine	144 g/L
SDS (10%)	10 g/L

1X used for electrophoresis

Gel monomer preparation (Monomer - Acrylamide/Bis-acrylamide solution)
Composition of resolving and stacking gel is as follows:

Gel %	d/w	Monomer	Gel buffer	10% SDS	10% APS	TEMED
Resolving gel (12%)	3.4mL	4mL	2.5mL resolving gel buffer	0.1mL	50µL	5µL
Stacking gel (6%)	5.4mL	2.0mL	2.5mL stacking gel buffer	0.1mL	50µL	10µL

Silver staining

Silver stain

silver nitrate	0.2%
formaldehyde	0.75µL
d/w	100mL

Developer

Na_2CO_3	6 g
formaldehyde	50 µL
10% $Na_2S_2O_3$	40µL
d/w	100mL

Hydrator

10% $Na_2S_2O_3$	1mL
d/w	49mL

Reagents for in solution digestion

Reagents	*Preparation*
6M urea in 50mM Tris HCl (pH 8.0)	0.36g was dissolved in 1mL nanopure water
50mM Ammonium bicarbonate	0.395g of Ammonium bicarbonate was dissolved in 100mL nanopure water
200mM DTT	30.86mg DTT in 1mL of 50mM Ammonium bicarbonate
200mM IAA	22mg IAA was dissolved in 0.6mL 50mM Ammonium bicarbonate

1mM HCl, Trypsin (1µg/ µL), Formic acid (MS grade)

Methanol precipitated protein pellet was dissolved in urea, treated with DTT and IAA for reduction and alkylation, in dark. The mixture was then treated with trypsin to digest proteins/peptides in solution, overnight. The mixture was acidifed with formic acid and transferred in to a MS autosampler vial for LC-MS QToF

References

Abadulla, E., Tzanov, T., Costa, S., Robra, K.H.A., Cavaco-Paulo, Gubitz, G.M. (2000) Decolorization and Detoxification of Textile Dyes with a Laccase from *Trametes hirsute*. *Appl Environ Microbiol*, 66, 3357.

Abbas, A., Mushtaq, A., Cheema, A.I., Mahmood, F., Khan, M.A., Naqqash, T., Khurshid, M., Manzoor, I., Muhammad, S., Shahid, M. (2020) Heterologous expression of azoreductase-encoding gene azrS of *Bacillus* sp. MR-1/2 for enhanced azo dye decolorization and wastewater treatment. *Archives of Microbiology*, 202, 2135-2145.

Abd El-Rahim, W.M., Moawad, H., Azeiz, A.Z.A., Sadowsky, M.J. (2017) Optimization of conditions for decolorization of azo-based textile dyes by multiple fungal species. *J Biotechnol*, 260, 11-17.

Abraham, K.J. (2007) Development of a Classification Scheme Using a Secondary and Tertiary Amino Acid Analysis of Azoreductase Gene. *J Med Biol Sci*, 1, 1.

Abrahart, E.N (1977) Dyes and their Intermediates. New York: Chemical Publishing. 1–12.

Acuner, E., and Dilek, F.B. (2004) "Treatment of Tectilon Yellow 2G by *Chlorella vulgaris*" *Process Biochem*, 39, 623.

Adeel, S., Usman, M., Haider, W., Saeed, M., Muneer, M., Ali, M. (2015) Dyeing of gamma irradiated cotton using Direct Yellow 12 and Direct Yellow 27: improvement in colour strength and fastness properties. *Cellulose*, *22*, 2095-2105.

Ajaz M., Elahi A., Rehman A. (2018) Degradation of azo dye by bacterium, *Alishewanella* sp. CBL-2 isolated from industrial effluent and its potential use in decontamination of wastewater. *J Water Reuse Desalin*, 8, 507–515.

Aksu, Z. (2003) Reactive dye bioaccumulation by *Saccharomyces cerevisiae*. *Process Biochem*, 38(10), 1437-1444.

Al-Amrani W.A., Lim P.E., Seng C.E., Ngah W.S.W. (2014) Factors affecting bio-decolorization of azo dyes and COD removal in anoxic–aerobic REACT operated sequencing batch reactor. *J Taiwan Inst Chem Eng*, 45, 609–616.

Al-Ansari, M.M., Li, Z., Masood, A., Rajaselvam, J. (2022) Decolourization of azo dye using a batch bioreactor by an indigenous bacterium *Enterobacter aerogenes* ES014 from the waste water dye effluent and toxicity analysis. *Environ Res*, 205, 112189.

Alaton, I.A., Balcioglu, I.A., Bahnemann, D.W., 2002. Advanced oxidation of a reactive dyebath effluent: comparison of O3, H2O2/ UV-C and TiO2/UV-A process. *Water Res*, 36, 1143–1154.

Ali, H. (2010) Biodegradation of synthetic dyes—a review. *Water Air Soil Pollut*, 213(1-4), 251-273.

Al-Kdasi, A., Idris, A., Saed, K., Guan, C.T., (2004) Treatment of textile wastewater by advanced oxidation processes—a Review. *Global Nest: The International Journal*, 6(3), 221–229.

Ambrósio, S.T., Vilar Júnior, J.C., Da Silva, C.A.A., Okada, K., Nascimento, A.E., Longo, R.L., Campos-Takaki, G.M. (2012) A biosorption isotherm model for the removal of reactive azo dyes by inactivated mycelia of *Cunninghamella elegans* UCP542. *Molecules*, 17(1), 452-462.

Amwele, H.R., Papirom, P., Chukanhom, K., Beamish, F.H.W., Petkam, R. (2015) Acute and subchronic toxicity of metal complex Azo acid dye and anionic surfactant oil on fish *Oreochromis niloticus*. *J Environ Biol*, 36(1):199–205.

An, X., Chen, Y., Chen, G., Feng, L., Zhang, Q. (2020) Integrated metagenomic and metaproteomic analyses reveal potential degradation mechanism of azo dye-Direct Black G by thermophilic microflora. *Ecotoxicol Environ Safety*, 196, 110557.

Anjaneya, O., Souche, S.Y., Santoshkumar, M., Karegoudar, T. B. (2011) Decolorization of sulfonated azo dye Metanil Yellow by newly isolated bacterial strains: *Bacillus* sp. strain AK1 and *Lysinibacillus* sp. strain AK2. *J Hazard Mater*, 190(1-3), 351-358.

Anjaneyulu, Y., Sreedhara Chary, N., Raj, S.S.D. (2005) Decolourization of Industrial Effluents-Available Methods and Emerging Technologies—A Review *Rev Environ Sci Biotechnol*, 4, 245.

Asad, S., Amoozegar, M.A., Pourbabaee, A., Sarbolouki, M.N., Dastgheib, S.M.M. (2007) Decolorization of textile azo dyes by newly isolated halophilic and halotolerant bacteria. *Bioresource Technol*, 98(11), 2082-2088.

Aslam, M.M., Baig, M.A., Hassan, I., Qazi, I.A., Malik, M., Saeed, H. (2004) Textile wastewater characterization and reduction of its COD and BOD by oxidation. *Elec J Env Agricult Food Chem, 3*(6), 804-811.

Asses, N., Ayed, L., Hkiri, N., Hamdi, M. (2018) Congo red decolorization and detoxification by *Aspergillus niger*: removal mechanisms and dye degradation pathway. *BioMed research international*, 1-9.

Babu S.S., Mohandass C., Vijayaraj A.S., Dhale M.A. (2015) Detoxification and color removal of Congo Red by a novel *Dietzia* sp. (DTS26)–a microcosm approach. *Ecotox Environ Safe*, 114, 52-60.

Babu, S.S., Mohandass, C., Raj, A.V., Rajasabapathy, R., Dhale, M.A. (2013) Multiple approaches towards decolorization and reuse of a textile dye (VB-B) by a marine bacterium *Shewanella decolorationis*. *Water Air Soil Pollut*, 224, 1-12.

Bafana, A., Chakrabarti, T. (2008) Lateral gene transfer in phylogeny of azoreductase enzyme. *Comput Biol Chem*, 32,191–197.

Bafana, A., Chakrabarti, T., Devi, S.S. (2008). Azoreductase and dye detoxification activities of *Bacillus velezensis* strain AB. *Appl Microbiol Biotechnol*, 77, 1139-1144.

Balakrishnan, V.K., Shirin, S., Aman, A.M., de Solla, S.R., Mathieu-Denoncourt, J., Langlois, V.S. (2016) Genotoxic and carcinogenic products arising from reductive transformations of the azo dye, Disperse Yellow 7. *Chemosphere*, 146, 206-215.

Banat, I. M., Nigam, P., Singh, D., Marchant, R. (1996) Microbial Decolorization of Textile Dye-Containing Effluents: A Review. *Bioresour Technol*, 58, 217.

Beliaev, A.S., Klingeman, D.M., Klappenbach, J.A., Wu, L., Romine, M.F., Tiedje, J.M., Nealson, K.H., Fredrickson, J.K., Zhou, J. (2005) Global transcriptome analysis of *Shewanella oneidensis* MR-1 exposed to different terminal electron acceptors. *J Bacteriol*, 187(20), 7138-7145.

Beliaev, A.S., Thompson, D.K., Khare, T., Lim, H., Brandt, C.C., Li, G., Murray, A.E., Heidelberg, J.F., Giometti, C.S., Yates Iii, J., Nealson, K.H. (2002) Gene and protein expression profiles of *Shewanella oneidensis* during anaerobic growth with different electron acceptors. *Omics: a journal of integrative biology*, 6(1),39-60.

Benkhaya, S., M'rabet, S., El Harfi, A. (2020) Classifications, properties, recent synthesis and applications of azo dyes. *Heliyon*, 6(1).

Bera, S.P., Tank, S.K. (2021) Microbial degradation of Procion Red by *Pseudomonas stutzeri*. *Scientific Reports*, 11(1), 1-12.

Bharathi, D., Nandagopal, J.G.T., Ranjithkumar, R., Gupta, P.K., Djearamane, S. (2022) Microbial approaches for sustainable remediation of dye-contaminated wastewater: a review. *Arch Microbiol*, 204(3), 1-11.

Blümel, S. and Stolz, A. (2003) Cloning and Characterization of the Gene Coding for the Aerobic Azoreductase from *Pigmentiphaga kullae* K24. *Appl Microbiol Biotechnol*, 62, 186.

Bor-Yann, C. (2002) Understanding decolorization characteristics of reactive azo dyes by *Pseudomonas luteola*: toxicity and kinetics. *Process Biochem*, 38(3), 437–446.

Bouraie M.E., Din, W.S.E. (2016) Biodegradation of reactive black 5 by *Aeromonas hydrophila* strain isolated from dye-contaminated textile wastewater. *Sustain Environ Res*, 26, 209–216.

Bradford, M.M. (1976) A rapid and sensitive method for the quantitation of microgram quantities of protein utilizing the principle of protein-dye binding. *Anal Biochem*, 72(1-2), 248-254.

Bras, R., Isabel, M., Ferra, A., Pinheiro, H.M., Goncalves, I.C. (2001) Batch tests for assessing decolorization of azo dye by methanogenic and mixed cultures. *J Biotechnol*, 89, 155–162

Brigé, A., Motte, B., Borloo, J., Buysschaert, G., Devreese, B., Van Beeumen, J.J. (2008) Bacterial decolorization of textile dyes is an extracellular process requiring a multicomponent electron transfer pathway. *Microb Biotechnol*, 1(1), 40-52.

Brown, S.D., Thompson, M.R., VerBerkmoes, N.C., Chourey, K., Shah, M., Zhou, J., Hettich, R.L. and Thompson, D.K. (2006) Molecular Dynamics of the *Shewanella oneidensis:* Response to Chromate Stress. *Mol Cell Proteomics*, 5(6), 1054-1071.

Brunello, F. (1973) The Art of Dyeing in the History of Mankind; (Hickey, B. trans.) Neri Pozza Editore: Vicenza

Bumpus, S.B., Evans, B.S., Thomas, P.M., Ntai, I., Kelleher, N.L. (2009) A proteomics approach to discovering natural products and their biosynthetic pathways. *Nat Biotechnol*, 27, 951-956.

Carliell, C.M., Barclay, S.J., Buckley, C.A. (1996) Treatment of exhausted reactive dyebath effluent using anaerobic digestion laboratory and full-scale trials. *Water SA*, 22, 225–233.

Cetin, D., Donmez, S., Donmez, G. (2008) The treatment of textile wastewater including chromium (VI) and reactive dye by sulfate-reducing bacterial enrichment. *J Environ Manag*, 88, 76–82.

Chagas, E.P. and Durrant, L.R. (2001) Decolorization of azo dyes by *Phanerochaete chrysosporium* and *Pleurotus sajorcaju*. *Enzyme Microb Technol*, 29(8-9), 473-477.

Champagne, P.P. and Ramsay, J. A. (2005) Contribution of manganese peroxidase and laccase to dye decoloration by *Trametes versicolor*. *Appl Microbiol Biotechnol*, 69, 276-285.

Chandanshive, V., Kadam, S., Rane, N., Jeon, B. H., Jadhav, J., Govindwar, S. (2020) In situ textile wastewater treatment in high-rate transpiration system furrows planted with aquatic macrophytes and floating phytobeds. *Chemosphere*, 252, 126513.

Chang, J.S. and Lin, Y.C. (2000) Fed-batch bioreactor strategies for microbial decolorization of azo dye using a *Pseudomonas luteola*. *Biotechnol Prog*, 16, 979–85.

Chang, J.S., Chou, C., Lin, Y.C., Lin, P.J., Ho, J.Y., Hu, T.L. (2001) Kinetic characteristics of bacterial azo-dye decolorization by *Pseudomonas luteola*. *Water Res*, 35(12), 2841-2850.

Chang, J.S. and Lin, C.Y. (2001) Decolorization kinetics of recombinant *Escherichia coli* strain harboring azo dye decolorization determinants for *Rhodococcus* sp. *Biotechnol Lett*, 23, 631-636.

Chen, K.C., Huang, W.T., Wu, J.Y., Houng, J.Y. (1999) Microbial decolorization of azo dyes by *Proteus mirabilis*. *J Ind Microbiol Biotechnol*, 23, 686–690.

Chen, B.Y., Chen, W. M., Wu, F.L., Chen, P.K., Yen, C.Y. (2008) Revealing Azo-dye Decolorization of Indigenous *Aeromonas hydrophila* from Fountain Spring in Northeast Taiwan. *J Chin Inst Chem Engrs*, 39, 495

Chen, G., An, X., Feng, L., Xia, X., Zhang, Q. (2020) Genome and transcriptome analysis of a newly isolated azo dye degrading thermophilic strain *Anoxybacillus* sp. *Ecotoxicol Environ Safety*, 203, 111047.

Chen, H. (2006) Recent advances in azo dye degrading enzyme research. *Curr Protein Pept Sci*, 7, 101–111.

Chen, H.L. and Burns, L.D. (2006) Environmental analysis of textile products. *Cloth Text Res J*, 24, 248–261.

Chen, H., Hopper, S.L., Cerniglia, C.E. (2005) Biochemical and molecular characterization of an azoreductase from *Staphylococcus aureus*, a tetrameric NADPH-dependent flavoprotein. *Microbiology*, 151, 1433-1441.

Chen, K.C., Wu, J.Y., Liou, D.J., Hwang, S.C.J. (2003) Decolorization of textile dyes by newly isolated bacterial strains. *J Biotechnol*, 10, 57–68

Chen, X., Xu, M., Wei, J., Sun, G. (2010) Two different electron transfer pathways may involve in azoreduction in *Shewanella decolorationis* S12. *Appl Microbiol Biotechnol*, 86(2), 743-51.

Chengalroyen, M.D., Dabbs, E.R. (2013) The microbial degradation of azo dyes: minireview. *World J Microbiol Biotechnol*, 29, 389–399.

Chivukula, M. and Renganathan, V. (1995) Phenolic Azo Dye Oxidation by Laccase from *Pyricularia oryzae*. *Appl Environ Microbiol*, 61, 4374.

Choi, J., Joo, W.A., Park, S.J., Lee, S.H., Kim, C.W. (2005) An efficient proteomics based strategy for the functional characterization of a novel halophilic enzyme from *Halobacterium salinarum*. *Proteomics*, 5, 907-917.

Chung, K.T., Fulk, G.E., Egan, M. (1978) Reduction of azo dye by intestinal anaerobes. *Appl Environ Microbiol*, 49: 47–51.

Chung, K.T. and Cerniglia, C.E. (1992) Mutagenicity of azo dyes: structure–activity relationships. *Mutat Res*, 277, 201–220

Dafale, N., Rao, N.N., Meshram, S.U., Wate, S.R. (2008) Decolorization of Azo Dyes and Simulated Dye Bath Wastewater Using Acclimatized Microbial Consortium—biostimulation and halo tolerance. *Bioresour Technol*, 99, 2552

Dash, H. R., Mangwani, N., Chakraborty, J., Kumari, S., Das, S. (2013) Marine bacteria: potential candidates for enhanced bioremediation. *Appl Microbiol Biotechnol*, 97(2), 561-571.

Dave, S.R., Patel, T.L., Tipre, D.R. (2015). Bacterial Degradation of Azo Dye Containing Wastes. In: *Microbial Degradation of Synthetic Dyes in Wastewaters*, Springer International Publishing, pp 57-83

Dawkar, V.V., Jadhav, U.U., Telke, A.A., Govindwar, S.P. (2009) Peroxidase from *Bacillus* sp. VUS and its role in the decolorization of textile dyes. *Biotechnol Bioprocess Eng*, 14, 361–368

Dawkar, V.V., Jadhav, U.U., Jadhav, S.U., Govindwar, S.P. (2008) Biodegradation of Disperse Textile Dye Brown 3REL by Newly Isolated *Bacillus* sp. VUS. *J Appl Microbiol*, 105, 14.

de Almeida, E.J.R. and Corso, C.R. (2016) Acid blue 161: decolorization and toxicity analysis after microbiological treatment. *Water Air Soil Pollut*, 227, 1-8.

de Aragao Umbuzeiro, G., Freeman, H.S., Warren, S.H., De Oliveira, D.P., Terao, Y., Watanabe, T., Claxton, L.D. (2005) The contribution of azo dyes to the mutagenic activity of the Cristais River. *Chemosphere*, 60(1), 55-64.

De Baere, L.A., Devocht, M., Van Assche, P., Verstraete, W. (1984) Influence of high NaCl and NH_4Cl salt levels on methanogenic associations. *Water Res*, 18(5), 543-548.

de Souza, N.A., Ramaiah, N., Damare, S., Furtado, B., Mohandass, C., Patil, A., De Lima, M. (2019) Differential protein expression in *Shewanella seohaensis* decolorizing azo dyes. *Current Proteomics*, 16(2), 156-164.

Deller, S., Macheroux, P., Sollner, S. (2008) Flavin-dependent quinone reductases. *Cell Mol Life Sci*, 65, 141–160

Deller, S., Sollner, S., Trenker-El-Toukhy, R., Jelesarov, I., Gübitz, G. M., Macheroux, P. (2006) Characterization of a thermostable NADPH: FMN oxidoreductase from the mesophilic bacterium *Bacillus subtilis*. *Biochemistry*, 45(23), 7083-7091.

Deng, D., Guo, J., Zeng, G., Sun, G. (2008) Decolorization of anthraquinone, triphenylmethane and azo dyes by a new isolated *Bacillus cereus* strain DC11. *Int Biodeterior Biodegrad*, 62(3), 263-269.

Dhanve, R.S., Shebalkar, U.U., Jadhav, J.P. (2008) Biodegradation of diazo reactive dye Navy Blue HE2R (Reactive Blue 127) by an isolated *Exiguobacterium* sp. RD3. *Biotechnol Bioprocess Eng*, 13, 53–60

Dias, A.A., Lucas, M.S., Sampaio, A., Peres, J.A., Bezerra, R.M. (2010) Decolorization of azo dyes by yeasts. In *Biodegradation of Azo Dyes*, Ed Hatice Atacag Erkurt, Springer, vol 9, 183-193.

Dong, X., Zhou, J., Liu, Y. (2003) Peptone-induced biodecolorization of reactive brilliant blue (KN-R) by *Rhodocyclus gelatinosus* XL-1. *Process Biochem*, 39(1), 89-94.

dos Santos, A.B., Cervantes, F.J., van Lier, J. B. (2007) Review Paper on Current Technologies for Decolourisation of Textile Wastewaters: Perspectives for Anaerobic Biotechnology. *Bioresour Technol*, 98, 2369.

D'Souza, D.T., Tiwari, R., Sah, A.K., Raghukumar, C. (2006) Enhanced production of laccase by a marine fungus during treatment of colored effluents and synthetic dyes. *Enzyme Microb Technol*, 38(3-4), 504-511.

Du, L.N., Li, G., Zhao, Y.H., Xu, H.K., Wang, Y., Zhou, Y., Wang, L. (2015) Efficient metabolism of the azo dye methyl orange by *Aeromonas* sp. strain DH-6: characteristics and partial mechanism. *Int Biodeterior Biodegrad*, 105, 66-72.

Dubbs, J.M. and Mongkolsuk, S. (2007) Peroxiredoxins in bacterial antioxidant defense In: *Peroxiredoxin Systems*; Flohé, L.; Harris, J.R., Eds.; Springer: pp. 143-193.

Duran, N. and Esposito, E. (2000) Potential Applications of Oxidative Enzymes and Phenoloxidase-like Compounds in Wastewater and Soil Treatment. A Review. *Appl Catalysis B Environ*, 28, 83.

El-Shora, H.M. and Metwally, M. (2008) Use of Tyrosinase Enzyme from *Bacillus thuringiensis* for the Decontamination of Water Polluted with Phenols. *Biotechnology*, 7, 305.

Enayatzamir, K., Alikhani, H.A., Yakhchali, B., Tabandeh, F., Rodríguez-Couto, S. (2010) Decolouration of azo dyes by *Phanerochaete chrysosporium* immobilised into alginate beads. *Environ Sci Pollut Res*, 17, 145-153.

Enayatzamir, K., Tabandeh, F., Yakhchali, B., Alikhani, H.A., Couto, S.R. (2009) Assessment of the joint effect of laccase and cellobiose dehydrogenase on the decolouration of different synthetic dyes. *J Hazard Mater*, 169(1-3), 176-181.

Eskandari, F., Shahnavaz, B., Mashreghi, M. (2019) Optimization of complete RB-5 azo dye decolorization using novel cold-adapted and mesophilic bacterial consortia. *J Environ Manage*, 241, 91-98.

Eslami, H., Shariatifar, A., Rafiee, E., Shiranian, M., Salehi, F., Hosseini, S.S., Eslami, G., Ghanbari, R. and Ebrahimi, A.A. (2019) Decolorization and biodegradation of reactive Red 198 Azo dye by a new *Enterococcus faecalis – Klebsiella variicola* bacterial consortium isolated from textile wastewater sludge. *World J Microbiol Biotechnol*, 35, 1-10.

Evangelista-Barreto, N.S., Albuquerque, C.D., Vieira, R.H.S.F., CamposTakaki, G.M. (2009) Cometabolic Decolorization of the Reactive Azo Dye Orange II by *Geobacillus stearothermophilus* UCP 986. *Textile Res J*, 79, 1266

Fareed, A., Zaffar, H., Bilal, M., Hussain, J., Jackson, C., Naqvi, T. A. (2022) Decolorization of azo dyes by a novel aerobic bacterial strain *Bacillus cereus* strain ROC. *PloS one*, 17(6), e0269559.

Feng, J., Cerniglia, C.E., Chen, H. (2012) Toxicological significance of azo dye metabolism by human intestinal microbiota. *Front Biosci* (Elite edition), 4, 568.

Feng, J., Kweon, O., Xu, H., Cerniglia, C. E., Chen, H. (2012) Probing the NADH-and Methyl Red-binding site of a FMN-dependent azoreductase (*AzoA*) from *Enterococcus faecalis*. *Arch Biochem Biophys*, 520(2), 99-107.

Forgacs, E., Cserhati, T., Oros, G. (2004) Removal of synthetic dyes from wastewaters: a review. *Environ Int, 30*(7), 953-971

Friedman, D.B. (2007) Quantitative proteomics for two-dimensional gels using difference gel electrophoresis. *Methods Mol Biol*, 367, 219-239

Gahr, F., Hermanutz, F., Oppermann, W. (1994) Ozonation- an important technique to comply with new German laws for textile wastewater treatment. *Water Sci Technol*, 30, 255–263

Gao, C., Mulder, D., Yin, C., Elliot, M. A. (2012) Crp is a global regulator of antibiotic production in *Streptomyces*. mBio 3, e00407-12.

Gao, H., Wang, Y., Liu, X., Yan, T., Wu, L., Alm, E., Arkin, A., Thompson, D.K., Zhou, J. (2004) Global transcriptome analysis of the heat shock response of *Shewanella oneidensis*. 7796-7803

Garg, V.K. and Kaushik, P. (2008) Influence of textile mill wastewater irrigation on the growth of sorghum cultivars. *Appl Ecol Environ Res*, 6(1),1–12.

Gerritse, J., Drzyzga, O., Kloetstra, G., Keijmel, M., Wiersum, L.P., Hutson, R., Collins, M.D. and Gottschal, J.C. (1999) Influence of different electron donors and acceptors on dehalorespiration of tetrachloroethene by *Desulfitobacterium frappieri* TCE1. *Appl Environ Microbiol*, 65(12), 5212-5221.

Ghaly, A.E., Ananthashankar, R., Alhattab, M.V.V.R., Ramakrishnan, V.V. (2014) Production, characterization and treatment of textile effluents: a critical review. *J Chem Eng Process Technol*, *5*(1), 1-19.

Ghodake, G.S., Kalme, S.D., Jadhav, J.P., Govindwar, S.P. (2009) Purification and partial characterization of lignin peroxides from *Acinetobacter calcoaceticus* NCIM 2890 and its application in decolourization of textile dyes. *Appl Biochem Biotechnol*, 152, 6–14

Ghodake, G., Jadhav, S., Dawkar, V., Govindwar, S. (2009a) Biodegradation of diazo dye Direct brown MR by *Acinetobacter calcoaceticus* NCIM 2890. *Int Biodeterior Biodegrad*, 63(4), 433-439.

Ghosh, D.K., Mandal, A., Chaudhuri, J. (1992) Purification and partial characterization of two azoreductases from *Shigella dysenteriae* type 1. *FEMS Microbiol Lett*, 98, 229–234

Gianfreda, L., Xu, F., Bollag, J.M. (1999) Laccases: a useful group of oxidoreductive enzymes. *Bioremediation J*, 3, 1e25

Golab, V., Vinder, A., Simonic, M. (2005) Efficiency of the coagulation/flocculation method for the treatment of dye bath effluent. *Dyes Pigments*, 67, 93-97.

Gomaa, O.M., Linz, J.E., Reddy, C.A. (2008) Decolorization of Victoria blue by the white rot fungus, *Phanerochaete chrysosporium*. *World J Microbiol Biotechnol*, *24*, 2349-2356.

Gomare, S. S., Jadhav, J. P., Govindwar, S. P. (2008) Degradation of sulfonated azo dyes by the purified lignin peroxidase from *Brevibacillus laterosporus* MTCC 2298. *Biotechnol Bioprocess Eng*, 13, 136-143.

Gonçalves, I.M.C., Gomes, A., Bras, R., Ferra, M.I.A., Amorim, M.T.P., Porter, R.S. (2000) Biological treatment of effluent containing textile dyes. *Coloration Technol*, 116(12), 393-397.

Gou, M., Qu, Y., Zhou, J., Ma, F., Tan, L. (2009) Azo dye decolorization by a new fungal isolate, *Penicillium* sp. QQ and fungal-bacterial cocultures. *J Hazard Mater*, 170(1), 314-319.

Gou, M., Qu, Y., Zhou, J., Ma, F., Tan, L. (2009) Azo dye decolorization by a new fungal isolate, *Penicillium* sp. QQ and fungal-bacterial cocultures. *J Hazard Mater*, 170(1), 314-319.

Gram, C. (1884) The differential staining of Schizomycetes in tissue sections and in dried preparations. *Fortschitte der Medicin*, 2, 185-189

Guo, G., Li, X., Tian, F., Liu, T., Yang, F., Ding, K., Liu, C., Chen, J. and Wang, C., (2020) Azo dye decolorization by a halotolerant consortium under microaerophilic conditions. *Chemosphere*, 244, 125510.

Guo, X., Zhou, S., Wang, Y., Song, J., Wang, H., Kong, D., Zhu, J., Dong, W., He, M., Hu, G. and Ruan, Z. (2016) Characterization of a highly thermostable and organic solvent-tolerant copper-containing polyphenol oxidase with dye-decolorizing ability from *Kurthia huakuii* LAM0618T. *PloS one*, 11(10), e0164810.

Gürses, A., Açıkyıldız, M., Güneş, K., Gürses, M.S. (2016) Classification of Dye and Pigments. In: *Dyes and Pigments*. Springer Briefs in Molecular Science. Springer, Cham pp 31-45

Gürses, A., Açıkyıldız, M., Güneş, K., Gürses, M.S. (2016) Colorants in Health and Environmental Aspects. In *Dyes and Pigments*; Springer International Publishing: Cham, Switzerland, pp. 69–83

Güzel, F., Sayğılı, H., Sayğılı, G. A., Koyuncu, F. (2014) Decolorisation of aqueous crystal violet solution by a new nanoporous carbon: Equilibrium and kinetic approach. *J Ind Eng Chem*, *20*(5), 3375-3386.

Hadibarata, T., Adnan, L.A., Yusoff, A.R.M., Yuniarto, A., Rubiyatno, Zubir, M.M.F.A., Khudhair, A.B., Teh, Z.C. and Naser, M.A. (2013) Microbial decolorization of an azo dye reactive black 5 using white-rot fungus *Pleurotus eryngii* F032. *Water Air Soil Pollut*, 224,1-9.

Hafeez, F., Farheen, H., Mahmood, F., Shahzad, T., Shahid, M., Iqbal, M., Rasul, S., Manzoor, H. and Hussain, S. (2018) Isolation and characterization of a lead (Pb) tolerant *Pseudomonas aeruginosa* strain HF5 for decolorization of reactive red-120 and other azo dyes. *Ann Microbiol*, *68*(12), 943-952.

Hafshejani, M.K., Ogugbue, C.J., Morad, N. (2014) Application of response surface methodology for optimization of decolorization and mineralization of triazo dye Direct Blue 71 by *Pseudomonas aeruginosa*. *3 Biotech*, 4, 605-619.

Haq, I., Raj, A., Markandeya. (2018) Biodegradation of Azure-B dye by *Serratia liquefaciens* and its validation by phytotoxicity, genotoxicity and cytotoxicity studies. *Chemosphere*, 196, 58–68.

Hassan, S., Sabreena, Khurshid, Z., Bhat, S.A., Kumar, V., Ameen, F., Ganai, B.A. (2022) Marine bacteria and omic approaches: A novel and potential repository for bioremediation assessment. *J Appl Microbiol*, 133(4), 2299-2313.

He, Q. and Sanford, R.A. (2003) Characterization of Fe(III) reduction by chlororespiring *Anaeromxyobacter dehalogenans*, *Appl. Environ. Microbiol*. 69 2712–2718.

Heidelberg, J.F., Paulsen, I.T., Nelson, K.E., Gaidos, E.J., Nelson, W.C., Read, T.D., Eisen, J.A., Seshadri, R., Ward, N., Methe, B., Clayton, R.A. (2002) Genome sequence of the dissimilatory metal ion– reducing bacterium *Shewanella oneidensis*. *Nat Biotechnol*, 20(11), 1118-1123.

Heukeshoven, J. and Dernick, R. (1985) Simplified method for silver staining of proteins in polyacrylamide gels and the mechanism of silver staining. *Electrophoresis* 6, 103– 112.

Holkar, C.R., Arora, H., Halder, D., Pinjari, D.V. (2018) Biodegradation of reactive blue 19 with simultaneous electricity generation by the newly isolated electrogenic

Klebsiella sp. C NCIM 5546 bacterium in a microbial fuel cell. *Int Biodeterior Biodegrad*, 133, 194–201

Holme, I. (2006) Sir William Henry Perkin: a review of his life, work and legacy. *Coloration Technol*, 122(5), 235-251.

Hong, Y., Chen, X., Guo, J., Xu, Z., Xu, M., Sun, G. (2007a) Effects of electron donors and acceptors on anaerobic reduction of azo dyes by *Shewanella decolorationis* S12. *Appl Microbiol Biotechnol*, 74, 230-238.

Hong, Y., Xu, M., Guo, J., Xu, Z., Chen, X., Sun, G. (2007b) Respiration and growth of Shewanella decolorationis S12 with azo compound as sole electron acceptor. *Appl Environ Microbiol*, 73(1), 64-72.

Hong, Y.G., and Gu, J.D. (2010) Physiology and biochemistry of reduction of azo compounds by *Shewanella* strains relevant to electron transport chain. *Appl Microbiol Biotechnol*, 88(3), 637-643.

Hsueh, C.C., Chen, B.Y., Yen, C. Y. (2009) Understanding Effects of Chemical Structure on Azo Dye Decolorization Characteristics by *Aeromonas hydrophila*,'' *J Hazard Mater*, 167, 995

Hunger, K. (2003) Dyes, general survey. Industrial Dyes: Chemistry, Properties, Applications, Wiley Subscription Services, Inc., A Wiley Company, Frankfurt, 1-10.

Igiri, B.E., Okoduwa, S.I., Idoko, G.O., Akabuogu, E.P., Adeyi, A.O. Ejiogu, I.K. (2018) Toxicity and bioremediation of heavy metals contaminated ecosystem from tannery wastewater: a review. *J Toxicol*, 16.

Imran, M., Shaharoona, B., Crowley, D.E., Khalid, A., Hussain, S., Arshad, M. (2015) The stability of textile azo dyes in soil and their impact on microbial phospholipid fatty acid profiles. *Ecotoxicol Environ Saf*, 120, 163–8.

Imran, M., Arshad, M., Asghar, H.N., Asghar, M., Crowley, D.E. (2014) Potential of *Shewanella* sp. Strain IFN4 to Decolorize Azo Dyes Under Optimal Conditions. *Int J Agri Biol*, 16(3).

Imtiazuddin, S.M., Mumtaz, M., Mallick, K.A. (2012) Pollutants of wastewater characteristics in textile industries. *J Basic App Sci*, 8, 554-556.

Jadhav, S.U., Jadhav, M. U., Kagalkar, A. N., Govindwar, S. P. (2008) Decolorization of Brilliant Blue G Dye Mediated by Degradation of the Microbial Consortium of *Galactomyces geotrichum* and *Bacillus* sp. *J Chin Inst Chem Engrs*, 39, 563

Jadhav, U.U., Dawkar, V.V., Ghodake, G.S., Govindwar, S. P. (2008a) Biodegradation of Direct Red 5B, a Textile Dye by Newly Isolated *Comamonas* sp. UVS. *J Hazard Mater*, 158, 507

Jaikumar, V. and Ramamurthi, V. (2009) Biosorption of acid yellow by spent brewery grains in a batch system: equilibrium and kinetic modelling. *Int J Biol*, *1*(1), 21.

Jayapal, M., Jagadeesan, H., Shanmugam, M., Murugesan, S. (2018) Sequential anaerobic-aerobic treatment using plant microbe integrated system for degradation of azo dyes and their aromatic amines by-products. *J Hazard Mater*, 354, 231-243.

Ji, J., Kulshreshtha, S., Kakade, A., et al (2020) Bioaugmentation of membrane bioreactor with *Aeromonas hydrophila* LZ-MG14 for enhanced malachite green and hexavalent chromium removal in textile wastewater. *Int Biodeterior Biodegrad,* 150, 104939.

Joint, I., Mühling M., Querellou, J. (2010) Culturing marine bacteria – an essential prerequisite for biodiscovery. *Microb Biotechnol*, 3 (5), 564-75.

Joshi, A.U., Hinsu, A T., Kotadiya, R.J., Rank, J.K., Andharia, K.N., Kothari, R.K. (2020) Decolorization and biodegradation of textile di-azo dye Acid Blue 113 by *Pseudomonas stutzeri* AK6. *3 Biotech*, 10(5), 214.

Joshi, T., Iyengar, L., Singh, K., Garg, S. (2008) Isolation, identification and application of novel bacterial consortium TJ-1 for decolorization of structurally different azo dyes. *Bioresour Technol*, 99, 115–7121.

Kalme, S.D., Parshetti, G.K., Jadhav, S.U., Govindwar, S.P. (2007) Biodegradation of benzidine based dye Direct Blue-6 by *Pseudomonas desmolyticum* NCIM 2112. *Bioresour Technol*, 98, 1405–1410

Kalme, S., Jadhav, S., Jadhav, M., Govindwar, S. (2009) Textile dye degrading laccase from *Pseudomonas desmolyticum* NCIM 2112. *Enzyme Microb Technol*, 44(2), 65-71

Kalyani, D.C., Patil, P.S., Jadhav, J.P., Govindwar, S. P. (2008) Biodegradation of reactive textile dye Red BLI by an isolated bacterium *Pseudomonas* sp. SUK1. *Bioresour Technol*, 99, 4635–4641.

Kalyani, D.C., Phugare, S.S., Shedbalkar, U.U., Jadhav, J.P. (2011) Purification and characterization of a bacterial peroxidase from the isolated strain *Pseudomonas* sp. SUK1 and its application for textile dye decolorization. *Ann Microbiol*, 61(3), 483-491.

Kalyani, D.C., Telke, A.A., Dhanve, R.S., Jadhav, J.P. (2009) Ecofriendly biodegradation and detoxification of Reactive Red 2 textile dye by newly isolated *Pseudomonas* sp. SUK1. *J Hazard Mater*, 163(2-3), 735-742.

Kang, C. H. and So, J. S. (2016) Antibiotic and heavy metal resistance in *Shewanella putrefaciens* strains isolated from shellfishes collected from West Sea, Korea. *Mar Pollut Bull*, 112(1-2), 111-116.

Kapustka, L.A. and Reporter, M. (1993)nTerrestrial Primary Producers,'' Handbook of Ecotoxicology, P. Calow, Ed., Blackwell Scientific Publications, Oxford, p. 278

Karcher, S., Kornmuller, A., Jekel, M. (2001) Screening of Commercial Sorbents for the Removal of Reactive Dyes. *Dyes Pigments*, 51, 111

Kaur, H., Kalotra, R., Walia, G.K., Handa, D. (2013) Dyeing industry effluent induced behavioral and morphological changes in the fish, *Cirrhinus mrigala*. *Int J Zool Res*, 3(3), 13–20

Kaushik, P. and Malik, A. (2009) Fungal dye decolourization: recent advances and future potential. *Environ Int*, 35, 127-141.

Khaled, J.M., Alyahya, S.A., Govindan, R., Chelliah, C.K., Maruthupandy, M., Alharbi, N.S., Kadaikunnan, S., Issac, R., Murugan, S., Li, W.J. (2022) Laccase producing bacteria influenced the high decolorization of textile azo dyes with advanced study. *Environ Res*, 207, 112211.

Khalid, A., Arshad, M., Crowley, D. (2010) Bioaugmentation of azo dyes. In *Biodegradation of Azo Dyes*, Ed Hatice Atacag Erkurt, Springer, vol 9; 1-37.

Khalid, A., Arshad, M., Crowley, D.E. (2008). Decolorization of azo dyes by *Shewanella* sp. under saline conditions. *Appl Microbiol Biotechnol*, 79, 1053-1059.

Khalid, A., Kausar, F., Arshad, M., Mahmood, T., Ahmed, I. (2012) Accelerated decolorization of reactive azo dyes under saline conditions by bacteria isolated from Arabian seawater sediment. *Appl Microbiol Biotechnol*, 96, 1599-1606.

Khan, R., Bhawana, P., Fulekar, M.H. (2013) Microbial decolorization and degradation of synthetic dyes: a review. *Rev Environ Sci Bio/Technol*, 12(1), 75-97.

Khehra, M.S., Saini, H.S., Sharma, D.K., Chadha, B.S., Chimni, S.S. (2005) Comparative studies on potential of consortium and constituent pure bacterial isolates to decolorize azo dyes. *Water Res*, 39, 5135–5141

Kilic, N.K., Nielsen, J.L., Yuce, M., Donmez, G. (2007) Characterization of a simple bacterial consortium for effective treatment of wastewaters with reactive dyes and Cr(VI). *Chemosphere*, 67(4), 826–831.

Kinter, M. and Sherman, N.E. (2000) Protein sequencing and identification using tandem mass spectrometry; Wiley & Sons: New York,

Kirk-Othmer. (1993) Encyclopedia of Chemical Technology, Volume 8, John Wiley & Sons, New York

Knapp, J. S. and Newby, P. S. (1995) The Microbiological Decolorization of an Industrial Effluent Containing a Diazo-Linked Chromophore. *Water Res*, 29, 1807.

Kodam, K.M., Soojhawon, I., Lohande, P.D., Gawai, K.R., (2005) Microbial decolorization of reactive azo dyes under aerobic conditions. *World J Microbiol Biotechnol*, 21, 367–370

Korniłłowicz-Kowalska, T., and Rybczyńska, K. (2012) Decolorization of Remazol Brilliant Blue (RBBR) and Poly R-478 dyes by *Bjerkandera adusta* CCBAS 930. *Open Life Sciences*, 7(5), 948-956.

Krishnan, J., Kishore, A.A., Suresh, A., Madhumeetha, B., Prakash, D.G. (2017) Effect of pH, inoculum dose and initial dye concentration on the removal of azo dye mixture under aerobic conditions. *Int Biodeterior Biodegrad*, 119, 16–27

Křížová, H. (2015) Natural dyes: Their past, present, future and sustainability. In Recent Developments in Fibrous Material Science; Křemenáková, D., Militký, J., Mishra, R., Eds.; Kanina: Prague, Czech Republic,; pp. 59–71.

Kudlich, M., Keck, A., Klein, J., Stolz, A. (1997) Localization of the enzyme system involved in the anaerobic degradation of azo dyes by *Sphingomonas* sp. BN6 and effect of artificial redox mediators on the rate of azo reduction. *Appl Environ Microbiol*, 63(9), 3691-3694.

Kumar, N., Sinha, S., Mehrotra, T., Singh, R., Tandon, S., Thakur, I. S. (2019) Biodecolorization of azo dye Acid Black 24 by *Bacillus pseudomycoides*: Process optimization using Box Behnken design model and toxicity assessment. *Bioresour Technol Rep*, 8, 100311.

Kumar, S., Stecher, G. Tamura, K. (2016) MEGA7: molecular evolutionary genetics analysis version 7.0 for bigger datasets. *Molecular biology and evolution*, *33*(7), 1870-1874.

Kurade, M.B., Waghmode, T.R., Kagalkar, A.N., Govindwar, S.P. (2012) Decolorization of textile industry effluent containing disperse dye Scarlet RR by a newly developed bacterial-yeast consortium BL-GG. *Chem Eng J*, 184, 33-41.

Laemmli, U.K., (1970) Cleavage of structural proteins during the assembly of the head of bacteriophage T4. *Nature*, 227, 680-5

Lauro, F.M., McDougald, D., Thomas, T., Williams, T.J., Egan, S., Rice, S., DeMaere, M.Z., Ting, L., Ertan, H., Johnson, J., Ferriera, S. (2009) The genomic basis of trophic strategy in marine bacteria. *Proc Natl Acad Sci*, 106(37), 15527-15533.

Leelakriangsak, M. (2013). Molecular approaches for bacterial azoreductases. *Songklanakarin J. Sci. Technol*, 35(6).

Leelakriangsak, M. and Borisut, S. (2012) Characterization of the decolorizing activity of azo dyes by *Bacillus subtilis* azoreductase AzoR1. *Songklanakarin J. Sci. Technol*, 34, 509–516.

Lenihan, H. S. (1999) Physical-biological coupling on oyster reefs: how habitat structure influences individual performance. *Ecological Monographs* 69: 251–275

Levin, L., Papinutti, L., Forchiassin, F. (2004) Evaluation of Argentinean white rot fungi for their ability to produce lignin-modifying enzymes and decolorize industrial dyes. *Bioresour Technol*, 94(2), 169-176.

Lin, J., Zhang, X., Li, Z., Lei, L. (2010) Biodegradation of Reactive Blue 13 in a Two-Stage Anaerobic/Aerobic Fluidized Beds System with a *Pseudomonas* sp. Isolate. *Bioresour. Technol*., 101, 34.

Linhoss, A. C. and Underwood, W. V. (2016) Modeling salt panne land-cover suitability under sea-level rise. *J Coastal Res*, 32(5), 1116-1125.

Liu, G., Zhou, J., Fu, Q. S., Wang, J. (2009a) The *Escherichia coli* azoreductase AzoR is involved in resistance to thiol-specific stress caused by electrophilic quinones. *J Bacteriol*, 191(20), 6394-6400.

Liu, G., Zhou, J., Wang, J., Zhou, M., Lu, H., Jin, R., (2009b) Acceleration of azo dye decolorization by using quinone reductase activity of azoreductase and quinone redox mediator. *Bioresour Technol*, 100, 2791–2795

Liu, G., Zhou, J., Wang, J., Zhang, X., Dong, B., Wang, N. (2015) Reductive Decolorization of Azo Dye by Bacteria. In *Microbial Degradation of Synthetic Dyes in Wastewaters*; Singh, S.N., Ed.; Springer International Publishing: Cham, Switzerland, 111–133

Liu, S., Meng, C., Xu, G., Jian, H., Wang, F. (2018) Validation of reference genes for reverse transcription real-time quantitative PCR analysis in the deep-sea bacterium *Shewanella psychrophila* WP2. *FEMS Microbiol Lett*, 365(7)

Liu, W., Chen, Y., Zhou, X., Liu, J., Zhu, J., Wang, S., Liu, C. Sun, D. (2020) The cyclic AMP receptor protein, Crp, is required for the decolorization of acid yellow 36 in *Shewanella putrefaciens* CN32. *Front Microbiol*, 11, 596372.

Livak, K.J. and Schmittgen, T.D. (2001) Analysis of relative gene expression data using real-time quantitative PCR and the 2(-Delta Delta C (T)) Method. *Methods*, 25(4), 402- 8.

Lopez-Grimau, V. and Gutierrez, M.C. (2006) Decolorization of simulated reactive dye bath effluents by electrochemical oxidation assisted by UV light. *Chemosphere* 62, 106-112.

Lowry, O.H., Rosebrough, N.J., Farr, A.L., Randall, R.J. (1951) Protein measurement with the Folin phenol reagent. *J Biol Chem*, 193(1), 265-275.

Lucas, M.S., Amaral, C., Sampaio, A. et al (2006) Biodegradation of the diazo dye Reactive Black 5 by a wild isolate of *Candida oleophila*. *Enzyme Microb Technol*, 39:51–55

Mahmood, F., Shahid, M., Hussain, S., Shahzad, T., Tahir, M., Ijaz, M., Hussain, A., Mahmood, K., Imran, M. Babar, S.A.K. (2017) Potential plant growth-promoting strain Bacillus sp. SR-2-1/1 decolorized azo dyes through NADH-ubiquinone: oxidoreductase activity. *Bioresour Technol*, 235, 76-184.

Mahmood, S., Arshad, M., Khalid, A., Nazli, Z. H., Mahmood, T. (2011) Isolation and screening of azo dye decolorizing bacterial isolates from dye-contaminated textile wastewater. *Soil & Environment*, 30(1).

Mahmood, S., Khalid, A., Arshad, M., Mahmood, T., Crowley, D.E. (2016) Detoxification of azo dyes by bacterial oxidoreductase enzymes. *Crit Rev Biotechnol*, 36(4), 639-651.

Majcherczyk, A., Johannes, C., Hüttermann, A. (1998) Oxidation of polycyclic aromatic hydrocarbons (PAH) by laccase of Trametes versicolor. *Enzyme Microb Technol*, *22*(5), 335-341.

Manickam, P., and Vijay, D. (2021) Chemical hazards in textiles. In *Chemical Management in Textiles and Fashion* (pp. 19-52). Woodhead Publishing.

Mansour, H. B., Corroler, D., Barillier, D., Ghedira, K., Chekir, L., Mosrati, R. (2007) Evaluation of genotoxicity and pro-oxidant effect of the azo dyes: acids yellow 17, violet 7 and orange 52, and of their degradation products by *Pseudomonas putida* mt-2. *Food Chem Toxicol*, 45(9), 1670-1677.

Manu, B. and Chaudhari, S. (2003) Decolorization of indigo and azo dyes in semicontinuous reactors with long hydraulic retention time. *Process Biochem*, 38(8), 1213-1221.

Martins, M.A.M., Cardoso, M.H., Queiroz, M.J. (1999) Biodegradation of azo dyes by the yeast *Candida zeylanoides* in batch aerated cultures. *Chemosphere*, 38:2455–2460

Mbuligwe, S. E. (2005) Comparative Treatment of Dye-Rich Wastewater in Engineered Wetland Systems (EWSs) Vegetated with Different Plants. *Water Res*, 39, 271

McMullan, G., Meehan, C., Conneely, A., Kirby, N., Robinson, T., Nigam, P., Banat, I.M., Marchant, R., Smyth, W.F. (2001) Microbial decolourisation and degradation of textile dyes. *Appl Microbiol Biotechnol*, 56:81–87

Meehan, C., Banat, I.M., McMullan, G., et al (2000) Decolorization of remazol black-B using a thermotolerant yeast, *Kluyveromyces marxianus* IMB3. *Environ Int* 26, 75–79

Mehra, S., Singh, M., Chadha, P. (2021) Adverse impact of textile dyes on the aquatic environment as well as on human beings. *Toxicol Int*, 28(2), 165.

Mendes, S., Pereira, L., Batista, C., Martins, L. O. (2011) Molecular determinants of azo reduction activity in the strain *Pseudomonas putida* MET94. *Appl Microbiol Biotechnol*, 92(2), 393-405.

Mielgo, I., López, C., Moreira, M. T., Feijoo, G., Lema, J. M. (2003) Oxidative degradation of azo dyes by manganese peroxidase under optimized conditions. *Biotechnol Progress*, 19(2), 325-331.

Millbern, Z., Trettin, A., Wu, R., Demmler, M., Vinueza, N. R. (2022) Synthetic dyes: A mass spectrometry approach and applications. Mass Spectrometry Reviews, e21818.

Misal, S. A. and Gawai, K. R. (2018) Azoreductase: a key player of xenobiotic metabolism. *Bioresour Bioprocess*, 5(1), 1-9.

Mishra, S., and Maiti, A. (2018) The efficacy of bacterial species to decolourise reactive azo, anthroquinone and triphenylmethane dyes from wastewater: a review. *Environ Sci Pollut Res*, 25, 8286-8314.

Modi, H. A., Rajput, G., Ambasana, C. (2010) Decolorization of water soluble azo dyes by bacterial cultures, isolated from dye house effluent. *Bioresour Technol*, 101(16), 6580-6583.

Mohan, S., Muralimohan, N., Vidhya, K., Sivakumar, C. (2017) A case study on-textile industrial process, characterization and impacts of textile effluent. *Indian J Sci Res*, 17(1), 080–084

Moosvi, S., Kher, X., Madamwar, D. (2007) Isolation, characterization and decolorization of textile dyes by a mixed bacterial consortium JW-2. Dyes Pigments 74:723–729

Moosvi, S., Kehaira, H., Madamwar, D. (2005) Decolorization of textile dye Reactive Violet 5 by a newly isolated bacterial consortium RVM 11.1. *World J Microbiol Biotechnol*, 21, 667–672

Mugerfeld, I., Law, B. A., Wickham, G. S., Thompson, D. K. (2009) A putative azoreductase gene is involved in the *Shewanella oneidensis* response to heavy metal stress. *Appl Microbiol Biotechnol*, 82, 1131-1141.

Murugesan, K., Kim, Y. M., Jeon, J. R., Chang, Y. S. (2009) Effect of metal ions on reactive dye decolorization by laccase from *Ganoderma lucidum*. *J Hazard Mater,* 168(1), 523-529.

Myslak, Z. W., and Bolt, H. M. (1998) Occupational exposure to azo dyes and risk of bladder cancer. *Zbl. Arbeitsmed*, 38, 310-321.

Nachiyar, C.V. and Rajkumar, G.S. (2005) Purification and characterization of an oxygen insensitive azoreductase from *Pseudomonas aeruginosa*. *Enzyme Microb Technol*, 36, 503–509

Nagevenkar, G.S. and Ramaiah, N. (2010) Abundance of sewage-pollution indicator and human pathogenic bacteria in a tropical estuarine complex. *N Environ Monit Assess* 155, 245

Naghdi, M., Taheran, M., Brar, S. K., Kermanshahi-Pour, A., Verma, M., Surampalli, R. Y. (2017) Immobilized laccase on oxygen functionalized nanobiochars through mineral acids treatment for removal of carbamazepine. *Sci Total Environ*, 584, 393-401.

Nakanishi, M., Yatome, C., Ishida, N., Kitade, Y., (2001) Putative ACP phosphodiesterase gene encodes an azoreductase. *J Biol Chem*, 49, 46394–46399

Neihsial, R., Singha, N. A., Singh, A. K. (2022) Taxonomic diversity and predictive metabolic functions of a heavy metal tolerant multiple azo dye degrading bacterial consortium from textile effluents. *Int Biodeterior Biodegrad*, 171, 105421.

Nigam, P., Banat, I.M., Dalel, S., Roger, M., (1995) Microbial process for the decolorization of textile effluent containing azo, diazo and reactive dyes. *Process Biochem*, 31, 435–442

Nilratnisakorn, S., Thiravetyanand, P., Nakbanpote, W. (2007) Synthetic Reactive Dye Wastewater Treatment by Narrow-Leaved Cattails (*Typha angustifolia* Linn.): Effects of Dye, Salinity and Metals. *Sci. Total Environ*, 384, 67

O'Neill, C., Hawkes, F. R., Esteves, S. R. R., Hawkes, D. L., Wilcox, S. J. (1999) Anaerobic and aerobic treatment of a simulated textile effluent. *J Chem Technol Biotechnol*: International Research in Process, Environmental & Clean Technology, 74(10), 993-999.

Ogugbue, C.J. and Sawidis, T. (2011) Bioremediation and Detoxification of Synthetic Wastewater Containing Triarylmethane Dyes by *Aeromonas hydrophila* Isolated from Industrial Effluent. *Biotechnol Res Int*

Ollikka, P., Alhonmäki, K., Leppänen, V. M., Glumoff, T., Raijola, T., Suominen, I. (1993) Decolorization of azo, triphenyl methane, heterocyclic, and polymeric dyes by lignin peroxidase isoenzymes from *Phanerochaete chrysosporium*. *Appl Environ Microbiol*, 59(12), 4010-4016.

Ooi, T., Shibata, T., Sato, R., Ohno, H., Kinoshita, S., Thuoc, T.L., Taguchi, S. (2007) An azoreductase, aerobic NADH-dependent flavoprotein discovered from *Bacillus* sp.: functional expression and enzymatic characterization. *Appl Microbiol Biotechnol*, 75, 377-386

Oturkar, C.C., Nemade, H.N., Mulik, P.M., Patole, M.S., Hawaldar, R.R., Gawai, K.R. (2011) Mechanistic investigation of decolorization and degradation of Reactive Red 120 by *Bacillus lentus* BI377. *Bioresour Technol*, 102(2), 758-764.

Pace, N.R. (1997) A molecular view of microbial diversity and the biosphere. *Science*, 276 (5313), 734–740

Pandey, A., Singh, P., Iyengar, L. (2007) Bacterial decolorization and degradation of azo dyes. *Int Biodeterior Biodegrad*, 59(2), 73-84.

Pandey, A.K., Dubey, V. (2012) Biodegradation of azo dye Reactive Red BL by *Alcaligenes* sp. AA09. *Int J Eng Sci*, 1, 54e60

Parsons, T. R., Maita, Y., Lalli, C. M. (1984) A manual of chemical and biological methods for seawater analysis. Oxford Pergamon Press.

Paszczyński, A., Crawford, R.L., Huynh, V.B. (1988) Manganese peroxidase of *Phanerochaete chrysosporium*: purification. In *Methods in enzymology* (Vol. 161, pp. 264-270). Academic Press.

Patil, P.S., Phugare, S.S., Jadhav, S.B., Jadhav, J.P. (2010) Communal action of microbial cultures for Red HE3B degradation. *J Hazard Mater*, 181(1–3):263–270.

Patil, P., Desai, N., Govindwar, S., Jadhav, J. P., Bapat, V. (2009) Degradation Analysis of Reactive Red 198 by Hairy Roots of *Tagetes patula* L. (Marigold). *Planta*, 230, 725.

Patterson, S. D. and Aebersold, R. H. (2003) Proteomics: The first decade and beyond. *Nat Genet*, 33, 311-323.

Pearce, C.I., Lloyd, J.R., Guthrie, J.T. (2003) The removal of colour from textile wastewater using whole bacterial cells: a review. *Dyes Pigments*, 58(3), 179-196.

Pereira, F., Kerkar, S., Krishnan, K.P. (2013) Bacterial response to dynamic metal concentrations in the surface sediments of a solar saltern (Goa, India). *Environ Monit Assess*, 185, 3625–3636

Petrucci, E., Di Palma, L., Lavecchia, R., Zuorro, A. (2015) Treatment of diazo dye Reactive Green 19 by anodic oxidation on a boron-doped diamond electrode. *J Ind Eng Chem*, *26*, 116-121.

Pieper, D.H. and Reineke, W. (2000) Engineering bacteria for bioremediation. *Curr Opin Biotechnol*, 11(3), 262-270.

Pinheiro, L.R.S., Gradíssimo, D.G., Xavier, L.P., Santos, A.V. (2022) Degradation of azo dyes: bacterial potential for bioremediation. *Sustainability*, 14(3), 1510.

Prasad, S.S. and Aikat, K. (2014) Study of bio-degradation and biodecolourization of azo dye by *Enterobacter* sp. SXCR. *Environ Technol*, 35, 956–965

Prasad, A. S. and Rao, K. V. (2013) Aerobic biodegradation of Azo dye by *Bacillus cohnii* MTCC 3616; an obligately alkaliphilic bacterium and toxicity evaluation of metabolites by different bioassay systems. *Appl Microbio Biotechnol*, 97(16), 7469-7481.

Punj, S., and John, G. H. (2009) Purification and identification of an FMN-dependent NAD(P)H azoreductase from *Enterococcus faecalis*. *Curr Issues Mol Biol*, 11(2), 59–65

Raffi, F., Hall, J.D., Cerniglia, C.E. (1997) Mutagenicity of azo dyes used in foods, drugs and cosmetics before and after reduction by *Clostridium* species from the human intestinal tract. *Food Chem Toxicol*, 35, 897-901.

Rafii, F., Franklin, W., Cerniglia, C.E. (1990) Azoreductase activity of anaerobic bacteria isolated from human intestinal microflora. *Appl Environ Microbiol*, 56, 2146–215.

Raghukumar, C. (2008) Marine fungal biotechnology: an ecological perspective. *Fungal Diversity*, 31: 19-35

Rai, H., Bhattacharya, M., Singh, J., Bansal, T.K., Vats, P., Banerjee, U.C. (2005) Removal of Dyes from the Effluent of Textile and Dyestuff Manufacturing Industry: A Review of Emerging Techniques with Reference to Biological Treatment. *Crit Rev Environ Sci Technol*, 35, 219.

Ramaiah, N., Kenkre, V.D., Verlecar, X.N. (2002) Marine environmental pollution stress detection through direct viable counts of bacteria. *Water Res*, 36 (9): 2383-93

Ramaiah, N. (2001) Coliform and human pathogenic bacteria in tourism affected water bodies in North Goa. *Coastin*, 7, 13-16.

Ramaiah, N., *et al.*, (2007) Sewage-pollution indicator bacteria. In: Shetye, S.R., Kumar, M.D., Shankar, D., (eds) The Mandovi and Zuari Estuaries. Research Publishing Services, Chennai, India

Ramakrishna, K. R. and Viraraghavan, T. (1997) Dye Removal Using Low Cost Adsorbents. *Water Sci Technol*, 36, 189

Ramalho, P.A., Cardoso, M.H., Cavaco-Paulo, A., *et al* (2004) Characterization of azo reduction activity in a novel ascomycete yeast strain. *Appl Environ Microbiol*, 70, 2279–2288

Ravikumar, G., Kalaiselvi, M., Gomathi, D., Vidhya, B., Devaki, K., Uma, C. (2013) Effect of laccase from *Hypsizygus ulmarius* in decolorization of different dyes. *J Pharm Sci*, 3, 150e152

Rekik, H., Jaouadi, N.Z., Bouacem, K., Zenati, B., Kourdali, S., Badis, A., Annane, R., Bouanane-Darenfed, A., Bejar, S. and Jaouadi, B. (2019) Physical and enzymatic properties of a new manganese peroxidase from the white-rot fungus *Trametes pubescens* strain i8 for lignin biodegradation and textile-dyes biodecolorization. *Int J Biological Macromol*, 125, 514-525.

Renganathan, S., Thilagaraj, W. R., Miranda, L. R., Gautam, P., Velan, M. (2006) Accumulation of acid orange 7, acid red 18 and reactive black 5 by growing *Schizophyllum commune*. *Bioresour Technol*, 97(16), 2189-2193.

Renner, R. (1997) On the trail of bioremediating microbes. *Environ Sci Technol*, 31(4), 188A-189A.

Reyes, P., Pickard, M.A., Vazquez-Duhalt, R. (1999) Hydroxybenzotriazole increase the range of textile dyes decolorized by immobilized laccase. *Biotechnol Lett*, 21, 875-880.

Reysenbach, A. L., Giver, L. J., Wickham, G. S., and Pace, N. R. (1992) Differential amplification of rDNA genes by polymerase chain reaction. *Appl Environ Microbiol*, 58, 3417–3418

Robinson, T., McMullan, G., Marchant, R., Nigam, P. (2001) Remediation of Dyes in Textile Effluent: A Critical Review on Current Treatment Technologies with a Proposed Alternative. *Bioresour Technol*, 77, 247.

Rodriguez, C.E., Fukuto, J.M., Taguchi, K., Froines, J., Cho, A.K. (2005) The interactions of 9,10-phenanthrenequinone with glyceraldehyde-3-phosphate dehydrogenase (GAPDH), a potential site for toxic actions. *Chem Biol Interact*, 155, 97–110.

Rodriguez, E., Pickard, M.A., Vazquez-Duhalt, R. (1999) Industrial dye decolorization by laccases from ligninolytic fungi. *Curr Microbiol*, 38, 27-32.

Russ, R., Rau, J., Stolz, A. (2000) The function of cytoplasmic flavin reductases in the reduction of azo dyes by bacteria. *Appl Environ Microbiol*, 66(4), 1429–34.

Ryan, A., Wang, C.J., Laurieri, N., Westwood, I., Sim, E. (2010a) Reaction mechanism of azoreductases suggests convergent evolution with quinone oxidoreductases. *Protein & cell*, 1, 780-790.

Ryan, A., Laurieri, N., Westwood, I., Wang, C.J., Lowe, E., Sim, E. (2010b) A novel mechanism for azoreduction. *J Mol Biol*, 400, 24-37

Rybicki, E., Swiech, T., Lesniewska, E., Albinska, J., Szynkowska, M.I., Paryjczak, T., Sypniewski, S. (2004) Changes in hazardous substances in cotton after mechanical and chemical treatments of textiles. *Fibres Text East Eur*, 12, 67–73

Šafaříková, M., Ptáčková, L., Kibrikova, I., Šafařík, I. (2005) Biosorption of water-soluble dyes on magnetically modified *Saccharomyces cerevisiae* subsp. *uvarum* cells. *Chemosphere*, 59(6), 831-835.

Sanghi, R., Bhattacharya, B., Singh, V. (2006) Use of *Cassia javahikai* seed gum and gum-g-polyacrylamide as coagulant aid for the decolorization of textile dye solutions. *Bioresour Technol*, 97(10), 1259-1264.

Saratale, G.D., Bhosale, S. K., Kalme, S.D., Govindwar, S.P. (2007) Biodegradation of Kerosene in *Aspergillus ochraceus* (NCIM 1146). *J Basic Microbiol*, 47, 400.

Saratale, R.G., Saratale, G.D., Chang, J.S., Govindwar, S.P. (2009a). Biodegradation of textile dye navy blue HER by *Trichosporon beigelii* NCIM-3326. *J Hazard Mater*, 166 (2–3), 1421–1428.

Saratale, R.G., Saratale, G.D., Chang, J.S., Govindwar, S.P. (2009b) Ecofriendly degradation of sulfonated diazo dye C.I. Reactive Green 19A using *Micrococcus glutamicus* NCIM-2168. *Bioresour Technol*, 100, 3897–3905.

Saratale, R.G., Saratale, G.D., Kalyani, D.C., Chang, J.S., Govindwar, S.P. (2009c) Enhanced decolorization and biodegradation of textile azo dye Scarlet R by using developed microbial consortium-GR. *Bioresour Technol*, 100(9), 2493-2500.

Saratale, R.G., Saratale, G.D., Chang, J.S., Govindwar, S.P. (2011) Bacterial decolorization and degradation of azo dyes: A review. *J Taiwan Inst Chem Eng*, 42, 138-157.

Sarayu, K. and Sandhya, S. (2010) Aerobic Biodegradation Pathway for Remazol Orange by *Pseudomonas aeruginosa*. *Appl Biochem Biotechnol*, 160, 1241

Sarkar, S., Banerjee, A., Halder, U., Biswas, R., Bandopadhyay, R. (2017) Degradation of synthetic azo dyes of textile industry: a sustainable approach using microbial enzymes. *Water Conserv Sci Eng*, 2, 121–131.

Sarnaik, S. and Kanekar, P. (1999) Biodegradation of methyl violet by Pseudomonas mendocina MCM B-402. *Appl Microbiol Biotechnol*, *52*, 251-254.

Selvam, K., Priya, M.S., Yamuna, M. (2012) Decolourization of azo dyes and dye industry effluents by lignin degrading fungus *Trametes versicolor*. *International Journal of Pharmaceutical & Biological Archives*, 3(3), 666-672.

Selvam, K., Swaminathan, K., Chae, K.S. (2003) Decolourization of azo dyes and a dye industry effluent by a white rot fungus *Thelephora* sp. *Bioresour Technol*, 88(2), 115-119.

Senan, R.C. and Abraham, E.T. (2004) Bioremediation of textile azo dyes by aerobic bacterial consortium. *Biodegradation*, 15, 275–280.

Serra, C., Kogevinas, M., Silverman, D.T., Turuguet, D., Tardon, A., García-Closas, R., Carrato, A., Castaño-Vinyals, G., Fernandez, F., Stewart, P. and Benavides, F.G.

(2008). Work in the textile industry in Spain and bladder cancer. *Occup Environ Med*, 65(8), 552-559.

Shah, P.D., Dave, S.R., Rao, M.S. (2012) Enzymatic degradation of textile dye Reactive Orange 13 by newly isolated bacterial strain *Alcaligenes faecalis* PMS-1. *Int Biodeterior Biodegrad*, 69, 41–50.

Shah, M.P. (2014) Microbe-mediated degradation of synthetic dyes in wastewater. In *Microbial degradation of synthetic dyes in wastewaters* (pp. 205-241). Cham: Springer International Publishing.

Shah, M.P., Patel, K.A., Darji, A.M. (2013) Microbial degradation and decolorization of methyl orange dye by an application of *Pseudomonas* spp. ETL-1982. *Int J Environ Biorem Biodegrad*, 1(1), 26-36.

Sharma, D.K., Saini, H.S., Singh, M., Chimni, S.S., Chadha, B.S. (2004) Isolation and characterization of microorganisms capable of decolorizing various triphenylmethane dyes. *J Basic Microbiol*, 44(1), 59-65.

Sharma, P., Singh, S.P., Iqbal, H.M., Tong, Y.W. (2022) Omics approaches in bioremediation of environmental contaminants: An integrated approach for environmental safety and sustainability. *Environ Res*, 211, 113102.

Si, J., Peng, F., Cui, B. (2013) Purification, biochemical characterization and dye decolorization capacity of an alkali-resistant and metal-tolerant laccase from *Trametes pubescens*. *Bioresour Technol*, 128, 49-57.

Si, J., Yuan, T.Q., Cui, B.K. (2015) Exploring strategies for adsorption of azo dye Congo Red using free and immobilized biomasses of *Trametes pubescens*. *Annals Microbiol*, 65(1), 411-421.

Silveira, E., Marques, P.P., Silva, S.S., Lima-Filho, J.L., Porto, A.L.F., Tambourgi, E.B. (2009) Selection of *Pseudomonas* for industrial textile dyes decolourization. *Int Biodeterior Biodegradation*, 63, 230–235.

Singh, R.L., Singh, P.K., Singh, R.P. (2015) Enzymatic decolorization and degradation of azo dyes–A review. *Int Biodeterior Biodegradation, 104*, 21-31.

Singh, R.P., Singh, P.K., Singh, R.L. (2014) Bacterial decolorization of textile azo dye Acid Orange by *Staphylococcus hominis* RMLRT03. *Toxicol Int*, 21, 160-166.

Singh, S., Chatterji, S., Nandini, P.T., Prasad, A.S.A., Rao, K.V.B. (2015) Biodegradation of azo dye Direct Orange 16 by *Micrococcus luteus* strain SSN2. *Int J Environ Sci Technol*, 12(7), 2161-2168.

Smibert, R.M. and Krieg, N.R. (1994) Phenotypic characterization. In: *Methods for general and molecular bacteriology*, Gerhardt P, Murray RGE, Wood WA, Krieg NR (Eds), American Society for Microbiology, Washington, DC, pp 607-654

Song, Z., Song, L., Shao, Y., Tan, L. (2018) Degradation and detoxification of azo dyes by a salt-tolerant yeast *Cyberlindnera samutprakarnensis* S4 under high-salt conditions. *World J Microbiol Biotechnol*, 34, 131.

Soni, P., Sharma, S., Sharma, S., Kumar, S., Sharma, K.P. (2006) A comparative study on the toxic effects of textile dye wastewaters (untreated and treated) on mortality and RBC of a freshwater fish *Gambusia affinis* (Baird and Gerard). *J Environ Biol*, 27(4), 623–628.

Souza, A.G.V., Maria, T.C., Saran, L.M., Alves, L.M.C. (2022) Enzymatic bioremediation of dyes from textile industry effluents. In: *The Toxicity of Environmental Pollutants*. IntechOpen.

Spadaro, J.T., Gold, M.H., Renganathan, V. (1992) Degradation of azo dyes by the lignin-degrading fungus *Phanerochaete chrysosporium*. *Apppl Environ Microbiol*, 58(8), 2397-2401.

Sponza, D.T. and Isik, M. (2004) Decolorization and inhibition kinetic of direct black 38 azo dye with granulated anaerobic sludge. *Enzyme Microb Technol*, 34, 147–158.

Sreedharan, V., Saha, P., Rao, K.V.B. (2021) Dye degradation potential of *Acinetobacter baumannii* strain VITVB against commercial azo dyes. *Biorem J*, 25(4), 347-368.

Srinivasan, S., Sadasivam, S. K., Gunalan, S., Shanmugam, G., Kothandan, G. (2019) Application of docking and active site analysis for enzyme linked biodegradation of textile dyes. *Environ Pollut*, 248, 599-608.

Staley, J.T. and Konopka, A. (1985) Measurement of in situ activities of nonphotosynthetic microorganisms in aquatic and terrestrial habitats. *Ann Rev Microbiol*, 39, 321–346.

Stolz, A. (2001) Basic and applied aspects in the microbial degradation of azo dyes. *Appl Microbiol Biotechnol*, 56(1-2), 69-80.

Sudha, M., Saranya, A., Selvakumar, G., Sivakumar, N. (2014) Microbial degradation of azo dyes: a review. *Int J Curr Microbiol App Sci*, 3(2):670–690.

Sudha, M., Bakiyaraj, G., Saranya, A., Sivakumar, N., Selvakumar, G. (2018) Prospective assessment of the *Enterobacter aerogenes* PP002 in decolorization and degradation of azo dyes DB 71 and DG 28. *J Environ Chem Eng*, 6(1), 95-109.

Suzuki, Y., Yoda, T., Ruhul, A., Sugiura, W. (2001) Molecular Cloning and Characterization of the Gene Coding for Azoreductase from *Bacillus* sp. OY1-2 Isolated from Soil. *J Biol Chem*, 276, 9059.

Sweeney, E.A., Chipman, J.K., Forsythe, S.J. (1994) Evidence for direct-acting oxidative genotoxicity by reduction products of azo dyes. *Environ Health Perspect*, 102(suppl 6), 119-122.

Tamura, K., Nei, M., Kumar, S., (2004) Prospects for inferring very large phylogenies by using the neighbor-joining method. *Proc Natl Acad Sci USA*, 101, 11030–11035.

Tan, N.C., Leeuwen, A.V., Voorthuizen, E.M.V., Slenders, P., Prenafeta-Boldu, F.X., Temmink, H., Lettinga, G., Field, J.A. (2005) Fate and biodegradability of sulfonated aromatic amines. *Biodegradation*, 16, 527-537.

Tang, J., Wang, Y., Yang, G., Luo, H., Zhuang, L., Yu, Z., Zhou, S. (2018) Complete genome sequence of the dissimilatory azo reducing thermophilic bacterium *Novibacillus thermophiles* SG-1. *J Biotechnol*, 284, 6-10.

Tang, X., Yi, W., Munske, G.R., Adhikari, D.P., Zakharova, N.L., Bruce, J.E. (2007) Profiling the membrane proteome of *Shewanella oneidensis* MR-1 with new affinity labeling probes. *J Proteome Res*, 6(2), 724-734.

Tanner, K., Vilanova, C., Porcar, M. (2017) Bioprospecting challenges in unusual environments. *Microb Biotechnol*, 10(4), 671.

Telke, A.A., Joshi, S.M., Jadhav, S.U., Tamboli, D.P., Govindwar, S.P. (2010) Decolorization and detoxification of Congo red and textile industry effluent by an isolated bacterium *Pseudomonas* sp. SU-EBT. *Biodegradation*, 21, 283-296.

Telke, A.A., Kalyani, D.C., Dawkar, V.V., Govindwar, S.P. (2009) Influence of organic and inorganic compounds on oxidoreductive decolorization of sulfonated azo dye CI Reactive Orange 16. *J Hazard Mater*, 172(1), 298-309.

Telke, A., Kalyani, D., Jadhav, J., Govindwar, S. (2008) Kinetics and Mechanism of Reactive Red 141 Degradation by a Bacterial Isolate *Rhizobium radiobacter* MTCC 8161. *Acta Chim Slov*, 55, 320

Thakur, J.K., Paul, S., Dureja, P., Annapurna, K., Padaria, J.C., Gopal, M. (2014) Degradation of sulphonated azo dye red HE7B by *Bacillus* sp. and elucidation of degradative pathways. *Curr Microbiol*, 69, 183-191.

Thatoi, H., Behera, B.C., Mishra, R.R., Dutta, S.K. (2013) Biodiversity and biotechnological potential of microorganisms from mangrove ecosystems: a review. *Annals Microbiol*, 63(1), 1-19.

Thorsten, D. and José, L.R. (2001) Do mangroves rather than rivers provide nutrients to coastal environments south of the Amazon River? Evidence from long-term flux measurements. *Mar Eco Prog Series*, 213, 67-77

Tian, F., Guo, G., Zhang, C., Yang, F., Hu, Z., Liu, C., Wang, S.W. (2019) Isolation, cloning and characterization of an azoreductase and the effect of salinity on its expression in a halophilic bacterium. *Int J Biol Macromol*, 123, 1062-1069.

Tien, M. and Kirk, T.K. (1984) Lignin degrading enzymes from *Phanerochaete chrysosporium*: purification, characterization, and catalytic properties of a unique hydrogen peroxide requiring oxygenase. *Proc Natl Acad Sci*, 81, 2280–2284.

Toes, A.C., Geelhoed, J.S., Kuenen, J.G., Muyzer, G. (2008) Characterization of heavy metal resistance of metal-reducing *Shewanella* isolates from marine sediments. *Geomicrobiol J*, 25(6), 304-314.

Tony, B.D., Goyal, D., Khanna, S. (2009) Decolorization of textile azo dyes by aerobic bacterial consortium. *Int Biodeterior Biodegrad*, 63(4), 462-469.

Töwe, S., Leelakriangsak, M., Kobayashi, K., Duy, N.V, Hecker, M., Zuber, P., Antelmann, H. (2007) The MarR-type repressor MhqR (YkvE) regulates multiple dioxygenases/glyoxalases and an azoreductase which confer resistance to 2-methylhydroquinone and catechol in *Bacillus subtilis*. *Mol Microbiol*, 66, 40-54.

Valenzuela-García, L.I., Zapata, B.L., Ramírez-Ramírez, N., Huchin-Mian, J.P., Robleto, E.A., Ayala-García, V.M., Pedraza-Reyes, M. (2020) Novel biochemical properties and physiological role of the flavin mononucleotide oxidoreductase *YhdA* from *Bacillus subtilis*. *Appl Environ Microbiol*, 86(20), e01688-20.

Vandevivere, P.C., Bianchi, R., Verstraete, W. (1998) Review: Treatment and reuse of wastewater from the textile wet-processing industry: Review of emerging technologies. *J Chem Technol Biot*, *72*(4), 289-302.

Varadharajan, D. and Soundarapandian, P. (2014) Effect of Physico-Chemical Parameters on Species Biodiversity with Special Reference to the Phytoplankton from Muthupettai, South East Coast of India. *J Earth Sci Clim Change*, 5 (5), 200.

Vasseur, C., Labadie, J., Hebraud, M. (1999) Differential protein expression by *Pseudomonas fragi* submitted to various stresses. *Electrophoresis*, 20 (11), 2204 -2213.

Verma, A.K., Raghukumar, C., Verma, P., Shouche, Y.S., Naik, C.G. (2010) Four marine-derived fungi for bioremediation of raw textile mill effluents. *Biodegradation*, 21, 217-233.

Verma, P. and Madamwar, D. (2003) Decolorization of Synthetic Dyes by a Newly Isolated Strain of *Serratia maerascens. World J Microbiol Biotechnol*, 19, 615.

Vijayaraghavan, K. and Yun, Y.S. (2008) Utilization of Fermentation Waste (*Corynebacterium glutamicum*) for Biosorption of Reactive Black 5 from Aqueous Solution. *J Hazard Mater*, 141, 45.

Vitor, V. and Corso, C.R. (2008) Decolorization of textile dye by *Candida albicans* isolated from industrial effluents. *J Ind Microbiol Biotechnol*, 35, 1353–1357

Wang, H., Su, J.Q., Zheng, X.W., Tian, Y., Xiong, X.J., Zheng, T.L. (2009) Bacterial decolorization and degradation of the reactive dye reactive red 180 by *Citrobacter* sp. CK3. *Int Biodeterior Biodegrad*, 63(4), 395–399.

Wang, B., Xu, M., Sun, G. (2010) Comparative analysis of membranous proteomics of *Shewanella decolorationis* S12 grown with azo compound or Fe (III) citrate as sole terminal electron acceptor. *Appl Microbiol Biotechnol*, 86(5), 1513-1523.

Wang, F., Xu, Z., Wang, C., Guo, Z., Yuan, Z., Kang, H., Li, J., Lu, F. Liu, Y. (2021) Biochemical characterization of a tyrosinase from *Bacillus aryabhattai* and its application. *Int J Biol Macromol*, 176, 37-46.

Weisburg, W.G., Barns, S.M., Pelletier, D.A., Lane, D.J. (1991) 16S ribosomal DNA amplification for phylogenetic study. *J Bacteriol*, 173 (2), 697–703.

Weisburger, J.H. (2002) Comments on the history and importance of aromatic and heterocyclic amines in public health. *Mut Res*, 506, 9-20.

Wheeler, D.L., Barrett, T., Benson, D.A., Bryant, S.H., Canese, K., Chetvernin, V., Church, D.M., DiCuccio, M., Edgar, R., Federhen, S., Feolo, M. (2007) Database resources of the national center for biotechnology information. *Nucleic Acids Res*, 36(suppl_1), D13-D21.

Won, S.W., Choi, S.B., Chung, B.W., Park, D., Park, J.M., Yun, Y.S. (2004) Biosorptive decolorization of Reactive Orange 16 using the waste biomass of *Corynebacterium glutamicum*. *Ind Eng Chem Res*, 43(24), 7865–7869.

Wong, P.K. and Yuen, P. Y. (1996) Decolorization and Biodegradation of Methyl Red by *Klebsiella pneumoniae* RS-13. *Water Res*, 30, 1736.

Wu, F.C., Tseng, R. L., Juang, R. S. (2001) Enhanced Abilities of Highly Swollen Chitosan Beads for Color Removal and Tyrosinase Immobilization. *J Hazard Mater*, 81, 167.

Wu, J., Kim, K.S., Sung, N.C., Kim, C.H., Lee, Y.C. (2009) Isolation and characterization of *Shewanella oneidensis* WL-7 capable of decolorizing azo dye Reactive Black 5. *J Gen Appl Microbiol*, 55(1), 51-55.

Wuhrmann, K., Mechsner, K., Kappeler, T. (1980) Investigations on rate-determining factors in the microbial reduction of azo dyes. *European J Appl Microbiol Biotechnol*, 9:325–338.

Xu, M., Guo, J., Sun, G. (2007) Biodegradation of Textile Azo Dye by *Shewanella decolorationis* S12 under Microaerophilic Conditions. *Appl Microbiol Biotechnol*, 76, 719.

Yan, H. and Pan, G. (2004) Increase in Biodegradation of Dimethyl Phthalate by *Closterium lunula* Using Inorganic Carbon. *Chemosphere*, 55, 1281

Yang, Q., Yang, M., Pritsch, K. *et al* (2003) Decolorization of synthetic dyes and production of manganese-dependent peroxidase by new fungal isolates. *Biotechnol Lett*, 25, 709–713.

Yang, Y., Lu, L., Gao, F., Zhao, Y. (2013) Characterization of an efficient catalytic and organic solvent-tolerant azoreductase toward methyl red from *Shewanella oneidensis* MR-1. *Environ Sci Pollut Res*, *20*, 3232-3239.

Yaseen, D.A. and Scholz, M. (2019) Textile dye wastewater characteristics and constituents of synthetic effluents: a critical review. *Int J Environ Sci Technol*, 16(2), 1193-1226.

Yoo, E.S., Libra, J., Wiesmann, U. (2000) Reduction of azo dyes by *Desulfovibrio desulfuricans*. *Water Sci Technol*, 1, 15–22

Yu, C.H., Wu, C.H., Ho, T.H., Hong, P.A. (2010) Decolorization of CI Reactive Black 5 in UV/TiO2, UV/oxidant and UV/TiO2/oxidant systems: A comparative study. *Chem Eng J*, 158(3), 578-583.

Zafar, S., Bukhari, D. A., Rehman, A. (2022). Azo dyes degradation by microorganisms - An efficient and sustainable approach. *Saudi J Biol Sci*, 103437.

Zhang, H.K., Lu, H., Wang, J., Liu, G.F., Zhou, J.T., & Xu, M.Y. (2013) Global transcriptome analysis of *Escherichia coli* exposed to immobilized anthraquinone-2-sulfonate and azo dye under anaerobic conditions. *Appl Microbiol Biotechnol*, 97, 6895-6905.

Zhang, S., An, X., Gong, J., Xu, Z., Wang, L., Xia, X., Zhang, Q. (2022) Molecular response of *Anoxybacillus* sp. PDR2 under azo dye stress: An integrated analysis of proteomics and metabolomics. *J Hazard Mater*, 438, 129500.

Zhao, B. and Poh, C.L. (2008) Insights into environmental bioremediation by microorganisms through functional genomics and proteomics. *Proteomics*, 8(4), 874-881

Zhao, R., Ma, L., Fan, F., Gong, Y., Wan, X., Jiang, M., Zhang, X., Yang, Y. (2011) Decolorization of different dyes by a newly isolated white- rot fungal strain *Ganoderma* sp. En3 and cloning and functional analysis of its laccase gene. *J Hazard Mater*, 192, 855e873

Zhou, Q. (2001) Chemical pollution and transport of organic dyes in water-soil-crop systems of the Chinese Coast. *Bull Environ Contam Toxicol*, 66(6), 0784–93

Zhou, X. and Xiang, X. (2013) Effect of different plants on azo-dye wastewater bio-decolorization. *Procedia Environ Sci*, 18, 540-546.

Publication:

- **De Souza, N. A**., Ramaiah, N., Damare, S., Furtado, B., Mohandass, C., Patil, A., & De Lima, M. (2019). Differential Protein Expression in *Shewanella seohaensis* Decolorizing Azo Dyes. *Current Proteomics*, *16*(2), 156-164.

Manuscript under preparation:

- Physiological and molecular characterization of rapid azo dye decolorization using a marine bacterial strain *Shewanella seohaensis* NIO_14d

Conference proceedings and presentations:

- Poster presented at National Conference of Young Researchers 2017 on "New Frontiers in Life Sciences & Environment", organized by Faculty of Life Sciences and Environment, Goa University on 16th & 17th March 2017

- Oral presentation on "Proteomic characterization of an azo dye decolorizing marine bacterium for bioremediation of textile effluent" presented at National Conference MiCON 2022 – *Advances in Microbiology* organized by Yenepoya Research Centre, Yenepoya (Deemed to be University) on 2nd February 2022

- Poster presented at International E-conference "Contribution of Biological Sciences for Sustainable Environment" organized by Department of Microbiology, Wilson College, Mumbai on 25th & 26th February 2022 (**Awarded First Place**)

Send Orders for Reprints to reprints@benthamscience.ae

Current Proteomics, 2018, *15*, 000-000

RESEARCH ARTICLE

Differential Protein Expression in *Shewanella seohaensis* Decolorizing Azo Dyes

Nadine Ana de Souza[1,2], Nagappa Ramaiah[1*], Samir Damare[1], Bliss Furtado[1,3], Chellandi Mohandass[1], Anushka Patil[1] and Marsha De Lima[1]

[1]*Biological Oceanography Division, CSIR-National Institute of Oceanography, Dona Paula, Goa 403 004, India;* [2]*Department of Microbiology, Goa University, Taleigao Plateau, Goa 403206, India;* [3]*Present Address: Department of Microbiology, Faculty of Biology and Environmental Protection, Nicolaus Copernicus University, Lwowska 1, 87-100 Torun, Poland*

ARTICLE HISTORY

Received: March 06, 2018
Revised: June 21, 2018
Accepted: July 24, 2018

DOI:
10.2174/1570164615666180731110845

Abstract: ***Background***: Microbial remediation is an ecologically safe alternative to controlling environmental pollution caused by toxic aromatic compounds including azo dyes. Marine bacteria show excellent potential as agents of bioremediation. However, a lack of understanding of the entailing mechanisms of microbial degradation often restricts its wide-scale and effective application.

Objective: To understand the changes in a bacterial proteome profile during azo dye decolorization.

Method: In this study, we tested a Gram-negative bacterium, *Shewanella seohaensis* NIODMS14 isolated from an estuarine environment and grown in three different azo dyes (Reactive Black 5 (RB5), Reactive Green 19 (RG19) and Reactive Red 120 (RR120)). The unlabeled bacterial protein samples extracted during the process of dye decolorization were subject to mass spectrometry. Relative protein quantification was determined by comparing the resultant MS/MS spectra for each protein.

Results: Maximum dye decolorization of 98.31% for RB5, 91.49% for RG19 and 97.07% for RR120 at a concentration of 100 mg L^{-1} was observed. The liquid chromatography-mass spectrometry - Quadrupole Time of Flight (LCMS-QToF) analysis revealed that as many as 29 proteins were up-regulated by 7 hours of growth and 17 by 24 hours of growth. Notably, these were common across the decolorized solutions of all three azo dyes. In cultures challenged with the azo dyes, the major class of up-regulated proteins was cellular oxidoreductases and an alkyl hydroperoxide reductase (SwissProt ID: A9KY42).

Conclusion: The findings of this study on the bacterial proteome profiling during the azo dye decolorization process are used to highlight the up-regulation of important proteins that are involved in energy metabolism and oxido-reduction pathways. This has important implications in understanding the mechanism of azo dye decolorization by *Shewanella seohaensis*.

Keywords: Azo dye, decolorization, mass spectrometry, proteomics, *Shewanella seohaensis*, up-regulation.

1. INTRODUCTION

Currently, there are over 100,000 different synthetic dyes in use worldwide [1]. They find useful applications in textile, pharmaceutical, leather, paper, cosmetic and food industries [2, 3] and are classified by their chemical composition or by the types of fibers to which they can be applied [4]. Chemical classification system groups synthetic dyes based on the nature of their chromophores. As such, the various classes of industrially significant dyes include azo, anthraquinone, diazonium, sulfur, indigoid, triarylmethane, triphenylmethyl (trityl), nitro and phthalocyanine derivatives [5].

In India, the dye manufacturing industry contributes to almost 6.6% of the global dye production [6]. The textile industry accounts for two-thirds of the total dyestuff market. The process of dyeing of one kilogram of fiber with reactive dyes utilizes 70 to 150 L water, 0.6 to 0.8 kg NaCl and about 30 to 60 g dyestuff [7]. Depending on the class of dye used, the dyeing process discharges approximately 2% to 50% of dye into wastewater [8, 9]. Reactive dyes used for dyeing of cellulosic fibers, wool and silk have low rates of fiber fixa-

*Address correspondence to this author at the Biological Oceanography Division, CSIR-National Institute of Oceanography, P.O. Box: 403004, Goa, India; Tel: +91 9420897437; E-mail: ramaiahnagappa@gmail.com

1570-1646/18 $58.00+.00 © 2018 Bentham Science Publishers

tion [10]. Consequently, textile effluents contain large amounts of unbound dye which enter aquatic bodies directly and impart intense coloration. It is estimated that 280,000 tons of textile dyes are discharged in industrial effluents per year worldwide [11]. Disposal of large volumes of azo dyes in textile industrial effluent poses an environmental and organismic health hazard. If left untreated, the deeply colored water causes a reduction in the penetration of sunlight to subsurface layers of the receiving water bodies. This leads to decreasing photosynthetic activity and increasing biological oxygen demand [12]. Oliveira *et al*. [13] and Shah [14] reported that many mutagenic and carcinogenic synthetic dyes which are resistant to microbial degradation can become highly persistent in natural water bodies leading to ecosystem degradation and implicit hazards of various kinds.

Azo dyes typically contain one or more azo (-N=N-) groups and are the most extensively used textile dyes [15]. A complex chemical structure and synthetic nature make these dyes xenobiotic and recalcitrant to biodegradation [16]. The toxic nature of certain azo dye breakdown products has prompted the European Union to impose a ban on the use of certain azo dyes [17].

Many of the world's textile industry hubs are present in developing countries. However, due to a lack of stringent monitoring and inadequate environmental management controls, effluents are discharged without proper treatment directly into water bodies [18].

High economic costs coupled with low efficiency and limited application make conventional physicochemical treatments of dye-containing wastewater less appealing. Biological systems capable of degrading and decolorizing azo dyes are therefore of great significance in bioremediation efforts. Various mechanisms of dye decolorization by microorganisms have been proposed in recent times [19]. However, bacteria receive attention for their ability to decolorize a wide range of structurally different dyes. Many species of bacteria adopt a number of mechanisms to remove or decolorize azo compounds from the environment including biosorption, bioaccumulation, reduction, oxidation and sequential reduction-oxidation processes [20]. Among them, *Shewanella* species are reported to possess diverse respiratory metabolic pathways and are indeed known potential agents for bioremediation [21]. In this regard, understanding and evaluating the changes in the proteome of an organism during its growth would prove pivotal. For instance, Zhao and Poh [22] describe how different cellular protein components of bacteria are known to respond differently to various environmental stimuli.

The ease and reliability of reproducible proteome analyses are facilitating large-scale descriptions of proteins from various organisms. Essentially, the expression of proteins by the bacterium exposed to synthetic dyes under experimental alterations helps to elucidate the possible expression of pertinent proteins. As Linsen *et al*. [23] suggest, differential protein expression analysis enables the identification of proteins and the pattern of their expression under different conditions of growth. This is implicit of the fact that the proteins expressed differentially are useful to discern their functional involvement in a given process. In this regard, their identification would contribute to recognize the role of specific proteins in the pathway of dye decolorization. Such a comprehensive understanding would enable selective alteration of certain proteins for targeted development of strains with maximum efficiency of dye decolorization.

In this study, a gel-free proteomic approach was used to evaluate the changes in protein expression of *Shewanella seohaensis* NIODMS14 during the decolorization of three reactive dyes, Reactive Black 5 (RB5), Reactive Green 19 (RG19) and Reactive Red 120 (RR120). We used a Liquid Chromatography-Mass Spectrometry - Quadrupole Time of Flight (LCMS-QToF) system to identify the proteins expressed and to measure their abundance with respect to differential regulation. This was done to understand the contrast in the expression of proteins when *Shewanella seohaensis* NIODMS14 is grown in a medium with an azo dye versus growth in the dye-free medium. The results demonstrate differences in the proteome of *Shewanella seohaensis* NIODMS14 during the decolorization process of the three azo dyes.

2. MATERIALS AND METHODS

2.1 Microorganism and Culture Conditions

The proteomic profiles of a Gram-negative, salt tolerant bacterial isolate collected from an estuarine location in Goa, India were analyzed in this study. The strain NIODMS14 was identified as *Shewanella seohaensis* on the basis of 16S rRNA gene sequencing and the sequence was submitted to GenBank with the accession number KR922404. The pure culture of the isolate was deposited at the Microbial Type Culture Collection (MTCC) of the CSIR-Institute of Microbial Technology, Chandigarh, India, under the accession number MTCC 25079**.** The culture was purified on seawater nutrient agar (SWNA containing [l^{-1}]: peptic digest of animal tissue 5.0 g, sodium chloride 5.0 g, beef extract 1.5 g, yeast extract 1.5 g, agar 15 g, distilled water 500 mL, sea water 500 mL, pH 7.4 ± 0.2) and a loopful of seed culture from an isolated colony was pre-cultured in 10 mL nutrient broth (NB, containing [l^{-1}] 5.0 g peptone and 3.0 g yeast extract) at pH 7.0 for 12 hours at 30°C, 120 rpm on a shaker incubator. Fresh NB (100 mL) was further inoculated with 1% (v/v) of the pre-cultured broth and grown under the same conditions. This was then used as the inoculum for decolorization experiments. Stock solutions of the dyes (10 g L^{-1}) were prepared and sterilized by membrane filtration using a 0.2-µm pore size membrane filter (Axiva, Delhi). All chemicals used in this study were of analytical grade.

2.2. Decolorization Assay and Growth Profiles

Decolorization experiments using three commercial reactive azo dyes, viz. RB5, RG19 and RR120 (Sigma-Aldrich), were performed by growing the culture in 500 mL Erlenmeyer flasks containing 250 mL of sterile nutrient broth supplemented with dyes added at a concentration of 100 mg L^{-1}. Flasks were incubated at 30°C and samples were aliquoted every 3 hours until decolorization was complete. The samples were then centrifuged at 20,000 g for 10 minutes at 4°C. The cell-free supernatant color was read at the wavelength of maximum absorption of the dyes used, i.e. 597 nm

for RB5, 630 nm for RG19 and 522 nm for RR120, using a Shimadzu UV-1800 spectrophotometer (Kyoto, Japan). Controls without dye and/or inoculum were maintained under identical conditions. The cell pellets were further used for protein extraction.

The decolorization efficiency was expressed using the following equation [24]:

$$\text{Decolorization (\%)} = (A_{initial} - A_{final})/ A_{initial} \times 100$$

where $A_{initial}$ is the initial absorbance and A_{final} is the absorbance after time t.

Bacterial growth was measured by determining the absorbance of culture samples at 600 nm [24].

2.3. Extraction of Proteins

The cell pellets, obtained at the time points 7 hours and 24 hours, were washed twice with 1X Phosphate Buffer (PB containing [l^{-1}]: disodium hydrogen phosphate 1.42 g, potassium dihydrogen phosphate 0.24 g, distilled water 1000 mL, pH 7.4 ± 0.2) and resuspended in 1 mL of protein extraction buffer along with zirconia beads and homogenized in a FastPrep24 homogenizer (MP Biomedicals, USA) at 6.5 m/s for 40 seconds. Whole cell proteins were extracted using a urea-thiourea buffer containing [ml^{-1}]: urea 0.42 g, thiourea 0.15 g, CHAPS 0.4 g, IPG buffer (Immobilized pH gradient) 80 microL, Dithiothreitol (DTT) 0.03 g and 1M tris solution 200 microL. Cell debris was removed by centrifugation at 20,000 g at 4°C for 20 minutes. The proteins in the supernatant were precipitated using methanol [25]. The vacuum dried samples were resuspended in 1 mL of TE buffer (pH 8.3) containing 10 µL of 1X protease inhibitor (Serva, Germany). The protein concentration was estimated using the Folin-Lowry method [26]. Based on this concentration, suitable aliquots were made and stored at -20°C until further processing.

2.4. Preparation of In-solution Digests

The method of in-solution trypsin digestion for the solubilization of proteins was followed (modified from Kinter *et al*. [27]). 6M urea was used as a chaotropic agent along with 200mM DTT and 200 mM iodoacetamide as reducing and alkylating agents, respectively. 100 µg of the extracted protein sample was digested with 1 mg mL^{-1} trypsin (20µg Proteomics grade Trypsin from porcine pancreas dissolved in 20µL of 1mM HCl, Sigma T6567, USA) at 37°C for 15 hours. After digestion, the samples were acidified to a pH of 2-3 using 100% formic acid (MS grade) before subjecting to mass spectrometry.

2.5. Mass Spectrometry and Protein Identification

Proteins were identified using the in-house LCMS-QToF facility (6538 UHD Accurate Mass QTOF LC/MS, Agilent Technologies, USA). Sub-volumes of 8 µL tryptic digests were injected into the auto-sampler. The LC separations were carried out on a Prot ID Chip 150 II 300A C18 150 mm column using water and 9:1 (v/v) acetonitrile: water. 0.1% Formic acid in water (1:999 v/v) was used as adduct in both the aqueous and organic phases (acetonitrile). The peptides were eluted using a standardized 71-minute protocol with a linear gradient of increasing acetonitrile concentration (2 to 90% for 50 min, 90% for 10 min and 90 to 2% for 3 min). The MS/MS spectra for the separated ions were acquired in the range of 50 to 2000 *m/z* in positive mode at 2 ppm accuracy. The spectral data was acquired using Mass Hunter Software ver. B.06.00 (Agilent Technologies, USA).

2.6. LC-MS/MS Data Analyses and Interpretation

Protein identification and quantification were performed using Spectrum Mill software ver. B.04.01.141 (Agilent Technologies, USA). The MS/MS spectra acquired were searched against the genus-specific UniProtKB/Swiss-Prot database for *Shewanella*. The following search criteria were used: minimum matched peak intensity of 50%, precursor mass tolerance of 50 ppm and product mass tolerance of 100 ppm. In addition, a maximum of 2 missed cleavages was allowed. Carbamidomethylation of cysteine residues was included as the fixed modification. The study was a high throughput discovery proteomics experiment and samples were run as four technical replicates.

2.7. Statistical Analyses

Mass Profiler Professional (MPP) software ver. 14.5 (Agilent Technologies, USA) was used to analyze the protein hits generated. The proteins were identified in each of the replicates and grouped for each sample (dye-free control, RB5, RG19 and RR120). Each identified protein entity in the sample was selected based on the frequency of occurrence in at least one condition. Auto-validation was carried out for the database matches using the default settings with a False Discovery Rate (FDR) of 1.2% (Supplemental file 1). Significant proteins had peptide scores in protein mode >1 with a scored peak intensity (SPI) of >10% for peptides. The differential significance between control samples (dye-free) and dye-amended samples was determined with a p-value cut-off of 0.2 and a fold-change cut-off of 2.0. The protein hits satisfying the cut-off criteria were functionally classified based on the Kyoto Encyclopedia of Genes and Genomes, ver. 37 (KEGG) pathways. Venn diagrams were created to identify proteins exclusively up-regulated during decolorization of different dyes and proteins common to all the dye conditions.

3. RESULTS

3.1. Cell Growth and Decolorization Assay

The growth assay of *Shewanella seohaensis* NIODMS14 and extent of decolorization of the three reactive dyes in dye-amended nutrient broth suggest rapid decolorization (Fig. **1**). The culture decolorized all three reactive dyes substantially. Dye decolorization was visible in the initial 3 hours of contact with the dye itself. In case of RB5, rapid decolorization (84.33%) was seen within the initial 3 hours and a maximum of 98.31% was achieved by 20 hours. Similarly, for RG19, decolorization of 78.5% was seen after 3 hours incubation of the culture with the dye whereas a maximum of 91.49% was achieved in 23 hours. Maximum decolorization of 97.07% of RR120 happened within 17 hours. It was observed that color reduction of the reactive dyes occurred concomitantly with

active cell growth and considerable decolorization occurred in the early stages of growth.

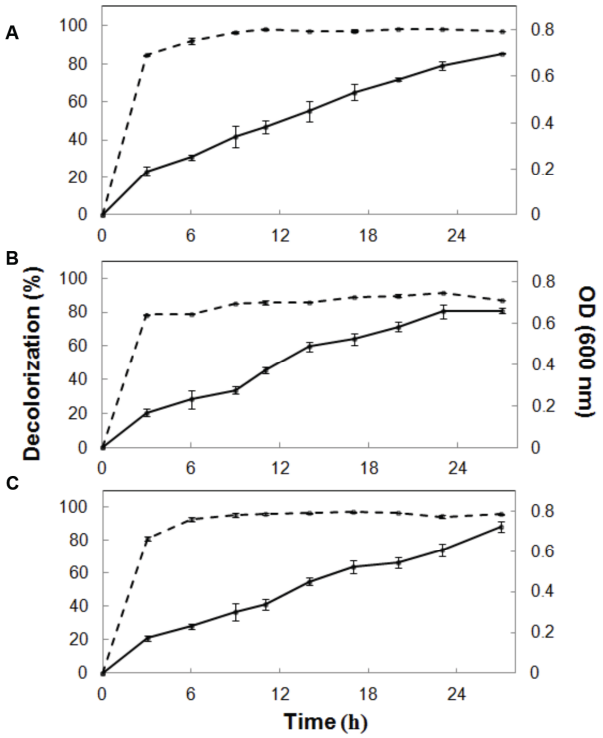


Fig. (1). Growth curve (solid line) and decolorization percent (dashed line) of *Shewanella seohaensis* NIODMS14 in nutrient broth amended with 100 ppm of (**A**) Reactive Black 5 (**B**) Reactive Green 19 (**C**) Reactive Red 120. Data are expressed as mean ± standard deviation (SD) of three replicate experiments.

3.2. Protein Identification

The numbers of expressed proteins in *Shewanella seohaensis* NIODMS14 in the medium with and without dyes (control) were compared to discern the changes in the protein profiles during dye decolorization. The accession numbers of the identified proteins were referenced using the UniProtKB database (www.uniprot.org).

Approximately, a total of 1182 functionally different protein hits were obtained from the data acquired using the MPP software ver. 14.5 (Agilent Technologies, USA). Of these, 507 entities were obtained from the culture grown in the absence of the dyes (control), whereas, 423, 417 and 677 proteins were detected in *S. seohaensis* NIODMS14 grown in medium with RB5, RG19 and RR120, respectively (Supplemental file 2).

3.3. Functional Characterization of Expressed Proteins

The identified proteins had a broad functional distribution and were classified as such. According to the physiological functions assigned using the Kyoto Encyclopedia of Genes and Genomes, ver. 37 (KEGG) metabolic pathways and Clusters of Orthologous Groups database (https://www.genome.jp/kegg/pathway.html), the proteins were classified into 15 functional categories (Fig. **2**). This allowed a comparison of differentially expressed proteins between control and dye treatment. It was observed that the number of proteins detected did not vary much with or without the presence of azo dyes. Major cellular processes were not affected during decolorization as the culture grew well and essential proteins were expressed in all three dye-challenged conditions. Proteins involved in the process of translation were maximal, contributing to 25% of the total classified proteins. The minimum numbers of proteins identified were those involved in the metabolism of other molecules including terpenoids, polyketides, flavonoids, etc., accounting for only 13% of the total classified proteins.

3.4. Comparison of Differentially Expressed Proteins

Significant differences in protein profiles were observed in *S. seohaensis* NIODMS14 grown in the presence of reactive azo dyes. At 7 hours of incubation, 176, 113 and

Table 1. Proteins up-regulated during decolorization of Reactive Black 5 azo dye.

Swiss-Prot ID	Protein Name	Gene Based on Protein ID	Protein Mass (Da)	Functional Category[a]	Fold Change[b]
A9L5Q8	Cytochrome c prime	*Sbal195_1300*	16506.6	Energy metabolism	16.00
P83223	Fumarate reductase flavoprotein	*SO_0970*	62903.3	Energy metabolism	1.29
A8GZW1	Oxidoreductase FAD/NAD(P)-binding domain protein	*Spea_0520*	26730	Energy metabolism	1.08
Q8EI38	NADH-quinone oxidoreductase, subunit K	*nuoK*	11211.3	Energy metabolism	16.00
A9KY42	Alkyl hydroperoxide reductase/ Thiol specific antioxidant	*Sbal195_1777*	22160.7	Peroxiredoxin activity	1.54
A4Y8D8	TRAP dicarboxylate transporter, DctP subunit	*Sputcn32_2500*	38006	Membrane transport	16.00
A9KTX7	Membrane protein involved in aromatic hydrocarbon degradation	*Sbal195_2866*	46196.6	Cellular process	3.59

[a]Functions are reported according to KEGG2 metabolic database (http://www.genome.jp/kegg/kegg2.html).

[b]Fold change compared to dye free control.

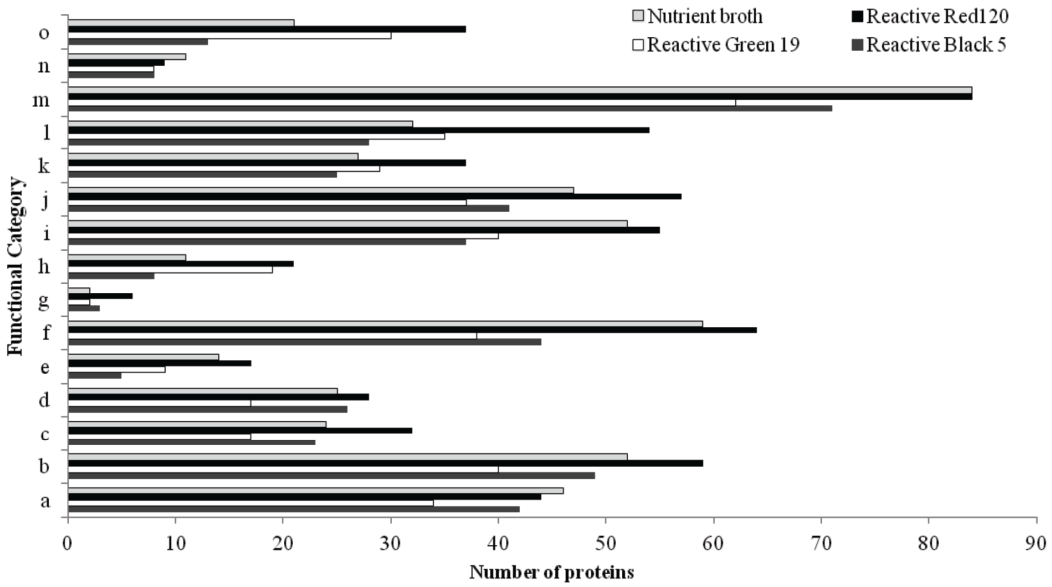


Fig. (2). Functional classification of identified proteins expressed in dye-free nutrient broth (light grey shaded bar) compared to those expressed during decolorization of the reactive dyes: RR120 (black shaded bar), RG19 (white shaded bar) and RB5 (dark grey shaded bar). Lowercase letters along the x-axis refer to the following categories of functional roles: (a) Carbohydrate metabolism; (b) Amino acid metabolism; (c) Lipid metabolism; (d) Nucleotide metabolism; (e) Cofactors and vitamins metabolism; (f) Energy metabolism; (g) Other metabolic processes; (h) Signal transduction; (i) Cellular process; (j) Transport; (k) Replication and repair; (l) Transcription; (m) Translation; (n) Protein folding, sorting and degradation; (o) Miscellaneous & Unknown function. (KEGG metabolic database, http://www.genome.jp/kegg/).

231 proteins were up-regulated during the decolorization of RB5, RG19 and RR120 respectively. Further, at 24 hours, as many as 138, 219 and 520 proteins were up-regulated in *S. seohaensis* NIODMS14 grown in RB5, RG19 and RR120 respectively as compared that grown in the dye-free control (Fig. **3**). As many as 29 up-regulated proteins were found to be common to all the three dyes at the early stages of the decolorization process (7 hours) while 17 commonly up-regulated proteins were identified in the samples after 24 hours of incubation (Fig. **3**). Of these, some prominent proteins expressed during the decolorization of Reactive Black 5 are listed in Table **1** along with their fold change and functional categorization. Similarly, up-regulated proteins identified during decolorization of Reactive Green 19 and Reactive Red 120 are summarized in Tables **2** and **3** respectively.

3.5. Changes in Abundance of Expressed Proteins Accompanying Dye Decolorization

Many proteins functioning in energy metabolism were predominantly up-regulated in the bacterium during dye decolorization, especially the cellular oxidoreductases. Proteins commonly expressed in all three dye decolorizing conditions were an oxidoreductase FAD/NAD (P)-binding domain protein (SwissProt ID: A8GZW1) and an alkyl hydroperoxide reductase (SwissProt ID: A9KY42). At 24 hours of exposure, the alkyl hydroperoxide reductase was up-regulated by 1.54, 1.25 and 7.68 folds under RB5, RG19 and RR120 dye decolorizing conditions respectively. This protein complex has oxido-reductase activity and can use either NADH or NADPH as an electron donor for direct reduction of redox dyes or of alkyl hydroperoxides. It functions in cellular response to oxidative stress and were notably absent in the control sample without dye.

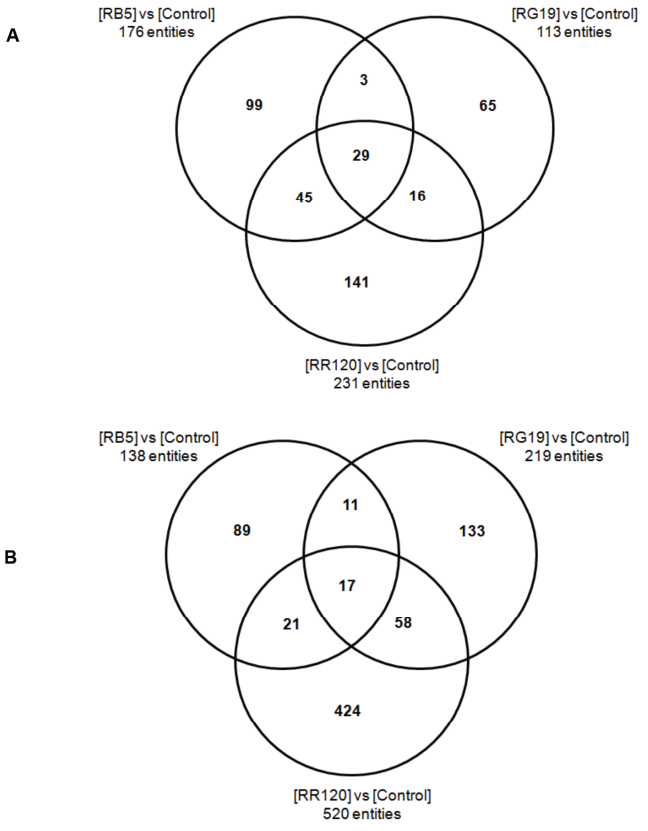


Fig. (3). Venn diagrams comparing up-regulated proteins entities in dye challenged *Shewanella seohaensis* NIODMS14 versus control (without dye). (**A**) Up-regulated entities at 7 hours; (**B**) Up-regulated entities at 24 hours of exposure to dyes.

Table 2. Proteins up-regulated during decolorization of Reactive Green 19 azo dye.

Swiss-Prot ID	Protein Name	Gene Based on Protein ID	Protein Mass (Da)	Functional Category[a]	Fold Change[b]
A9L5Q8	Cytochrome c prime	*Sbal195_1300*	16506.6	Energy metabolism	16.00
A8GZW1	Oxidoreductase FAD/NAD(P)-binding domain protein	*Spea_0520*	26730	Energy metabolism	2.94
A8FPZ7	FMN-dependent NADH-azoreductase	*azoR*	21205.9	Energy metabolism	16.00
P83223	Fumarate reductase flavoprotein subunit	*SO_0970*	62903.3	Energy metabolism	16.00
B0TT30	NADH:flavin oxidoreductase/NADH oxidase	*Shal_2030*	74360.4	Energy metabolism	1.49
A9KY42	Alkyl hydroperoxide reductase/ Thiol specific antioxidant	*Sbal195_1777*	22160.7	Peroxiredoxin activity	1.25
A8FYW2	Na(+)-translocating NADH-quinone reductase subunit A	*nqrA*	47902.9	Membrane transport	16.00
B1KNE0	TRAP dicarboxylate transporter, DctP subunit	*Swoo_1732*	39527.3	Membrane transport	16.00

[a]Functions are reported according to KEGG2 metabolic database (http://www.genome.jp/kegg/kegg2.html).

[b]Fold change compared to dye free control.

Table 3. Proteins up-regulated during decolorization of Reactive Red 120 azo dye.

Swiss-Prot ID	Protein Name	Gene Based on Protein ID	Protein Mass (Da)	Functional Category[a]	Fold Change[b]
A9L5Q8	Cytochrome c prime	*Sbal195_1300*	16506.6	Energy metabolism	1.18
A8GZW1	Oxidoreductase FAD/NAD(P)-binding domain protein	*Spea_0520*	26730	Energy metabolism	3.32
P83223	Fumarate reductase flavoprotein subunit	*SO_0970*	62903.3	Energy metabolism	1.66
BOTT30	NADH:flavin oxidoreductase/NADH oxidase	*Shal_2030*	74360.4	Energy metabolism	16.00
A9KY42	Alkyl hydroperoxide reductase/ Thiol specific antioxidant	*Sbal195_1777*	22160.7	Peroxiredoxin activity	7.68
A4Y3Y6	Na(+)-translocating NADH-quinone reductase subunit A	*nqrA*	47856.1	Membrane transport	1.36

[a]Functions are reported according to KEGG2 metabolic database (http://www.genome.jp/kegg/kegg2.html).

[b]Fold change compared to dye free control.

Proteins functioning in electron transport were observed to be up-regulated during dye decolorization. A fumarate reductase flavoprotein subunit (SwissProt ID: P83223) was up-regulated by 1.29, 16.00 and 1.66 in RB5, RG19 and RR120 decolorizing conditions respectively. Cytochrome c protein (SwissProt ID: A9L5Q8) which is also an electron transport protein, was identified in all three dye-challenged samples as well as in dye-free control with a fold change of 1.18 (in RR120 decolorizing condition) and 16.00 (in RB5 and RG19 decolorizing conditions). The up-regulation of these two proteins points to their role in dye reduction and decolorization by electron transfer. NADH: flavin oxidoreductase/NADH oxidase (SwissProt ID: B0TT30) was up-regulated by 1.49 fold in RG19 decolorizing condition and by 16.00 fold in RR120 decolorizing condition. Another protein with similar function, NADH-quinone oxidoreductase, subunit K found in the RB5 decolorized sample was up-regulated with a high fold change of 16.00. An FMN-dependent NADH-azoreductase was also obtained under RG19 decolorizing condition.

Two transport proteins were notably up-regulated wherein, Na (+)-translocating NADH-quinone reductase subunit A (SwissProt ID: E6XLW6) was detected during decolorization of RG19 (fold change of 16.00) and RR120 (fold change of 1.36) and TRAP dicarboxylate transporter (SwissProt ID: A4Y8D8; fold change of 16.00) was detected in *S. seohaensis* NIODMS14 decolorizing RB5 and RG19 and was not detected in the dye-free control. A membrane protein with 3.59 fold increase, reported to be involved in aromatic hydrocarbon degradation was identified in RB5 decolorizing condition at 7 hours. Gene Ontology (GO) annotation indicated that this 46.197 kDa polypeptide functions in membrane transport associated with the catabolism of aromatic hydrocarbons. The protein was identified based on amino acid similarity hit to the polypeptide present in *Shewanella baltica (strain OS195)*. Studies aimed at ex-situ expression of this and other up-regulated proteins would be highly valuable.

4. DISCUSSION

Shewanella strains have the ability to use a range of electron donors and acceptors, thereby reducing the toxic effects of many contaminants which have earned them the reputation of being excellent candidates for bioremediation [28]. Various cellular proteins which play a role in the reductive metabolism of *Shewanella* species include cellular oxidoreductases as well as *c*-type cytochromes and peroxiredoxins. Chen *et al*. [29] propose that some of these proteins have also been implicated in azo dye decolorization.

Various species of bacteria are known to accomplish decolorization and detoxification of azo dyes [30]. Pearce *et al*. [31] observed the lower efficiency of decolorization in case of complex structured and high molecular weight dyes such as azo dyes. However, in this study *Shewanella seohaensis* NIODMS14 exhibited rapid and efficient decolorization of three reactive diazo dyes at a concentration of 100 mg L^{-1}. In fact, complete decolorization of the dye RB5 was achieved within 24 hours. The strain also effectively decolorized more than 90% of RG19 and RR120 in a short time of 23 hours and 6 hours respectively. This is in contrast to previous reports by Wu *et al*. [32] where *Shewanella oneidensis* WL-7 was found to decolorize only 36% of 100 μM of RB5 in about 12 hours.

There are many studies aimed at identifying and characterizing the molecular components of the dye decolorization process [28, 33, 34, 35]. Kudlich *et al*. [36] first proposed the involvement of the bacterial electron transport chain in azo dye reduction. Dubbs and Mongkolsuk [37] suggested peroxiredoxins as a class of enzymes that play an antioxidant protective role in cells. The up-regulation of pertinent oxidoreductases (oxidoreductase FAD/NAD(P)-binding domain protein) and peroxiredoxins (alkyl hydroperoxide reductase) in dye-exposed *Shewanella seohaensis* NIODMS14 points to the involvement of these proteins in the dye decolorization process. Experimental validation of these proteins was not carried out as this was a discovery proteomic experiment.

As described by Hong and Gu [28], Hong *et al*. [33] and Wang *et al*. [35] fumarate reductase enhances decolorization by transferring electrons during bacterial azo reduction. The analysis of results showed a significantly up-regulated fumarate reductase flavoprotein subunit suggesting it plays a similar role in *Shewanella seohaensis* NIODMS14.

Transport proteins constitute an integral part of the response mechanism of bacteria to heavy metals and other environmental contaminants including azo dyes. The up-regulation of two transport proteins (Na (+) -translocating NADH-quinone reductase and TRAP dicarboxylate transporter) in *Shewanella seohaensis* NIODMS14 points to their possible involvement in transferring reducing electrons to the azo dye during the decolorization process (also described by Tang *et al*. [38]).

Brigé *et al*. [34] observed the involvement of cytochrome c proteins in the reduction of reactive dyes. These crucial components of the electron transport chain function in reducing dye molecules and thereby facilitating the decolorization process. In concurrence with these findings, multiple up-regulated cytochrome c proteins were observed in *Shewanella seohaensis* NIODMS14 associated with decolorization of the three reactive azo dyes.

The protein profiles generated from this study reveal the up-regulation of cellular oxidoreductases which may function in electron transfer during azo dye decolorization. However, it is necessary to further deduce the specific metabolic pathways in which these proteins function. This can be achieved by integrating computational and other 'omics' techniques.

CONCLUSION

Using a discovery proteomic approach, this study provides an insight into the induction, expression and catabolic pathway of certain proteins of *Shewanella seohaensis* NIODMS14 which rapidly decolorized three reactive azo dyes. Results obtained are used to directly correlate the function of various proteins to the process of azo dye decolorization based on observed differential regulation and/or expression and accompanying fold change values. During dye decolorization, the study identifies proteins in oxido-reduction pathways (for example, oxidoreductase FAD/NAD (P)-binding domain protein, NADH: flavin oxidoreductase/ NADH oxidase, alkyl hydroperoxide reductase and FMN-dependent NADH-azoreductase) to be up-regulated. Synergistic up-regulation of these proteins coupled with membrane transport proteins (Na (+)-translocating NADH-quinone reductase and TRAP dicarboxylate transporter) and electron transport (by fumarate reductase and cytochrome c proteins) serves to rapidly and efficiently decolorize azo dyes by *Shewanella seohaensis* NIODMS14.

Our results provide additional information to support that the electron transfer pathway contributes to azo dye recognition, metabolism and finally decolorization. This information has useful implications for targeted manipulation of specific dye decolorizing proteins in order to augment their activity and further design bioremediation strategies using *Shewanella seohaensis* in particular and other decolorizing bacterial strains in general.

LIST OF ABBREVIATIONS

DTT	=	Dithiothreitol
FDR	=	False Discovery Rate
GO	=	Gene Ontology
IPG	=	Immobilized pH gradient
KEGG	=	Kyoto Encyclopedia of Genes and Genomes
LCMS-QToF	=	Liquid Chromatography-Mass Spectrometry - Quadrupole Time of Flight
MPP	=	Mass Profiler Professional
MTCC	=	Microbial Type Culture Collection
NB	=	Nutrient broth
PB	=	Phosphate buffer
RB5	=	Reactive Black 5

RG19 = Reactive Green 19

RPM = revolutions per minute

RR120 = Reactive Red 120

SPI = scored peak intensity

SWNA = Sea water nutrient agar

TE = Tris-EDTA

ETHICS APPROVAL AND CONSENT TO PARTICIPATE

Not applicable.

HUMAN AND ANIMAL RIGHTS

No Animals/Humans were used for studies that are the basis of this research.

CONSENT FOR PUBLICATION

Not applicable.

CONFLICT OF INTEREST

The authors declare no conflict of interest, financial or otherwise.

ACKNOWLEDGEMENTS

This work was conceptualised by NR, SD and NdeS and exectued by NdeS, AP, MDeL. NdeS analyzed the data and wrote and revised this manuscript. SD, CM and NR supervised experimental design and helped revise this manuscript. BF and SD helped in carrying out proteomic experiments and acquisition of data. Ram Murti Meena helped in sequencing and identification of the isolate. All authors read and approved the final manuscript. The authors thank the Director, Council of Scientific and Industrial Research (CSIR) - National Institute of Oceanography for the facilities and encouragement. Financial support from CSIR funded project PSC0206 (MAR-BIOTECH) and BSC0111 (INDEPTH) is gratefully acknowledged. This is NIO contribution number 6275.

This study is funded by project Nos: PSC0206 and BSC0111. The funders had no role in study design, data collection and analysis, decision to publish, or preparation of the manuscript.

SUPPLEMENTARY MATERIAL

Supplementary material is available on the publisher's web site along with the published article. Supplemental File 1 contains all the files of auto validation carried out on the MS results. Supplemental File 2 shows a complete summary of all protein entities.

REFERENCES

[1] Chen, K.C.; Wu, J.Y.; Liou, D.J.; Hwang, S.C.J. Decolorization of the textile dyes by newly isolated bacterial strains. *J. Biotechnol.*, **2003**, *101*(1), 57-68.

[2] Zollinger, H. *Color Chemistry – Synthesis, Properties and Applications of Organic Dyes and Pigment*; VCH: New York, **1987**.

[3] Carmen, Z.; Daniela, S. In: *Organic pollutants ten years after the Stockholm Convention - environmental and analytical update*; Puzyn, T., Ed.; InTech, **2012**; pp. 55-86.

[4] Kirk, R.E.; Othmer, D.F. *Kirk-Othmer Encyclopedia of Chemical Technology*; Kroschwitz J.I.; Howe-Grant, M., Eds.; John Wiley & Sons: New York, **1993**; pp. 653-666.

[5] Forgacs, E.; Cserhati, T.; Oros, G. Removal of synthetic dyes from wastewaters: a review. *Environ. Int.*, **2004**, *30*(7), 953-971.

[6] Teli, M.D. Textile coloration industry in India. *Color Technol.*, **2008**, *124*(1), 1-13.

[7] Dupont, G. *La teinture*; Les Editions de l'industrie Textile: Paris, **2002**.

[8] McMullan, G.; Meehan, C.; Conneely, A.; Kirby, N.; Robinson, T.; Nigam, P.; Banat, I.M.; Marchant, R.; Smyth, W.F. Microbial decolourisation and degradation of textile dyes. *Appl. Microbiol. Biotechnol.*, **2001**, *56*(1-2), 81-87.

[9] Khalid, A.; Arshad, M.; Crowley, D.E. Decolorization of azo dyes by *Shewanella* sp. under saline conditions. *Appl. Microbiol. Biotechnol.*, **2008**, *79*(6), 1053-1059.

[10] Joo, D.J.; Shin, W.S.; Choi, J.H.; Choi, S.J.; Kim, M.C.; Han, M.H.; Ha, T.W.; Kim, Y.H. Decolorization of reactive dyes using inorganic coagulants and synthetic polymer. *Dyes Pigments*, **2007**, *73*(1), 59-64.

[11] Jin, X.; Liu, G.; Xu, Z.; Tao, W. Decolourisation of a dye industry effluent by *Aspergillus fumigatus* XC6. *Appl. Microbiol. Biotechnol.*, **2007**, *74*(1), 239-243.

[12] Bae, J.S.; Freeman, H.S. Aquatic toxicity evaluation of copper-complexed direct dyes to the *Daphnia magna*. *Dyes Pigments*, **2007**, *73*(1), 126-32.

[13] Oliveira, D.P.; Carneiro, P.A.; Sakagami, M.K.; Zanoni, M.V.B.; Umbuzeiro, G.A. Chemical characterization of a dye processing plant effluent—identification of the mutagenic components. *Mutat. Res. Genet. Toxicol. Environ. Mutagen*, **2007**, *626*(1), 135-142.

[14] Shah, M.P. Microbial degradation of textile dye (Remazol Black B) by *Bacillus* spp. ETL-2012. *J. Appl. Environ. Microbiol.*, **2013**, *1*(1), 6-11.

[15] Stolz, A. Basic and applied aspects in the microbial degradation of azo dyes. *Appl. Microbiol. Biotechnol.*, **2001**, *56*(1), 69-80.

[16] Dave, S.R.; Patel, T.L.; Tipre, D.R. Bacterial Degradation of Azo Dye Containing Wastes In: *Microbial Degradation of Synthetic Dyes in Wastewaters*; Singh, S.N., Ed.; Springer International Publishing: Switzerland, **2015**; pp. 57-83.

[17] de Lima, R.O.A.; Bazo, A.P.; Salvadori, D.M.F.; Rech, C.M.; de Palma Oliveira, D.; de Aragão Umbuzeiro, G. Mutagenic and carcinogenic potential of a textile azo dye processing plant effluent that impacts a drinking water source. *Mutat. Res. Genet. Toxicol. Environ. Mutagen.*, **2007**, *626*(1), 53-60.

[18] Sinha, S.; Singh, R.; Chaurasia, A.K.; Nigam, S. Self-sustainable *Chlorella pyrenoidosa* strain NCIM 2738 based photobioreactor for removal of Direct Red-31 dye along with other industrial pollutants to improve the water-quality. *J. Hazard. Mater.*, **2016**, *306*, 386-394.

[19] Khan, R.; Bhawana, P.; Fulekar, M.H. Microbial decolorization and degradation of synthetic dyes: a review. *Rev. Environ. Sci. Biotechnol.*, **2013**, *12*(1), 75-97.

[20] Mahmood, S.; Khalid, A.; Arshad, M.; Mahmood, T.; Crowley, D.E. Detoxification of azo dyes by bacterial oxidoreductase enzymes. *Crit. Rev. Biotechnol.,* **2016**, *36*(4), 639-651.

[21] Heidelberg, J.F.; Paulsen, I.T.; Nelson, K.E.; Gaidos, E.J.; Nelson, W.C.; Read, T.D.; Eisen, J.A.; Seshadri, R.; Ward, N.; Methe, B.; Clayton, R.A. Genome sequence of the dissimilatory metal ion–reducing bacterium *Shewanella oneidensis*. *Nat. Biotechnol.*, **2002**, *20*(11), 1118-1123.

[22] Zhao, B.; Poh, C.L. Insights into environmental bioremediation by microorganisms through functional genomics and proteomics. *Proteomics*, **2008**, *8*(4), 874-881.

[23] Linsen, L.; Löcherbach, J.; Berth, M.; Becher, D.; Bernhardt, J. Visual analysis of gel-free proteome data. *IEEE Trans. Vis. Comput. Graph.*, **2006**, *12*(4), 497-508.

[24] Dong, X.; Zhou, J.; Liu, Y. Peptone-induced biodecolorization of reactive brilliant blue (KN-R) by *Rhodocyclus gelatinosus* XL-1. *Process Biochem.*, **2003**, *39*(1), 89-94.

[25] Friedman, D.B. Quantitative proteomics for two-dimensional gels using difference gel electrophoresis. *Methods Mol. Biol.*, **2007**, *367*, 219-239.

[26] Lowry, O.H.; Rosebrough, N.J.; Farr, A.L.; Randall, R.J. Protein measurement with the Folin phenol reagent. *J. Biol. Chem*., **1951**, *193*(1), 265-275.

[27] Kinter, M.; Sherman, N.E. *Protein sequencing and identification using tandem mass spectrometry*; Wiley & Sons: New York, **2000**.

[28] Hong, Y.G.; Gu, J.D. Physiology and biochemistry of reduction of azo compounds by *Shewanella* strains relevant to electron transport chain. *Appl. Microbiol. Biotechnol*., **2010**, *88*(3), 637-643.

[29] Chen, X.; Xu, M.; Wei, J.; Sun, G. Two different electron transfer pathways may involve in azoreduction in *Shewanella decolorationis* S12. *Appl. Microbiol. Biotechnol*., **2010**, *86*(2), 743-51.

[30] Ali, H. Biodegradation of synthetic dyes- a review. *Water Air Soil Pollut*., **2010**, *213*(1-4), 251-273.

[31] Pearce, C.I.; Lloyd, J.R.; Guthrie, J.T. The removal of colour from textile wastewater using whole bacterial cells: a review. *Dyes Pigments*, **2003**, *58*(3), 179-196.

[32] Wu, J.; Kim, K.S.; Sung, N.C.; Kim, C.H.; Lee, Y.C. Isolation and characterization of *Shewanella oneidensis* WL-7 capable of decolorizing azo dye Reactive Black 5. *J. Gen. Appl. Microbiol*., **2009**, *55*(1), 51-55.

[33] Hong, Y.; Xu, M.; Guo, J.; Xu, Z.; Chen, X.; Sun, G. Respiration and growth of *Shewanella decolorationis* S12 with azo compound as sole electron acceptor. *Appl. Environ. Microbiol*., **2007**, *73*(1), 64-72.

[34] Brigé, A.; Motte, B.; Borloo, J.; Buysschaert, G.; Devreese, B.; Van Beeumen, J.J. Bacterial decolorization of textile dyes is an extracellular process requiring a multicomponent electron transfer pathway. *Microb. Biotechnol*., **2008**, *1*(1), 40-52.

[35] Wang, B.; Xu, M.; Sun, G. Comparative analysis of membranous proteomics of *Shewanella decolorationis* S12 grown with azo compound or Fe (III) citrate as sole terminal electron acceptor. *Appl. Microbiol. Biotechnol*., **2010**, *86*(5), 1513-1523.

[36] Kudlich, M.; Keck, A.; Klein, J.; Stolz, A. Localization of the enzyme system involved in the anaerobic degradation of azo dyes by *Sphingomonas* sp. BN6 and effect of artificial redox mediators on the rate of azo reduction. *Appl. Environ. Microbiol*., **1997**, *63*(9), 3691-3694.

[37] Dubbs, J.M.; Mongkolsuk, S. Peroxiredoxins in bacterial antioxidant defense In: *Peroxiredoxin Systems*; Flohé, L.; Harris**,** J.R., Eds.; Springer: Netherlands, **2007**; pp. 143-193.

[38] Tang, X.; Yi, W.; Munske, G.R.; Adhikari, D.P.; Zakharova, N.L.; Bruce, J.E. Profiling the membrane proteome of *Shewanella oneidensis* MR-1 with new affinity labeling probes. *J. Proteome. Res*., **2007**, *6*(2), 724-734..